SCV Notes

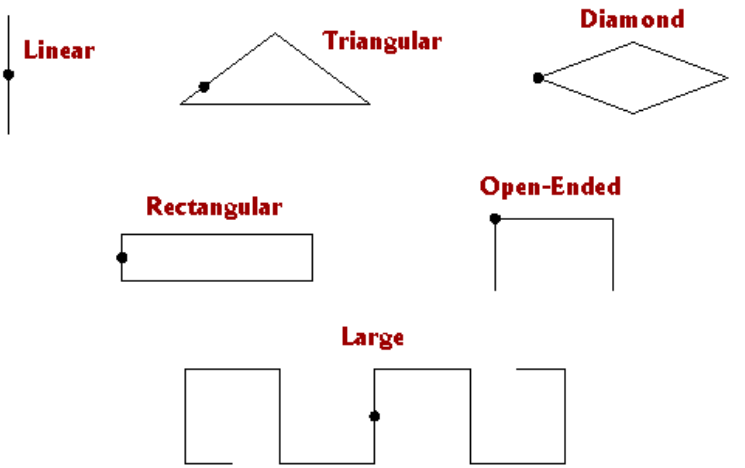

L. B. Cebik, W4RNL

Published by
antenneX Online Magazine
http://www.antennex.com/
POB 72022
Corpus Christi, Texas 78472 USA

ISBN: 1-877992-46-1

Table of Contents

Dedication (Posthumous)

This volume of studies of long-wire antennas is dedicated to the memory of Jean, who was my wife, my friend, my supporter, and my colleague. Her patience, understanding, and assistance gave me the confidence to retire early from academic life to undertake full-time the continuing development of my personal web site (http://www.cebik.com). The site is devoted to providing, as best I can, information of use to radio amateurs and others–both beginning and experienced–on various antenna and related topics. This volume grew out of that work–and hence, shows Jean's help at every step.

Preface to SCVs

In 1998, I published a series of short articles on SCV antennas in *The National Contest Journal*. Nearly a decade has gone by, and I still receive questions about these interesting antennas. Therefore, I decided to return to ground zero and re-formulate the information in those articles—and much, much more—to create this volume. I have expanded coverage in terms of several factors: the fundamentals upon which SCVs operate, antenna types that fit within the group, frequency coverage, and special applications and opportunities.

What is an SCV?

The letters SCV are an abbreviation for self-contained vertical. Although I generally do not favor adding terms to the lexicon of antennas, circumstances in the late 1990s led me to introduce the term. First, a debate was going on within amateur circles about whether all vertical antennas, especially those near to the ground, required a ground radial system in order to perform correctly. That discussion has largely ended, as folks began to understand some of the distinctions that mark talk about the ground relative to various parts of an antenna system.

Second, many amateurs seemed not to realize the close inter-relationship among members of the SCV family, let alone the fundamentals of their operation. Even the highly regarded compendium called *Low-Band Dxing* by ON4UN (John Devoldere) scattered members of the family in separate chapters (10 and 12) of his book (2nd Edition). In order to create a family union, I coined the term SCV.

An SCV is a self-contained vertically polarized antenna, usually constructed from copper wire for upper MF and lower HF use. Most basic family members use 1-λ of wire for the antenna structure, although there are also doubles and even larger members of the family. Among the basic SCV shapes are deltas (triangles), diamonds, rectangles, and open-ended versions (the half-square). **Fig. 0-1** shows some (but not all) of the basic family members.

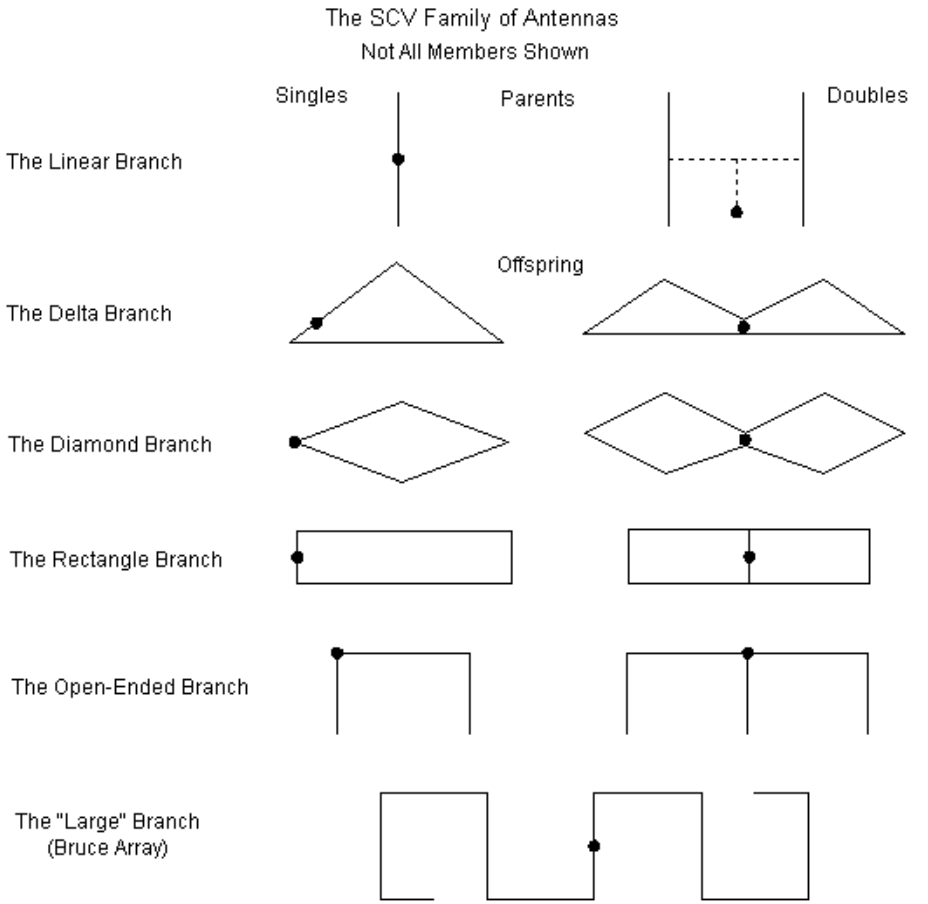

Fig. 0-1

None of the SCV family requires a buried or surface ground radial system. Such systems are necessary with vertical monopoles, since the radials form a portion of the antenna structure. The SCV family members are each complete in themselves. We shall have occasion along the way to see what a ground radial

system and other forms of ground treatment may do for this collection of antennas.

The SCVs are offspring of more basic antennas, indicated at the top of **Fig. 0-1**. All basic or single members of the family are forms of phased vertical dipoles, called a double in the figure. Of course, phased vertical dipoles derive from the single vertical dipole, the most fundamental vertically polarized antenna of all. (Despite the fact that much antenna lore begins with the ¼-λ vertical monopole and its radial system, we shall treat the monopole and its radials as a version of the dipole.) One consequence of using the vertical dipole as our fundamental antenna is that this volume will not discuss monopoles and their radials systems. For information on these types of antennas, consult *Ground-Plane Notes* published by *antenneX*.

The offspring of the vertical dipoles have a special feature: they all use a single feedpoint. The reduction in the number of feedpoints simplifies questions of matching the antenna to a desired feedline. However, that same fact presents some challenges, because for many SCV users, a 50-Ω coaxial cable is the favored transmission line. This fact alone has a role in shaping some of the SCVs in the collection.

Why Use an SCV?

The primary realm for the SCV is the upper MF region (160 meters) and the lower HF region (80 through 30 meters). Although we shall examine some special VHF and UHF applications for SCVs, the primary motivation for turning to the SCV designs was to improve performance of vertically polarized antennas without requiring a complex and often uncertain phasing system to interconnect vertical elements. In addition, all of the SCV designs require only inexpensive copper wire.

Fig. 0-2 presents a few overlaid elevation patterns for some typical 40-meter antennas. Within the group is a pair of wire horizontal dipoles, one at the amateur average backyard height of 35', the other at a more beneficial 50' level. The elevation angle of maximum radiation depends upon the antenna height as

measured in wavelengths. Even the higher dipole is only about 0.7-λ high on the sample frequency.

Sample 40-Meter Elevation Patterns Fig. 0-2

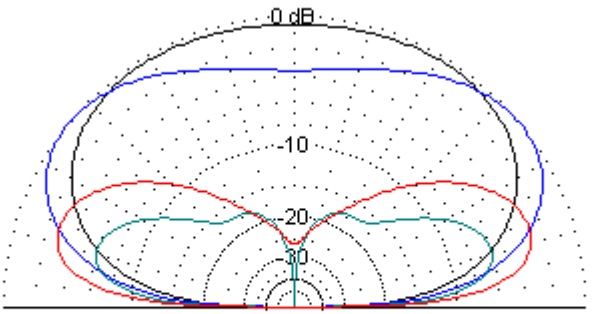

Black: Horizontal dipole at 35'
Blue: Horizontal dipole at 50'
Green: Vertical dipole at 10' to 77'
Red: Half-square at 10' to 49'

All sample antennas use AWG #12 copper wire at 7.15 MHz above average ground.

The figure also contains the elevation pattern for a wire vertical dipole that extends from 10' to about 77' above ground. Its pattern is omni-directional, and therefore we expect lesser gain in any particular direction. However, the SCVs are all bi-directional, as are the horizontal dipoles. The half-square is the representative SCV for this exercise. We may note that below 20°, the region most favorable to DX skip, the half-square has more gain than either of the two dipoles. In addition, both of the vertical antennas have very weak far-fields at high angles, which is often a source of QRN. Hence, many operators from 160 through 30 meters prefer vertical antennas as much for their quietness as for their low-angle gain. (Of course, there are noise sources, usually local, that may affect vertically polarized antennas more than horizontal antennas. Hence, one may not reap the benefits of the SCV at every possible location for an amateur installation, where control of local noise sources may range from limited to none.)

The SCV does not pretend to compete with directional beams that are at least ½-λ above ground. Unfortunately, that height becomes more difficult to achieve

as we lower the operating frequency. For reference, **Table 0-1** lists the height of 1 λ, ½ λ, and ¼ λ in both feet and meters for the lowest amateur bands.

Table 0-1. Heights of a wavelength and some fractions of a wavelength at typical amateur "low-band" frequencies

Band	Frequency	Height in Feet			Height in meters		
Meters	MHz	1 λ	0.5 λ	0.25 λ	1 λ	0.5 λ	0.25 λ
160	1.85	531.66	265.83	132.92	162.05	81.03	40.51
80	3.55	277.06	138.53	69.27	84.45	42.22	21.11
75	3.95	249.01	124.50	62.25	75.90	37.95	18.97
60	5.368	183.23	91.61	45.81	55.85	27.92	13.96
40	7.15	137.56	68.78	34.39	41.93	20.96	10.48
30	10.125	97.14	48.57	24.29	26.61	13.30	6.65

In the end, an SCV is a practical antenna. In absolute terms, it is far from the perfect radiator. Nevertheless, when we add in a healthy dose of realism in the form of acreage and height restrictions that surround the average amateur installation, it may become the perfect practical choice for a given situation.

How Shall We Study the SCV?

A wide-ranging survey of antenna types calls for a systematic means of study. Antenna modeling software is the obvious tool for the investigation for two reasons. First it permits a rapid survey of antenna performance potential in a variety of situations in which we may vary the soil quality, the antenna size and height above ground, and the wire size. Second, modeling software is completely reliable with respect to these antennas because the antenna construction does not press any of the limits of most modeling software. The software of choice for these notes is NEC-4. For most models, NEC-2 would do very well. However, a few models used in the study will involve buried radial systems, which only NEC-4 can handle. Most of the models used in this study will employ EZNEC Pro/4.

Models carry with them a few notable presumptions that may vary from an average amateur installation. Foremost among variables is the amount of ground

clutter in the immediate area of the antenna. The models will contain no clutter to adversely interact with the antenna. Most amateur antenna sites are not so fortunate. In fact, trees and posts that already exist in a yard may be necessary as supports for an SCV. All that I can do is give somewhat abstract advice: keep the vertical radiators of the antenna as far as feasible from conductive or semi-conductive objects, especially vertical ones. As well, keep the broadside areas of the antenna's fields as free of vertical objects as possible. Among the SCV designs, we shall note that some versions show a higher gain potential than others. Anecdotal reports sometimes reverse the order in terms of successful operation. In many, if not most, cases, the reversal arises from the difference in the antenna geometries relative to interactions with nearby objects.

We shall divide the work in each chapter or set of chapters into different categories. The first or initial foray into an SCV design will examine general principles. To even the playing field for all such initial entries, I shall use a standard frequency (7.15 MHz), a standard wire size (copper AWG #12 or 0.0808" diameter), and a standard ground (average: conductivity 0.005 S/m, permittivity 13).

Next, we shall examine some factors that contribute to SCV effectiveness for selected bands. Here, I shall use 160, 80, and 40 meters (1.85, 3.55, and 7.15 MHz) as targets, as we examine how SCV dimensions and height above ground influence performance—and with what rates of changes as we vary these dimensions. We shall have occasion to see changes (or their absence) as we vary the soil quality. **Table 0-2** lists the three standard soil qualities that we shall use.

Table 0-2. Standard soil quality parameters for SCV tests

Soil Label	Conductivity (S/m)	Relative Permittivity
Very Good	0.0303	20
Average	0.005	13
Very Poor	0.001	5

We may in fact perform the category-2 survey more than once, since some of

the antennas have both single and double versions.

The final category of investigation is for each SCV a potpourri of special considerations. Some of them may involve methods of feeding the wire antenna. In addition, we shall look at extended applications. Many of the SCV forms that we think of as lower HF antennas also have VHF and UHF applications. We shall examine those applications only far enough to show their intimate relationship to the wire versions that form main object of study.

Attached to this volume is a collection of models in EZNEC (.EZ) formats. The Appendix provides the dimensions for each basic (1-λ) SCV form. The collection cannot include the hundreds of models and variations required to perform the surveys. Instead, for each type of SCV, I shall include what I believe to be an optimized version of the antenna using AWG #12 copper wire over average ground. These models will provide a foundation for antenna installation planning and a vehicle for modification in case you wish to replicate any of the surveys that appear here. I recommend that you transfer the files to your hard drive before opening them so that you can save any interesting variations.

What Is the Plan of Attack?

Since all SCVs rest on a foundation anchored by the vertical dipole, Part 1 of the study will examine some of the basic properties of this antenna, especially as the behavior of the vertical dipole over ground differs from the behavior of its horizontal brother. Chapter 1 will look at the single vertical dipole. As simple as the antenna may be, as shown by the omni-directional pattern in **Fig. 0-3**, it may still contain a few surprises for amateurs who have experience only with horizontal dipoles. We shall see how elevation patterns change as we alter the height above ground. As well, we shall discover whether a ground radial system beneath the antenna has a significant affect on its performance. In fact, we shall digress into a discussion of different types of ground as they apply to different aspects of antenna performance, with special attention to various methods of feeding the vertical dipole—at its center and at its base, either with a high-impedance circuit or network or with a transmission line section (the J-pole). We shall even briefly explore how to bend the vertical dipole to form an inverted-L.

3-Dimensional Pattern of
a Vertical Dipole over Ground

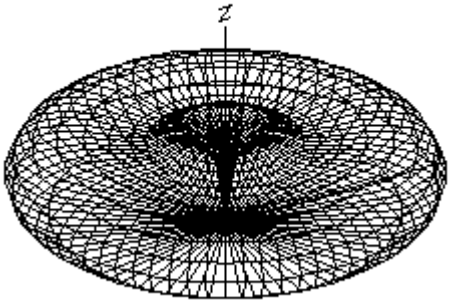

Fig. 0-3

In Chapter 2, we shall expand our view of vertical dipoles to include 2 or 3 of them in a line, all fed in phase. **Fig. 0-4** shows the bi-directional pattern for 2 such dipoles over ground. We shall want to find the conditions for optimizing the pattern and to learn of any limitations associated with the technique.

3-Dimensional Pattern of
2 Verticals In Phase over Ground

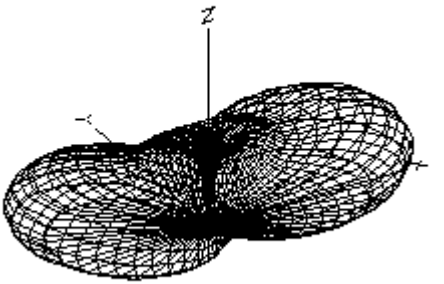

Fig. 0-4

Not all uses of multiple vertical dipoles involve feeding every element. We shall briefly look at some ways to create parasitic beams, including triangular arrays that allow an operator to cover the full horizon with a switch rather than a rotator. Finally, we shall explore an "ideal" vertical array in which the parasitic elements are pseudo-guy wires.

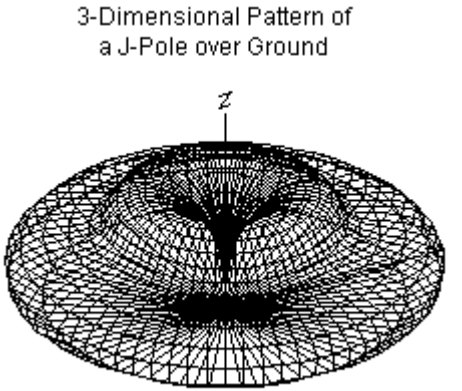

Fig. 0-5

The final chapter of Part 1 will introduce special considerations that apply to the use of the vertical dipole in VHF and UHF service. For example, the antenna height is many times that of the same antenna in the lower HF region, and that fact will make a large difference in the patterns that we obtain. We shall also explore the use of radials with such antennas, with emphasis on the relationship of a so-called sloping-radial monopole to a true vertical dipole. The J-pole that has such limited use in the HF region (see **Fig. 0-5** for a representative pattern) becomes commonplace. As well, we can create antennas in the VHF and UHF region that low-band operators can only dream about, such as collinear vertical dipoles.

Part 2 of our work takes us into the region of SCVs, understood as resting on a 1-λ length of wire in fundamental forms. We shall examine them in roughly an ascending order of performance potential. See **Fig. 0-1** to review the basic SCV

shapes. Chapter 4 begins with the delta or triangular form, a pattern for which appears in **Fig. 0-6**. We shall look at both the physical and performance differences between the two most common delta forms: the equilateral and the right triangle. The exercise will help us understand just how all SCVs work. The delta has a doublewide variation, and we shall look at its requirements and its promise of improved performance.

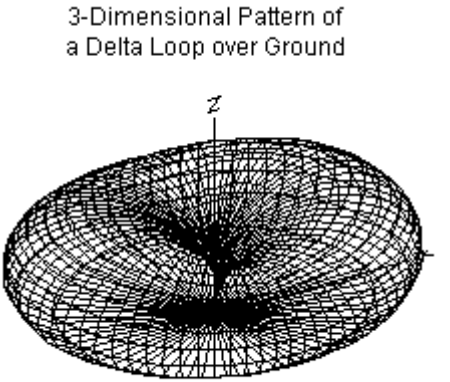

Fig. 0-6

The side-fed square diamond loop is an alternative to the delta. However, in the lower HF region, few amateurs have experimented with stretching the loop into an elongated diamond form both to increase the gain and to lower the impedance to coax-compatible values. **Fig. 0-7** shows the pattern for such an antenna. We shall discover how far we may stretch a diamond before we lose the benefits of the process. Even less common in the lower HF region are double diamond arrays with a single feedpoint. The rarest form of the diamond is a single or a double used in conjunction with a planar reflector to obtain a directional beam with broader-band characteristics than we can obtain from either the driver alone or from a parasitic diamond array. However rare these forms are in the HF region, they are commonplace in the UHF spectrum. We shall sample some of those potentials.

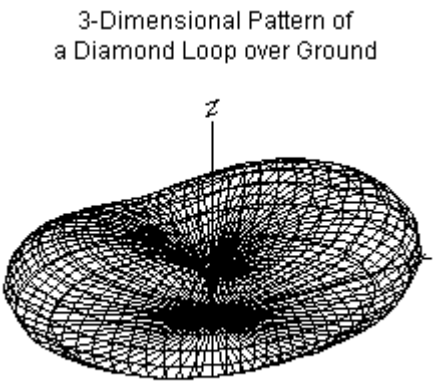

Fig. 0-7

Chapter 6 investigates a different form of SCV also derived from the side-fed square quad loop. This time, we begin with a square, with two wires parallel to ground and two wires vertical. If we stretch the loop parallel to the ground and shrink its height, we increase the gain and lower the side feedpoint impedance. **Fig. 0-8** gives us a representative pattern. In principle, stretching the square into a rectangle does the same job as stretching the diamond into an elongated diamond. Nevertheless, there are some interesting differences. For example, maximum gain for a stretched rectangle requires a shape that yields very low impedance values. One answer to this potential matching problem is to double the rectangular winding to create a parallel transmission line. The result is a multiplication of the feedpoint impedance by a factor of 4, creating a better match for the ubiquitous coaxial cable feedline. Alternatively, we may create a doublewide rectangle for additional bi-directional gain. We shall look at potential feedpoint positions for this long and thin array. Unlike the diamond, we may also create asymmetrical double rectangles (a generalized term coined by Dan Handelsman, N2DT). The most common version is the horizontally polarized hentenna. However, we may easily lay the antenna on its side and acquire its benefits with vertical polarization.

3-Dimensional Pattern of
a Rectangular Loop over Ground

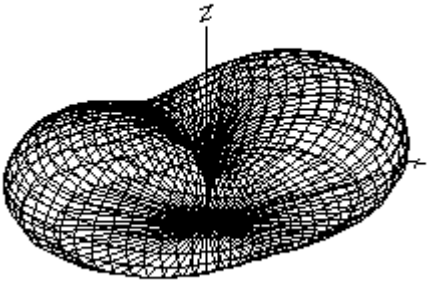

Fig. 0-8

All of the SCV versions that we have examined so far use closed loop structures. However, we may open the loop and obtain a better phase relationship between the vertical elements. The half-square is the most fundamental version of this technique, even though it appeared in amateur literature after the development of its doublewide big brother, the bobtail curtain. **Fig. 0-9** provides a representative pattern for the half-square. Fundamental theory tells us that the horizontal sections of each antenna should be ½-λ, while the verticals should be ¼-λ. However, we shall discover that these rough dimensions require considerable variation in order to achieve maximum performance. Moreover, the ratios required for vertical to horizontal sections are not the same for the half-square and the bobtail curtail. Among all of the SCV forms, the half-square and the bobtail curtain lend themselves best to the creation of parasitic beams. In fact, we may even create reversible beams using the half-square. Like all SCV forms, the half-square and the bobtail curtain have VHF and UHF applications, especially with planar reflectors. Both of these open-ended forms of the SCV also allow us some versatility in feeding them. We can feed the antenna at the upper junction with horizontal wire for a low-impedance system. Alternatively, we can feed one of the verticals at the lower end using standard high-impedance techniques. In the earliest days of their lives, high-impedance feed systems were most common.

3-Dimensional Pattern of
a Half-Square over Ground

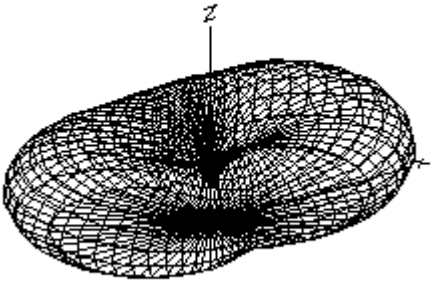

Fig. 0-9

Our final chapter works with an array that we might not think of as an SCV had we skipped the half-square. The Bruce array, whose pattern appears in **Fig. 0-10** is an open-ended array with indefinitely great potential.

3-Dimensional Pattern of
a Bruce Array over Ground

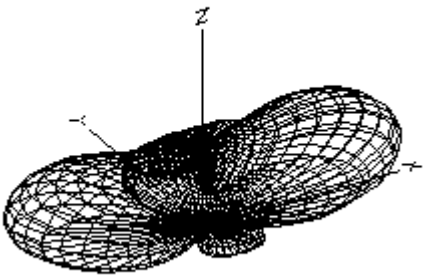

Fig. 0-10

The outline sketch of the Bruce array appears in only one guise in **Fig. 0-1**. It has 5 vertical sections, using a center feedpoint for the systems. Hence, many Bruce arrays use an odd number of sections. 4- and 5-section arrays are the most common amateur forms. The end wires point inward, although we can easily point them outward as well. The twist on the Bruce array is that it is ¼-λ tall, with ¼-λ between vertical wires. Hence, in its most rudimentary form, it is a side-fed quad that forgot to turn back upon itself. The result is a relatively high-gain array with a narrowing beamwidth as we increase the number of sections.

Like the Bruce array, our investigation is unending in principle. As a practical matter, we must draw these notes to a close somewhere, and the Bruce array is as appropriate a point as any. However, this preliminary survey has only begun our detailed look at SCVs and their roots. It is now time to acquire some data to give our understanding a firmer foundation.

Part I: Basics

1. The Vertical Dipole

The SCV in all of its forms derives from one of the most fundamental antennas in the repertoire of all transmitters or receivers of radio waves: the vertical dipole. Understanding the performance potential, limitations, and general behavior of SCVs begins with an understanding of how vertical dipoles behave over ground. Most radio amateurs are quite familiar with the behavior of the horizontal dipole, but for some reason, they fail to appreciate fully how that behavior changes when we tilt the antenna by 90°. As a consequence, they encounter information on one of the SCV forms and think only that the radiation patterns are odd and interesting, but somehow disconnected from the patterns with which they are familiar.

In fact, SCVs are an outgrowth of more general vertical antenna behavior. So we shall return to the beginning of self-contained vertical antennas: the dipole that has its entire length above ground. In fact, we shall begin with the dipole in free space, as shown in **Fig. 1-1**. The curved line attached to the outline sketch shows the relative current magnitude distribution along the wire. As with all dipoles, there is a small but definite phase shift (a few degrees at most) in the current along the wire's length, although the trace does not show it. Many amateur sources report that the current distribution trace is a sine curve, but that is not quite correct. The curve is nearly sinusoidal, but varies just enough to require complex mathematical techniques to analyze it precisely. That is one reason why antenna-modeling software does not use simple trigonometric relationships to calculate antenna behavior. Instead, NEC and MININEC require complex matrices associated with the method of moments in order to provide accurate antenna performance analysis.

In all respects the radiation patterns of the vertical dipole in free space are complete normal to dipoles in general. The free-space environment has no intrinsic up or down. The only way that we can call the antenna shown a vertical dipole is by reference to the Cartesian conventions of the modeling software. If we set the dipole along the +Z to –Z axis, it is vertical.

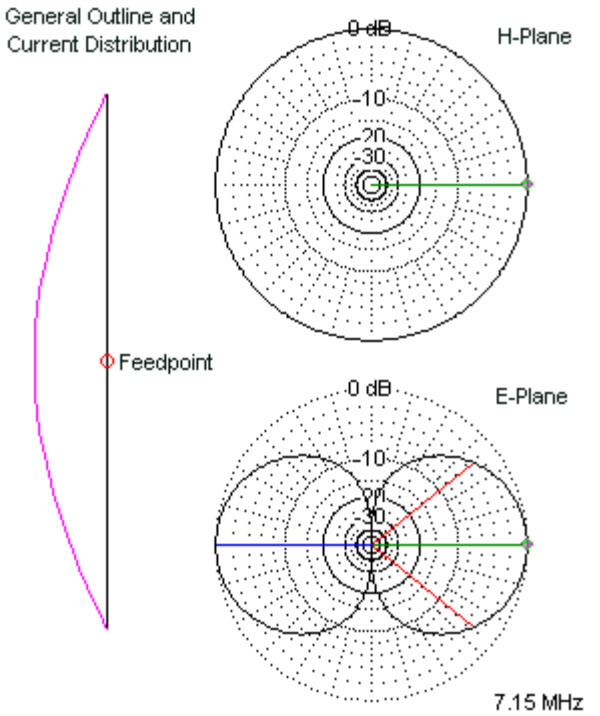

Fig. 1-1

In free-space, we apply the terms E-plane and H-plane to linear antennas. The E-plane is in the plane formed by the linear antenna wire. For a horizontal dipole above ground, the E-plane corresponds to the azimuth pattern. However, when we place a vertical dipole above ground, the E-plane translates to the elevation pattern.

The H-plane is at right angles to the plane of the antenna wire or wires. If we use a dipole horizontally above ground, the H-plane turns into the elevation pattern. However, if the dipole is vertical relative to the ground, the H-plane

corresponds to the azimuth pattern. From the patterns in **Fig. 1-1**, we would expect that the azimuth pattern of a vertical dipole would always be circular (in the absence of objects that might distort the pattern).

The Vertical Dipole over Ground

Let's set the vertical dipole to a resonant frequency of 7.15 MHz and place it over ground. In **Table 1-1**, we find the modeled performance figures for the dipole as we do two things. First, we gradually raise the bottom of the dipole above the ground, as measured in wavelengths. Second, we vary the soil quality of the ground below the vertical dipole. The table shows us what happens.

Performance of a Vertical Dipole over Various Soil Qualities with Various Base Heights					Table 1-1
Soil Type	Height	Gain dBi	TO deg	Feed R	Feed X
VG	0.01	1.93	15	100.50	8.55
	0.125	2.03	12	74.17	-7.25
	0.25	1.25	10	69.35	0.47
	0.375	2.72	43	73.26	2.99
	0.5	3.93	37	74.86	0.60
Average	0.01	-0.12	18	97.66	4.98
	0.125	0.29	15	73.15	-5.98
	0.25	0.17	13	70.10	0.92
	0.375	1.57	42	73.51	2.51
	0.5	2.61	36	74.51	0.44
VP	0.01	-0.72	21	91.60	2.22
	0.125	0.51	18	72.68	-3.94
	0.25	1.27	16	71.17	1.07
	0.375	1.88	15	73.56	1.85
	0.5	2.53	14	74.06	0.41
Notes:	Soil Type: VG = Very Good; VP = Very Poor				
	Gain dBi = maximum gain at TO angle				
	TO deg = TO angle in degrees				
	Feed R/Feed X = Feedpoint impedance in Ohms				
	Frequency: 7.15 MHz				

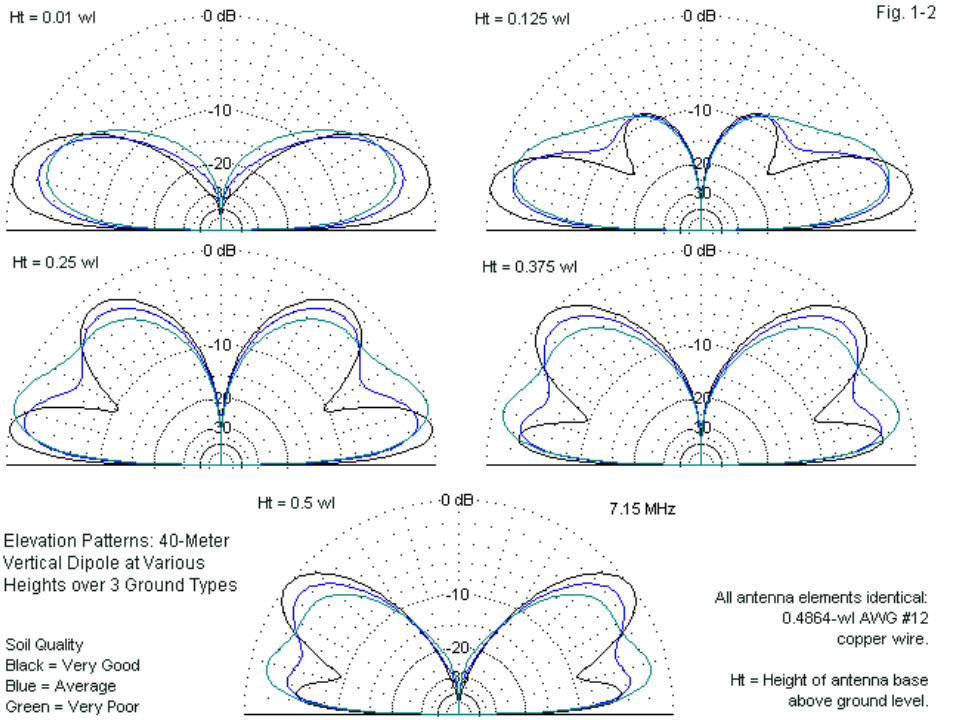

Fig. 1-2 provides some elevation patterns to help us understand the numbers. (We only need elevation patterns, since all azimuth patterns would be circles.) When the base of the vertical dipole is very close to the ground, the high-current region near the feedpoint is already ¼-λ above ground. For the cleanest pattern without any high-angle lobes, the low height is best, although we pay a price. The gain is low, and the ground has a strong influence on the feedpoint impedance. The dipole in the example has a resonant length in free space with a 73-Ω feedpoint impedance. (The impedance would be slightly lower if the model had used lossless wire, but all models will use AWG #12 copper wire. In the lower HF and the MF regions, the wire is very thin relative to a wavelength. Hence, there will be small losses that affect some of the numbers but not

practical performance.)

As we raise the antenna base above ground, several things happen at the same time. First, the feedpoint impedance more closely approximates its free-space value and fluctuates by only a very small amount with different heights. (In contrast, a horizontal dipole would show much larger changes in feedpoint impedance as we raise it from near-ground level to perhaps 1-λ above ground.)

Second, even the first step in the elevation of the vertical dipole shows the emergence of a second elevation lobe at a higher angle. The higher we raise the antenna above ground, the stronger the second lobe becomes. As shown by the TO angle column in the table, for certain types of ground quality, the second lobe grows stronger than the lower lobe, reducing the effectiveness of the antenna as a low-angle DX aerial. For average through very good soils, that height is somewhere between 0.25-λ and 0.375-λ. Add ¼-λ to these heights to get an idea of where the high-current region of the antenna is located relative to the ground.

The third aspect of the vertical dipole's behavior as we raise it above ground calls attention to the differences in lobe formation as we vary the quality of the soil beneath the antenna. The better the soil quality in terms of its conductivity and permittivity, the crisper will be the higher angle lobes, with deeper nulls between lobes. As the soil quality grows worse, the lobes lose some of their definition and become interconnected bulges in the pattern.

Moreover, as the soil quality improves, the upper lobes increase their strength more rapidly than when the soil is poor. It pays to attend to the details of both the patterns and the tabular data. For example, with base heights of 0.125-λ and 0.25-λ, the maximum gain of the dipole over average soil is lower than the maximum gain over either very good or very poor soil. This seemingly anomalous result is a result of two major factors: the higher gain that we obtain with very good soil and the slow growth of the second lobe over very poor soil.

As we continue to raise the base of the dipole without changing its end-to-end length, the differences in lobe formation over varying soil qualities becomes even

more evident. At a base height of 0.375-λ and above, the low-angle performance of the antenna over very good soil becomes marginal at best. In contrast, the same antenna over very poor soil shows its strongest lobe at a low angle even when the base height increases to 0.5-λ.

The importance of this initial exercise lies in its ability to help develop reasonable expectations from vertical antennas in general. For horizontal antennas, we use a simple rule of thumb: higher is better, both in terms of improving gain and in terms of lowering the elevation angle of maximum radiation (the TO or take-off angle). That rule does not apply to vertical antennas for the MF and HF regions. (It does apply to vertical antennas used in the VHF and UHF regions, where the antenna is many wavelengths above ground. Unless we suspend a vertical dipole below an aircraft, we cannot obtain the same base heights for antennas in the 1.8- to 10-MHz region.)

Virtually all HF and MF vertical antennas will show a height above ground that yields for a given soil quality the maximum gain at the lowest desired angle of radiation. Since that height is partially a function of soil quality, anyone using any type of vertical antenna must have a good general idea of the soil quality at a planned antenna site. In this way, vertical dipoles also differ from their horizontal counterparts. We may raise the height of a horizontal dipole with full confidence that every added increment of height will be beneficial, regardless of soil quality. (In the region below 1-λ, there are a few less-desirable heights for horizontal antennas, but they apply to all soil qualities.) For a vertical dipole and all of its SCV descendents, there will be a small range of nearly optimal heights that vary with the soil quality.

The results that we obtained from our 40-meter exercise are general, but not completely universal. The effects of ground interactions change somewhat with frequency. So obtain a feel for the differences, let's place the vertical dipole over our array of soil qualities using a base height of 0.125-λ. However, we shall add vertical dipoles at 1.85 and 3.55 MHz. Each dipole is resonant in free space. **Table 1-2**, we find the results of our small survey. The table has reference entries for each free-space model, showing the effects of decreasing frequency on AWG #12 wire. The gain goes down and the feedpoint resistance rises as the

wire becomes thinner when measured against a wavelength. Of course, the differences are numerical and have no operational significance.

Performance of Vertical Dipoles for 160, 80, and 40					Table 1-2
Meters at 0.125-Wavelength Base Height					
Freq MHz	Soil Type	Gain dBi	TO deg	Feed R	Feed X
1.85	Fr. Sp.	2.00		74.30	-0.41
	VG	4.11	10	75.89	-8.55
	Average	1.05	13	74.85	-8.08
	VP	-1.07	16	73.40	-6.67
3.55	Fr. Sp.	2.04		73.76	0.54
	VG	3.17	11	75.06	-7.53
	Average	0.26	14	73.40	-6.64
	VP	-0.28	18	72.77	-4.76
7.15	Fr. Sp.	2.07		73.26	0.63
	VG	2.03	12	74.17	-7.25
	Average	0.29	15	73.15	-5.98
	VP	0.51	18	72.68	-3.94
Notes:	All antennas use AWG #12 copper wire.				
	Free-Space entry is for reference.				
	Soil Type: VG = Very Good; VP = Very Poor				
	Gain dBi = maximum gain at TO angle				
	TO deg = TO angle in degrees				
	Feed R/Feed X = Feedpoint impedance in Ohms				

As we lower the frequency, the gain anomaly that we found at 7.15 MHz disappears. Average soil at the two lower frequencies yields a higher maximum gain than at the highest frequency in the trio. Indeed, as we lower the frequency, the difference in maximum gain between very poor and average soil increases.

Still we find interesting oddities in the pattern of values in the table and in the patterns that appear in **Fig. 1-3**. With very good soil, lowering the frequency increases the maximum gain. However, over very poor soil, lowering the frequency reduces the gain. The patterns show the changing relationship of the maximum gain levels for the 3 soil types for the antennas at each frequency. The

lesson is simple to state but often more difficult to implement: the vertical antenna user should know the effects of his or her soil quality on antenna performance for each frequency used.

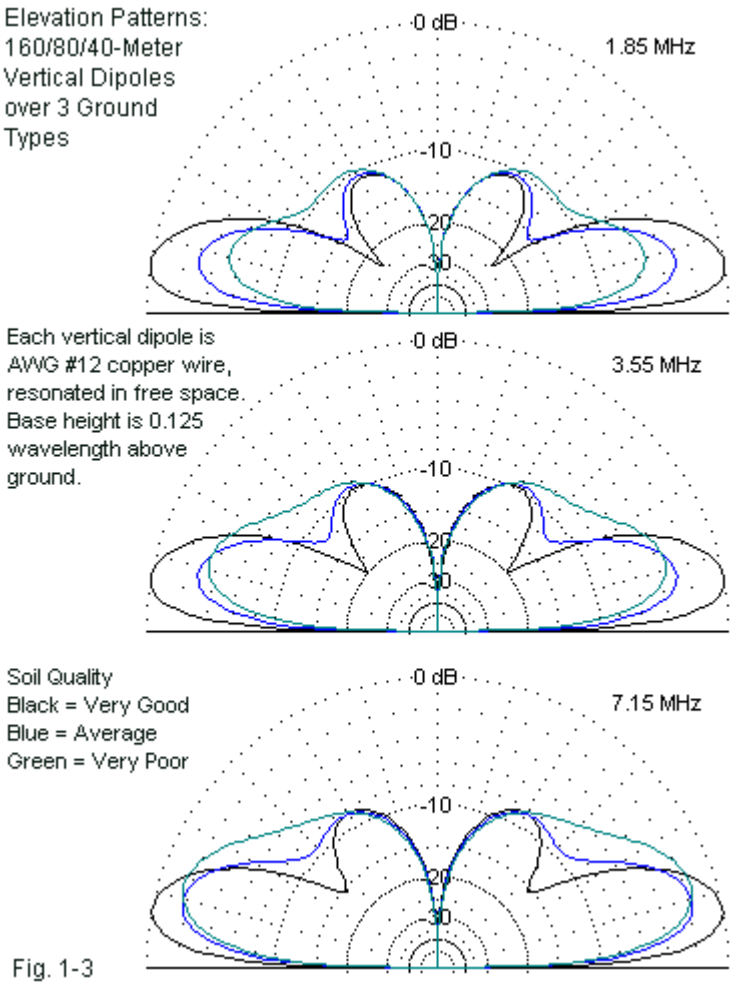

Fig. 1-3

Ground-Level Radials?

One perennial question that arises in connection with the vertical dipole is whether or to what degree its performance benefits from the presence of a ground radial system directly below the dipole. Some commercial and governmental installations require radial systems while a number of manufacturers of amateur vertical dipole systems suggest that a radial system will not improve antenna performance. Of course, the radial system for a vertical dipole that does not touch the ground will have no direct connection to the antenna. **Fig. 1-4** shows the general outline of the system that we shall subject to modeling tests.

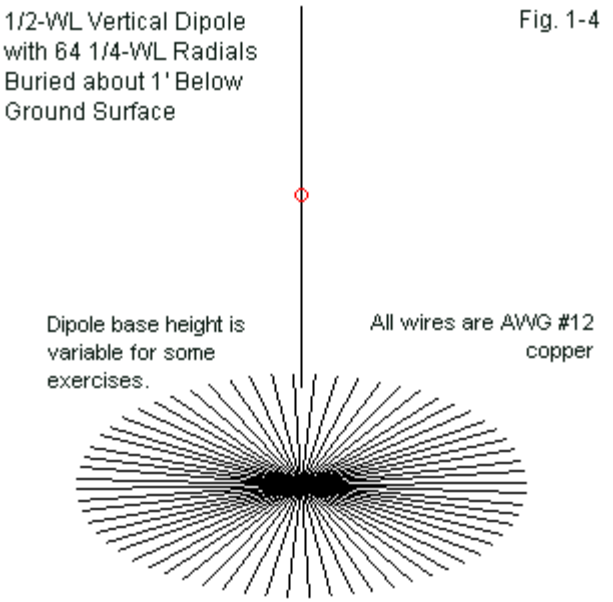

Commercial installations generally use about 120 radials, while amateur systems tend to be much skimpier. The modeled system uses 64 ¼-λ radials

composed of AWG #12 copper wire. As an initial test, let's re-gather the data in **Table 1-2** but this time use the radial system buried about 1' below the ground surface. The antenna will be a constant 0.125-λ distance above ground and sample our three soil quality levels. The results of our revised survey appear in **Table 1-3**.

Performance of Vertical Dipoles for 160, 80, and 40					Table 1-3
Meters at 0.125-Wavelength Base Height with 64 Buried Radials					
Freq MHz	Soil Type	Gain dBi	TO deg	Feed R	Feed X
1.85	Fr. Sp.	2.00		74.30	-0.41
	VG	4.12	10	76.01	-8.44
	Average	1.11	13	75.25	-7.53
	VP	-0.90	16	74.16	-5.22
3.55	Fr. Sp.	2.04		73.76	0.54
	VG	3.19	11	75.27	-7.38
	Average	0.36	14	74.58	-5.87
	VP	-0.11	18	73.89	-3.08
7.15	Fr. Sp.	2.07		73.26	0.63
	VG	2.06	12	74.57	-7.08
	Average	0.40	15	74.27	-5.12
	VP	0.68	18	74.15	-2.18
Notes:	All antennas use AWG #12 copper wire.				
	Free-Space entry is for reference.				
	Soil Type: VG = Very Good; VP = Very Poor				
	Gain dBi = maximum gain at TO angle				
	TO deg = TO angle in degrees				
	Feed R/Feed X = Feedpoint impedance in Ohms				

Regardless of the operating frequency between 1.85 and 7.15 MHz, the gain differential is almost constant for each soil quality. Over very poor soil, the radial system improves gain by about 0.17 dB. Over average soil, the improvement ranges between 0.06 and 0.12 dB. Over very good soil, the difference is 0.02 dB or less. These differences fall well below the level that one would be able to detect in operation. There are no changes in the TO-angle column. The feedpoint impedance variations fall well within the range that normal construction

variables would mask. For the base height of the vertical dipole used in this multi-band test (0.125-λ) the radial system offers no benefits that would justify the use of 2000' of radial wire at 40 meters, let alone 8000' at 160 meters. However, the radial system in no way detracts from the performance of the vertical dipole. Indeed, we may find another use for a radial system when we later alter the feedpoint of the vertical antenna.

Performance of a Vertical Dipole over Various					Table 1-4
Soil Qualities with Various Base Heights with 64 Buried Radials					
Soil Type	Height	Gain dBi	TO deg	Feed R	Feed X
VG	0.01	2.04	15	100.50	10.78
	0.125	2.06	12	74.57	-7.08
	0.25	1.26	10	69.43	0.37
	0.375	2.72	43	73.23	2.96
	0.5	3.94	37	74.84	0.61
Average	0.01	0.27	18	96.82	12.17
	0.125	0.40	15	74.27	-5.12
	0.25	0.20	13	70.42	0.89
	0.375	1.53	42	73.44	2.38
	0.5	2.61	36	74.45	0.46
VP	0.01	-0.06	22	90.01	14.74
	0.125	0.68	18	74.15	-2.18
	0.25	1.30	16	71.76	0.87
	0.375	1.86	15	73.54	1.62
	0.5	2.51	14	73.96	0.41
Notes:	Soil Type: VG = Very Good; VP = Very Poor				
	Gain dBi = maximum gain at TO angle				
	TO deg = TO angle in degrees				
	Feed R/Feed X = Feedpoint impedance in Ohms				
	Frequency: 7.15 MHz				

For most amateur installations, a base height of 0.125-λ is unreasonably high, even at 40 meters. Therefore, let's duplicate the test that resulted in the data in **Table 1-1**. In that test, we confined ourselves to 7.15 MHz, but surveyed the soil qualities using a large number of base heights above ground: from 0.01-λ

up to 0.5-λ. We may repeat these tests with the 64-radial system in place about 1' below the surface of the ground. The resulting data appear in **Table 1-4**.

Virtually no changes occur in the TO-angle columns as we compare the two tables. As well, the changes in the impedance columns occur mostly in the reactance column and only for the 0.01-λ base height. We may conveniently compare the gain values for the three soil types by graphing the differences between the values in the two tables, as shown in **Fig. 1-5**.

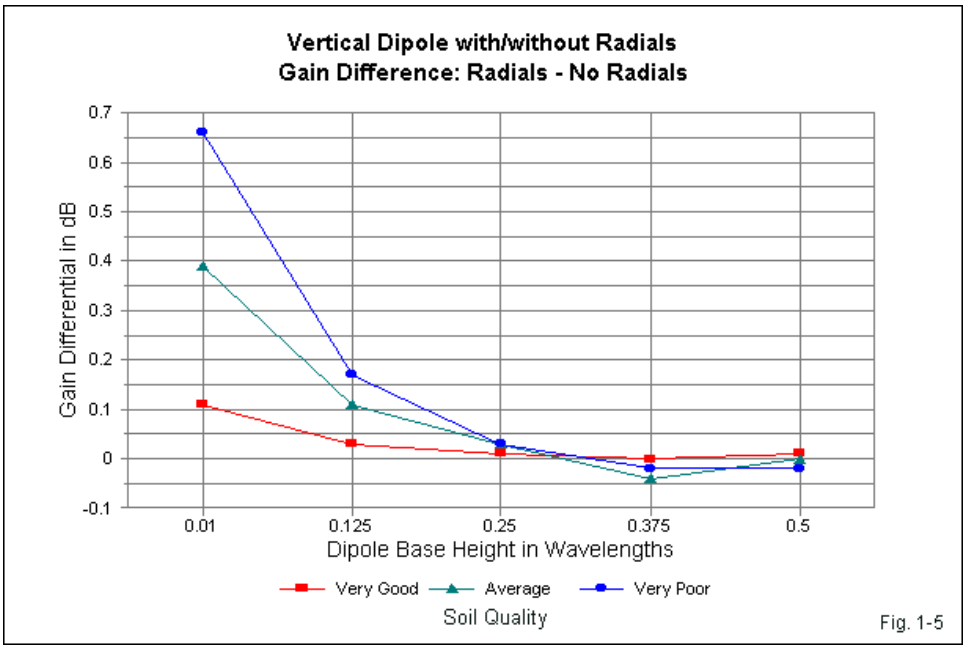

Fig. 1-5

At and above a base height of 0.125-λ, the gain differences decrease to an inconsequential level. Only at the lowest base height do we find some improvement in the vertical dipole gain. However, the gain improvement over average soil is less than 0.4 dB. Over very poor soil, the gain improvement is a little over 0.64 dB. Of course, the increase even at the very low base height will

dwindle as we decrease the number of radials in the field.

The reason for the relatively low improvement in the gain values is that the reflection zone for the far-field radiation pattern extends well beyond the limits of most radial systems. Where the zone begins depends upon the base height of the antenna. Only at the lowest height does the radial system begin to play any kind of role at all in strengthening the reflected rays, and then only where the soil quality falls below the very good level. The major and relatively constant effect of the radial field regardless of the soil quality is in the increase in the reactive component of the feedpoint impedance.

One Ground or Many?

Understanding why a ground radial system as large as 64 radials has so little effect upon the performance of vertical dipoles requires that we digress a moment to sort out various meanings that we may apply to the general term "ground." Chapter 1 of *Ground-Plane Notes* contains a detailed survey of ground concepts. Here we may simply list and summarize them.

1. The circuitry common buss or ground: This sense of a ground may or may not have any relationship to the earth. However, it has an application to earth-related ground in the sense of forming a reference level against which we may measure all voltages, from DC to high-frequency RF.

2. DC and static discharge grounds: Antennas that are isolated from the earth can build up static charges from various sources, including the wind. Many antennas have a provision for discharging static by isolating the RF feedpoint terminals via an RF choke or a high-value resistor. RF goes to and from the feedline, while static charges have a direct path to the earth.

3. Lightning ground: Although we may think of a lightning ground as a long rod that goes into the earth and to which we connect tall metallic structures, the concept is far broader. Relative to all of the equipment, antennas, and other structures at a given communications site, a lightning ground system should establish as low a voltage differential as possible (ideally zero) between each element in the system

and to ground. As well, the system should provide very low impedance paths to ground for any lightning strike or lightning-induced charge.

4. RF ground: A good RF ground at the frequencies of operation does not have the same requirements as a lightning ground system, although the same components may do double duty. The RF ground system establishes the zero-voltage reference system for RF energy from all points including the equipment, feedlines, and the antenna. It does not require deep rods, although deep rods do not detract from the RF ground. However, it may require more rods and more interconnections among them to ensure a zero or near-zero difference in the RF voltage potential between various points in a communications installation.

5. Far-field reflection ground: An antenna's far field (or Fraunhofer zone) begins at a point about twice the square of the antenna's maximum dimension divided by a wavelength at the operating frequency. The near-field region (or Fresnel zone) lies closer to the antenna than the specified limit. As a result, the base height of a vertical dipole has a stronger affect on the feedpoint impedance than on the far-field gain. In virtually all cases, the reflection zone for the far field lies outside the range over which the antenna installer has any control. Far-field reflections are at the mercy of the environment surrounding the antenna at distances from 2 to many wavelengths away.

6. Antenna-completion "ground": A ground-mounted monopole requires a radial system to complete the antenna structure. The radial system may perform other functions as well. However, the radials of the system complete the antenna, as evidenced by the fact that elevated monopoles need at least a few radials. The relationship of the elevated monopole to the vertical dipole becomes evident if we gradually slope the radials downward until they form essentially a single element that is 180° from the upper half of the antenna. In the process, we shall encounter a continuous increase in the feedpoint impedance until it reaches the dipole value.

For a vertical dipole with a center feedpoint, many of the ground concepts that we have distinguished are inapplicable. The most applicable ground is the far-field ground. As we lower the vertical dipole base height, the near field comes

into play by virtue of stronger coupling to the ground. Because the antenna makes no direct connection to the earth, the antenna-completion concept is inapplicable. Like a horizontal dipole, the vertical dipole does not require an RF ground in order to operate correctly. However, a number of the other ground concepts may give us good reason for concern with a vertical dipole. For safety and for quiet operation, we may wish to provide a vertical dipole with both a static discharge path and with a lightning-strike protection path. Hence, obtaining a certain performance level from a vertical dipole may not end the antenna design process.

Shortened Vertical Dipoles

A full-length vertical dipole is normally impractical for most amateur installations. At 1.85 MHz, the resonant vertical dipole using AWG #12 copper wire is about 259' tall, plus whatever base height the installer selects. At 3.55 MHz, the length is 130'. Even at 7.15 MHz, we need about 67' of wire length. As a consequence, many vertical dipole users develop shortened versions.

In broadest terms, we may use two methods to shorten a vertical dipole. One involves the use of one or more inductors. If we place the inductor at the center of the vertical dipole, we believe that we have added a single inductance, simply because we have added one coil. (We may open the coil at the center to provide feedpoint terminals or we might use a small secondary winding to create the feedpoint.) However, we may equally view center loading as adding an inductance to each dipole leg.

The alternative view of center loading gives us a clearer sense of how this form of inductive loading relates to the use of inductors that we place farther away from the feedpoint. We sometimes call this form of inductive loading "mid-element" loading. In one of those misplaced sound bites derived from mobile antenna practices, some claim that mid-element loading is less lossy than center loading. In fact, we would find only small numerical differences in performance, differences that we cannot detect in practice.

The reason why we do not find significant advantages for mid-element

loading derives from one fundamental fact about inductors. They have Q. Most well designed loading coils have a Q between 200 and 400. Q is the ratio of reactance to resistance. Therefore, as the coil's inductance increases, so too do both its reactance and its resistance. For a given short dipole length, if we move the inductors away from the center or feedpoint, the required value of inductance for the coil on each side of center increases. Coils that we place midway between the feedpoint and the dipole end will require nearly twice the inductance of coils places at the feedpoint. The mid-element coils will each be the same size (or just about) as the single center-loading coil. Since Q is constant, the sum of all losses occasioned by loading coils will be double for mid-element loading, although the losses affect only the outer halves of each leg.

In most cases, we find well under 0.1-dB difference in far-field gain between center and mid-element loading. Mid-element loading does yield a somewhat higher feedpoint impedance. However, this factor tends to be more significant to ground-mounted monopoles than to vertical dipoles. In exchange for the higher feedpoint, we double or triple the construction challenges, since we now have three breaks in the dipole, rather than a single break at the feedpoint. Consequently, center inductive loading tends to remain the most common form of vertical dipole shortening.

The alternative to inductive loading bears a very old and misleading name: capacitive hat loading. In this technique, we add wires to both the top and bottom ends of the shortened dipole. The wires are horizontal and symmetrical. As a result, any radiation from the hat wires largely self-cancels, leaving vertically polarized radiation from the central portion of the antenna.

The "capacitive" portion of the name for this shortening technique derives from an old method of calculating hat size. It proved effective for very large-scale hats with many wires in early LF and MF antennas, where the hat simulated a solid circular surface. However, the technique becomes spurious at higher frequencies and with sparser hats. In fact, the only reason that we sometimes use many wires in a hat structure is to shorten the length of the individual wires. As few as two symmetrical wires per dipole end prove to be as effective as a 60-wire hat. **Fig. 1-6** shows the current distribution from a simple T-hatted dipole.

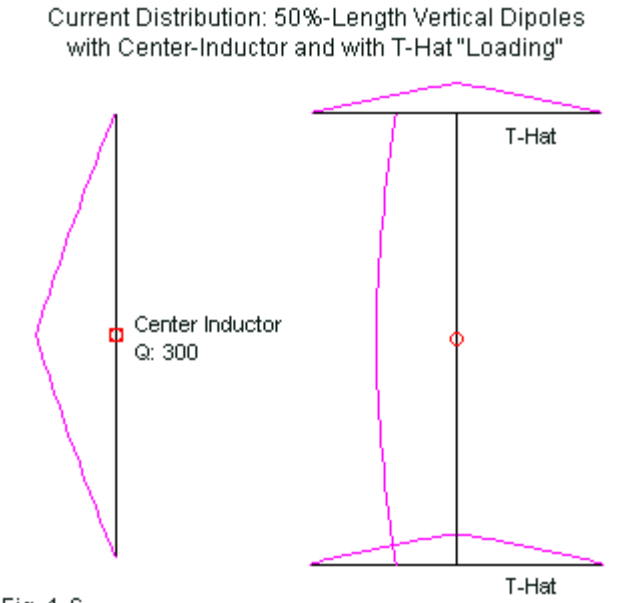

Fig. 1-6

As the right side of the figure shows, the central portion of the shortened vertical dipole operates at full current throughout its length. At the junction with the T-hats, each hat wire receives half the current at that point. The self-canceling current in the horizontal wires are at a much lower level than the current occupied by a center loading inductor. Compare the hat curve with the current distribution on the center-loaded vertical dipole to the left.

Table 1-5 compares the potential performance of two shortened vertical dipoles in free space with the performance of a full-length vertical dipole. The shortened dipoles are 70% and 50% of full length, respectively. The center loading inductors use a Q of 300. The table shows the required inductance values necessary to bring the dipole to resonance. The T-hatted dipoles show the length of each wire in each T assembly. The test frequency is 7.15 MHz, although the general principles involved would apply at any frequency.

Shortened Loaded Vertical Dipole Performance at 7.15 MHz								Table 1-5
Length %	Ld Type	Gain dBi	Pre-Ld R	Pre-Ld X	Ld R	Ld X	Ind uH	Len T
100		2.07	73.24	0.63	73.24	0.63		
70	Induct	1.59	28.39	-498.60	30.05	0.05	11.10	
50	Induct	0.81	13.35	-930.60	16.45	0.04	20.71	
70	T-Hat	1.94			59.88	0.63		5.80
50	T-Hat	1.77			39.33	-0.01		10.96
Notes:	All antennas are free-space models.							
	Length is the percentage of full size AWG #12 copper wire resonant dipole.							
	Induct = inductive center loading with a Q of 300.							
	T-Hat is a 2-wire hat applied to both the top and bottom of the shortened dipole							
	Pre-Ld R and X apply to center loading; the feedpoint impedance without the inductor.							
	Ld R and X are the feedpoint values for the loaded vertical dipole.							
	Ind uH = the required center inductor to resonate the shortened dipole.							
	Len T = hat wire length on each side of the dipole end.							

The relative effectiveness of the two loading methods is clear from two columns: the gain and the feedpoint resistance. Especially at a length of 50% of full size, the T-hatted dipole shows a significant gain advantage over center loading. In addition, the T-hats show a higher feedpoint resistance. Indeed, a dipole length of about 60% full-size would provide a relatively good match to the ubiquitous coaxial cable used in amateur installations.

In contrast, center inductive loading shows both lower gain and lower feedpoint resistance values. The inductive loading entries have two extra columns to show the pre-loading feedpoint impedance. The capacitive reactance at the pre-loaded condition translates into the required inductance of the loading coil. The differential in the resistive component of the feedpoint impedance shows the coil resistance that is a function of its Q of 300.

For most wire vertical dipole installations, T-hatting or even multi-legged hatting is a practical form of vertical dipole shortening if the dipole itself suspends from a rope between two non-conductive support posts. Such installation techniques are not only convenient for hanging wire vertical dipoles, they also provide a support for the heavy feedline that should emerge from the center feedpoint at right angles for as far as practical. The feedline will tend to bend the vertical wire toward its side, but a convenient rope to the other support can easily compensate to keep the dipole vertical.

Center or Base Feeding

Many amateurs find that a center feedpoint is mechanically inconvenient. Therefore, for vertical dipoles with a low base height, they turn to base feeding. In principle, we may feed a ½-λ wire element at any point along its length, from center to either end. **Fig. 1-7** shows a comparison of the current distribution using both center feeding and base feeding. Peak current still occurs at the dipole's center region.

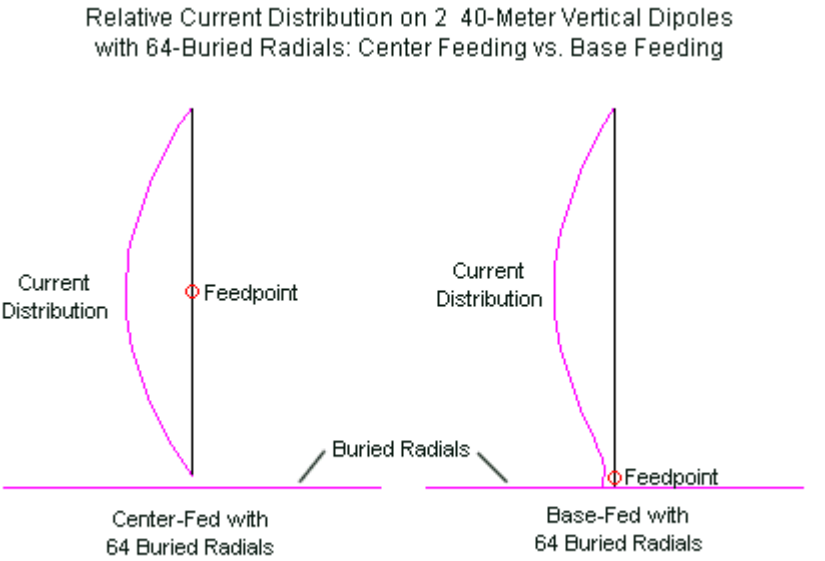

Fig. 1-7

Both curves employ models with a base height of 0.01-λ. Both use a 64-radial system 1' below average ground at 7.15 MHz. The radials are not wholly necessary, as shown earlier, but they do provide a ready reference to ground level in the outline sketches. As well, they show an important feature of base feeding: a connection to ground.

The end of a dipole, with or without a radial system, shows a very high impedance. We sometimes call this “voltage feeding” in contrast to the “current feeding” that occurs at the element center. Essentially, we require a method of transforming the very high end-impedance down to a level that corresponds to the characteristic impedance of a feedline. At or very near to the ground in most amateur installations, the feedline will be a coaxial cable. **Fig. 1-8** outlines two techniques for effecting the match.

Two Generic Methods of Base-Feeding a Vertical Dipole

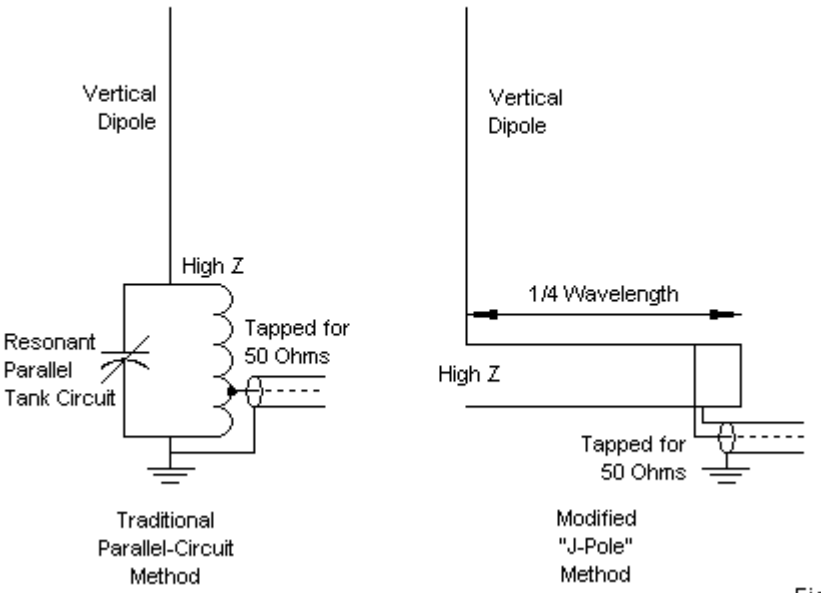

Fig. 1-8

The method on the left goes back to the earliest days of radio. The parallel tank circuit is resonant at the frequency of operation. Technically, one sets it to provide maximum power to the antenna, which may involve more or less capacitance depending on the impedance of the antenna base at the operating

frequency. In some versions of this matching circuit, you may find taps on the turns of the coil at the antenna end to refine the match. You may also find variations at the point shown for a low-impedance tap to the coaxial cable. Some versions use a separate low-impedance secondary or link winding. This winding may also use a series capacitor, depending upon the complexity that the user is willing to have at the base of his or her antenna.

An alternative system appears on the right of **Fig. 1-8**. If we were to stand the total system upright to place the parallel feedline in line with the antenna element, we would have a J-pole antenna. If we placed the system as shown at a right angle to its orientation in the sketch, we would have a horizontal ½-λ end-fed wire (Zepp) antenna with a matching line. In all cases, the parallel transmission line is about ¼-λ long and shorted at the end away from the antenna. Such a line transforms a high impedance at one end to a low impedance at the shorted end. Somewhere close to the shorted end you will find a pair of tapping points that will provide a good match to a 50-Ω cable.

The J-pole, Zepp, and base-fed vertical dipole have something in common. In all three cases, the currents on the matching section at any given point will not be equal in magnitude and opposite in phase. This condition results from the fact that the antenna end impedance will not be identical to the impedance at the free-end of the matching line. Therefore, the matching line will have on it both the normal transmission line current (I_T) and also some radiation current (I_R). Let's take a pair of facing points anywhere along the line, calling one line A and the other B. At these points, the currents will be the sum of radiation and transmission-line current on one line and the difference between the transmission-line and the radiation current on the other.

$$I_A = I_T + I_R \qquad I_B = I_T - I_R$$

It is possible therefore to sort out the currents at any given point along the transmission line.

$$I_T = \frac{I_A + I_B}{2} \qquad I_R = \frac{I_A - I_B}{2}$$

The actual calculation requires consideration of the current phase in each case.

Hence, the actual calculation is lengthier than indicated by the general forms shown in these notes. In most cases, radio amateurs have found a way to reduce calculation time. They simply bypass the calculations and adjust the tapping point until they have a good match for the main feedline.

Base feeding a vertical dipole is as effective as center feeding in terms of antenna performance. Models of center and base fed antenna show gain values that are within about ¼-dB of each other both with and without a ground radial system. However, base-fed systems have a further requirement for greatest efficiency of power transfer to the antenna. There must be a good RF ground between the point at which we establish ground for the feed network and the earth ground for the equipment. A good RF ground system means a near-zero voltage differential between the antenna point and the equipment point at the frequency of operation. Coax braid may not be sufficient to ensure such a condition. Hence, the installer should pay special attention to this aspect of the antenna system as a whole. Of course, the continuity between the antenna and the earth provides a good discharge path for static discharge. However, further attention may be necessary to ensure that the pathway is adequate for good lightning protection as well.

The Bent Base-Fed Vertical Dipole or the Inverted-L

A ½-λ inverted-L is an alternative method of shortening the length of a true vertical. Most such antennas are base fed. Very often, amateurs use them as multi-band antennas and substitute a remote antenna tuner for the tank circuit that we just explored. The degree to which the ½-λ inverted-L emulates a true vertical dipole depends on where we make the bend.

Let's review some of the performance numbers that attach to models of a center-fed vertical dipole over average ground at 7.15 MHz. The maximum gain is between –0.1 and 0.1 dBi with the antenna base close to the ground. The TO angle is 18°, and the feedpoint impedance is 96-97-Ω. If we base feed the same antenna wire, we obtain a high impedance, but the TO angle remains the same. The gain increases to between 0.1 and 0.2 dBi. These numbers form a reference background for a couple of inverted-L modeling experiments.

First, let's bend the ½-λ base-fed vertical about 2/3 of the way toward the top. **Fig. 1-9** shows the current distribution on this version of the L, along with the radiation patterns that result from the bend.

Fig. 1-9

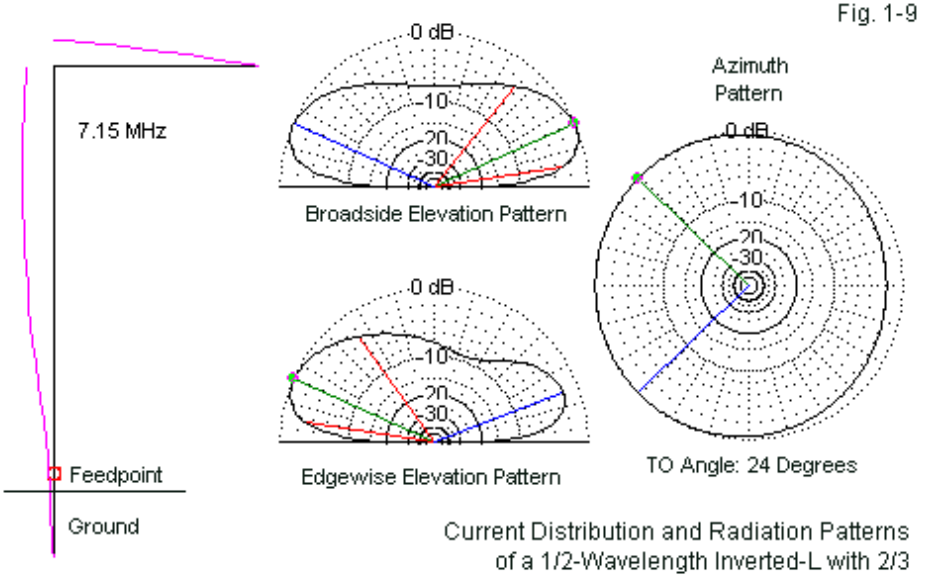

Current Distribution and Radiation Patterns of a 1/2-Wavelength Inverted-L with 2/3 Vertical and 1/3 Horizontal: Base-Fed

Unlike the T-hat vertical dipole, the radiation from the horizontal section of the L does not cancel. Hence, we find a small but definite distortion in the anticipated circular azimuth pattern. Broadside to the horizontal section, the elevation pattern is symmetrical. However, edgewise to the top wire, we find a slightly stronger signal in the direction away from the bent portion of the antenna. Maximum gain of about 0.48 dBi, but that figure applies only within the region on the azimuth pattern between the headings indicated. The average gain is similar to the value for the standard vertical dipole. Because the inverted-L is not as tall as its true-dipole counterpart, the TO angle has risen to about 24°. If the bend permits a usable antenna, then the compromises in performance do not seem excessive.

Next, let's create a second ½-λ inverted-L, but this time bend it only 1/3 of the distance along its total length. Although this height is unnecessarily low at the test frequency of 7.15 MHz, such a procedure might well be necessary on 80 or 160 meters. **Fig. 1-10** shows the outline and current distribution, along with the resulting azimuth and elevation patterns.

Fig. 1-10

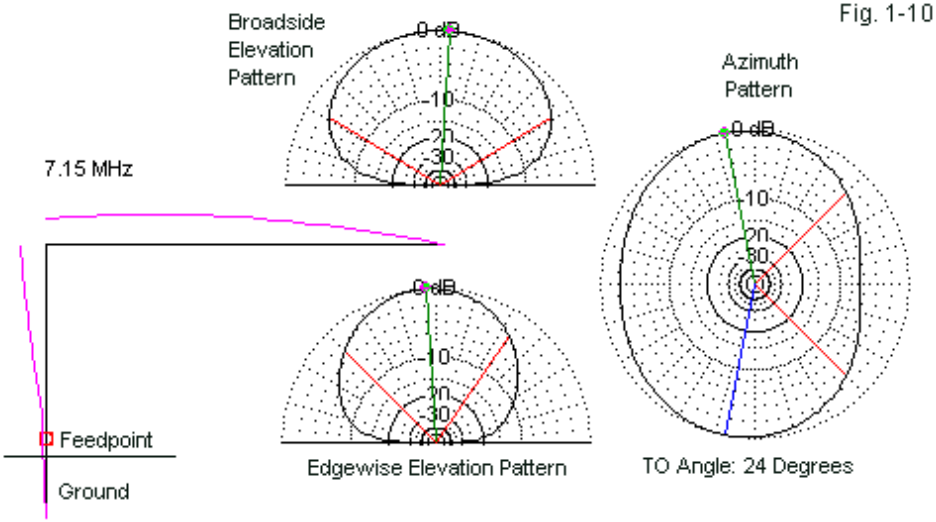

Current Distribution and Radiation Patterns
of a 1/2-Wavelength Inverted-L with 1/3
Vertical and 2/3 Horizontal: Base-Fed

Since the region of highest current occurs in the horizontal section of the antenna, the system acts most like a low horizontal antenna. Maximum gain is nearly straight upward and shows a value of 4.17 dBi. As the elevation patterns reveal, this signal strength is useful mostly for NVIS (near vertical incidence skywave) operation. The azimuth pattern uses an elevation angle of 24° for comparison with the pattern for the inverted-L with a high bend. The maximum gain is about –0.2 dB at this angle and occurs nearly (but not quite) broadside to the horizontal portion of the antenna. In line with the horizontal top wire, the

pattern is considerably weaker.

To obtain performance more coincident with a true vertical dipole, the bend for an inverted-L should be as far as possible above the center of the antenna's overall length. With a suitable ground radial system, one may operate the 7.15-MHz ½-λ inverted-L as a bent monopole on 80 meters. The overall length will be close to ¼-λ. Since our focus is upon ½-λ dipoles and their variants, we shall not pursue that option here.

The Center-Fed Multi-Band Vertical Doublet

If we cut a vertical wire to ½-λ at a certain frequency and place its base end close to the ground, we may operate that antenna over a considerable range of frequencies. The condition for the operation is that we replace the usual coaxial cable with a parallel feedline that runs at right angles to the antenna for as far as possible before reaching a wide-range antenna tuner that provides an impedance match to the low-impedance transmitting and receiving equipment.

Multi-band Performance of a Center-Fed Vertical Doublet						Table 1-6
Len wl	Base Ht	Gain dBi	TO deg	Feed R	Feed X	
1.5	0.3	4.23	62	95.41	-50.48	
1.25	0.25	4.36	9	210.6	-924.9	
1	0.2	2.84	11	4329	-1018	
0.75	0.15	1.4	13	381.3	933.1	
0.5	0.1	0.53	16	76.4	-0.54	
0.375	0.075	0.08	18	41.21	-399.8	
Notes:	Vertical doublet is AWG #12 copper wire above average ground.					
	Len wl = doublet length in wavelengths at the operating frequency.					
	Base Ht = distance above ground of the boublet base in wl.					
	Gain dBi = maximum gain at TO angle					
	TO deg = TO angle in degrees					
	Feed R/Feed X = feedpoint impedance in Ohms					

Table 1-6 provides some representative data for a modeling exercise over average ground. Each line entry shows a different length for the antenna,

although the physical length remains constant. Hence, the base height also changes for each entry. The remaining data show the gain, TO angle, and feedpoint impedance for each frequency. Immediately, one limitation becomes apparent. As we lower the operating frequency and reduce the electrical length of the vertical antenna, the feedpoint resistance decreases while the capacitive reactance increases. A length of about 0.375-λ is roughly a limit beyond which the losses even on a parallel transmission line become excessive. In addition, the feedpoint impedance is not the impedance that will appear at the antenna tuner terminals. That impedance depends on the impedance transformation that results from the combination of the feedpoint impedance, the line's characteristic impedance, and the electrical length of the line.

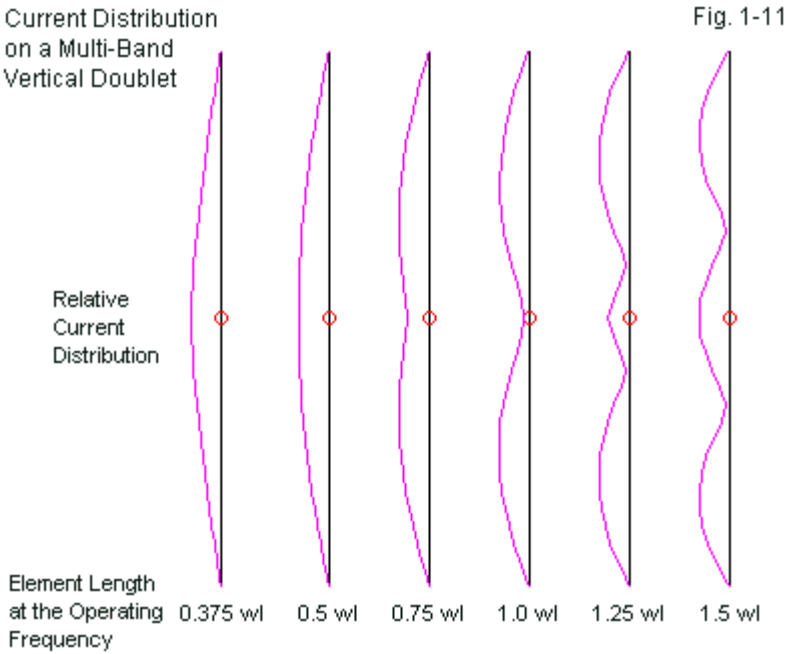

Fig. 1-11 shows the current distribution along the antenna at each of the

frequencies listed in the table. These distribution curves accompany a rising gain and falling TO angle until we pass an electrical length of 1.25-λ. At a length of 1.5-λ, the antenna behavior changes radically, as shown in the elevation plots in **Fig. 1-12**. At this length, the low-angle gain is back down to about 1 dBi.

Fig. 1-12

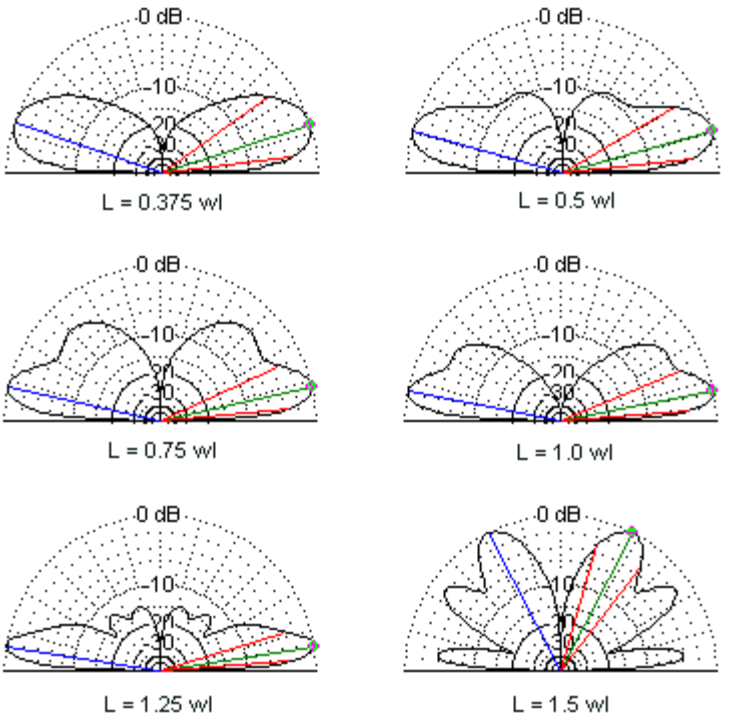

Elevation Patterns for a Multi-Band Vertical Doublet
as the Electrical Length Increases with the Operating Frequency

The vertical doublet is thus capable of effective use from at least 0.5-λ

through 1.25-λ. Less efficient operation may be possible for electrical lengths down to 0.375-λ. In practical terms, a 44' wire, which is about 1.25-λ on 10 meters, will operate effectively down through at least 20 meters and possibly at 30 meters. Likewise, an 88' doublet will handle 20 through 60 meters, with possible operation on 80 meters.

We refer to the multi-band center-fed antenna as a doublet because on many operating frequencies, we are not operating a dipole. Technically, a dipole has only one peak-to-minimum current transition each side of center, with the peak current (and minimum voltage) exactly at the element center point. As shown in the current distribution curves in **Fig. 1-11**, when the wire is electrically longer than 0.5-λ, we encounter multiple current peaks. Hence, the better name for the multi-band wire is the more generic term "doublet."

Conclusion

Although we have examined many facets of the vertical dipole and its variations, these notes are largely a review of what is well known about the antenna. The information forms a background for following steps through the family tree that leads eventually to the SCV members. Indeed, we have not yet reached the parents of the SCV, but only a fundamental grandparent. All SCVs are variations on the theme of multiple vertical dipoles. Therefore, multiple vertical dipoles will be the next stop on our journey.

2. Multiple Vertical Dipoles

The immediate parents of all forms of single-feedpoint SCV antennas are a pair of vertical dipoles fed in phase. Rather than simply model this one pair of antennas, we shall survey a host of different antennas involving 2 or 3 vertical dipoles, including both phase-fed and parasitic arrays. Parasitic arrays will become part of our standard coverage of SCVs, so that portion of the exercise will not be idle by any means.

Since we shall just be sampling various forms of multiple-dipole arrays, most of our work will be at 7.15 MHz. Moreover, we shall restrict ourselves to vertical dipoles with a base height of 4' above average ground. When we perform a small bit of work over various soils and various frequencies, we shall keep the base height of each vertical dipole at 4'. When we examine the performance of the shortened dipoles (to 70% of full length), we shall use the feedpoint or center height of the full-size vertical dipole as our marker, since that height will equalize the region of highest current for both full-size and shortened dipoles. In the realm of shortened dipoles, we shall skip the inefficient center-loaded versions and use only T-hatted models.

Before we complete this chapter, we shall not only have seen optimized dipole pairs fed in phase, and 2-element vertical dipole parasitic beams, but as well, we shall examine some dipole triangles and in-phase-fed pairs of parasitic vertical dipole beams. The final example will be an odd sort of parasitic vertical dipole array consisting of a single driver with 6 sloping pseudo-guy-wire parasitic elements.

Our first step is to review the performance of a single vertical dipole composed—like all others in these notes—of AWG #12 copper wire. In the new configuration, the dipole extends from 4' to 71' above average ground. **Fig. 2-1** shows the general outline, the current distribution, and the elevation and azimuth patterns. Maximum gain is 0.01 dBi, with a TO angle of 18°. The feedpoint impedance is 90.7 – 0.3 Ω. These numbers form a reference against which we

may compare all of the other arrays to come. Although the gain is not high, the omni-directional pattern that shows significant radiation (and receiving sensitivity) only at low elevation angles has drawn this antenna type into very widespread use.

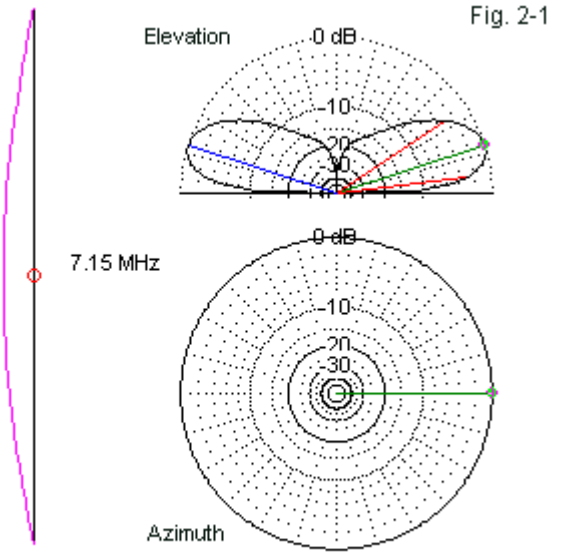

Reference Patterns for a Single Vertical Dipole

Pairs of Vertical Dipoles Fed Out-of-Phase with Each Other

One common way to use multiple vertical dipoles (or monopoles) is to create a directional pattern along the line formed by the elements. The general scheme appears in **Fig. 2-2**, with a general elevation pattern overlaid on the array outline at the left. In order to achieve the overlaid pattern, which also appears in the central portion of the figure, we must provide each element with the correct current magnitude and phase angle. Variations in either category will not achieve the cardioidal pattern with the deep rear inset or null. For the simple case in the

exercise, the elements are exactly ¼-λ apart. Since we can feed the model with separate feedpoint current values, we may use equal current magnitude, but set the phase angle for one current value 90° to the other. The rear element must be +90° relative to the forward element (or the forward element must be -90° relative to the rear one). The patterns in the center of the figure reflect this model set-up.

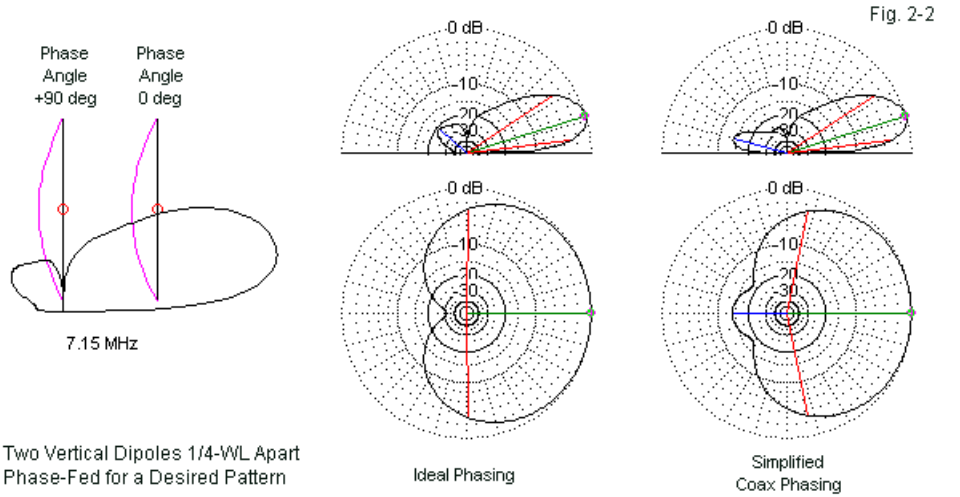

Unfortunately, many radio amateurs try to simplify the phasing task by running a single quarter-wavelength of feedline between the two antennas. When they allow for the line's velocity factor, they discover that the cable will not reach. Then they simply add a further ½-λ section. Still the pattern fails to achieve the desired goal. The right side of **Fig. 2-2** shows the best patterns achieved by this technique using a variety of transmission lines having available characteristic impedance values from 35 Ω up to 125 Ω.

Table 2-1 summarizes the results of this somewhat misguided exercise. For reference, it includes the single dipole data, the ideally phased pair of elements, and the simplified attempt to achieve proper phasing with a single feedline between the elements. For some purposes, the resulting patterns may be

acceptable, but they are all far from the ideal. However, we are defining what is ideal by reference to a certain pattern shape—the cardioidal pattern. Note that all of the approximations do manage a bit more gain at the cost of a few degrees of beamwidth. Perfect phasing does not mean maximum forward gain.

1/4-Wavelength-Separated Vertical Dipoles Fed 90-Degrees Out of Phase						
Type	Gain dBi	TO Deg	F-B dB	BW Deg	Feed R	Feed X
Ideal	3.07	17	31.43	177.4	46.7	-39.2
					131.9	38.8
Casual Single Coaxial Cables, 90 Degrees Long						
35 Ohm	3.75	17	12.94	147.2	7.1	-3.5
50 Ohm	3.61	17	14.34	151.4	12.1	-5.8
70 Ohm	3.51	17	14.06	156.4	18.9	-8.7
93 Ohm	3.30	17	12.32	161.8	26.3	-11.3
125 Ohm	3.01	17	10.05	168.8	35.3	-13.4
Reference: Single Vertical Dipole Data						
	0.01	18			90.7	-0.3
Notes:	Ideal feed uses 2 separate source at a 90-degree phase angle.					
	Casual feeds use a single trasmission line between feedpoints.					
	Gain dBi = maximum gain at TO angle					
	TO deg = TO angle in degrees					
	F-B dB = 180-degree front-to-back ratio in dB					
	BW Deg = horizontal beamwidth in degrees.					
	Feed R/Feed X = feedpoint impedance in Ohms					
	Frequency: 7.15 MHz					
	All vertical dipoles use a base height of 4', are 67' long, and use					
	AWG #12 copper wire over average soil.					
						Table 2-1

Note that in the ideal case with separate feedpoints, we obtain very different feedpoint impedance values for the two dipoles. The elements exhibit considerable mutual coupling. As a consequence, a transmission line for which either element is a load will not normally show the required current magnitude and phase angle at its end when fed in parallel with the other element if the line is an odd multiple of ¼-λ. In short, current and impedance do not change values at

the same rate if the line is not matched to the load.

Properly phasing 2 or more elements requires a considerable amount of calculation and planning to arrive at conditions that are close to the ideal. Chapter 8 of recent editions of *The ARRL Antenna Book* contains a wealth of information on the subject. Even more comprehensive is Chapter 11 of ON4UN's *Low-Band DXing*. Our foray into phased arrays only notes that such arrays are feasible. Since the arrays do not play a significant role with respect to SCV antennas, we shall bypass further discussion.

In-Phase Fed Vertical Dipoles

If we do not wish the pattern to be inline with the dipoles, we may simplify the matter of feeding. We may feed each vertical dipole—either at the center or the base—in phase. **Fig. 2-3** shows in outline form how we can easily achieve in-phase feeding. We need only use exactly equal lengths of transmission line between the individual feedpoints and join them in parallel at the center. The line length and the degree of mismatch between the line and the feedpoint impedances will determine the transformation of current magnitude and phase. However, since both lines are identical, each element will be in phase with the other one.

Fig. 2-3

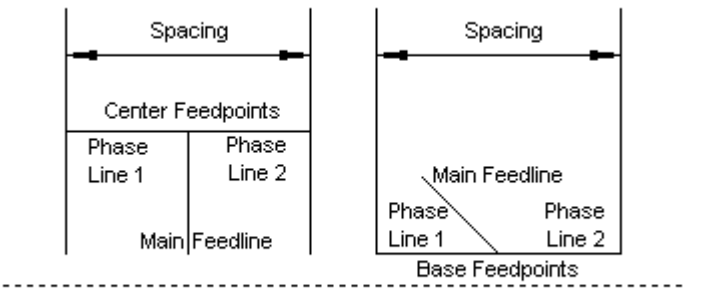

Two Methods of Feeding a Pair of Vertical Dipoles in Phase

The pattern that we achieve by this technique is a bi-directional "figure 8" (usually, more like a well-formed peanut), as shown in **Fig. 2-4**. The shape of the pattern is similar to those that we associate with SCV antennas. The similarity is more than accidental, since the in-phase-fed dipole pair is the direct parent of all SCV antennas.

Fig. 2-4

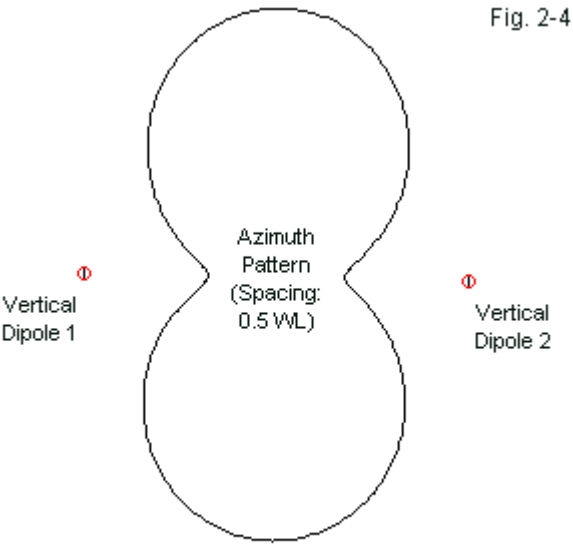

Relationship of the Vertical Dipoles Fed In Phase
to the Resulting Azimuth Pattern

The gain, beamwidth, and feedpoint impedance of the individual dipole center feedpoints varies according to the space between the dipoles. **Table 2-2** shows the effects of spacing on all of these factors at 7.15 MHz using our standardized dipole with a base height of 4' above average earth. The absence of beamwidth values in the first two entries only indicates that the azimuth pattern does not show a 3-dB gain reduction relative to maximum gain. Although somewhat oval, these patterns are too circular to exhibit a –3-dB beamwidth.

2 Vertical Dipoles Fed In Phase with Various Spacing Values					
Sp WL	Gain dBi	TO Deg	BW Deg	Feed R	Feed X
Ideal Feed: Separate Sources			Feed values are for each source.		
0.125	0.37	17		165.8	-17.2
0.25	1.35	17		128.3	-42.8
0.375	2.8	17	88.4	91.7	-44.4
0.5	4.26	17	62.9	66.6	-27.4
0.625	4.81	17	49.4	59.9	-2.6
Practical Feed: 2 Equal Lengths of 70-Ohm VF-1 Feedline					
Spacing = 0.5 WL		Feed values is for a single source.			
Len WL	Gain dBi	TO Deg	BW Deg	Feed R	Feed X
0.3	4.26	17	62.9	40.5	14.2
0.4	4.26	17	62.9	51.4	-5.1
0.5	4.26	17	62.9	33.3	-13.7
Notes:	SP WL = spacing between dipoles in wavelengths.				
	Len WL = length of each feedline leg in wavelengths.				
	Gain dBi = maximum gain at TO angle				
	TO deg = TO angle in degrees				
	BW Deg = horizontal beamwidth in degrees.				
	Feed R/Feed X = feedpoint impedance in Ohms				
	Frequency: 7.15 MHz				
	All vertical dipoles use a base height of 4', are 67'				
	long, and use AWG #12 copper wire over average soil.				
					Table 2-2

The table also illustrates the fact that if we use exactly equal line lengths from each dipole feedpoint to a center junction, we do not change the behavior of the array relative to the idealized case. All that we change is the resulting feedline impedance at the junction. The models contain no feedline losses, but these are ordinarily close to negligible in the lower HF and upper MF regions, even with standard coaxial cables. If a single feedline is a hallmark of an SCV, then the in-phase-fed dipole pair is our first true SCV.

In conjunction with **Table 2-2**, also examine the gallery of azimuth patterns in **Fig. 2-5**. Assume that the dipoles are arranged in a vertical line at the center of

each pattern. Remember that far-field patterns exist at an indefinitely large distance from the antenna, so any physical representation of the antenna itself would be too small to see.

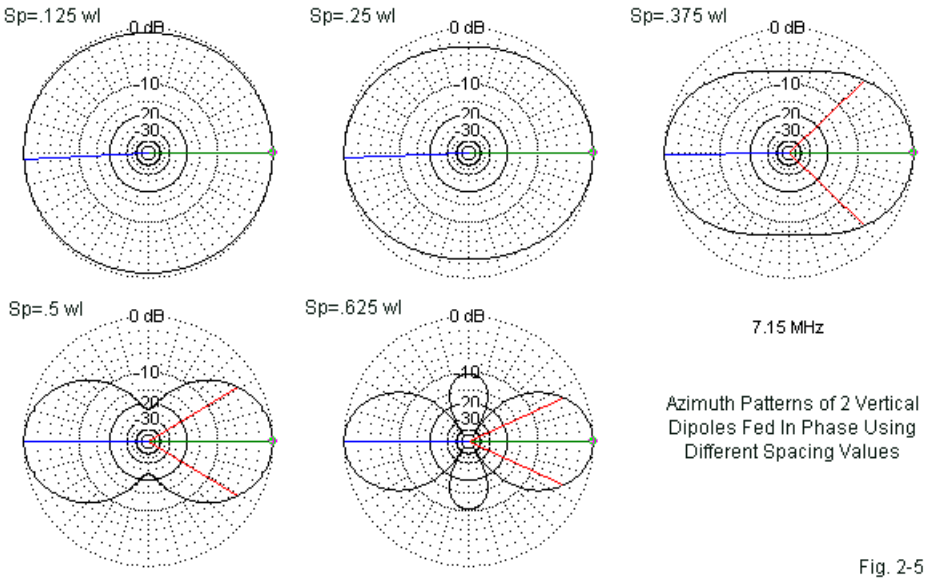

Azimuth Patterns of 2 Vertical Dipoles Fed In Phase Using Different Spacing Values

Fig. 2-5

Each pattern is normalized, that is, its maximum gain coincides with the outer circle of the polar plot. In fact, the patterns increase in maximum gain as we increase the spacing. In the table, we may note the rapid change in gain as we increase the spacing until we reach the 0.5-λ distance. Further increases in gain are small as the pattern develops sidelobes that are edgewise to or in line with the dipoles, as is evident in the pattern for a spacing of 0.625-λ. Eventually, the sidelobes grow to equal the broadside lobes. At this point, the pattern loses its bi-directional character. As a consequence, ½-λ spacing between vertical dipoles (or monopoles) often bears the label “ideal” when it comes to evaluating in-phase array performance, as the best compromise between gain and pattern cleanliness.

We should not overlook that fact that the exact performance numbers will vary somewhat with both frequency and soil quality, just as they did with simple vertical dipoles. **Table 2-3** traces in-phase-fed pairs of dipoles spaced 0.5-λ apart for 1.85, 3.55, and 7.15 MHz using very good, average, and very poor soil. The table contains the raw data reports for the models at each frequency and soil type, plus 2 supplementary records.

If we examine the range of gain values across the soil types at each test frequency, we find a somewhat normal spread. At 40 meters, the gain difference between very good and very poor soil is only 2.6 dB. The range increases to about 4.3 dB on 80 meters and climbs to 5.3 dB on 160 meters. These are spreads for which the study of single vertical dipoles in the preceding chapter has prepared us.

Now let's look at the data from the opposite direction, examining for each soil type the range of gain from 1.85 to 7.15 MHz. Over very good soil, the gain on 160 meters is about 1.6 dB greater than at 7.15 MHz. Over average soil, the 1.85-MHz value is about 1.1 dB higher than the 7.15-MHz value. However, over very poor soil, we find the opposite curve. The gain actually increases with rising frequency, by about 1.1 dB.

Fig. 2-6 present a gallery of elevation patterns for the three test frequencies. Each section of the graphic overlays patterns for the 3 soil types. At all three test frequencies, the difference between the maximum gain value over very good soil and the value over average soil is approximately the same (between 2.1 and 2.7 dB). The most significant difference in the progression of patterns is between maximum gain at 3.55 and at 7.15 MHz. As we raise the test frequency in approximate 2:1 ratios, the gain differential shrinks by about 1 dB per step. At 160 meters, the difference is over 2.5 dB, while at 40 meters, the difference is down to about 0.5 dB.

The small set of tests suggests that the changes we find in performance when we change frequency and soil type are regular, but not at all simple. The lesson is the same that we learned in the last chapter: know both the soil quality in your area and the behavior of your antenna over that soil.

2 Vertical Dipoles Spaced 1/2-Wavelength Using Various Frequencies and Various Soil Types						
Freq MHz	Soil	Gain dBi	TO Deg	BW Deg	Feed R	Feed X
	VG	7.93	12	61.3	75.0	-22.4
1.85	Ave	5.35	16	62.6	74.4	-22.5
	VP	2.63	19	63.6	73.1	-23.5
	VG	7.22	13	61.6	72.1	-25.7
3.55	Ave	4.50	17	63.0	71.2	-25.5
	VP	2.90	20	63.2	69.1	-26.1
	VG	6.31	14	61.9	67.7	-28.3
7.15	Ave	4.26	17	62.9	66.6	-27.4
	VP	3.70	20	64.2	64.8	-26.3
Gain Range by Bands (from 1.85 to 7.15 MHz) over Soil Range						
	Soil	Delta Gn				
	VP	-1.62				
	VG	-1.09				
	Ave	1.07				
Gain Range by Soil Type (from VG to VP) over Frequency Range						
Freq MHz		Delta Gn				
1.85		5.30				
3.55		4.32				
7.15		2.61				
Notes:						
	Freq MHz = frequency in MHz					
	Soil = VG = very good, Ave = average, VP = very poor					
	Gain dBi = maximum gain at TO angle					
	TO deg = TO angle in degrees					
	BW Deg = horizontal beamwidth in degrees.					
	Feed R/Feed X = feedpoint impedance in Ohms					
	Feed values are for each feedpoint.					
	All vertical dipoles use a base height of 4', and					
	use AWG #12 copper wire.					
						Table 2-3

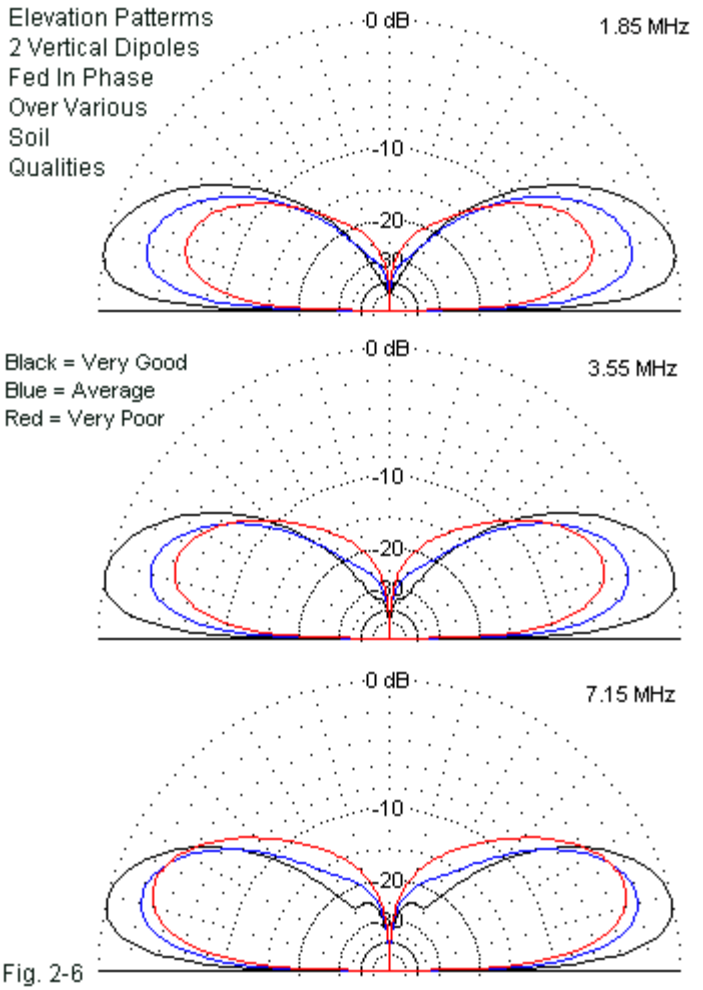

Fig. 2-6

Three Vertical Dipoles Fed In Phase

Let's add one more dipole to the line, also spaced 0.5-λ from the adjacent

dipole. The array that we obtain looks like the outline in **Fig. 2-7**. The graphic also contains the elevation and azimuth pattern for the 3-dipole array with a base height of 4' at 7.15 MHz.

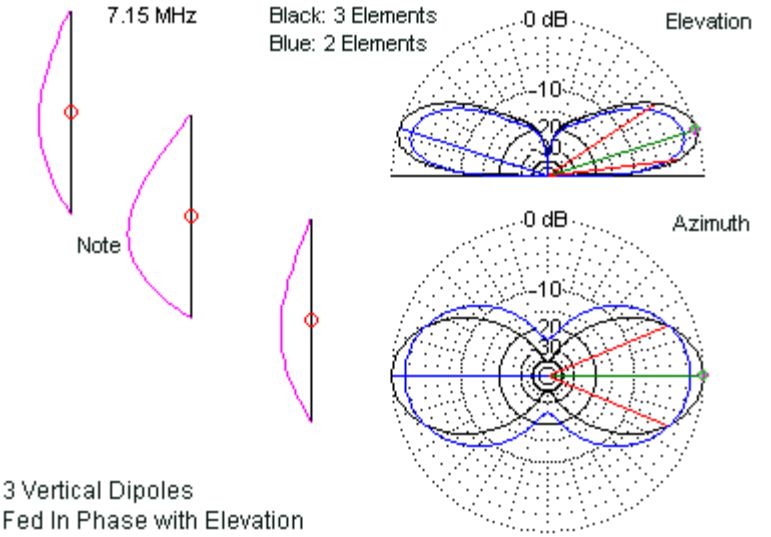

Fig. 2-7

From 3 dipoles fed in phase, we obtain more gain and a narrower beamwidth relative to a 2-dipole array. The plots overlay the patterns for these two arrays for an easy comparison. More exacting data appear in **Table 2-4**. In fact, the table provides data for 1, 2, and 3 dipoles for ready comparison. The sharp rise in gain occurs in the move from 1 to 2 dipoles, as the azimuth pattern changes from a circle to a peanut. We gain only about 1.5 dB additional bi-directional gain from adding a third dipole, with about a 20° reduction in the beamwidth in each direction. Since wire arrays generally have fixed positions, we must always measure increases in gain against reductions in horizontal coverage. Before we close this chapter, we shall examine some rudimentary ways to overcome the gaps in horizonal coverage.

Performance of 1 to 3 Vertical Dipoles with 1/2-Wavelength					
Spacing and Fed In Phase					
Ideal Feed: Separate Sources			Feed values are for each source.		
No Ele	Gain dBi	TO Deg	BW Deg	Feed R	Feed X
1	0.01	18		90.7	0.3
2	4.26	17	62.9	66.6	-27.4
3	5.72	17	44.8	55.5	-38.4
				66.8	-27.4
Notes:					
	Frequency: 7.15 MHz				
	All vertical dipoles use a base height of 4', are 67'				
	long, and use AWG #12 copper wire over average soil.				
	Gain dBi = maximum gain at TO angle				
	TO deg = TO angle in degrees				
	BW Deg = horizontal beamwidth in degrees.				
	Feed R/Feed X = feedpoint impedance in Ohms				
	Feed values are for each feedpoint for 2 elements.				
	For 3 elements, first entry is for end dipoles, second				
	entry is for the center dipole.				
					Table 2-4

We shall have occasion to refer to the sample gain values when we examine SCV antennas, since some of the versions will have three vertical legs or their equivalent. For the moment, the key element to note about the 3-dipole array is the current distribution curves in **Fig. 2-7**. Also note in the table that we have different impedance values for the end dipoles than for the center dipole. (I shall add a reminder here that all of the models use the element center as the feedpoint.) The difference in the curves and the impedance values results from the fact that a line of dipoles requires a binomial distribution of current at the feedpoints for optimal operation. All three source currents have a phase angle of 0° (or any other values, so along as all three are the same). However, the magnitude of the currents at the feedpoints of the end dipoles is 1, while the magnitude of the current on the center dipole is 2. (A 4-dipole line would use magnitude values of 1-3-3-1, while a 5-dipole line would use 1-4-6-4-1, etc.)

One immediate and practical consequence of this outcome is that we can no longer use the simple feed system that we employed with a 2-dipole system. For optimal operation, we must turn to networks and other means of ensuring that each dipole feedpoint receives the correct relative current magnitude, while maintaining the same phase angle at all three feedpoints. Therefore, we find many commercial applications of 3-dipole (and 3-monopole) arrays, but few amateur applications. Nevertheless, the 3-dipole phased array remains the parent of such antennas as the double delta, the double diamond, the double rectangle, and the bobtail curtain.

Expectations of Shortened Vertical Dipole Arrays

In Chapter 1, we learned that we may shorten a vertical dipole at least to 70% of full length without serious impact to antenna gain under the condition that we do not use inductive loading. Instead, the preferred method of compensating for the shorter length and of bringing the antenna back to resonance is the hat structure. The hat does not need to be complex so long as it is symmetrical. Hence, a T-hat is as effective as a disk, although the legs of the T will be considerably longer than the radius of a solid or screen disk hat.

We may use shortened verticals in phased arrays. The only difference will appear in the individual feedpoint impedance values. For nearly equal performance, we need to maintain two features of the full-length vertical dipole in the same in-phase-fed configuration. First, we must maintain the spacing. A common tempting thought among builders of shortened-element antennas of all sorts is the idea that when we shorten the element length, we also shorten the spacing between elements. Resist this temptation at all costs. An in-phase-fed dual-dipole array requires 0.5-λ spacing for optimal performance regardless of the dipole lengths.

The second feature to maintain is the height of the high current region of the antenna. With ground-mounted monopoles, this feature is automatic, since the high current occurs just above ground level. However, when we use a vertical dipole, the high current region is elevated, with a center at the feedpoint (or the virtual feedpoint, if we base feed the element). When we use a shortened vertical

dipole, its center should be at the same height as the center of a full-length vertical dipole for equivalent performance.

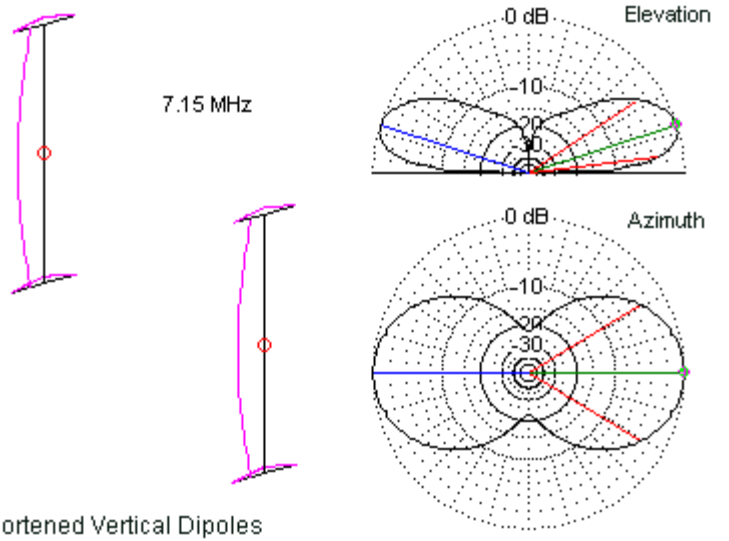

2 Shortened Vertical Dipoles
Fed in Phase: Current Distribution
and Elevation and Azimuth Patterns

Fig. 2-8

Fig. 2-8 shows the outline of a pair of T-hat 70% vertical dipoles for 7.15 MHz using AWG #12 copper wire and spaced 0.5-λ apart. The legs are 6.3' each, but the base is 14.1' above ground to place the center at the same height as the corresponding full-length dipole with a base height of 4'. If we compare the azimuth pattern with the 0.5-λ pattern in **Fig. 2-5**, we should find virtually no difference. **Table 2-5** provides data on modeled shortened 70% vertical dipoles with T-hats for 160, 80, and 40 meters over average soil. The table includes information for both 1 and 2 dipoles. In each case, the shortened dipole has a center point at the same height as its full-length counterpart. You may usefully compare this data with the data in **Table 2-3**. In fact, you may uncover a surprise or two.

Performance of Single and In-Phase Fed Pairs of 70% Dipoles with T-Hats						
at Various Frequencies over Average Soil						
Fr MHz	No Ele	Gain dBi	TO Deg	BW Deg	Feed R	Feed X
1.85	1	1.13	16		79.5	0.5
	2	5.40	16	62.5	58.6	-24.7
3.55	1	0.31	17		76.3	-0.2
	2	4.57	17	62.9	56.3	-23.9
7.15	1	0.09	18		71.7	1.9
	2	4.32	18	63.3	53.3	-20.8
Notes:	All vertical dipoles use a base height of 4', and					
	use AWG #12 copper wire.					
	Dimensions:		Fr MHz	Len ft	T-leg ft	
			1.85	181.03	23.8	
			3.55	94.34	12.5	
			7.15	46.84	6.3	
	Fr MHz = frequency in MHz					
	Gain dBi = maximum gain at TO angle					
	TO deg = TO angle in degrees					
	BW Deg = horizontal beamwidth in degrees.					
	Feed R/Feed X = feedpoint impedance in Ohms					
	Feed values are for each feedpoint.					
	Len ft = length of vertical section					
	T-leg ft = length of each T-hat leg; x2 for total width.					
						Table 2-5

At all three frequencies, the shortened dual-dipole array shows a slightly higher gain value than the corresponding full-length array. The difference is far too small to be operationally significant, but it is numerically interesting for what it reminds us about concerning vertical dipoles that are close to ground. The shortened vertical dipole has less gain by a small amount than the full-length dipole. However, the full-length dipole approaches the ground surface more closely—just about 10' more closely at 40 meters. As a consequence, the full-length dipoles show slightly higher ground losses than their shorter brethren. The two factors balance out in this series of simulations so that the shorter and the longer systems have roughly equal performance. If we shorten the T-hat dipoles

further, the reduction in gain will gradually outweigh the benefits of a higher base level.

Whatever version of a dual-dipole in-phase fed array that we choose, it lies at the heart of all of its SCV offspring. However, we shall eventually convert some SCVs into beams. Therefore, we need some basic familiarity with an alternative way to use multiple vertical dipoles.

Parasitic Vertical Dipoles (Vertical Yagis)

We may create a two element driver-reflector vertical Yagi or parasitic beam using vertical dipole elements as easily as we do the same job with 2 horizontal elements. However, several features change in the process. To examine what is the same and what differs, let's examine a few AWG #12 copper wire beams for 40 meters. The outline and pattern for our array appears in **Fig. 2-9**. The figure also includes a modeled SWR graph for the antenna.

One factor that does not change is the SWR curve. It does not cover the entire 40-meter band because we are using very thin elements (as measured in fractions of a wavelength) and because the beam has been designed for the maximum front-to-back ratio at the test frequency (7.15 MHz). As is the case with any driver-reflector Yagi, the gain will be highest at the low end of the band and lowest at the upper end. The front-to-back ratio will decrease as we move away from the design frequency. Nevertheless, the beam is a good and useful performer.

The parasitic beam does not achieve the deep rear null of the ideal phased array. However, it is fully competitive with any of the casually phased beams that we encountered at the beginning of this chapter. Those who are familiar only with horizontally oriented Yagi may find the azimuth pattern in **Fig. 2-9** somewhat surprising. The two orientations yield different patterns because the horizontal Yagi shows the E-plane pattern as the azimuth plot. When we change the orientation to vertical, the H-plane becomes the azimuth pattern. For the same element configuration, we obtain lower forward gain, but an extremely wide beamwidth. That fact offers us both limitations and opportunities.

Fig. 2-9

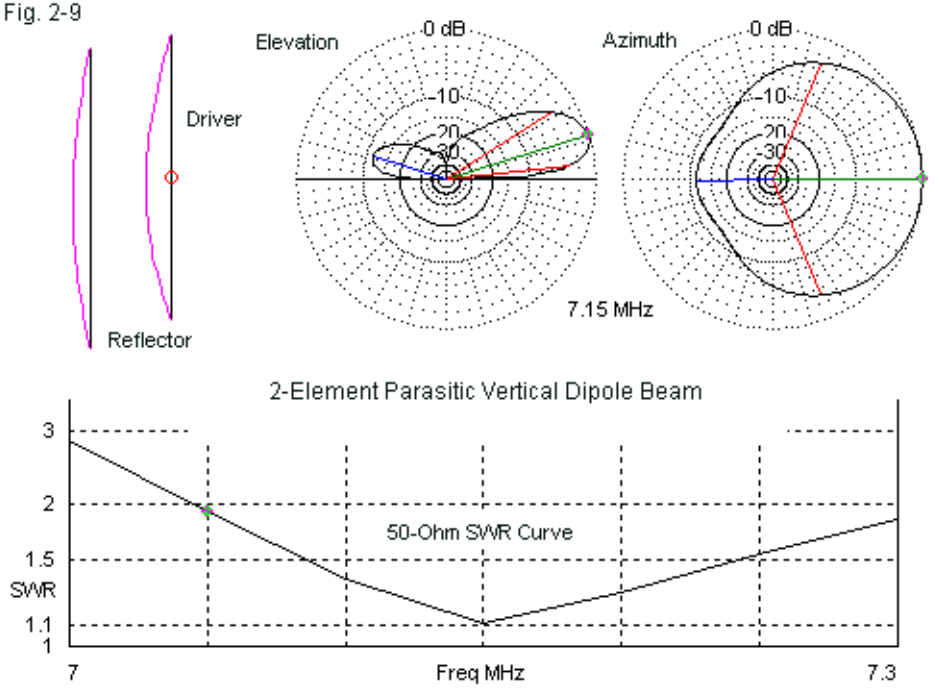

Since the array derives its forward gain or directivity from the mutual coupling between the elements without the benefit of a direct feed to the reflector element, the elements require different lengths. In the models, I retained the element center point. Hence, the driver's natural need to be a bit shorter than an independent vertical dipole resulted in shortening at both ends of the element. The longer reflector is not only taller than an independent vertical dipole; it also comes a bit closer to the ground. The dimensions appear in **Table 2-6**, along with the dimensions and performance data for several versions of the same 2-element parasitic beam.

One variation on the basic 2-element Yagi is to make both elements the same length, namely the length of the driver element. At the center of the

reflector, we may introduce an inductive load to electrically lengthen the element to the former level, usually indicated by achieving the same front-to-back ratio. The table indicates two loading conditions. The first uses a lossless inductor that yields about j75-Ω of reactance at the test frequency. The loaded reflector actually performs better (but not to a noticeable degree) than the full size reflector. Since the inductance (about 1.67 μH) is small, assigning it a Q of 300 shows only a tiny drop in performance.

Performance of 7.15-MHz Driver-Reflector Vertical-Dipole Parasitic Beams						
Type	Gain dBi	TO Deg	F-B dB	BW Deg	Feed R	Feed X
Std	3.63	17	11.44	135.8	50.8	2.1
Ld Qinf	3.72	17	11.77	134.8	50.3	3.2
Ld Q300	3.70	17	11.7	134.8	50.3	3.1
Ld TL	3.72	17	11.77	134.8	50.3	3.2
Triangle	4.02	17	15.15	129.6	63.8	12.8
Notes:	All vertical dipole use AWG #12 copper wire.					
	All drivers extend from 4.75 to 70.25 feet above ground					
	Std reflector extends from 3.5 to 72.5 feet above ground.					
	All loaded reflector (including triangle) are driver length.					
	Spacing (except triangle) is 18.5 feet from driver to reflector.					
	Triangle is 24.25 feet on each side					
	Ld inductor is 1.67 uH (X = j75 Ohms).					
	Ld TL is 21.5 feet of 50-Ohm, VF-1 transmisson line.					
	Triangle Reflector TLs are 22' of 70-Ohm, VF-1 transmission line.					
	Gain dBi = maximum gain at TO angle					
	TO deg = TO angle in degrees					
	BW Deg = horizontal beamwidth in degrees.					
	Feed R/Feed X = feedpoint impedance in Ohms					
						Table 2-6

We may replace the inductor with a shorted transmission-line stub. Because the feedpoint impedance of the 2-element array is just about 50 Ω, we may use 50-Ω coax for our stub. A length of about 21.5' will yield the required inductive reactance with lower losses than the Q-300 inductor. (The actual stub length will be the assigned value times the line's velocity factor.)

The use of a shorted stub offers us the opportunity to convert our beam into a reversible Yagi. We may run the stubs that we attach to each element to a central switching position, as suggested in **Fig. 2-10**. In one position, the switches short the stub of the designated reflector. The same switches route the other stub—unshorted—to the main feedline so that the stub becomes simply a small addition to the overall driver feedline. Flipping the switches reverses the process and the direction of the beam. The condition of using this system effectively is to keep the braids of the two stubs completely independent. The driver braid connects to the main feedline braid via the switch (or relay) system.

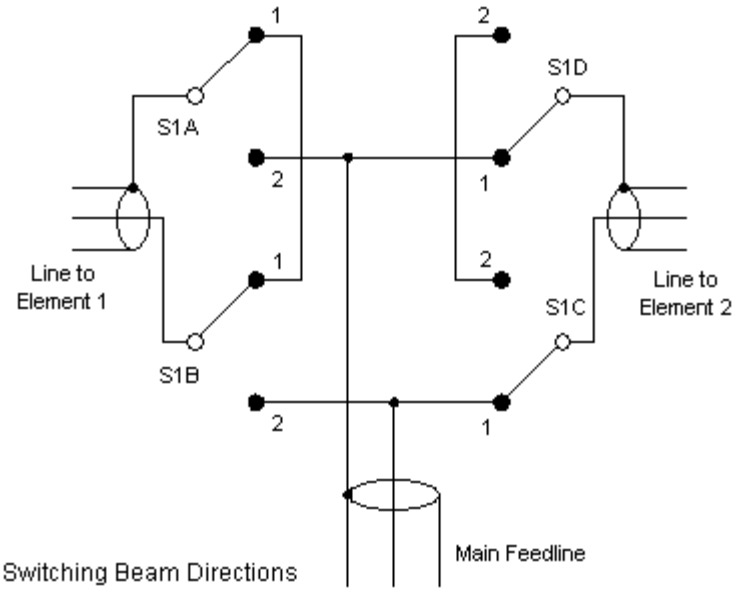

Fig. 2-10

To increase the effectiveness of the 2-element Yagi for worldwide coverage, we may set up three vertical dipoles in an equilateral triangle. At 40 meters, the triangle requires about 24.25' on a side, which is about 21' from any apex to the midpoint on the opposite side. At any given time, as suggested in **Fig. 2-11**, one

vertical dipole functions as a driver while the other two act as parasitic reflectors. In the model, all of the elements are identical to the driver element in the 2-element beams.

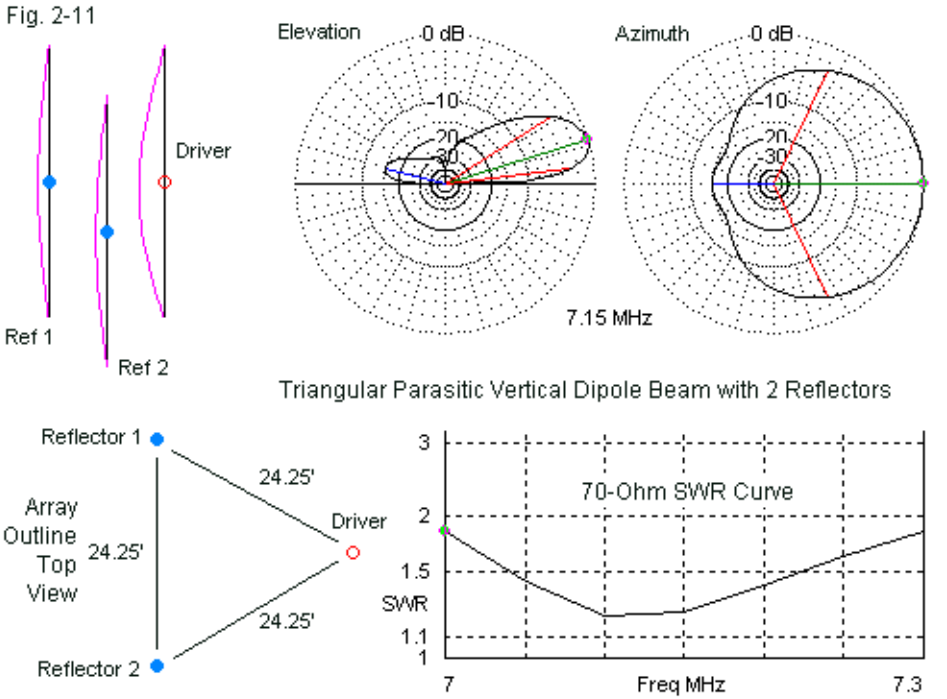

The modeled array is only a demonstration version and not a finished product. Hence, its performance is set for 70 Ω rather than 50 Ω. The data in **Table 2-6** and in the SWR graph suggest marginally better performance, but too marginally to be significant. The system uses shorted reflector stubs to set their electrical lengths for good parasitic duty. That fact allows us to bring all three stubs to a central point to select which element will be the driver and which elements will be the reflectors. If we notice the beamwidth of the array pattern, the switching system (more complex than for the basic reversible beam) offers us

full coverage of the horizon without significant loss of transmitted or received signal strength. As shown in **Fig. 2-12**, the triangle loses only about 2 dB of gain at the pattern overlap points, compared to a loss of about 6 dB where the reversible beam patterns overlap.

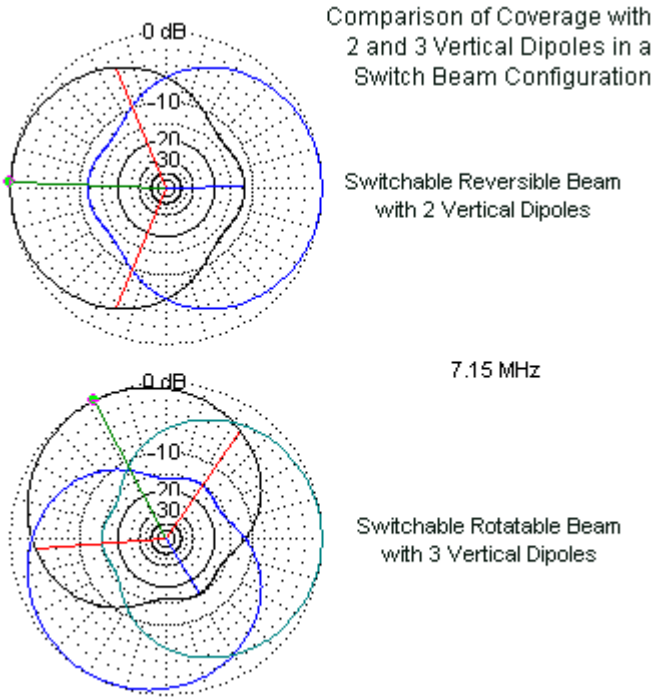

Fig. 2-12

We are not restricted to single drivers in creating parasitic beams with vertical dipoles. Indeed, we may create a parasitic beam by adding reflector elements to a phased pair of dipole drivers, as shown in **Fig. 2-13**. Each parasitic element set uses the same dimensions as the original simple 2-element Yagi. However, the model sets each Yagi 0.5-λ from the other. We may feed the driver pair through equal lengths of transmission line to achieve in-phase feeding. Horizontally, we

would call the array a parasitic lazy-H. Vertically, it becomes simply a standing-H.

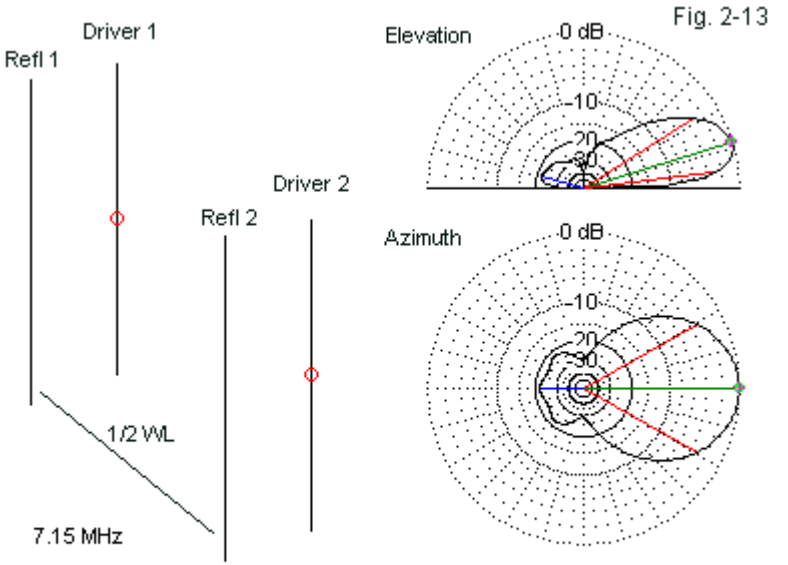

2 Parasitic Vertical Dipole Beams Spaced 0.5-WL
with Drivers Fed In Phase

The array shows about 7.37 dBi gain, about 3-dB higher than a single array. Equally significant is the reduction in beamwidth to 58°. Hence, the 4-dipole hybrid beam requires careful planning to point it at a specific region that is the communications target. Whether measured in terms of the 180° values, the worst-case value, or the average, the front-to-back ratio exceeds 20 dB, as the azimuth pattern clearly shows.

The hybrid phased-parasitic beam or standing-H falls into the realm of a special-needs beam. Due to the narrower beamwidth, reversing the beam may or may not yield any benefits, depending upon the relationship of communications

targets to the installation site. Nevertheless, like all of the elevation patterns associated with the multiple-dipole arrays in this chapter, the antenna enjoys the same low-angle pattern without the high-angle components that add noise without improving our reception of DX signals.

Parasitic Beams with Shortened Dipoles

To complete the picture of what multiple vertical dipoles may accomplish, I created a number of models using the T-hat shorter dipoles that we met earlier. In each case, I used elements with the length of the first T-hat driver, although with shorter legs. Each reflector has an inductive load, since we are only sampling the territory. **Fig. 2-14** shows the outlines of the sample beams: a basic 2-element version, a triangle, and a standing-H hybrid.

Fig. 2-14

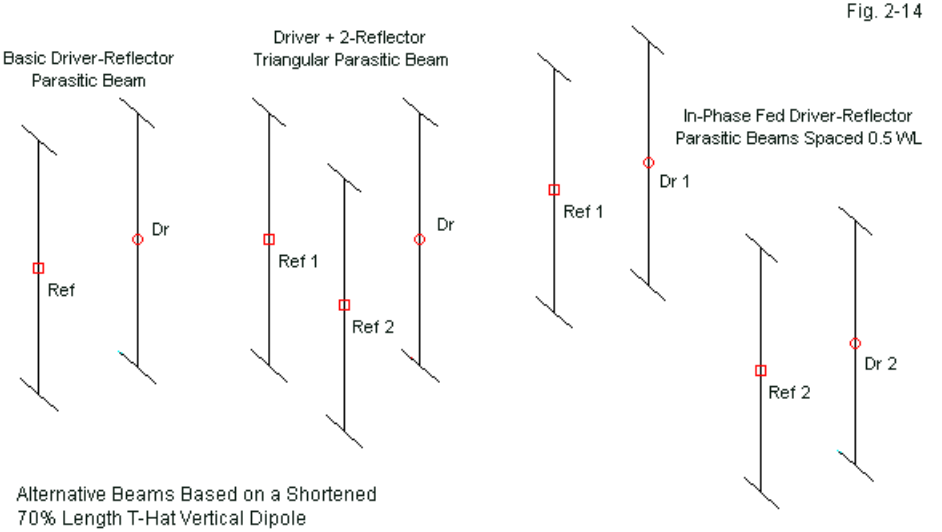

The results appear in **Table 2-7**. In general, with 70% elements and T-hats, we may accomplish everything that we can achieve using full-length elements, including reversibility, where applicable.

Performance of 7.15-MHz Driver-Reflector Vertical-Dipole Parasitic Beams							
Using 70% Dipoles with T-Hats							
Type	No Ele	Gain dBi	TO Deg	F-B dB	BW Deg	Feed R	Feed X
Ld Qinf	2	3.75	17	13.81	139.8	44.5	5.3
Ld Qinf	4	7.37	17	18.79	58.8	59.5	-5.2
Triangle	3	4.29	17	13.73	123	47.8	10.6
Notes:	All vertical dipoles use a base height of 4', and						
	use AWG #12 copper wire.						
	All 70% dipoles extend from 14.08' to 60.92' above average ground						
	T-Hat legs are each 5.8'.						
	Driver-reflector spacing for 2- and 4-element beams is 18'.						
	Triangle array is 24.25' on each side.						
	2 and 4 element beams use 65-Ohm inductive loads in reflector.						
	Triangle (3-element beam) uses 80-Ohm inductive loads in each reflector,						
	in the form of shorted transmission line stubs.						
	Gain dBi = maximum gain at TO angle						
	TO deg = TO angle in degrees						
	BW Deg = horizontal beamwidth in degrees.						
	Feed R/Feed X = feedpoint impedance in Ohms						
	4-element beam consists of 2 in-phase-fed driver-reflector beams; hence,						
	feedpoint values are for each of 2 drivers.						
							Table 2-7

All of the modeled beams are susceptible to improvements. Here, they serve only to prove the principle that moderate vertical dipole shortening is possible. Shortening below the 70% level will likely reduce gain, although we may always load a reflector to its full electrical length. Shortening may also reduce the feedpoint impedance, which is close to the 50-Ω mark with 70% elements. Nevertheless, the entire arena of complex arrays using shortened elements remains a fertile ground for experimentation.

Our goal has been only to demonstrate some of the possibilities for using vertical dipoles as elements in a lower HF array with significant performance potential. Many of these possibilities will re-emerge when we consider SCVs in detail. When we do encounter SCV arrays, we shall understand better from where they derive their performance.

A "Nearly Ideal" Parasitic Beam

To complete our survey of multiple vertical dipole arrays, we should note that standard configurations are not strictly necessary to produce a set of results. When we first examined phased arrays, we noted that many users prefer the cardioidal pattern produced by certain types of phasing. Some consider that to be an "ideal" pattern. It is possible to capture a cardioidal pattern with a suitable parasitic array. However, as **Fig. 2-15** shows in the outline sketch, the configuration will be far from standard.

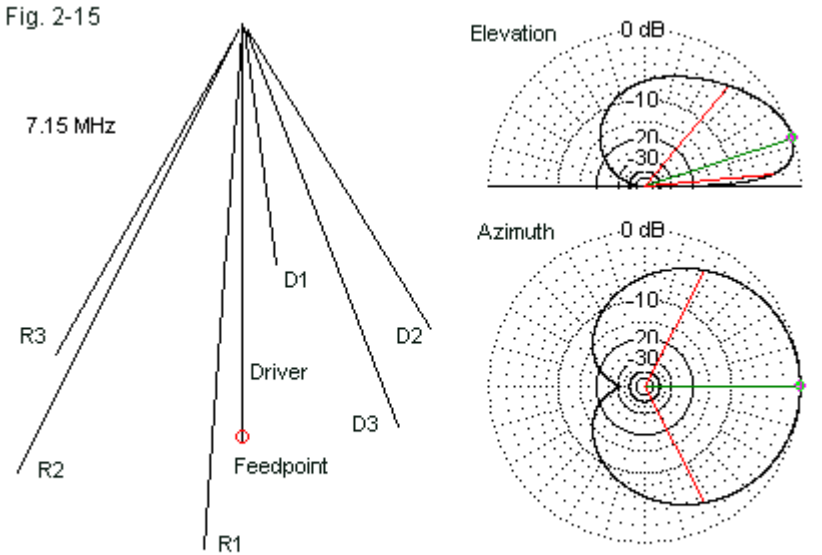

A Base-Fed Vertical Dipole Driver with
6 Pseudo-Guy Sloping Parasitic Elements

The array consists of a central vertical dipole. This particular model uses a base-fed ½-λ driver element. Unlike most of our models, this element is 2.5" diameter aluminum, more closely reflecting the likely construction of such an

antenna. The driver extends from 2.85' to 66.52' above ground. The interesting feature of the array is the use of 6 parasitic pseudo-guys as the parasitic elements. (The actual guying would consist of non-conductive fiberglass or similar ropes, with the wires applied to them.) Each parasitic make a 27° angle with the driver element. Three guys are directors and three are reflectors. None of the parasitic elements touches the driver. Rather, they terminate 6" from the element horizontally at a level that is 65.58' above ground. The directors are 57' long and terminate 14.8' above ground. The reflectors are 68.5' long and terminate 4.55' above ground.

With this arrangement (over average ground), the maximum array gain is 5.36 dBi, about 2.3 dB stronger than the original idealized phased array. Because the gain is higher, the beamwidth decreases to 125° (compared to 177° for the 2-element phased array). Because the parasitic elements slope, the pattern exhibits considerably greater high-angle radiation than the idealized phased array or any of the other patterns that we have observed. Hence, it qualifies as only "nearly ideal" for those who favor a cardioidal pattern. The driver, of course, requires high-impedance matching techniques.

This antenna serves only to let us know that we have not exhausted all of the techniques by which we may produce bi-directional and directional antennas for 160 meters through 40 meters. Indeed, most of our survey efforts have focused on basic designs that will eventually find their way into variations of SCVs.

Conclusion

In this chapter, we have examined phased arrays and parasitic arrays, as well as hybrids of both types. We restricted ourselves to arrays using 2, 3, or 4 elements as the types of antennas that form the parentage of SCVs and SCV beams. Most of our examples have focused on the 40-meter band, because vertical dipoles tend to be too tall for common use on 160 and 80. Nevertheless, with due adjustment for both frequency and soil quality, the principles involved apply at any frequency that we may choose to use.

There are applications for SCV designs at VHF and UHF frequencies,

although we tend not to recognize the link to the antennas with which we have been working. The most distinctive feature of these antennas is their environment many wavelengths above the ground. The added height forces us to take a somewhat different view of the resulting patterns, especially elevation patterns. Therefore, before we close the book on the parents of SCVs, we should spend at least a little time looking at the older generation in the VHF and UHF region.

3. VHF/UHF Applications

When we shift our operating frequency above 50 MHz, we encounter many changes in the expectations that we should bring to antenna performance. Since SCV designs are as functional and advantageous in the VHF and UHF regions as they are in the lower HF and upper MF regions, we should spend a little time developing some of those basic expectations. By using the vertical dipole as our basic antenna, we can more easily anticipate how more complex SCV arrays will perform.

One set of changes results from the fact that we operate VHF and UHF antennas many wavelengths above ground, in contrast to the low base heights used by our HF antennas. Not all performance features of low verticals are applicable to high ones. We can place antennas at greater heights, when measured in wavelengths, simply because the length of a wave grows much shorter as we raise the frequency. **Table 3-1** provides a rough guide to the length of a full wave at the center of the most-used VHF and UHF amateur bands.

A Wavelength on Various Higher Amateur Bands				
Freq MHz	WL m	WL mm	WL ft	WL in
52	5.7652	5765.2	18.915	226.98
146	2.0534	2053.4	6.737	80.84
223.5	1.3414	1341.4	4.401	52.81
435	0.6892	689.2	2.261	27.13
915	0.3276	327.6	1.075	12.90
1270	0.2361	236.1	0.774	9.29
Notes:	Freq MHz = band center in MHz			
	WL m = wavelength in meters			
	WL mm = wavelength in millimeters			
	WL ft = wavelength in feet			
	WL in = wavelength in inches			
				Table 3-1

Another set of changes results from our ability at higher frequencies to use array types that are impractical from 160 to 40 meters. For example, except for certain NVIS antenna, we generally do not use planar reflectors at lower frequencies. However, planar techniques are common in VHF and UHF antennas. As well, J-pole antennas may be perfectly straight at these frequencies.

To survey some of the possibilities and antenna properties in the upper frequency ranges, we shall fix a test frequency: 299.7925 MHz, at which frequency a meter and a wavelength coincide. We shall also provide dimensional information in wavelengths so that you may scale any antenna to any desired amateur band or other frequency. We shall also fix the dipole element diameter at 8 mm (0.315”). The diameter is approximately 5/16”, a value that falls within the range of self-supporting elements that are common in the VHF/UHF region. When scaling any antenna design, be certain to scale the element diameter as well as the element lengths and spacing between elements. Most of our work will use average ground (conductivity 0.005 S/m, relative permittivity 13). However, we shall pause to examine the effects of soil quality on upper range vertical antennas.

The Vertical Dipole at Various Heights over Various Soils

A resonant vertical dipole in free space at 299.2925 MHz is 0.432-λ long (or 0.432 m) when we use our 8-mm diameter lossless wire. The modeled free-space gain is 2.13 dBi. One reason why the gain does not reach the theoretical 2.15-dBi that we often use to define a dBd is the fact that the element diameter is so large. As we increase the element diameter of a linear dipole, the length required for resonant operation becomes shorter, slightly reducing the gain. (Remember that these remarks hold numerical interest but are not operationally significant.) If we reduce the diameter to 0.0001-mm, the required resonant length increases to 0.492-λ and the gain climbs to 2.14 dBi. Even with such a thin dipole, we have some end effect and fall short of the indefinitely thin wire upon which basic dipole theory is based.

Since we know what a dipole looks like and know that its azimuth pattern is

circular, we can turn directly to the antenna's elevation performance. **Table 3-2** summarizes data for the dipole at heights of 2, 5, 10, and 20 λ above very good, average, and very poor soils. 2 λ equals only about 40' at 6 meters and much lower at higher bands. Nevertheless, we find that at the lowest height in the survey, the feedpoint impedance coincides closely with the free-space value. The antenna is already high enough so that ground conditions immediately below the antenna have little influence on performance.

Performance of a Resonant Vertical Dipole at Various Base Heights above Ground and over Various Soil Qualities					
Ht WL	Soil	Gain dBi	TO deg	Feed R	Feed X
2	VG	4.70	5.2	72.15	-0.38
	Ave	5.21	5.4	72.14	-0.38
	VP	6.03	5.7	72.10	-0.38
5	VG	6.46	2.5	72.05	-0.38
	Ave	6.74	2.5	72.05	-0.38
	VP	7.18	2.6	72.04	-0.38
10	VG	7.23	1.3	72.04	-0.38
	Ave	7.38	1.3	72.04	-0.38
	VP	7.63	1.4	72.03	-0.38
20	VG	7.67	0.7	72.03	-0.39
	Ave	7.76	0.7	72.03	-0.39
	VP	7.89	0.7	72.03	-0.39
Fr Sp		2.13		72.03	-0.38
Notes:	Ht WL = base height of dipole in wavelengths				
	Free-Space entry is for reference.				
	Soil Type: VG = Very Good; VP = Very Poor				
	Gain dBi = maximum gain at TO angle				
	TO deg = TO angle in degrees				
	Feed R/Feed X = Feedpoint impedance in Ohms				
	All antenna elements = 8 mm diameter, lossless				
					Table 3-2

However, antenna height relative to the ground reflection zone for far-field pattern formation remains a very important factor in the determination of

maximum gain and the TO angle. Maximum gain increases and the TO angle decrease with rising antenna height. However, we must revise some of our HF expectations. For example, the poorer the soil quality, the higher the maximum gain value that we obtain. As we increase the antenna height, the differential among maximum gain values decreases.

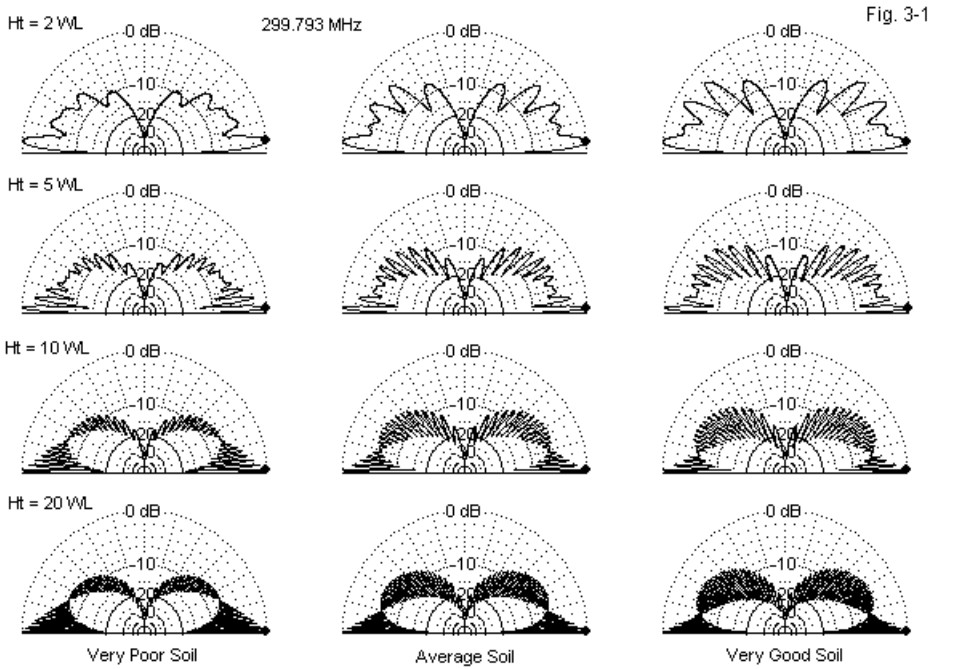

Elevation Patterns of Vertical Dipoles at Various Heights over Various Soil Qualities

Fig. 3-1 provides a gallery of modeled elevation patterns for the 3 soil types and 4 antenna base heights in the survey. Had we shown only the patterns for a 2-λ height, we might set aside the pattern differences as simply an oddity. However, by increasing the height in significant steps, we begin to see some interesting patterns. Of course, increasing antenna height yields more lobes and nulls. Some wags have described the patterns at 5-λ and higher as resembling

kissing porcupines.

For each soil type, we also begin to see a uniformity in the development of those nulls and lobes. For each soil quality, there is an elevation angle at which both the lobes and the nulls are weakest. The elevation angle for this condition is independent of antenna height and rests on the soil quality values. For very poor soil, the angle is about 25°. Over average soil, the angle decreases to about 15°, and over very good soil, the angle is about 12°. As we improve the soil quality, the reduction in lobe strength at the critical angle increases. Although the reduction is unimportant to point-to-point communications in the VHF and UHF region, it may have some importance to ground-to-air and to low-angle satellite communications. We shall see the same elevated gain depression in patterns formed by some of the more complex arrays that we may construct using vertical dipoles.

The survey that we have just examined used lossless or perfect wire. Indeed, all of the models in this chapter will also use lossless wire. Because 8-mm wire is such a large fraction of a wavelength, skin effect plays almost no role in reducing the dipole's gain. **Table 3-3** provides a brief survey of what happens to the free-space gain of a vertical dipole when we construct it with a number of practical materials. Only type 303 stainless steel can reduce the gain relative to the lossless-wire version, but the reduction is insufficient to count against the use of this very durable material in VHF and UHF antenna construction.

Dipole Free-Space Gain with				Table 3-3
Various Materials				
Material		Resis	Cond	Gain dBi
Perfect				2.13
Copper		1.74E-08	5.75E+07	2.13
Aluminum		4.00E-08	2.50E+07	2.13
Brass		6.40E-08	1.56E+07	2.13
Stainless Steel		7.20E-07	1.39E+06	2.11
Notes:	Resis = resistivity in Ohms/meter			
	Cond = conductivity in mhos/meter			
	Gain dBi = maximum gain at TO angle			

How Vertical Dipoles Relate to Vertical Monopoles

Because vertical monopole theory began with ground-mounted versions that used buried radial systems, we continue to labor under a variety of misunderstanding of how monopoles and dipoles relate to each other. Essentially, when we place a vertical antenna well above the ground, a monopole is simply a dipole with its lower half splayed into 4 or more sloping or straight (horizontal) radials. **Fig. 3-2** shows the evolution of the 90°-monopole from the vertical dipole passing through a sloping-radial stage, with the radials at 45° relative to the vertical upper element half. Note that in each case, the feedpoints are at the same level (5-λ above ground for this sample). As well, the length of the element above the feedpoint is identical in all cases. The vertical part of each antenna is 8-mm in diameter, but the radials use 4-mm diameter elements. We can clearly see that as we increase the angle of the radials, the high-angle lobes increase their strength.

Fig. 3-2

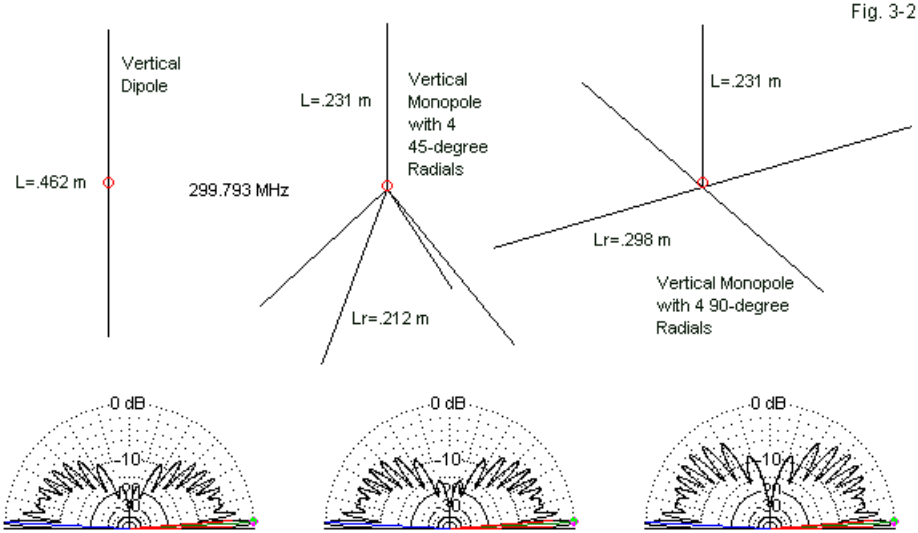

Dimensions and Elevation Patterns of 3 Types of Vertical Antennas

Table 3-4 provides numerical data from the models used to produce the patterns. Interestingly, the sloping-radial version of the antenna yields the highest maximum gain, but the 90° or straight-radial version of the antenna yields the lowest TO angle (but only by 0.1°). Even more interesting are the impedance values at the feedpoint. The 45°-radial version is a reasonable match for a 50-Ω feedline, but the builder can decrease the angle for a perfect match.

Relative Performance of Vertical Antennas with Feedpoints 5 Wavelengths above Average Soil							
Antenna	Len V	Len R	Gain dBi	TO deg	Feed R	Feed X
Vertical Dipole	0.462		6.69	2.7	72.0	-0.4
Monopole w/4 sloping radials	0.231	0.212	7.05	2.7	44.0	0.4
Monopole w/4 straight radials	0.231	0.298	5.07	2.6	26.2	-0.3
Monopole w/4 straight radials						
set for 50-Ohms	0.310	0.110	6.08	2.6	48.8	0.9
Notes:	Vertical elements 8 mm diameter, radials 4 mm diameter					
	Len V = length of vertical element in wavelengths					
	Len R = length of a radial in wavelengths					
	Sloping radials at 45 degrees, straight radials at 90 degrees relative to vertical					
	Gain dBi = maximum gain at TO angle					
	TO deg = TO angle in degrees					
	Feed R/Feed X = Feedpoint impedance in Ohms					Table 3-4

Perhaps the impedance value that catches most amateurs by surprise is the resonant resistance of the 90°-radial version of the antenna. Popular literature continues to record this value as 35-36-Ω, that is, half the value for the resonant vertical dipole. However, the required length of the radials to achieve resonance lowers the value, even though an exploration of the current levels shows that each 90° radial receives ¼ of the feedpoint current.

In fact, 90°-radial monopoles that one might construct for 50-Ω feedlines are much modified from the standard version. The table shows the dimensions for one such monopole, using a longer vertical section and much shorter radials. If we compare the current distribution of the two antennas, as shown in **Fig. 3-3**, we discover that the 50-Ω monopole uses an off-center feedpoint to achieve the desired impedance. In exchange for the off-center feedpoint, the maximum gain increases by a full dB over the standard version of the monopole. In fact, most ¼-λ monopoles for VHF and UHF with 90° radials are not 1/4-λ long.

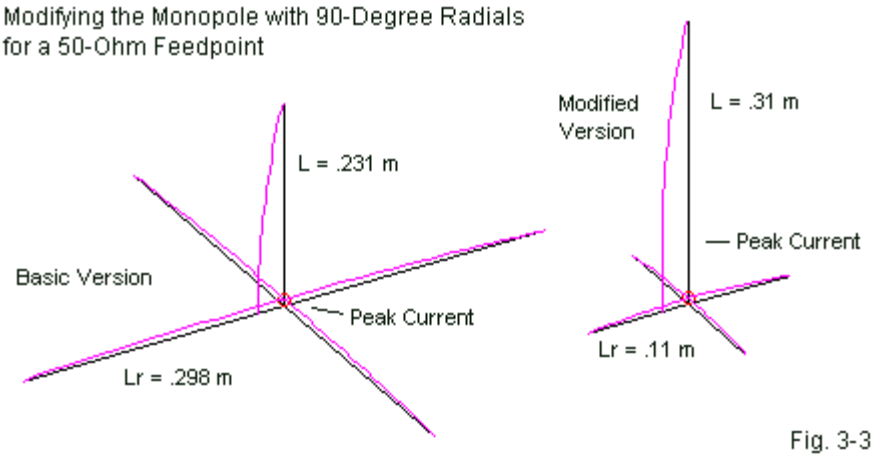

Fig. 3-3

The use of an off-center feedpoint raises the operational specter of common-mode currents. In fact, many feedpoint systems for sloping radials and for vertical dipoles also may be prone to such currents. For example, some installations run the feedline through the lower half of the vertical dipole element, resulting in close capacitive coupling between the element end and the coaxial cable braid. Hence, attenuation methods are in order, although we find them under two seemingly distinct names: chokes and decoupling devices. Both methods effectively attenuate common mode currents, avoiding significant radiation from the feedline.

Base-Feeding the Vertical Dipole and the J-Pole

The most common way to feed a vertical ½-λ element in the VHF and UHF regions is to use a ¼-λ matching section. The result is the very well known J-pole antenna. Less well known is the fact that there are two major variations on the feed system (and a larger number of variations on the upper end of the antenna).

Fig. 3-4 shows the more compact version of the J-pole, with the feedpoint at the center of the bottom cross piece. **Table 3-5** contains dimensions for the

model used as a sample. Like the other vertical elements in this chapter, the entire structure uses 8-mm diameter lossless material.

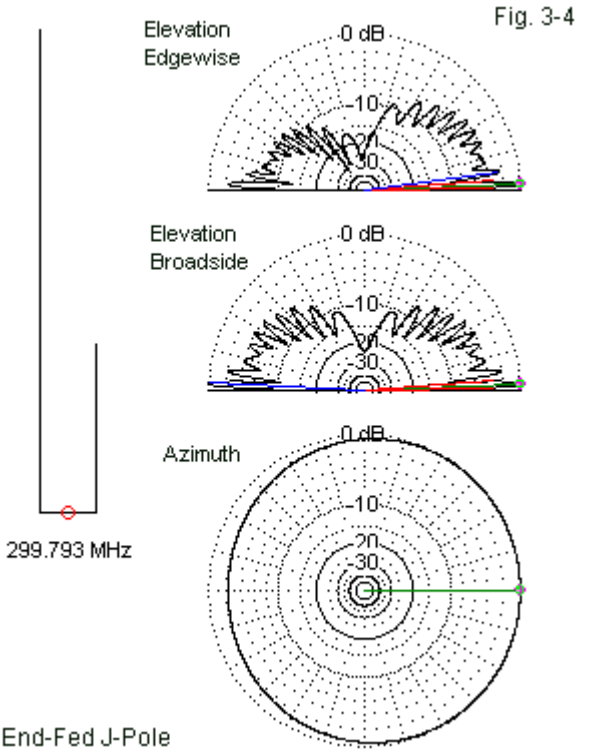

Because the junction of the matching section and the upper radiator does not have the same impedance as the open end of the matching section, we find radiation from all parts of the antenna. As a result, the figure presents two elevation patterns, one broadside to the pair of wires, the other edgewise to the assembly. In the direction of the short open-end wire, we find a slightly stronger pattern with numerous higher-angle lobes. The azimuth patterns shows that the antenna provides nearly a circular pattern.

Sample J-Pole Dimensions and Performance			
Parameter	End-Fed	Tap-Fed	Vert Dpl
Total Length	0.649	0.720	0.462
Exposed Element Length	0.420	0.485	
Parallel Section Length	0.229	0.235	
Tap-to-Shorted End Length		0.023	
Space between 8-mm Elements	0.073	0.046	
Max. Gain in dBi	7.75	7.27	6.74
TO angle in degrees	2.5	2.5	2.5
Front-Back Ratio in dB	2.26	1.46	
Feed resistance in Ohms	52.1	49.6	72.1
Feed Reactance in Ohms	0.2	2.4	-0.4
Note:	All antenna use a base height of 5 wavelengths		
	above average soil		
	All dimensions in wavelengths		Table 3-5

The alternative and perhaps more common feed system appears in **Fig. 3-5**. The matching section is a true shorted transmission-line stub, and the user experimentally determines the tapping points across the section, normally by reference to a 50-Ω SWR meter. As shown by the data in **Table 3-5**, the tapping point is not very far removed from the shorting bar. Part of the popularity of this version of the J-pole stems from a greater ease of construction. The end-fed version requires considerable experimentation with the length of each vertical segment. The tapped version tends to permit a more generalized construction with follow-up field-testing for the feedpoint tapping points.

The patterns are similar to those produced by the end-fed version of the J-pole. The lower front-to-back ratio is a function of the narrower spacing between the vertical elements. However, the elevation patterns show the same characteristics as we found in the end-fed version: a slightly stronger signal in the direction of the matching section open end and stronger high-angle lobes in this direction. Both versions of the J-pole yield about the same performance, with a maximum gain slightly higher than for a vertical dipole with the same base height. Of course, the high current region of the two J-poles is ¼-λ higher than for the center-fed vertical dipole.

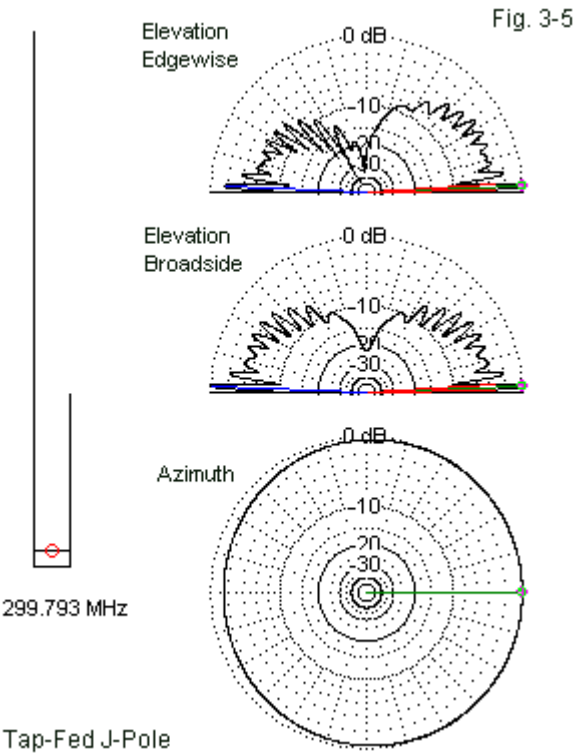

In principle, the end-fed version of the J-pole has a broader SWR bandwidth than the tapped version. **Fig. 3-6** presents the curves for the two versions used as samples in these notes. The tapped version does provide a wide enough bandwidth to cover the FM repeater portions of virtually all of the ham bands for which one might scale the sample design, (the most common application for a J-pole in the VHF and UHF amateur bands). The end-fed version would be more applicable to various land-mobile and maritime services that might require a wide operating bandwidth. The totally vertical J-pole has been used down into the upper HF amateur bands. However, the proximity to the ground of the shorting bar may call for tapping points that account for soil quality as well as for the basic

antenna geometry.

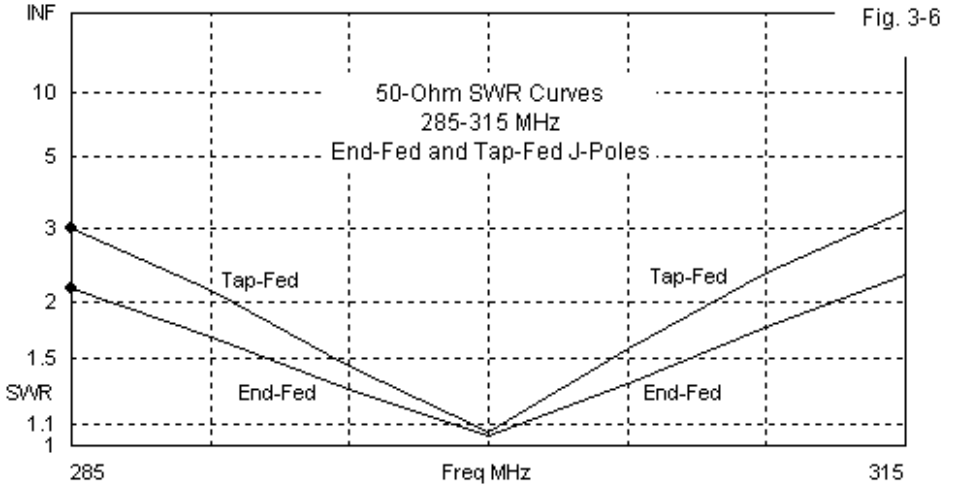

Fig. 3-6

Since the impedance values at the top of the matching section for either version of the J-pole are not the same, the currents on the two matching section wires will not have the same magnitude and opposite phase angles. The currents that do appear are a combination of transmission-line and radiation currents. **Fig. 3-7** shows current magnitude curves overlaid on the wires. (It does not show the relative phase angles.) The end-fed current magnitude at the junction of the matching section and the upper radiator does not go to zero. The zero-current point for the tapped version of the J-pole does not occur at a point that matches the end of the open-end matching section wire.

The figure also provides a review of the basic equations necessary to sort the radiation from the transmission-line currents. (An actual analysis would need to take both the magnitude and the phase angle into account, resulting in a more complex calculation procedure than the basic equations would suggest.) In lieu of a detailed analysis of the current components in the matching section wires, the non-symmetrical patterns becomes the best indication that the matching

section wires have a radiation as well as transmission-line current components. Ideally, the matching section would not radiate and the radiation azimuth pattern would be perfectly symmetrical, while the elevation pattern would not show stronger high-angle lobes in the direction of the open-ended matching section wire.

Fig. 3-7 Analyzing J-Pole Currents

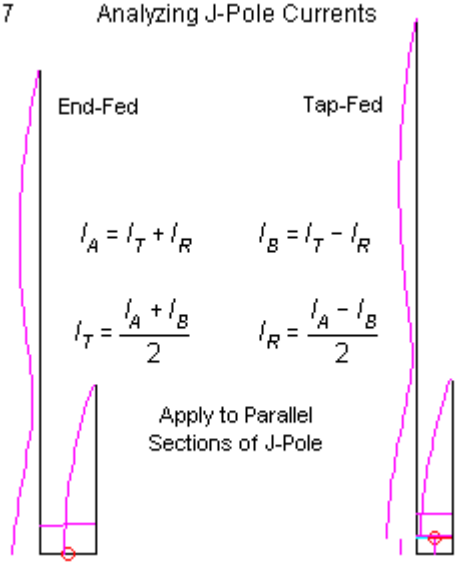

Collinear Vertical Dipoles

Certain designs that are highly impractical in the HF region become commonplace in the VHF and UHF region. For example, we may find vertical dipoles in a vertical stack and fed in phase. To achieve maximum gain requires close attention to the tip-to-tip spacing between the dipoles, as shown in **Table 3-6**. A spacing of about 0.5-λ, which corresponds to a feedpoint-to-feedpoint spacing of about 0.95-λ to 1.0-λ, yields the highest gain in the simple series of model runs at the test frequency. **Fig. 3-8** shows the general set-up and pattern.

Free-Space Gain of Vertically Separated Dipoles				
Tip Space in WL		Gain dBi		
0.4		5.32		
0.5		5.40		
0.6		5.36		
0.7		5.26		Table 3-6

Fig. 3-8

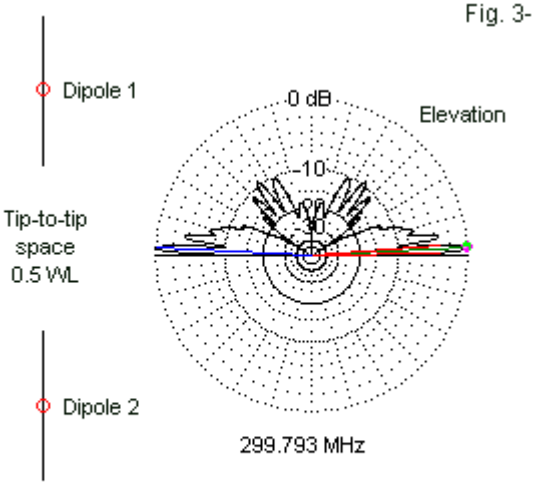

Vertically Separated Vertical Dipoles Fed In Phase
Center Height: 5 Wavelengths

One less desirable feature of the elevation pattern is the amount of energy devoted to higher-angle radiation. There are methods of controlling the waste by first controlling the phase change from one vertical dipole section to the next. The pair of independently fed dipoles has a total vertical length of close to 1.5-λ. If we add a pair of phase lines and use 4 ½-λ sections, we can go far toward achieving higher gain with less high-angle radiation.

Fig. 3-9 shows the outline of a collinear array that consists of 4 ½-λ sections.

Fed at the center, the array uses ¼-λ phase lines between the inner and outer section on each side of the feedpoint. The array produces nearly 11 dBi maximum gain when centered at the 5-λ height mark. A pair of optimally spaced dipoles centered at the same height yields about a dB less. As the elevation pattern shows, the phased collinear array derives the added gain by "moving" high-angle radiation down to lower angles.

Fig. 3-9

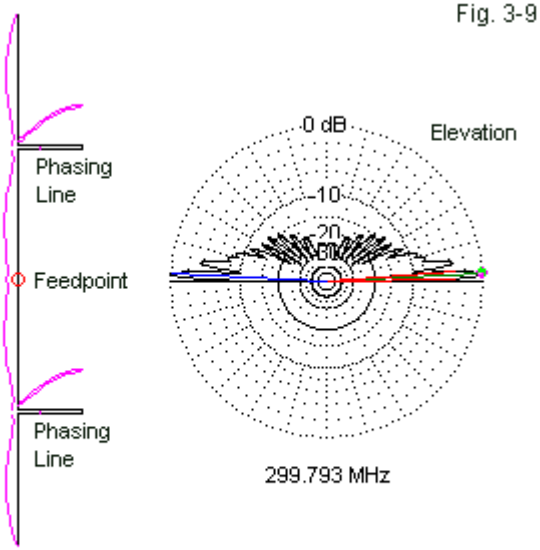

Collinear Array with 4 Half-Wavelength Sections and
Phasing Sections Center Height: 5 Wavelengths

The current patterns on the outline sketch show only the current magnitude, but the gain value informs us that the sections are all in phase. Had we omitted the phase lines and directly connected the ½-λ sections, the current would have undergone a phase reversal at each junction, negating much of the gain. The array shown has some common uses in the HF region, but virtually always placed horizontally with respect to ground. In the VHF and UHF region, we may easily create the vertical version to good effect. In many practical installations, the

straight phase lines shown in the model are curved to form a near circle around the main element. The curvature tends to minimize any pattern distortion resulting from phase-line radiation currents.

When modeling collinear arrays that use phase lines at high-voltage, low-current points, we obtain greatest accuracy by modeling the lines as physical wires. The NEC transmission-line facility (the TL command) is most accurate when the current magnitude and phase do not changes across the phase-line junctions with the main element. Hence, the TL command is most accurate in high current regions of an antenna. The collinear array in our sample forces us to place phase lines in regions where the current changes very rapidly, reducing the accuracy of NEC-created transmission lines. The cure for this limitation is to model the lines with physical wires as part of the overall model geometry.

VHF and UHF Parasitic Vertical Dipole Arrays (Yagis)

We may create directional arrays from vertical dipoles by making use of parasitic principles by which we feed a single driver and rely on the mutual coupling between otherwise passive elements to yield a desired antenna pattern. A closely spaced element that is longer than the driver will have a positive current phase angle relative to the driver and serve as a reflector. The term reflector only means that the main forward lobe is in the direction from the reflector element toward the driver. A closely spaced element that is shorter than the driver will have a negative current phase angle relative to the driver and serve as a director. The actual element spacing values may vary from 0.05-λ to about 0.2-λ (or more for some director elements).

One of the banes of VHF and UHF Yagi design are some very archaic and misguided cutting formulae for making small Yagis. All of these erroneous attempts to simplify Yagi design pay no heed to the element diameter. Yet, the element diameter plays a crucial role in determining the final properties of the directional beam. Furthermore, by careful attention to details of the design, we may tailor a beam for maximum gain, for maximum front-to-back ratio, or for maximum operating bandwidth. Each type of design requires elements with different lengths and with different spaces between elements, and both of those

values depend upon the diameter of the elements used in the design.

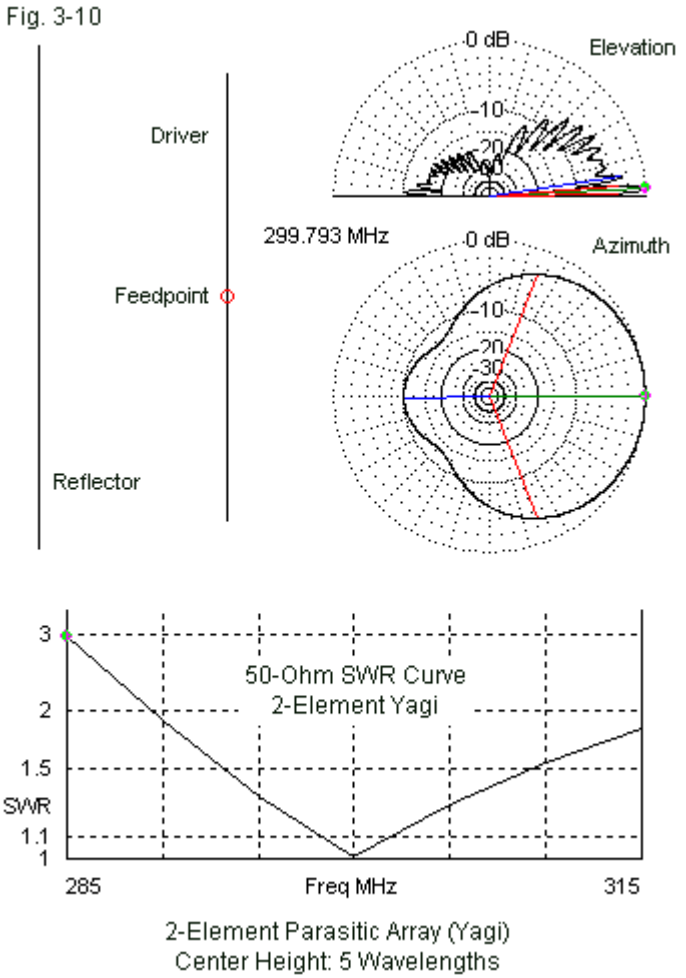

Fig. 3-10 shows the outline of a two-element Yagi using a driver and a

reflector. The dimensions for 8-mm elements appear in the left columns of **Table 3-7**. For the same level of performance with thinner elements, the driver-reflector spacing would be narrower.

Sample Yagi Dimensions and Performance			
Parameter	2-Element		3-Element
Reflector Length	0.490		0.523
Driver Length	0.438		0.472
Director Length			0.413
Reflector-Driver Space	0.185		0.248
Driver Director Space			0.126
Total Boom Length	0.185		0.374
Max. Gain in dBi	10.84		11.56
TO angle in degrees	2.7		2.6
Front-Back Ratio in dB	10.22		22.95
Beamwidth in degrees	137.6		124.1
Feed resistance in Ohms	49.7		48.1
Feed Reactance in Ohms	-0.1		-4.4
Note:	All antenna use a base height of 5 wavelengths		
	above average soil		
	All elements 8 mm diameter		
	All dimensions in wavelengths		Table 3-7

The array does not achieve the absolute maximum gain and front-to-back ratio that we might obtain from a driver and a reflector. This beam uses a spacing that provides a direct 50-Ω connection to coaxial cable and a very wide operating bandwidth (relative to Yagis designs in general). The SWR curve in the figure shows that the beam would easily cover almost any of the amateur bands. Like all 2-element driver-reflector arrays, the forward gain is highest at the low end of the passband and decreases almost linearly as we raise the operating frequency within the passband. The design also aligns reasonably well the lowest 50-Ω SWR value and the peak front-to-back ratio at the test frequency. Like the rise in SWR, the front-to-back ratio decrease slowly both above and below the test or design frequency.

Fig. 3-11

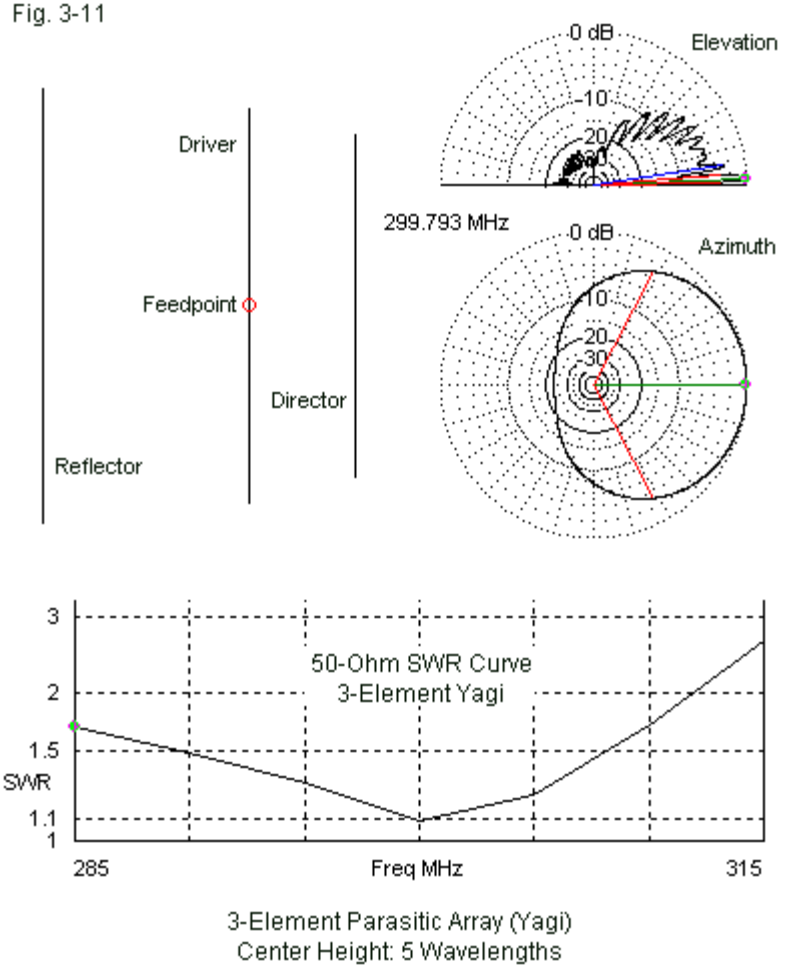

3-Element Parasitic Array (Yagi)
Center Height: 5 Wavelengths

The 2-element elevation and azimuth patterns are both interesting. The elevation pattern shows the same depressed gain at 15° over average soil that we found in the patterns for the simple dipole. The azimuth pattern has a

beamwidth of almost 138°. Therefore, if we did not wish to use a rotator, we might switch among three such Yagis, properly spaced from a central support. The horizontal coverage would be about as complete, but with a considerable cost saving.

Fig. 3-11 provides us with similar information about a 3-element Yagi designed for maximum bandwidth. The dimensions appear in the right columns of **Table 3-7**. The general outline of the Yagi would have a much different appearance had we designed it for maximum gain or maximum front-to-back ratio. The peak front-to-back ratio version has intermediate gain and nearly equal spacing between each pair of elements. The maximum-gain version shows nearly a full dB of gain over the wide-bandwidth model using close to the same total boom length. However, for that narrow-band design, the driver-reflector spacing would be smaller and the driver-director spacing larger.

Because the 3-element Yagi uses a director, the gain curve shows a rising value of forward gain as we increase the operating frequency within the passband. (Note that we always specify the gain curve within the operating passband. As we continue to increase the operating frequency, the antenna will show a relatively sudden reversal of direction.) The version shown in the figure and the table also uses a 50-Ω feedpoint for a direct connection to coaxial cable. As well, the minimum 50-Ω SWR and the maximum front-to-back value occur on the design frequency (or very close to it). Like the dipole and the 2-element Yagi, the elevation pattern shows depressed gain at an elevation angle of 15° above average soil. The azimuth pattern shows the benefit of an increased front-to-back ratio relative to the 2-element model. The forward gain is about 1 dB higher for the 3-element Yagi. The beamwidth has dropped to about 124°, still sufficient to allow 3 such Yagis to cover the horizon.

We may improve the forward gain of any parasitic beam by judiciously adding directors. Very long-boom Yagis with up to 50 elements exist for long distance point-to-point communications. Most of these Yagis employ horizontal polarization, but rotating them 90° along the boom axis converts them into vertically polarized beams. However, as we increase the forward gain, we pay a penalty in terms of the beamwidth. A very long-boom Yagi may have a

beamwidth that is only about 18°. Hence, in all applications, we must carefully weigh the need for gain against the need for coverage.

These brief notes are no substitute for fuller coverage of the subject of parasitic beams. *Wide-Band Yagi Notes* and *Long-Boom Yagi Studies* are both available for anyone interested in understanding the behavior of various types of Yagi designs and in seeing some of the options for achieving various kinds of performance from parasitic arrays. These notes are only a sample of parasitic possibilities. They go only as far as we went with some wire beams for the lower HF and the upper MF region. Indeed, if we had enough acreage and enough tall supports, we might create a long-boom Yagi for 160 or 80 meters.

In-Phase-Fed Pairs of Vertical Dipoles

Just as we did in the lower frequency regions, we may space a pair of VHF or UHF vertical dipoles 0.5-λ apart and feed the two elements in phase to obtain bi-directional gain over a single vertical dipole. **Fig. 3-12** shows the general outline of such a simple array. The figure also contains the elevation pattern over average ground, once more with the gain depression at 15° above average ground. The azimuth pattern for the array with a height of 5 λ above ground shows the well-formed figure-8 pattern.

The free-space gain of the dipole pair is nearly 6 dBi, just a bit less than 4-dB higher than a single dipole. At the listed height, the gain is about 10.5 dBi in each favored direction. The beamwidth is about 60° in each direction.

We may feed the VHF/UHF version of the phased dipole pair as independent dipoles or we may treat the array as a standing-H, with equal lengths of transmission line to a central connection to the main feedline. The exact impedance that we obtain at the line junction will be a function of the characteristic impedance of the line used and the length of the line.

Our introduction to the VHF/UHF phased pair of dipoles adds little to the general notes in Chapter 2 about such antennas. However, we shall return to this antenna in a later chapter when we discuss half-square antennas for VHF use.

As well, we shall very shortly see how we may use such a pair to form a directional beam without employing parasitic elements.

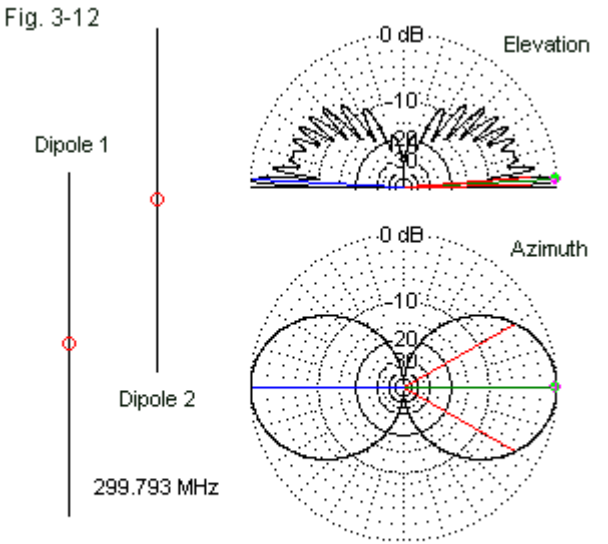

Two Dipole Fed In Phase
Center Height: 5 Wavelengths

Planar Reflectors

Although very rare in the lower HF region, planar reflectors are very common and useful for VHF and UHF antennas. When adequately designed, planar reflectors provide a very useful means of achieving the performance improvements that we wish from various types of drivers. To understand their operation, we must set aside most of what we think we know about parasitic reflectors, since the operating principles for the two types of reflectors are so different. A parasitic reflector is an element that receives its energy from the fed element (the driver) and is sized and spaced to produce currents having a

desirable relative current magnitude and phase angle so as to yield a directional radiation pattern. A Yagi director operates in the same manner, but with different required values of relative current magnitude and phase angle. Parasitic reflectors do not reflect in the flashlight sense.

In contrast, a planar reflector belongs to a family of reflectors based on principles derived ultimately from optics. Other members of the family include corners, troughs, and parabolas. **Fig. 3-13** shows the basic parameters of a planar reflector.

Limitations of a Planar Reflector Having a Finite H-Plane Dimension

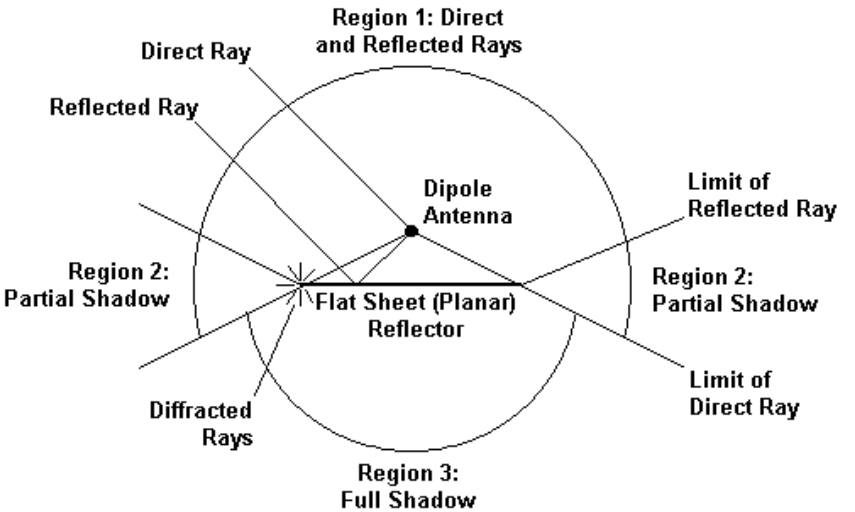

Fig. 3-13 Adapted from Kraus, Antennas, 2nd Ed., p. 548

The flat sheet that forms an ideal planar reflector has 3 regions. The forward

region is subject to both direct and reflected rays from the driver element. Hence, any optically based reflector does not benefit from trying to combine parasitic and optical techniques, such as adding a director to the driver. Indeed, such attempts simply increase the difficulty of obtaining a desired performance level. The region of partial shadow, of course, depends upon the size of the planar reflector. (Parabolic reflectors tend to reduce this region to an absolute minimum, but the level of success is dependent upon reflector size, as it is for the planar reflector.) Theoretically, the region of full shadow should produce an infinitely large front-to-back ratio. However, the diffraction of rays at the reflector edge reduces that ratio to a good but finite value.

Planar reflectors have two properties that deserve special note. In the extensive exploration of these arrays in *Planar and Corner Reflectors*, I discovered that the optimal size planar reflector is relatively constant for any type of driver. For maximum array gain, the reflector surface should extend between 0.4 λ and 0.5 λ beyond the limits of the driver element in both horizontal and vertical directions. Moreover, the exact dimensions of a planar reflector are far less critical than the dimensions of a parasitic reflector. Therefore, the planar reflector array is inherently a broadband device.

The vertical dipole and a pair of vertical dipoles fed in phase are two very good drivers to use with a planar reflector. Designing and modeling the total array involves two processes. One requirement is developing a model of the planar reflector using wire-grid techniques. The models that we shall use as samples employ standard wire-grid squares that are 0.1" per side. To simulate a solid surface, the wire diameter is the grid-square side length divided by π. The second requirement is to size and place the driver element(s) according to some set of design specifications. We might easily choose maximum gain, maximum front-to-back ratio of narrowest beamwidth as design goals. For our samples, I chose instead to achieve a 50-Ω feedpoint impedance. This goal results in very good performance from a planar array and is consistent with the parasitic array (Yagi) designs that we have already sampled. For any selected feedpoint impedance, we may vary both the dipole length (while retaining the 8-mm diameter) and the spacing from the reflector plane. Let's begin with a single dipole driver. **Fig. 3-14** outlines the array appearance in modeled form and

provides some basic far-field patterns with the antenna at a height of 5-λ above average ground. The dimensions and performance data are in the left columns of **Table 3-8**.

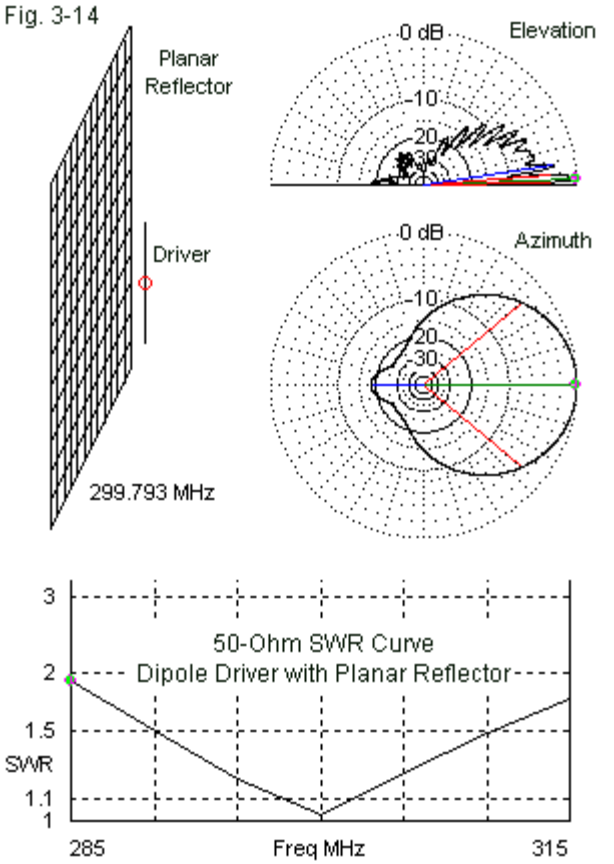

Dipole Driver with Planar Reflector
Center Height: 5 Wavelengths

Sample Planar Array Dimensions and Performance		
Parameter	1 Dipole	2 Dipoles
Reflector Width	1.2	1.6
Reflector Height	1.2	1.2
Driver Length	0.437	0.466
Reflector-Driver Space	0.176	0.25
Max. Gain in dBi	13.84	15.39
TO angle in degrees	2.7	2.7
Front-Back Ratio in dB	18.41	19.27
Beamwidth in degrees	79.7	53.0
Feed resistance in Ohms	50.2	51.1
Feed Reactance in Ohms	0.3	0.8
Note:	All antenna use a center height of 5 wavelengths	
	above average soil	
	All elements 8 mm diameter	
	All dimensions in wavelengths	
	2-dipole version: drivers fed in phase	
	Reflector models use standard wire-grid set-up	
		Table 3-8

An 8-mm dipole with a length of 0.437-λ spaced 0.176-λ from the planar screen yields the desired feedpoint impedance within close tolerances. Optimum performance for this configuration occurs with a reflector that is about 1.2-λ by 1.2-λ per side. The maximum gain is about 2-dB higher than for the wide-band 3-element Yagi, with a narrower beamwidth. The SWR operating bandwidth extends beyond the limits of the frequency range shown for that parameter in **Fig. 3-14**. As well, since we are not concerned with a shifting set of current phase angles on multiple elements, the gain and front-to-back ratio undergo only small changes across the passband. Hence, the planar reflector array is a wide-band antenna with respect to multiple operating parameters.

We may replace the single-dipole array with a pair of dipoles spaced ½-λ apart. For this version of the array, the horizontal dimension of the reflector increase to 1.6-λ. Each dipole has a length and spacing from the reflector to yield a 100-Ω impedance. Therefore, the length increases to 0.466-λ and the spacing

value is 0.25-λ. **Fig. 3-15** outlines the array with additional data.

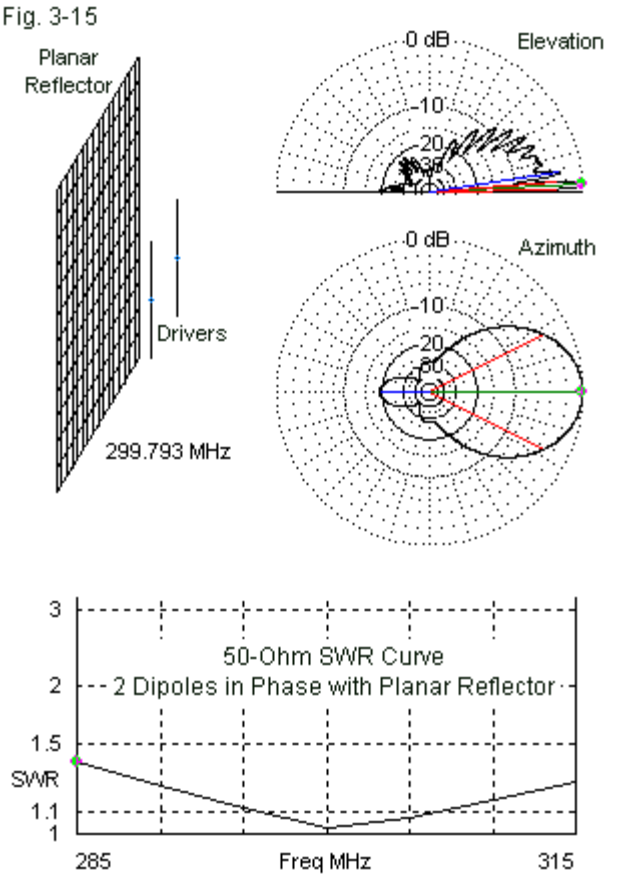

2 Dipoles in Phase with Planar Reflector
Center Height: 5 Wavelengths

The use of a 100-Ω driver allows us to use a pair of 100-Ω lines to a center

feedpoint for the total array. At the junction, the impedance is about 51 Ω for use with the usual coaxial cable feedline. Adding a second dipole in phase with the first increases the gain by about 1.5-dB relative to a single dipole driver. The beamwidth decreases to 53°. The elevation patterns for the two types of drivers are similar, and both show the gain depression at 15° since the models use average ground quality. The azimuth pattern shows the highly directional nature of the dual-driver planar array.

These sample planar arrays are not idle additions to the collection of SCV parents. We shall find offspring that use some of the SCV antennas as drivers to provide either additional performance capability or other special properties for VHF and UHF communications. The baseline data for these basic models will tell us if the offspring achieve as much or more than the parent models.

Conclusion

Our survey of VHF and UHF applications for vertical dipoles has sampled a number of ways in which operation in this frequency range differs from operation in the lower HF range that we ordinarily associate with SCV antennas. The greater height above ground makes a considerable difference to our expectations from the vertical dipole arrays. We may extend those altered expectations to the true SCVs to come.

In addition, we have looked at a few arrays that are highly impractical (but not impossible) at lower frequencies, but that are quite feasible and common at very high frequencies. The J-pole took on full vertical form as a means of base feeding a ½-λ element. Parasitic arrays became more complex. Finally, the planar reflector provided us with an alternative means of creating a practical directional beam.

Having examined the parentage of SCVs with enough detail to give us a good idea of the family's foundation, we reach a complex fork in the trail that we are following. In Part 2 of this study, we shall begin an exploration of the many forms that true SCVs may take.

Part II: SCVs

4. Deltas (Triangular SCVs)

The next generation of vertical antennas includes the true SCV forms. Each self-contained vertical array, in its basic form, includes about 1-λ of wire and contains two modified vertical dipoles. Perhaps the most desirable aspect of the SCV is that it requires a single feedpoint and uses the modifications to the geometry of a pair of vertical dipoles to allow it to provide in-phase feeding to both dipoles.

One of the oldest SCV forms is the triangle or delta loop. **Fig. 4-1** shows the two most common delta forms.

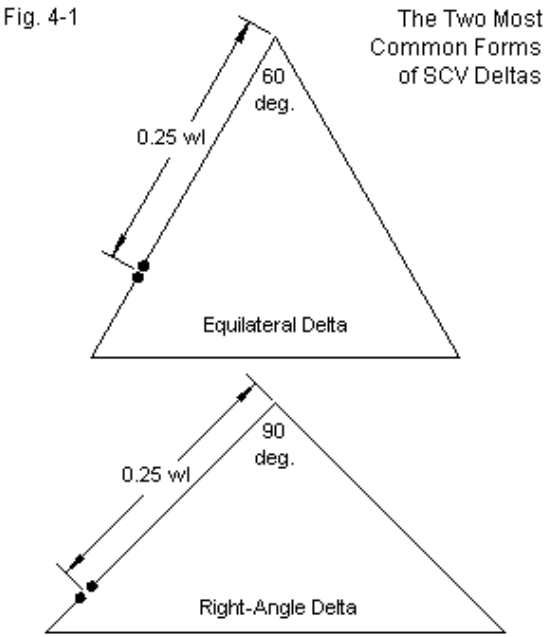

Both forms have one common feature: the placement of the feedpoint. To obtain essentially vertical polarization, the feedpoint must be about ¼-λ downward from the apex of the triangle. The second vertical dipole is on the opposite sloping leg. We might imagine a second virtual feedpoint at this position. The lower half of each dipole extends to a corner and then proceeds horizontally until the two dipole ends meet in the middle. If the real and virtual feedpoints represent high-current, low-voltage regions of the antenna, then the apex and the lower midpoint of the triangle point to high-voltage, low current regions. Essentially, then, we have two vertical dipoles, fed in phase.

Closed loops, whatever their shape, have some interesting properties. They may take the form of circles, squares, diamonds, triangles, or any other polygon. Unlike a linear element, if we increase the diameter of the element, the required length of the loop (or circumference) for resonance becomes larger. Hence, almost all SCV basic forms represent variations on the closed-loop theme. However, each form has some special features that deserve extended attention.

Fig. 4-2

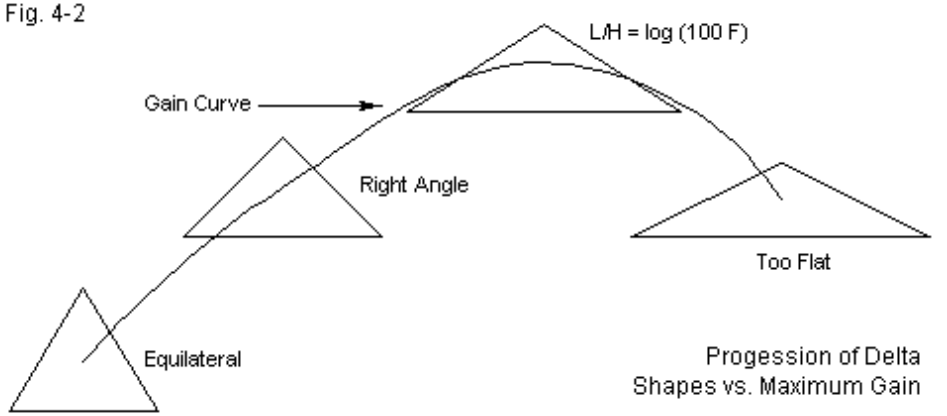

As suggested by **Fig. 4-2**, the two most common forms of the delta loop actually form two points in a rough progression of triangular shapes. As we flatten the delta—up to a certain point—we obtain slightly higher gain. The peak

gain occurs with a certain ratio of horizontal length to triangle height as measured from the apex to the bottom wire. The ratio of length to height is approximately the log of 100 times the frequency in MHz. If we flatten the triangle any further, the sloping wires become too horizontal for effective vertical service.

Let's remove one temptation at the beginning of our discussion. Radio amateurs are unduly fond of so-called cutting formulas. All such formulas have a similar form:

$$L = k_{(ft)} / F_{(MHz)}$$

where L is the total wire length in feet, F is the operating frequency in MHz, and k is a simple number. The traditional number to use for k in all loop exercises is 1005. The number actually derives from an exercise, now about 40 years out of date, for the elements of a 3-element quad beam, a design that has long since been supplanted by more effective designs. It never had any application to a single loop, whatever its shape. However, the number has persisted as the gold standard for pre-measuring loop wire. Alas, the standard is fool's gold, since the required length of wire needed to form a resonant loop, especially in the lower HF region of the spectrum, will vary with several factors. The diameter of the wire, the quality of the soil beneath the antenna, and the height of the antenna above ground will all affect the required circumference for resonance. Hence, we may discard all cutting formulas at the outset. NEC-4 models, which allow us to change the wire diameter and material, the ground quality, and the height of the antenna, will provide far better guidance to the required wire that we must purchase, not only to build a delta, but as well to build any of the SCV forms.

Feeding the Delta SCV

The delta loop has many uses. Not only do we use the antenna to form a bi-directional vertically polarized array, we often press it into service as a multi-band antenna. However, each service has a different feedpoint to obtain the most desirable operation that we can obtain from a triangle. Moreover, we may set up the triangle in two forms: apex up and apex down. The end result is a collection of 6 favored feedpoints for the seemingly simple triangular loop. **Fig. 4-3** shows the general positions of the possible feedpoints, applied to a right-angle delta. In both the upright and the inverted forms, the position that is about ¼-λ from the

apex is best in terms of providing the most nearly vertically polarized radiation pattern. However, this position is inconvenient for routing feedlines to and from the antenna. Hence, many builders prefer a corner position that allows them to route the feedline along a support rope. Still other builders prefer to place the feedpoint at the center of the lower wire in the antenna, which is the midpoint of the base wire in the upright position and the apex itself in the inverted version.

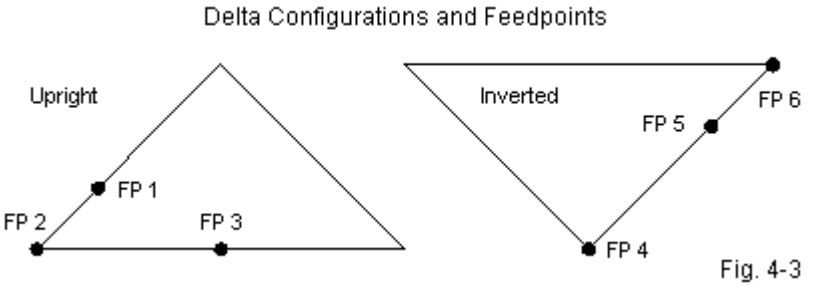

Fig. 4-3

Let's set up a test case at 7.15 MHz, using average soil below the antenna. The lowest height of the antenna or base height will be 20' above ground. Of course, we shall make two versions of the antenna, one upright, the other inverted. I have not specified the top height because we shall size each right triangle so that it is nearly resonant with the specified feedpoint, that is, within a very few Ohms reactance of perfect resonance. The antenna itself will be AWG #12 copper wire.

Table 4-1 summarizes some of the findings from the exercise. First, we find 4 different circumferences necessary for resonance. The midpoint feed positions require very different lengths relative to the corner and the side-feed positions. Although the corner and the side-feed positions use the same loop circumference within each series, the side-feed position shows slightly higher gain from the loop. The upright and the inverted series each require different lengths partly due to the difference in the influence of ground upon the wires in the loop. You may multiply the circumference values in the table by the operating frequency to obtain so-called cutting formulas, but that will do little good at other frequencies at other heights with different soils beneath the antenna.

Performance Variations with Changes in						Table 4-1
Right-Angle Delta Feedpoint Position						
(See Fig. 4-3 for physical positions of designated feedpoints.)						
Upright Series		Base Height: 20'				
Position	Gain dBi	TO deg	BW Deg	Feed R	Feed X	Circum ft
1	1.9	20	115.7	61.1	-0.6	146.4
2	1.69	20	116.7	67.5	-0.7	146.4
3	5.24	66		201.8	0.4	140.9
Inverted Series		Base Height: 20'				
4	5.81	43	105	244.7	-0.4	143.3
5	1.65	17	127.4	57.3	-1.5	146.4
6	1.48	18	128.3	63	-2.3	146.4
Notes:	Gain dBi = maximum gain at TO angle					
	TO deg = TO angle in degrees					
	BW Deg= beamwidth in degrees					
	Feed R/Feed X = feedpoint impedance in Ohms					
	Circum ft: total loop circumference in feet					
	All delta loops AWG #12 copper wire					
	Test frequency: 7.15 MHz					
	Soil quality: average					

In the upright series, the corner and the side feedpoints yield very low elevation angles of maximum radiation (the take-off or TO angle). The side position not only shows slightly higher gain, but also a slightly lower feedpoint impedance than the corner position. Both positions are suitable for using the delta in SCV service, although the mid-side position is electrically optimal, despite its physical inconvenience.

The center baseline position (3) yields an antenna that is largely horizontally polarized. Although outside the scope of these notes, the center baseline feedpoint is best for using a delta loop as a multi-band wire with reasonably effective results across the entire HF spectrum. The SCV positions tend to yield only high-angle radiation in the upper HF region. However, the center baseline feedpoint disables the loop from SCV service on the frequency for which the wire is about 1-λ long, as shown by the high TO angle value. **Fig. 4-4** shows patterns

and current distributions for each feedpoint position in the upright series. The patterns for the bottom center feedpoint disqualify the antenna as an SCV. Note the increase in the SCV horizontal component when we shift from the side position to the lower corner position.

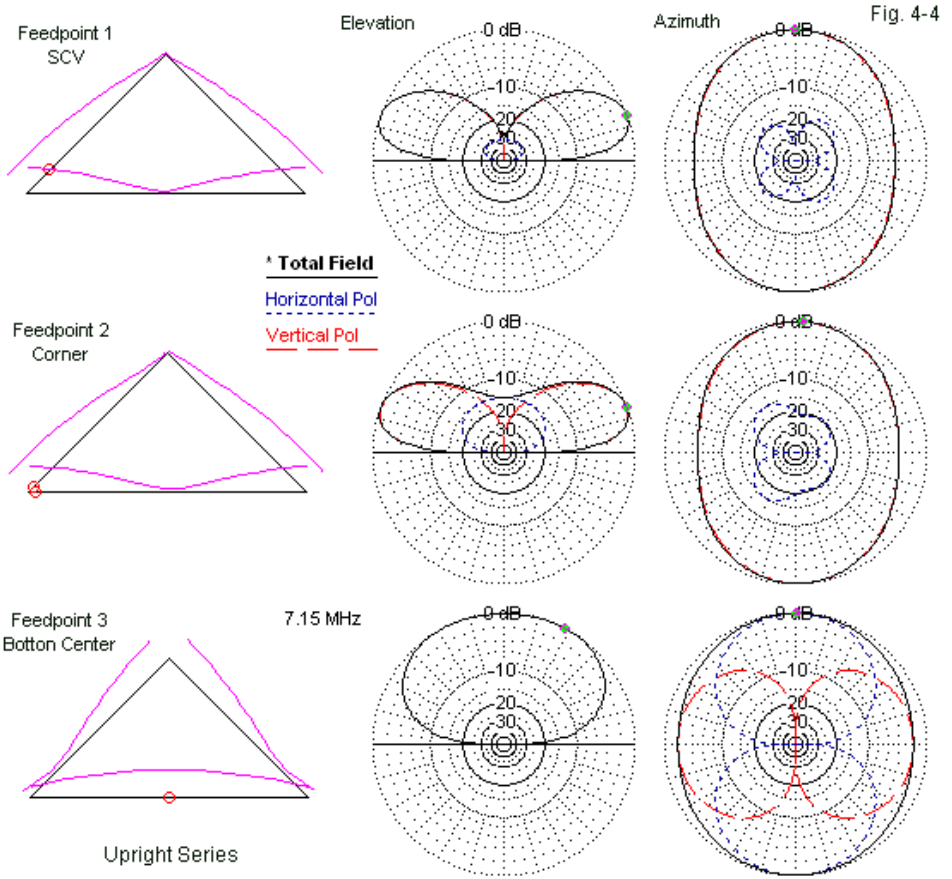

Changing Feedpoints of a 40-Meter Right-Angle Delta with a Base Height of 20' Above Average Soil

Fig. 4-5 shows the patterns for the inverted series of potential feedpoints. Apex feeding produces a non-SCV antenna (that may still be useful for multi-band service). Upper corner feeding yields a stronger horizontal component than the more ideal side position.

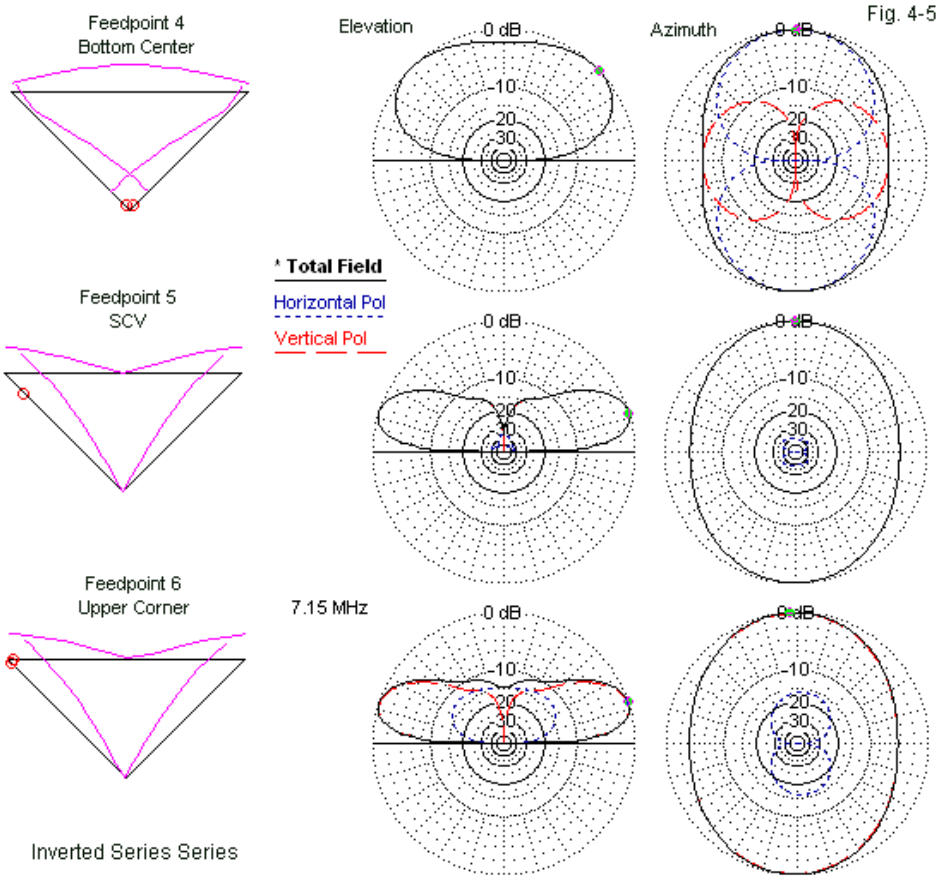

Changing Feedpoints of a 40-Meter Right-Angle Delta with a Base Height of 20' Above Average Soil

The exercise is more than idle. Rather, it shows the relationship of the SCV form to its roots in the vertical dipole. Indeed, for all of the sample SCVs in this chapter, we shall use a side feedpoint placed as close to the optimal position as modeling will permit.

The Equilateral Delta SCV

The equilateral delta SCV gains its popularity for two major reasons. First, it is relatively easy to calculate. We have three legs of equal length. The height is 0.866 times the length of a side. In **Fig. 4-6** we have the outline of the equilateral delta with key dimensions for 160-, 80-, and 40-meter versions. Each version is approximately resonant at the optimal height above ground for maximum gain over average soil, of course, using AWG #12 copper wire as the element material. The feedpoint position is 75% of the distance from the apex down toward a lower corner.

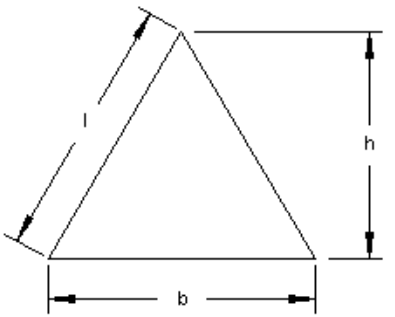

Equilateral Deltas for SCV Use

Dimensions

Freq.	1.85 MHz	3.55 MHz	7.15 MHz
B (base)	186.6'	97.6'	48.8'
H (height)	161.6'	84.52'	42.26'
L (leg)	186.6'	97.6'	48.8'
Circumference	559.8'	292.8'	146.4'

Fig. 4-6

Every SCV has an optimum height above ground at which the antenna yields maximum bi-directional gain. The height varies with two factors: the frequency of operation and the quality of the soil below the antenna. Therefore, we should look at what happens on each band (160, 80, and 40) over a fair sampling of soil qualities (very good, average, and very poor) to obtain some general trends in performance and in the optimal height for the antenna. At 1.85 MHz, I used 20'

increments of base height between 10' and 130'. **Table 4-2** shows the results of this modeling exercise.

Equilateral Deltas for 160 Meters					Table 4-2
Base Height and Soil Quality vs. Performance					
1.85 MHz					
Soil	Ht ft	Gain dBi	TO deg	Feed R	Feed X
VG	10	4.07	15	213.3	121.7
	30	4.39	14	184.5	40.0
	50	4.64	13	163.5	11.1
	70	4.87	12	146.1	-1.1
	90	5.06	11	132.1	-4.8
	110	5.18	11	121.5	-3.4
	130	5.21	10	114.5	0.8
Ave	10	1.94	20	220.1	113.0
	30	2.22	19	183.9	32.2
	50	2.35	17	160.3	6.5
	70	2.42	16	142.5	-3.0
	90	2.43	15	129.1	-4.6
	110	2.35	14	119.5	-2.1
	130	2.18	13	113.6	2.5
VP	10	-0.75	25	224.1	86.1
	30	-0.34	23	177.8	18.4
	50	-0.16	21	152.1	0.4
	70	-0.06	20	135.0	-4.1
	90	0.00	18	123.6	-2.8
	110	0.02	17	116.4	1.1
	130	0.03	17	112.6	6.0

We find an approximate 2-dB difference in average gain as we change soil types, regardless of height. Over very good soil, the equilateral delta reaches maximum gain with a base height of 130', a wholly impractical height, considering the added height of the antenna. Over average soil, the gain peaks at a base height of 90'. However, over very poor soil, the gain does not reach a maximum value within the sampling range. **Fig. 4-7** graphically portrays the data.

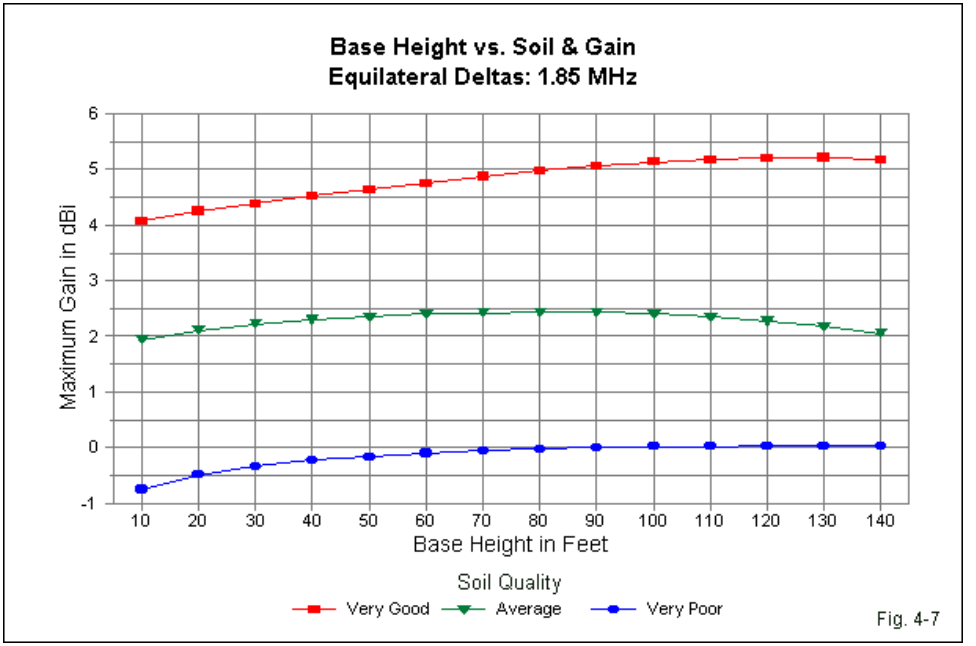

Fig. 4-7

All of the curves are fairly flat. Still the curve for average soil has distinct downward slope at higher base levels. Of course, the difference in gain between the lowest sampled height and the peak gain is only on the order of 1-dB, thus making the antenna usable at low levels. When considering an equilateral delta below 40' on 160 meters, note the rapid increase in both the resistive and the reactive components of the feedpoint impedance. Very low base heights will require a somewhat smaller loop circumference to achieve near-resonance.

We may usefully compare the 160-meter data with the 80-meter (3.55 MHz) information in **Table 4-3**. (The corresponding gain graph appears in **Fig. 4-8**.) For this sample I used 10' increments from 10' up to 70' for the base height. The heights for maximum gain are 60' for very good soil and 40' for average soil. These two values are not quite direct scalings of the 160-meter values. Once more, the progression of values for very poor soil does not show a distinct peak.

Equilateral Deltas for 80 Meters					Table 4-3
Base Height and Soil Quality vs. Performance					
3.55 MHz					
Soil	Ht ft	Gain dBi	TO deg	Feed R	Feed X
VG	10	3.63	16	198.7	66.4
	20	3.87	16	174.0	20.8
	30	4.06	14	154.8	2.0
	40	4.21	13	139.2	-5.4
	50	4.32	12	126.9	-6.5
	60	4.35	12	118.0	-3.9
	70	4.28	11	112.3	0.6
Ave	10	1.29	21	198.6	53.9
	20	1.50	20	169.6	13.3
	30	1.60	18	149.3	-1.4
	40	1.64	17	134.3	-5.9
	50	1.61	16	123.4	-5.1
	60	1.52	15	116.1	-1.7
	70	1.37	14	111.8	3.0
VP	10	-0.66	25	188.3	33.2
	20	-0.25	24	158.0	5.1
	30	0.04	22	139.5	-2.9
	40	0.28	21	127.2	-3.7
	50	0.48	19	119.2	-1.2
	60	0.67	19	114.4	2.6
	70	0.83	18	112.1	6.7

The data and the graph show an interesting trend when we compare the values with those for 160 meters. Over very good and average soils, the ratio of peak gain to lowest gain is smaller on 80 meters. Moreover, the average gain values for 160 meters are about 0.8-dB higher than on 80 meters. In contrast, over very poor soil, the range of peak to low gain values is twice as high on 80 meters as it is on 160 meters. In addition, the highest value shown is about 0.8-dB higher on 80 than on 160. Gain trends that apply to very good through average soil show a reversal when we reduce the soil quality to a very poor level. However, trends in the TO angle and the impedance remain consistent.

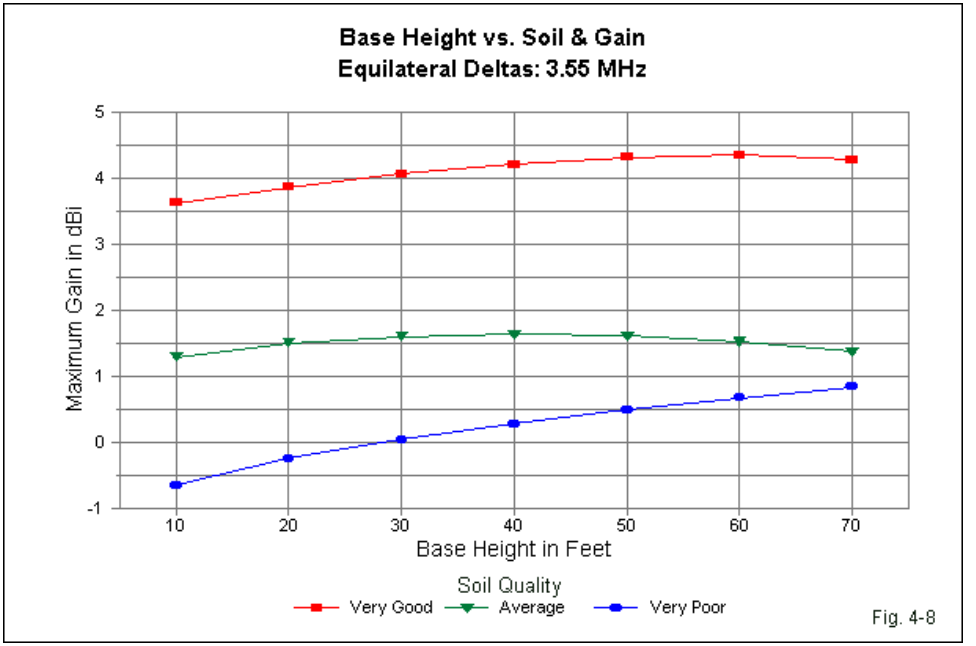

Fig. 4-8

The gain graphs show clearly the differences in behavior with changes in soil quality. Perhaps the most vivid sample occurs with the highest base level in both graphs. On 160 meters, the gain value for average soil is about 2-dB higher than the value for 80 meters. On 80 meters, the difference has shrunk to about 0.5-dB.

Once more, the overall antenna height of an 80-meter equilateral delta is too great to expect installation at the optimal base height. Using a lower base height, especially a base height below about 30', requires attention to the proper loop size if the builder wishes to achieve near resonance. Even a near-resonant condition will leave a relatively high resistive feedpoint impedance. As a result, many equilateral delta builders use parallel transmission line and an antenna tuner as part of the feed system.

Equilateral Deltas for 40 Meters					Table 4-4
Base Height and Soil Quality vs. Performance					
7.15 MHz					
Soil	Ht ft	Gain dBi	TO deg	Feed R	Feed X
VG	5	2.84	18	200.3	67.1
	10	3.06	17	173.3	23.2
	15	3.20	16	153.3	6.1
	20	3.30	15	137.6	0.0
	25	3.33	14	125.7	-0.2
	30	3.28	13	117.4	2.9
	35	3.14	12	112.2	7.7
Ave	5	0.86	23	195.1	52.8
	10	1.13	21	166.0	16.4
	15	1.30	20	146.4	4.0
	20	1.41	18	132.2	0.8
	25	1.47	17	122.3	2.3
	30	1.47	16	115.8	6.0
	35	1.42	15	112.3	10.5
VP	5	-0.25	26	179.0	38.0
	10	0.23	24	153.0	13.1
	15	0.60	22	137.1	6.0
	20	0.91	21	126.6	5.2
	25	1.19	20	119.8	7.1
	30	1.44	19	115.7	10.3
	35	1.65	19	113.7	13.7

The trends that we saw when comparing 160-meter and 80-meter data continue as we explore the 40-meter (7.15-MHz) data in **Table 4-4** and the corresponding gain graph in **Fig. 4-9**. Peak gain over very good soil drops by another full dB, but only by about 0.2-dB on 80 meters. Over very poor soil, we again find no absolute peak. However, with a base height of 35', the gain of the delta loop actually exceeds the peak gain that we achieve over average soil at a base height between 25' and 30'. The slope of the gain curve for very poor soil does not give any evidence of peaking within the next 5' to 10' at least. The very-poor soil line shows a very wide gain range.

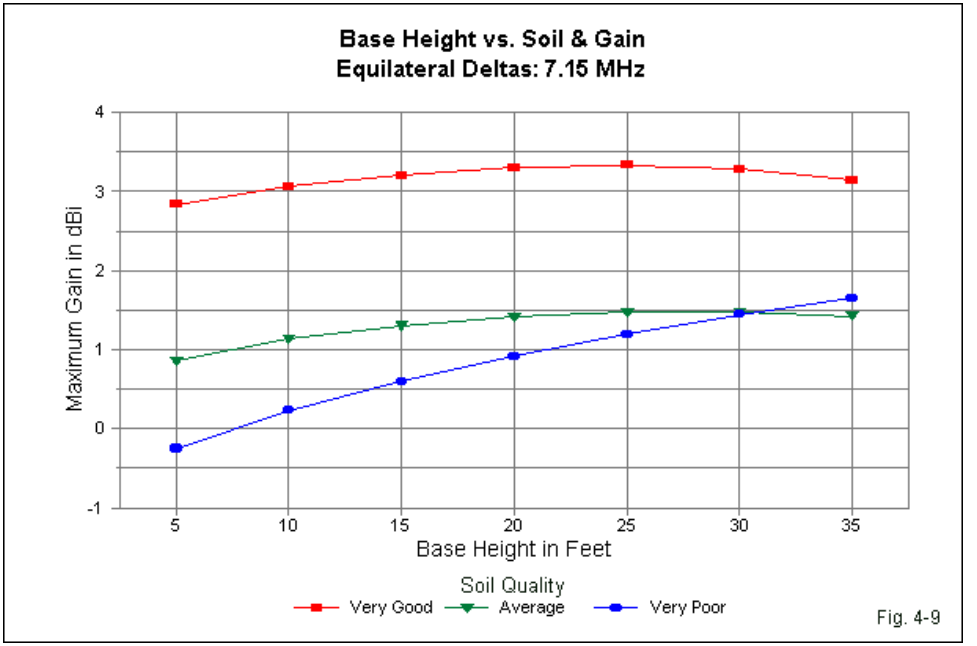

Fig. 4-9

Indeed, on 40 meters, the gain curves are flat enough to allow effective use of an equilateral delta SCV at virtually any reasonable height above ground. (Of course, one must allow for the reactance increase as we decrease the base height if one wishes near-resonant operation.) By way of contrast, base height may be more critical to the use of an equilateral delta over very poor soil: within reason, the higher, the better.

Elevation patterns differ according to soil quality. **Fig. 4-10** overlays elevation patterns for the 3.55-MHz delta with a base height of 50', the mean between peak-gain heights for very good and average soil. The patterns include all three soil types. As we improve the soil quality, the general level of high-angle radiation goes down and the secondary elevation lobes at higher angles become more distinct. These general properties appeared in Chapter 1, when we examined the behavior of elevation patterns produced by simple vertical dipoles.

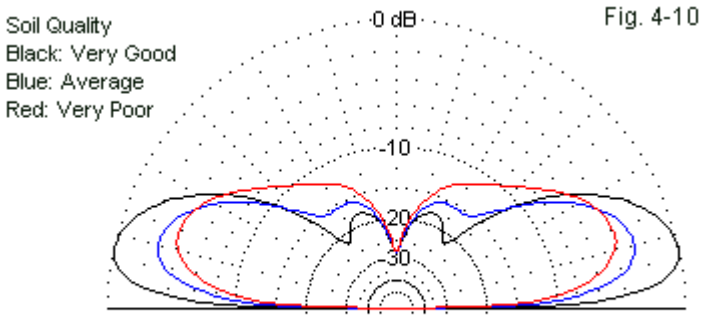

Fig. 4-10

Comparative Elevation Patterns: 3.55-MHz Equilateral Delta at a 50' Base Height above Various Soils

On 80 meters, the optimal base height for maximum gain is about 40’ over average soil. We may usefully compare the elevation pattern over this soil with patterns taken about 20’ below optimum and 20’ above optimum, as shown in **Fig. 4-11**. Note that at either non-optimal level, higher-angle radiation is greater, in one case by virtue of the general pattern shape, in the other case as a result of emerging secondary elevation lobes.

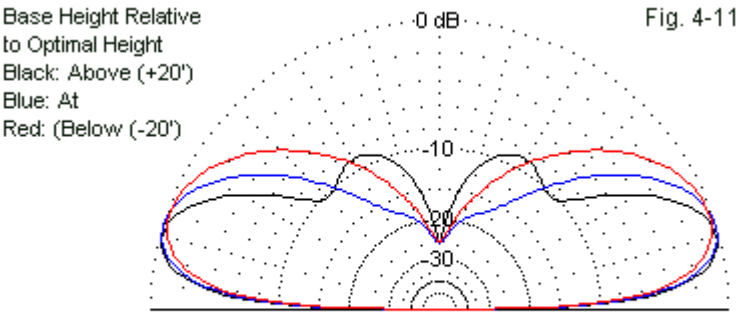

Fig. 4-11

Comparative Elevation Patterns: 3.55-MHz Equilateral Delta over Average Soil above, at and below Optimal Gain Height

The equilateral delta SCV is perhaps the lowest-gain SCV of any common form. Its use tends to result from that fact that it does provide some bi-directional gain over a single vertical dipole and it requires only one very high support point. The lower corners can use sloping tensioned ropes to hold the antenna in place, even with fairly high base levels. Of our delta options, the equilateral version also requires the least horizontal real estate. Nevertheless, many delta fans have gravitated to flatter triangles.

The Right-Angle Delta SCV

Within limits, the flatter that we make the triangle, the higher will be the bi-directional gain potential. Therefore, many delta users have moved toward the right-angle delta, which provides at optimal base heights a 0.4 to 0.5 dB gain benefit. The antenna has a number of added advantages. One is the ease of calculating the proportions. The height is ½ the base, and the sloping legs are 1.414 times the height. When we install the antenna close to the optimum base level for maximum gain, we obtain an impedance that is compatible with common 50-Ω coaxial cables. **Fig. 4-12** provides the basic outline of a right-angle delta along with the dimensions used in this exercise. The listed dimensions result in near-resonant impedances when the base level is in the vicinity of the level needed for maximum gain.

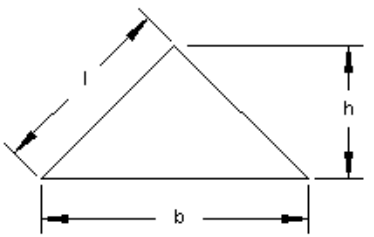

Right-Angle Deltas for SCV Use

Dimensions

Freq.	1.85 MHz	3.55 MHz	7.15 MHz
B (base)	232.6'	121.7'	60.8'
H (height)	116.3'	60.85'	30.4'
L (leg)	164.5'	86.1'	43.0'
Circumference	561.6'	293.8'	146.8

Fig. 4-12

On 160 meters, the right-angle-delta base levels that yield maximum gain are quite comparable to the values required for the equilateral delta. **Table 4-5** provides the data, supplemented by the gain graph in **Fig. 4-13**.

Right-Angle Deltas for 160 Meters					Table 4-5
Base Height and Soil Quality vs. Performance					
1.85 MHz					
Soil	Ht ft	Gain dBi	TO deg	Feed R	Feed X
VG	10	4.23	17	103.0	88.3
	30	4.65	16	87.7	30.8
	50	4.90	15	78.0	11.2
	70	5.12	13	69.8	2.1
	90	5.33	12	62.8	-1.9
	110	5.50	12	57.1	-2.7
	130	5.59	11	52.8	-1.8
	150	5.59	10	50.0	0.3
Ave	10	2.13	22	110.3	88.4
	30	2.59	20	89.2	26.8
	50	2.77	19	77.2	8.2
	70	2.86	17	68.2	0.5
	90	2.89	16	61.2	-2.4
	110	2.86	15	55.8	-2.5
	130	2.75	14	52.0	-1.1
	150	2.55	13	49.7	1.1
VP	10	-0.60	27	117.3	73.6
	30	0.04	25	88.4	18.2
	50	0.27	23	74.0	3.5
	70	0.37	21	64.5	-1.5
	90	0.41	20	58.0	-2.4
	110	0.42	18	53.6	-1.4
	130	0.41	17	50.9	0.5
	150	0.39	17	49.5	2.7

The data has one surprise. On 160 meters, and only on 160 meters, the curve for very poor soil shows a definite peak with a base height of 110'. Otherwise, the data is consistent with equilateral-delta data once we make a suitable gain adjustment. One of those consistent properties is the need to reduce the size of the loop if we wish to obtain a near-resonant feedpoint impedance in installations that use relatively low base heights. This need is

relatively independent of the soil quality.

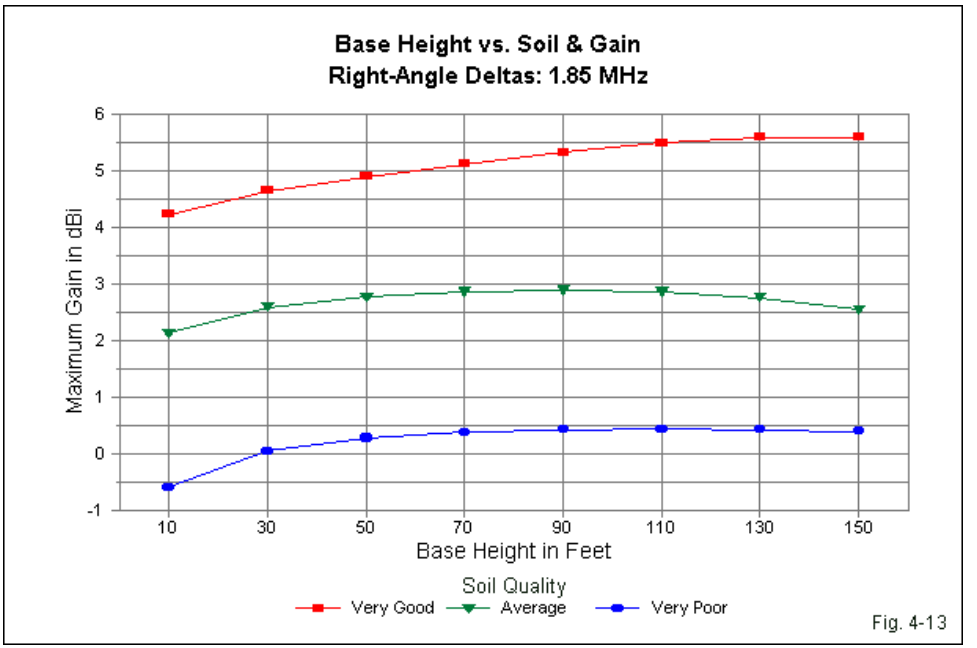

Fig. 4-13

A detailed look at the gain curves also yields another way in which the right-angle delta differs from its equilateral brother. Whereas the equilateral showed downward bends in the lines for very good and average soil, those bends now occur with the right-angle delta's average and very poor soil curves.

At 3.55 MHz, the data in **Table 4-6** and the curves in **Fig. 4-14** appear somewhat more akin to the corresponding information for the equilateral delta. The optimal base heights for the right-angle delta are about 1 step higher than for the equilateral delta. In addition, the gain progression over very poor soil no longer shows a peak value within the sampling range, since the rate of gain increase with increasing height is greater as we increase the operating frequency. In other words, the curve for very poor soil is steeper as we increase the

frequency. However, the very-poor-soil curve is not steep enough to permit its line to intersect with the average soil line within the sampling limits. For both the equilateral and the right-angle deltas, there remains a 0.5-dB difference in gain at the highest sampled base level between the two soil types. Indeed, except for the slightly higher gain values, the 80-meter curves for both type of deltas look amazingly similar.

Right-Angle Deltas for 80 Meters					Table 4-6
Base Height and Soil Quality vs. Performance					
3.55 MHz					
Soil	Ht ft	Gain dBi	TO deg	Feed R	Feed X
VG	10	3.93	18	94.7	49.2
	20	4.22	17	82.4	17.6
	30	4.42	16	73.3	4.3
	40	4.59	14	65.7	-1.9
	50	4.73	13	59.3	-4.3
	60	4.81	12	54.3	-4.4
	70	4.82	12	50.7	-2.0
	80	4.73	11	48.4	-0.9
Ave	10	1.63	23	97.7	43.3
	20	1.95	22	81.6	12.9
	30	2.09	20	71.1	1.5
	40	2.15	18	63.2	-3.1
	50	2.16	17	57.2	-4.3
	60	2.10	16	52.9	-3.6
	70	1.99	15	50.0	-1.9
	80	1.81	14	48.3	0.2
VP	10	-0.47	27	94.7	29.6
	20	0.05	25	76.6	6.5
	30	0.36	24	66.1	-0.9
	40	0.59	22	59.1	-3.2
	50	0.78	21	54.3	-3.0
	60	0.96	20	51.2	-1.7
	70	1.11	19	49.4	0.0
	80	1.25	18	48.6	1.8

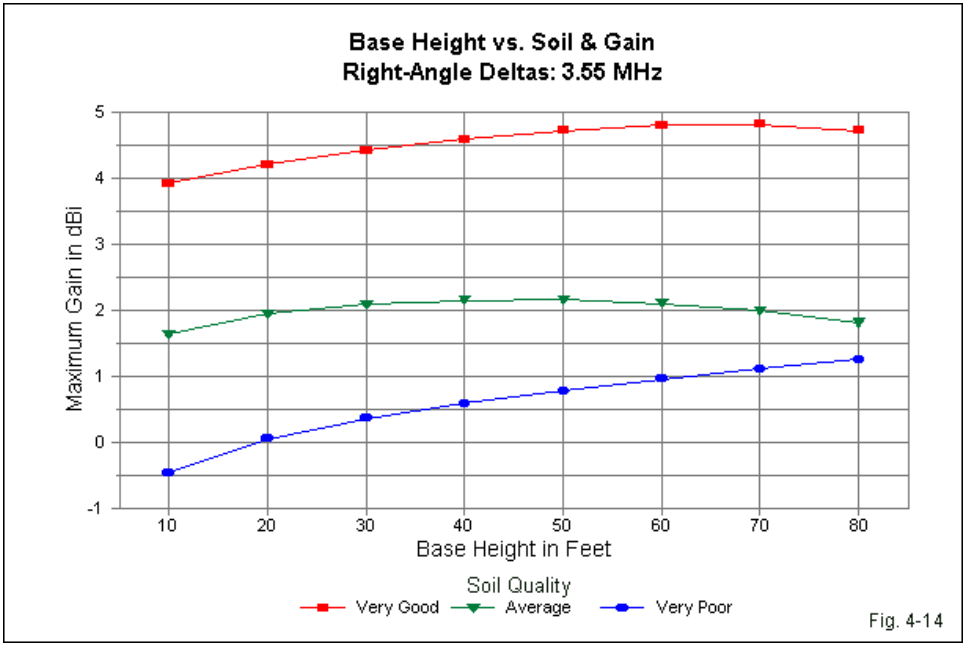

Fig. 4-14

Except for a half-dB gain advantage over the equilateral deltas, the 7.15-MHz right-angle delta gain numbers (**Table 4-7**) and curves (**Fig. 4-15**) look just like the ones for the taller antenna. The peak values for very good and average soil occur about 5' higher than for the equilateral triangle. The gain curve for very poor soil is even steeper than the one for the earlier antenna, with a total range of over 2.2 dB between base heights of 5' and 40'. The gain curves on the graph cross at about the 35' base level, where both soil types show a gain value of about 2 dBi. It is useful to remember that while all gain values over very good and average soil decrease as frequency increases, the curves for very poor soil show the opposite trend. The peak gain over very poor soil at 7.15 MHz is about 1.5 dB higher than at 1.85 MHz.

With a base height of at least 20' over any of the soil types, the feedpoint impedance for the SCV feedpoint is roughly compatible with coaxial cable

service. The modeled SCV feedpoint is 85% of the distance along a sloping leg counting from the apex downward. Because the feedpoint is so far along the sloping leg, corner-feeding a right-angle delta creates smaller reductions in performance than the same feedpoint on the equilateral delta, where the feedpoint is about 75% of the distance down a sloping leg.

Right-Angle Deltas for 40 Meters					Table 4-7
Base Height and Soil Quality vs. Performance					
7.15 MHz					
Soil	Ht ft	Gain dBi	TO deg	Feed R	Feed X
VG	5	3.19	20	95.7	49.5
	10	3.49	19	81.8	18.1
	15	3.66	17	71.9	5.5
	20	3.79	16	64.1	-0.1
	25	3.87	15	57.8	-1.9
	30	3.88	14	53	1.7
	35	3.81	13	49.6	-0.1
	40	3.65	12	47.6	2.1
Ave	5	1.16	24	95.5	41.5
	10	1.55	23	79.2	13.3
	15	1.76	21	68.8	3.1
	20	1.9	20	61.1	-0.6
	25	1.97	18	55.6	-1.3
	30	2.01	17	51.6	-0.4
	35	1.98	16	49.1	1.3
	40	1.91	15	47.7	3.3
VP	5	-0.12	28	87.9	30.1
	10	0.46	26	72.5	9.3
	15	0.86	24	63.4	2.7
	20	1.18	23	57.5	0.7
	25	1.46	21	53.4	0.8
	30	1.71	20	50.8	1.8
	35	1.93	19	49.2	3.2
	40	2.13	19	48.5	4.7

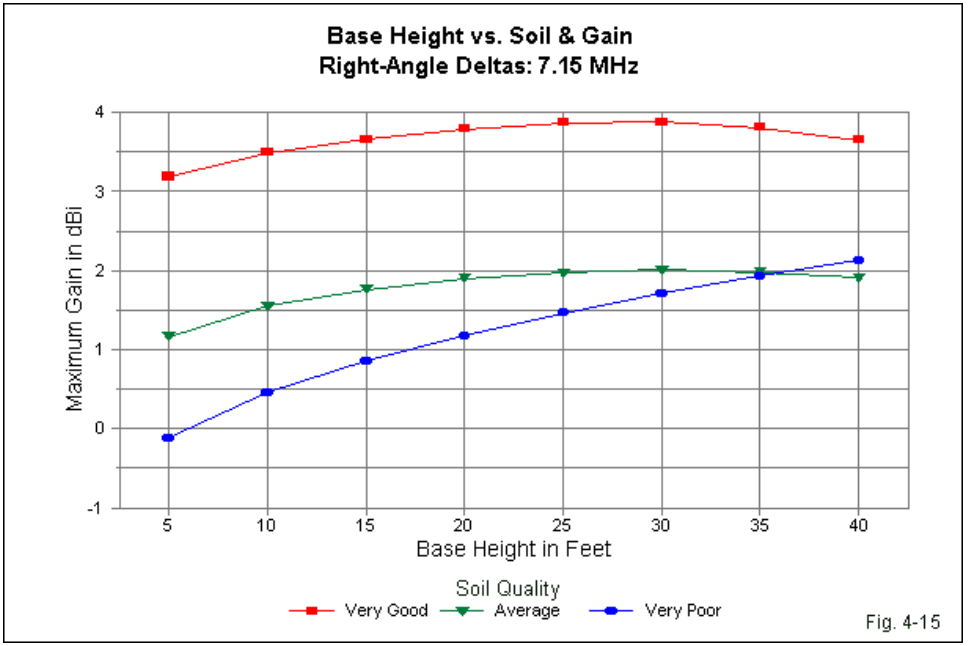

Fig. 4-15

The gain advantage of the right-angle delta over the equilateral delta is between 0.4 and 0.5 dB. In addition the right angle delta is a shorter antenna at any of the frequencies, although it does require addition horizontal room for the longer base. We can obtain a small amount of additional gain by further flattening the delta, but at a cost of further reductions in the feedpoint impedance. For this practical reason, most amateur users of deltas limit themselves to the right-angle version of the array.

A Few Comparisons

The review of delta performance using two versions of the array has confirmed a number of properties of vertically polarized antennas above various soil types as we change frequency. We shall see similar properties in future chapters as we compare delta performance to other SCV forms. Indeed, the data

presentation is designed for relatively easy comparison among antenna types.

We may also compare the right-angle and equilateral deltas in terms of radiation patterns, as shown in **Fig. 4-16**.

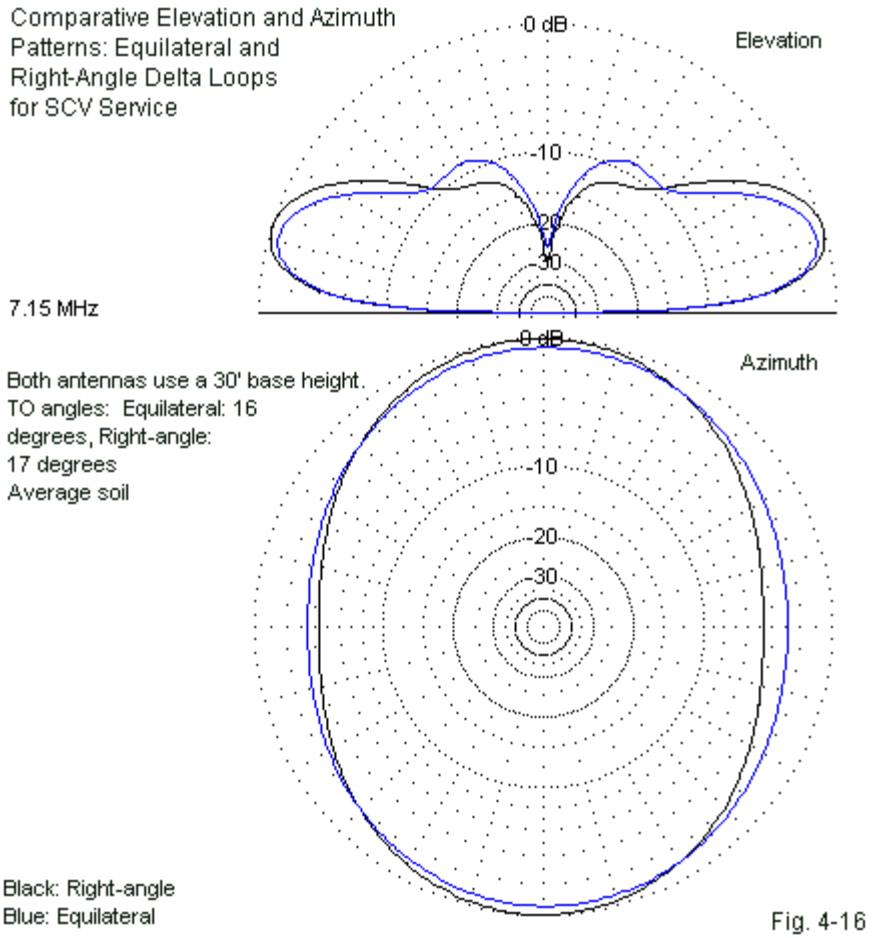

Fig. 4-16

The patterns are for 7.15-MHz deltas with a base height of 30' above average soil. The equilateral delta is the taller antenna, and its feedpoint is a bit higher from the ground than the feedpoint of the right-angle delta. As a consequence, the equilateral delta elevation pattern shows a more distinct beginning for a secondary elevation lobe.

The TO angles for the azimuth patterns are 1° apart. Both patterns show slightly higher side gain to the right in the patterns than to the left. Indeed, on the feedpoint side of the pattern, the equilateral delta shows a larger gain increment than the right-angle version. The average difference in the edgewise gain values for the two deltas provides broadside gain advantage for the right-angle delta.

The gain differences stem from the fact that the spacing between the real feedpoint and its virtual counterpart is larger for the right-angle delta than for the equilateral triangle. An SCV increases in gain as it comes closer to an "ideal" half-wavelength spacing between real and virtual feedpoints. No closed SCV form can achieve a true half-wavelength spacing and still remain closed, although some forms will come close. As well, practicality dictates that we end the gain chase when the feedpoint impedance becomes too low for easy matching.

Table 4-8 compares the performance of the right-angle delta with a single vertical dipole and with 2 fed in phase.

Comparative Performance: Right-Angle Delta, Single Vertical Dipole, and 2 Vertical Dipoles Fed In Phase
7.15 MHz, Average Ground, Base Height 20'

Ant	Top Ht	Gain dBi	TO Deg	BW Deg
1 V Dpl	87	0.29	14	
2 V Dpl	87	4.38	15	62
RA Delta	50.4	1.9	20	116
Notes:	1 V Dpl = single vertical dipole			
	2 V Dpl = 2 vertical dipoles, 1/2-wl apart,			
	fed in phase			
	RA Delta = right-angle delta loop			
				Table 4-8

All of the antennas have a 20' base level, which gives the vertical dipoles a feedpoint height advantage. This fact appears in the well-developed secondary elevation lobe in both dipole patterns. The delta pattern shows only a single elevation lobe.

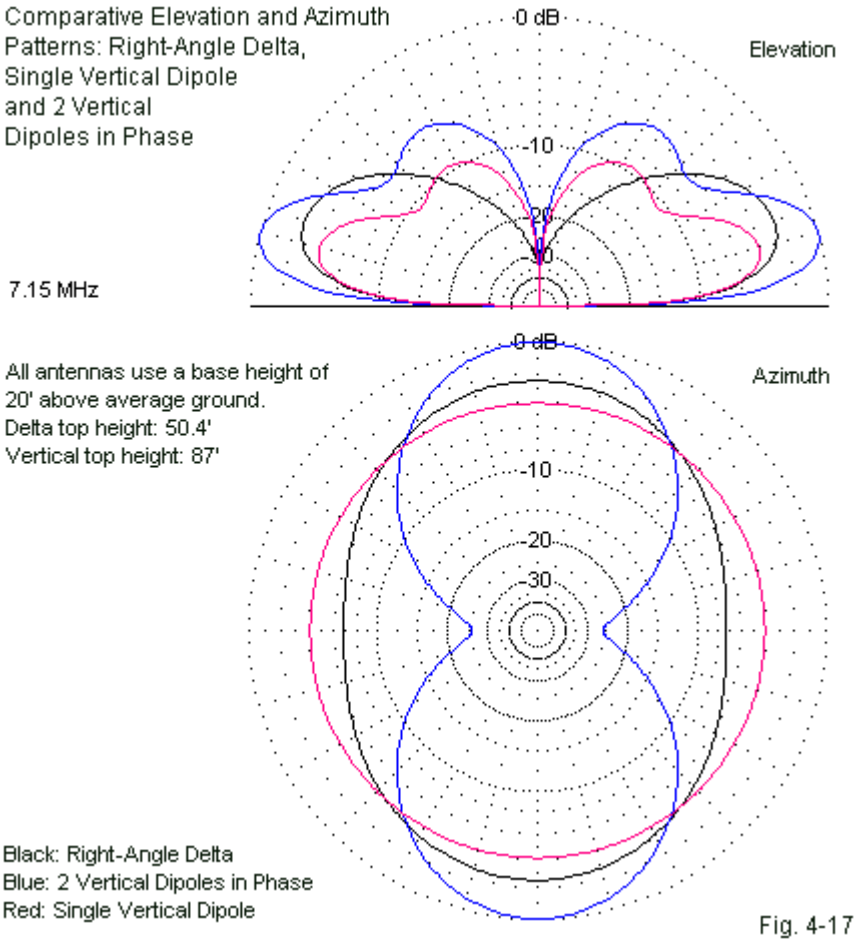

Fig. 4-17

The single dipole shows a circular azimuth pattern, as we would expect. In contrast, the in-phase-fed dipoles with a half-wavelength spacing show a well-developed peanut that is verging on a true figure 8. The right-angle delta has a broadly oval pattern, even though it is more elongated than the corresponding pattern for the equilateral delta might be. We may use the azimuth pattern shape as a measure of how far from ideal a delta SCV is. Indeed, the delta gain is considerably closer to the gain of a simple dipole than it is to the gain of phase-fed dipole pairs in a standing H.

Feeding the Right-Angle Delta SCV

Because we normally feed an equilateral delta using parallel transmission line and an antenna tuner, we tend not to be concerned about precise loop lengths or precise feedpoint impedance values. The proximity of the right-angle delta feedpoint impedance to 50 Ω brings these concerns front and center. **Fig. 4-18** shows the resistance and reactance curves for a 40-meter right-angle delta with a base height of 30'. Both lines are nearly linear. However, pay close attention to the Y-axis scales as they apply to resistance and reactance, respectively.

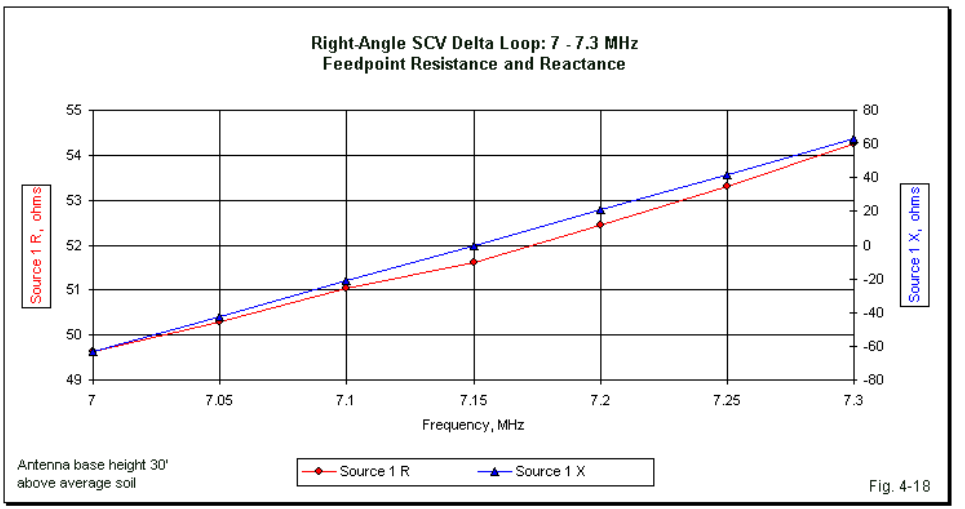

Fig. 4-18

Across a bandwidth greater than 4%, the feedpoint resistance changes by only 4 Ω. In contrast, the reactance changes by about 120 Ω. The reactance is the chief limitation in feeding a right-angle delta via coaxial cable. One design solution is to begin with a delta that is somewhat inductively reactive at the lower operating frequency. For any given base height, this procedure would involve making the loop larger and a bit flatter than the dimensions with which we started. (See **Fig. 4-12**.) At the feedpoint, the designer installs a series capacitor capable of remote tuning (and weatherproofing). For operation across the entire 40-meter band, the operator then needs only to tune the capacitor for the lowest SWR.

The same technique is applicable on 80 and 160 meters, although its utility is restricted to a subpart of these wider bands. As well, these lower bands will require capacitors with wider ranges to exceed a 4% bandwidth. Remember that the capacitor's minimum capacitance level must match the highest inductive reactance on the antenna's feedpoint. For practical reasons of component support, the technique often appears at corner rather than true SCV feedpoints.

Improving the Local Ground

In Chapter 1, we explored whether the use of a radial system beneath a vertical dipole had any positive benefits that would justify the expense and energy required to put one in place. We concluded that if the base of a vertical dipole was quite close to the ground and if the soil was quite poor to very poor, then improving the local ground beneath the antenna might be useful. As we elevated the base of the antenna above ground or moved the antenna over better soil, the benefits shrunk accordingly. An amateur installation rests upon the considered decision by a station operator about the balance between performance level and installation effort and cost. Therefore, we cannot make a final decision. Nevertheless, the data may be useful to the operator's decision-making process.

We can perform a similar function relative to improving the local ground beneath a delta loop. Let's consider a 40-meter right-angle delta with a base height of 20'. Then we shall add one of three forms of local ground improvement, as shown in **Fig. 4-19**. The first is a set of 64 30' radials centered under the apex of the delta. These radials approximate the usual ¼-λ radial set that we often

think about first when considering monopoles. Note that we are using, by amateur standards, a rather full radial set. We shall bury the AWG #12 copper radials 1' below ground level.

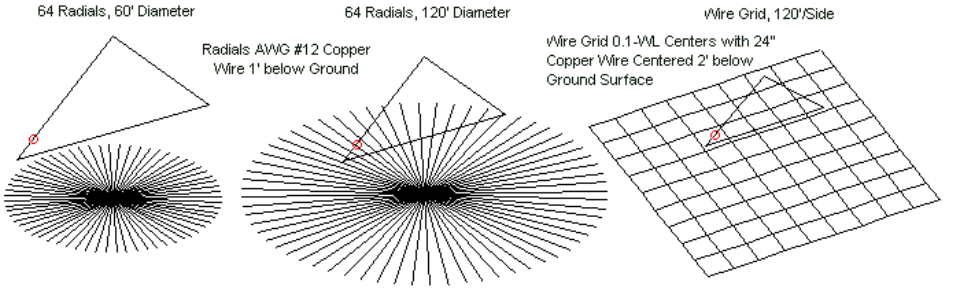

Right-Angle Delta at 7.15 MHz with 3 Forms of Local Ground Improvement

Fig. 4-19

The second system doubles the length of each radial. The system diameter is now 120' and extends over 30' beyond both the actual feedpoint and the virtual feedpoint on the opposing sloping leg of the delta. This system is also AWG #12 copper wire that is 1' below the surface of the ground. The final ground improvement consists of a wire-grid in the model to simulate as reasonably well as possible the use of a wire mesh to improve the local ground. The grid extends for 120' on a side. Relative to the extended radial system, the grid fills in the corners. The modeling constraints on a wire-grid of this sort consist of calling for a wire diameter that is very large so that a relatively small number of wires, as shown in the sketch, can simulate a solid surface. I used a wire diameter smaller than normal. By placing the wire centers 2' below ground and using a 2' wire diameter, the surface of the grid is at the 1' level. However, the grid is not sufficient to call it a solid surface simulation. Hence, we may think of it as a mesh.

Table 4-9 provides the data from the 3 experiments for our 3 soil quality values. The table also includes the data for the antenna's modeled performance without any ground improvement. The goal is not to be definitive. Instead, we wish only to obtain some indication of whether the work improves performance.

Improving the Ground Beneath a Delta Loop for 7.15 MHz					
Right-Angle Delta with 20' Base Height					
Ground	Soil	Gain dBi	TO deg	Feed R	Feed X
None	VG	3.79	16	64.1	-0.1
	Ave	1.90	20	61.1	-0.6
	VP	1.18	23	57.5	0.7
Rad-30	VG	3.82	16	64.3	0.5
	Ave	2.03	20	61.4	1.0
	VP	1.38	23	57.4	3.0
Rad-60	VG	3.87	16	65.3	0.1
	Ave	2.27	20	67.2	-0.1
	VP	1.90	24	70.3	3.7
WG-60	VG	3.90	16	65.0	-0.9
	Ave	2.54	20	67.1	-4.3
	VP	2.37	25	70.9	-3.6
Notes:	None = no ground treatment				
	Rad-30 = 64 30' radials centered beneath delta				
	Rad-60 = 64 60' radials centered beneath delta				
	WG-60 = wire grid 60' on a side				
	Radial buried 1' below surface; wire-grid 2' below				
	surface with 24" diameter wires				Table 4-9

When we think of local ground improvement, we often immediately think of radials. However, since the local ground improvement does not also perform an antenna-completion function, the key to obtaining any sort of improvement is area coverage, not the wire layout. Wherever in the table that we find improvement, the square wire-grid provides the best coverage and the most improvement.

Just as we found for the simple vertical dipole, improvement varies with soil quality. With very good soil, even the largest coverage provides a gain improvement of about 0.1 dB. Over average soil, the range of improvement is only about 0.6 dB. The small radial field with a 60’ diameter that barely reaches the limits of the delta base improves performance by about 0.1 dB. We require the full 120’ coverage to obtain maximum improvement.

If we have very poor soil, we obtain the greatest improvement: about 1.2 dB using the wire-grid mesh. Note that, unlike the situation with better soil qualities, we obtain a considerable portion of the improvement by shifting from a 120' diameter radial system to the grid that is 120' on a side.

Most of the benefit consists in reducing the losses directly beneath the antenna. Since most of the far-field reflection occurs beyond the limit of the local ground improvement effort, we do not see any changes in the TO angle for the 2 better soils and only a small rise in the angle over very poor soil. Whether the performance improvements justify the time, energy, and expense of local ground improvement remains a user decision.

Smaller and Bigger Deltas

At ant given frequency, an equilateral delta is about 40% taller than a right-angle delta. To shrink the equilateral delta to a workable size, builders have employed a number of techniques. All of them involve the use of wires placed at one or another high-voltage, low-current region of the antenna. The top or apex of the delta is the more popular point for adding the wire, although the center of the horizontal base wire is in principle equally apt for treatment. Similar treatments have appeared on the elements for shrunken quad elements and beams.

Fig. 4-20 shows some of the techniques translated into working models of equilateral delta quads. The STW or single top wire method runs a wire from the apex downward. In the 40-meter models, a 27.7' foot wire allows us to arrive at resonance with an equilateral triangle that is only as tall as the full size right-angle delta. We may shrink the delta even further if we add T-hats to the wire, as shown in the STWT model. The SBW or single bottom wire technique runs a 23.75' wire upward from the center of the bottom wire and arrives at a triangle the same size as the STW version. Using the same size triangle, we may substitute a shorted transmission line section, as shown in the outline for the STL model. The line is 24.7' long and uses 1' spacing between the parallel wires. The outline sketches also show the current distribution on each wire, including the ones used to shrink the overall delta size.

The feedpoint position varies with the shortening method in an effort to reduce the horizontal radiation component to a minimum. **Fig. 4-20** provides a typical set of elevation and azimuth patterns, since all of the models produce almost identical patterns. Note that the horizontal component in the azimuth pattern is somewhat higher than we obtain with a full-size delta.

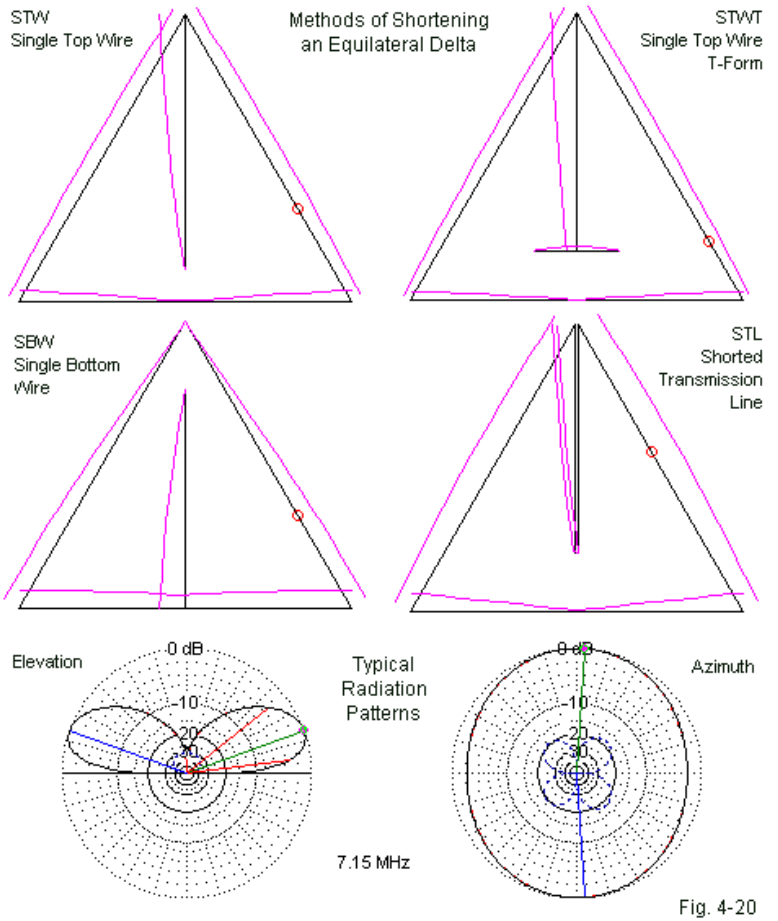

Fig. 4-20

Equally important is the performance data for these shrunken deltas, compared to the performance of a full-size equilateral triangle. **Table 4-10** supplies the model reports, including the base length and height for each triangle. Perhaps the most striking fact is the loss of gain relative to the full-size delta. However, note that the version using the T-hat wire (STWT) to effect a modest further size reduction reduces gain by a sizable amount. Therefore, we immediately see that there are limits to the shrinking process before the gain drops to an unacceptable level.

Comparison of Methods of Shortening a 7.15-MHz Equilateral Delta Loop								Table 4-10
AWG #12 Copper Wire; Base Height 20' Above Average Soil								
Method	Base	Height	Wire	Feed Pos	Gain dBi	TO deg	Feed R	Feed X
None	48.8	42.26		75	1.41	18	132.2	0.83
STW	36	31	27.7	70	0.75	20	44.4	-3.1
STWT	32	27.7	22.75	80	0.18	21	26.2	-2.2
SBW	36	31	23.75	70	0.69	19	20.8	2.4
STL	26	31	24.7	45	0.68	20	48.2	-1.6
Notes:	None = full-size equilateral delta loop							
	STW = single top wire: 1 wire from apex downward							
	STWT = single top wire with T" one wire from apex downward with two 4.32' T wires							
	SBW = single bottom wire: 1 wire from center of base upward							
	STL = single shorted parallel transmission line stub with 1' wire spacing							
	Feed Pos = feedpoint position as a percentage of distance from apex down one leg							

Among the 31'-tall models, the two versions that shorten from the apex downward (STW and STL) achieve feedpoint impedances similar to those that we obtain from a right-angle delta. Shortening from the bottom up (SBW) yields a much lower feedpoint impedance that may call for complex matching efforts.

For comparison, a right-angle delta with a base height of 20' and a top height just over 50' on 40 meters shows a potential gain of about 1.9 dBi. The shrunken equilateral deltas have gain values over a full dB lower. However, the full-size right-angle delta requires a base length of about 60'. The final decision among the various delta options may ultimately rest upon the physical properties of the installation site.

Not only can we shrink a delta, we may also expand it, assuming that we have the necessary space. The most common form for such antennas is the so-

called double-delta, actually a junction of two right-angle deltas in a line. **Fig. 4-21** shows the general outline of a version of the antenna for 40 meters. The dimensions are those of the single right-angle delta doubled in overall length to 121.6' total. The height remains the same at 50.4', but now consists of twin peaks.

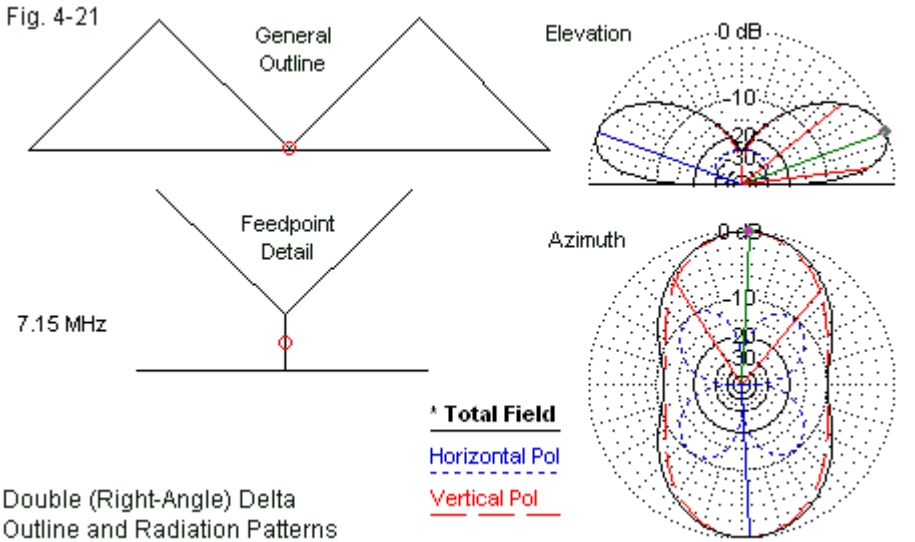

Double (Right-Angle) Delta
Outline and Radiation Patterns

The inset in the figure shows the detail of the feedpoint. We feed the two deltas in parallel, which forces us to feed the array at the corner of each delta rather than at the optimal SCV position. Each outer corner of the array will show a current level about half the value of the current at the feedpoint, indicating close to binomial feeding of the three elements. (The inner sloping legs of the array count as one element, while the outer sloping legs each count as an additional element. The counterpart to the double delta is the 3-element vertical dipole array with the elements properly phase fed.)

As a consequence of feeding the double delta at a corner, the horizontal

component of the azimuth pattern is higher than we find in single deltas, but still 10 dB below the gain of the total field. We may vary the feedpoint impedance to some degree by altering the separation between the base wire and the top of the feed wire.

The gain of a right-angle double delta is about 3.8 dBi (compared to 1.9 dBi for a single right-angle delta with the same base height). The TO angle remains at 20° elevation. Unlike the broad oval of the single right-angle delta, the double version has a distinct shape that begins to show slight side nulls regions. The beamwidth in each broadside direction is about 73°. These modeled values are for average soil.

The double delta is only the first of many doubled SCV forms. By the end of our journey, we shall be interested in comparing the potential performance of them all. (See the Appendix for the performance comparisons of 40-meter models over average soil and for the dimensions of single deltas for 160 through 30 meters.)

Parasitic Delta Beams

One largely untapped potential for deltas, especially right-angle deltas, is the creation of parasitic beams. (I hesitate to call them Yagis, lest someone re-dub them delta Yagis or Dagis for short.) The techniques required to form a working 2-element parasitic beam that is reversible are far simpler than trying to tame the array for phased service. We begin by forming two identical driver-size deltas, as shown in **Fig. 4-22**.

Because the driver element for a reflector-driver bream will be shorter (or smaller, in the case of a closed loop) than a single element, the sample 40-meter delta beam will use triangles with a base that is 59.3’ long, with a height of 29.65’. These dimensions are about 2.5% smaller than the single right-angle delta that we have used on this band, with both antennas having a 20’ base height. However, the final dimensions are a function of the element spacing, and the spacing in turn rests on the desired feedpoint impedance. For direct feed with a 50-Ω transmission line, 20’ between delta loops works very well.

Since the reflector must be electrically larger than the driver, we must add one or another form of inductive loading. A j50-Ω load at the position on the reflector that corresponds to the feedpoint on the driver provides the elevation and azimuth patterns shown in the figure. The forward gain is 5.19 dBi over average soil, a gain advantage of about 3.3 dB over the bi-directional gain of a single delta. The front-to-back ratio is 11.37 dB. It is possible to adjust the load value to obtain higher front-to-back ratios, but one may also have to reset the spacing to achieve a 50-Ω feedpoint impedance. The beamwidth is about 85° in the forward direction.

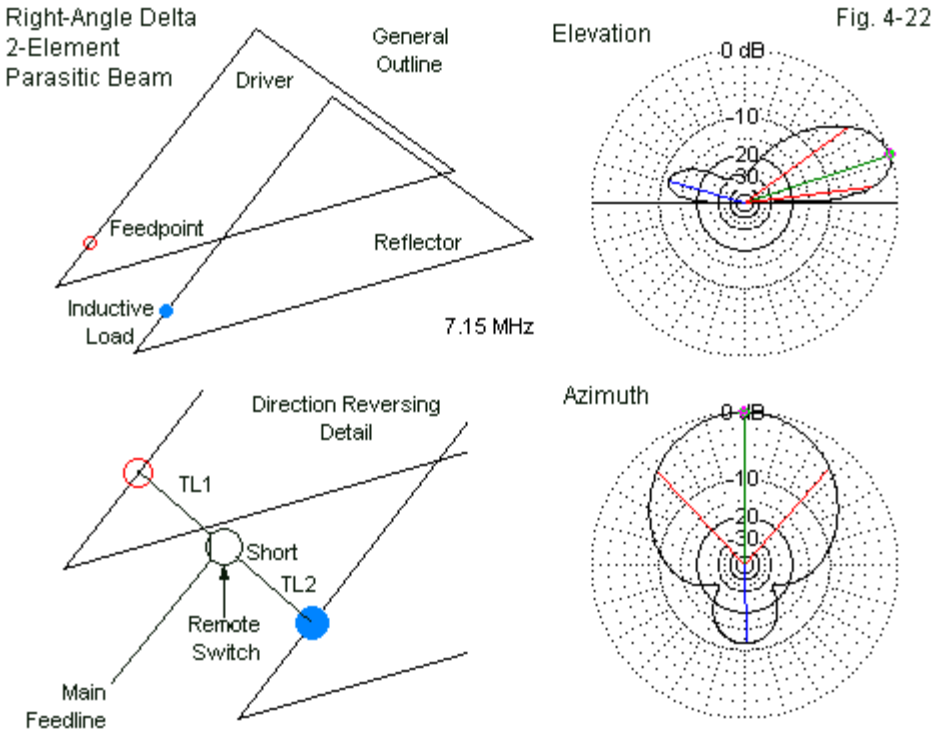

The lower left portion of the outline sketch provides us with the importance of arriving at close to a 50-Ω impedance. (The model shows an impedance of 50.3 + j1.8 Ω.) To achieve a j50-Ω reflector load, we might use an inductor. Alternatively, we may use a shorted transmission-line stub calculated to yield the proper inductive reactance. If we select a 50-Ω line for the stub, it will be about 17.2' long with a velocity factor of 1.0. Even a velocity factor of .67 will yield a physical stub length of 11.5', just enough to reach the centerline between the two elements.

Next, let's bring the same length of feedline from the driver to the centerline. At the potential junction, we may install a manual or a remote switch that accomplishes the functions shown in **Fig. 2-10**. One short line becomes a simple extension of the transmission line to the driver. The other short line becomes a shorted stub. The switch alternates functions, resulting in a reversible fixed-position beam.

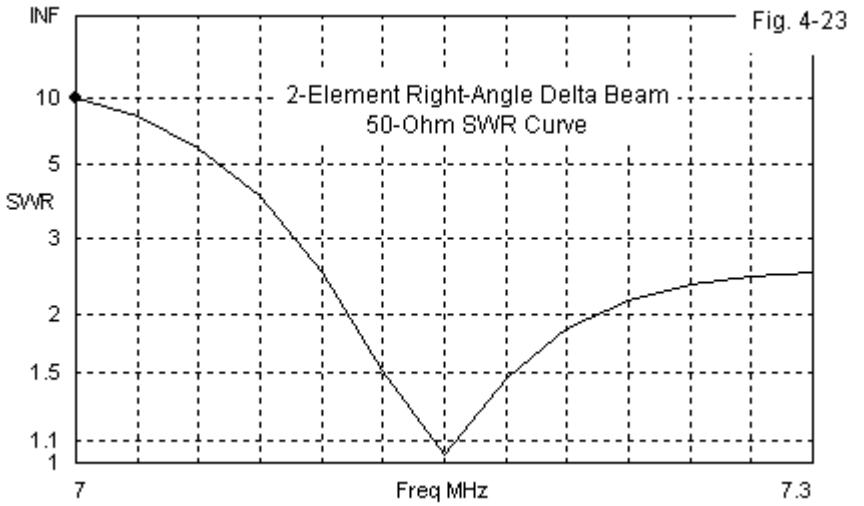

One limitation of the 40-meter 2-element delta beam is that is has a fairly narrow operating bandwidth that does not quite cover half of 40 meters. See **Fig.**

4-23. Consequently, the beam may prove somewhat finicky to adjust initially. We may apply the same technique used to form the delta beam to other SCV forms. Although the gain of each reversible SCV beam will vary somewhat, they all will exhibit the same limitation in the SWR bandwidth.

Conclusion

Although there are possible VHF and UHF applications for the delta SCV, triangles are rare at the higher frequencies, that is, above the HF region. Other SCV forms have found more extensive use due to their improved performance and, in many cases, simpler construction. For example, it is often easier to construct the crossing supports for a square quad loop than it is to form 3 legs to support a delta loop, especially if the legs use unequal angles to form a right-angle triangle.

We began our journey among the SCVs by examining the delta because this particular form has perhaps the lowest performance level of any of the overall group. The fundamental reason for the relatively low gain of even a right-angle delta is the limitation on the spacing between the two vertical elements that are in-phase with each other. Many of the SCV forms to come will improve upon that spacing, while still falling short of an ideal ½-λ.

Modelers who examine the current tables for any of the SCV forms may raise an eyebrow over the fact that the current at the virtual second feedpoint is 180° out of phase with the feedpoint current. For example, the segment facing the feedpoint on the opposing leg of one delta shows a current of 0.992 at 179.4° in contrast to a feedpoint current of 1.0 at 0°. A voltage phase reversal also occurs in the model, even though voltage data is usually not accessible in the output reports. Hence, the two sloping elements remain in-phase with each other, with a minor allowance for the losses associated with copper wire at the operating frequency. The reversal in the model occurs as a result of the fact that we model triangles (and other loops) as continuous ribbons. Ideally, we should start each side of the triangle at the base-wire midpoint, working outward and then upward to the apex. This practice would reflect that same procedure that we generally apply to modeling independent vertical dipoles. (Of course, in both cases, we

may also model from the top down, so long as we are consistent within a given model.) The resulting model would then show the phasing conditions that exist in a physical antenna. See the Appendix for a small set of exercises on the relationship of model set-ups to physical antennas.

Despite its limitations, the delta remains a favored option for creating a bi-directional vertically polarized array for lower HF use among a wide group of amateurs who have access to only one high support. With the correct orientation, the array provides gain over a vertical dipole in two major directional areas. (The beamwidth of a single delta is too wide to think of definite directions. The better idea is directional areas.)

In addition, the delta illustrates almost all of the possibilities and potentials that we may expect of any SCV form, including the ability to create a doublewide array and to construct reversible parasitic beams. So we may view the delta as a prototype of SCVs to come. We briefly noted the absence of significant VHF and UHF applications for the delta. Those applications will abound for our next SVC form, the diamond.

5. Diamond (Quad) SCVs

The SCV that we call the “diamond” is actually an elongated diamond, that is, lengthened parallel to the ground and flattened vertically. It derives from the square diamond shape that we sometimes see in horizontally polarized quad beams for the upper HF region. Even in its long, squat form, we shall not initially become enthused with the diamond, especially if we keep in mind the performance figures for the right-angle delta. However, we shall discover some interesting properties when we double the diamond and even more when we examine some of the many VHF and UHF applications for this SCV form. We shall develop these fascinating aspects of the diamond slowly so that we fully understand how the diamond relates to the entire family of SCVs.

The Square Diamond SCV

We shall note the square diamond shape as a wire SCV for the lower HF region only long enough to see why we shall elongate the form. **Fig. 5-1** sketches the basic outline and 40-meter dimensions of the square diamond.

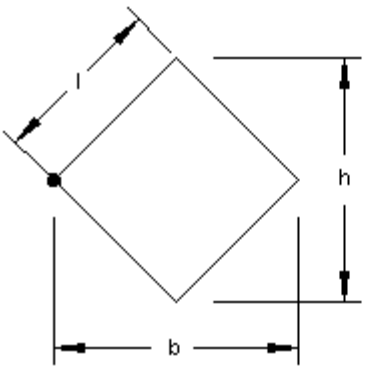

7.15-MHz Diamond-Shaped Quad Loop for SCV Use

Dimensions

Freq.	7.15 MHz
B (base)	51.3'
H (height)	51.3'
L (leg)	36.3'
Circumference	145.0'

Fig. 5-1

We recognize the square diamond as simply a side-fed quad loop. Since the form is square, the base and height are identical. Each side is 0.707 times either value. The circumference is similar to the circumference of a delta, since both types of antennas rest on the use of loops just over 1-λ to achieve a near-resonant feedpoint impedance. The square quad loop is largely impractical on 40-meters and below, since it requires more height than any other SCV form. **Table 5-1** provides some further reasons why the squared diamond has few uses as an SCV. The table does not go beyond the data over average soil. Even with the restricted data set, we can see the antenna's lower gain relative to a right-angle delta, as well as its higher impedance. The impedance may be a problem to those who prefer coax feedlines, but a blessing to those opting for parallel feedlines.

Square Quad for 40 Meters					Table 5-1
Base Height and Soil Quality vs. Performance					
7.15 MHz					
Soil	Ht ft	Gain dBi	TO deg	Feed R	Feed X
Ave	5	1.08	20	181.1	13.3
	10	1.29	18	158.4	-0.8
	15	1.43	17	143.2	-3.6
	20	1.50	16	133.0	-1.6
	25	1.52	15	126.8	2.6
	30	1.48	14	123.6	7.4
	35	1.42	14	122.8	11.9

In the preceding chapter, we found that flattening a triangle—for example, from an equilateral form to a right-angle form—gave us two advantages. First, it spread the distance from the actual feedpoint to its virtual counterpart toward an ideal half-wavelength spacing. Although no closed loop can reach the ideal spacing, every increase shows a rise in gain until the vertical legs become short enough to result in a gain reduction. Second, as we elongate the triangle, we see the feedpoint impedance decrease. Normally, we stop the stretching process when the impedance is near the 50-Ω mark. However, the arrest is arbitrary in the sense that if we continue to strength and flatten a triangle, the gain will continue to rise, although the impedance may fall to undesired levels.

The “stretch-and-flatten” process is not unique to triangles. Rather, it is inherent to any SCV form. **Fig. 5-2** compares the bi-directional elevation and azimuth patterns of a square diamond to an elongated diamond when both use the same base height at 7.15 MHz. The elongation yields about a dB of added gain, accompanied by a reduction in the energy to the sides (that is, edgewise to the diamond plane). Even when we cut off the elongation process upon reaching a 50-Ω feedpoint impedance, we obtain worthwhile advantages. As well, we lower the overall height of the array.

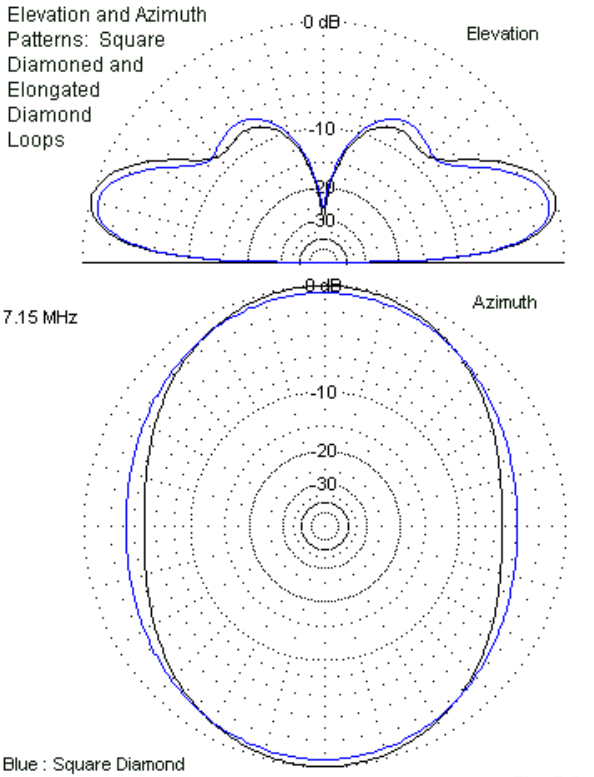

Fig. 5-2

The Elongated Diamond SCV

We shall focus our attention on diamonds that we have stretched to produce a 50-Ω feedpoint impedance. For many SCV users, the form shown in **Fig. 5-3** is among the most practical. The figure also charts the dimensions used to develop 160-, 80-, and 40-meter versions of the antenna using AWG #12 copper wire. These antennas, like all of the SCVs in these notes, represent a compromise design that is usable over soil qualities that range from very good to very poor. Note that the side-corner feedpoint position does not change in the process of flattening.

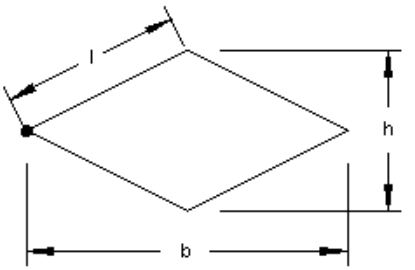

Diamond Loop for SCV Use

Dimensions

Freq.	1.85 MHz	3.55 MHz	7.15 MHz
B (base)	254.0'	131.4'	64.4'
H (height)	117.0'	64.4'	34.0'
L (leg)	139.8'	73.2'	46.4'
Circumference	559.3'	292.7'	145.6

Fig. 5-3

Because AWG #12 wire becomes thinner as a function of a wavelength as we lower the operating frequency, the base-to-height ratio is not constant. It ranges from 2.17:1 at 1.85 MHz down to 1.89:1 at 7.15 MHz. Like almost all antennas based on the vertical dipole, the feedpoint impedance does not change very rapidly as we move the antenna from some high base level closer to the ground—until we reach a quite low base height. Because the feedpoint of the diamond is elevated relative to the comparable point on a delta, the increase in both the resistive and reactive components does not occur until we reach a lower base level. The impedance levels are not very far apart for any given base height, regardless of soil type.

Although feedpoint impedance is stable relative to soil type, the shape of the elevation patterns may vary considerably when we place the diamond at the optimal height for maximum gain relative to a given soil quality. **Fig. 5-4** shows overlaid elevation patterns for a 160-meter diamond under these conditions for very good, average, and very poor soil.

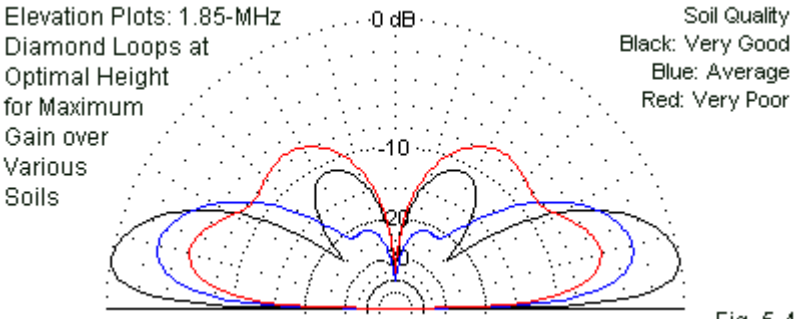

Fig. 5-4

The diamond achieves maximum gain on 160 meters at relatively high base levels when the soil is either very good or very poor. Hence, the elevation patterns show well-developed secondary elevation lobes at high angles. (By now, we expect secondary elevation lobes over very good soil to be quite distinct with a deep null between lobes. In contrast, we also expect secondary lobes over very poor soil to blend more seamlessly with the lower main lobe, with no distinct null angle to mark their boundary.) In contrast to the extremes in soil quality, average soil produces a lower height at which maximum gain occurs. As a result, the secondary elevation lobe is just beginning to emerge. One consequence of this condition is that the antenna is relatively insensitive to signals and noise from high-angle sources.

Because we shall be interested in comparing the performance of the diamond to the right-angle delta in the preceding chapter, we should explore the 4-sided SCV on each of the bands that we have selected for detailed study. The data for 1.85 MHz appear in **Table 5-2**, while **Fig. 5-5** graphs the gain curves over the range of sampled base heights, that is, the height of the antenna's lowest point.

Elongated Diamonds for 160 Meters					Table 5-2
Base Height and Soil Quality vs. Performance					
1.85 MHz					
Soil	Ht ft	Gain dBi	TO deg	Feed R	Feed X
VG	10	4.55	16	81.6	54.7
	30	4.83	15	71.0	20.2
	50	5.06	14	63.2	7.0
	70	5.28	13	56.6	0.9
	90	5.47	12	51.0	-1.5
	110	5.61	11	46.6	-1.7
	130	5.67	10	43.4	-0.5
	150	5.62	10	41.5	1.4
Ave	10	2.39	21	86.0	50.3
	30	2.67	20	71.6	16.7
	50	2.80	18	62.4	4.8
	70	2.87	17	55.3	-0.1
	90	2.88	15	49.8	-1.7
	110	2.82	14	45.7	-1.3
	130	2.69	13	43.0	0.1
	150	2.46	12	41.4	1.9
VP	10	-0.38	26	89.8	38.4
	30	0.07	24	70.2	10.2
	50	0.26	22	59.9	1.5
	70	0.37	20	52.3	-1.3
	90	0.43	19	47.4	-1.4
	110	0.47	17	44.2	-0.3
	130	0.50	17	42.2	1.4
	150	0.51	16	41.4	3.2

The relevant right-angle delta information to use for comparison appears **Table 4-5** and **Fig. 4-13**. Perhaps the most surprising fact may be the tiny differences in performance between the two 50-Ω SCVs. The diamond performs slightly better at lower heights due to the elevated feedpoint. However, virtually any differences in performance between the two SCVs would be so small that construction and site variables would override them.

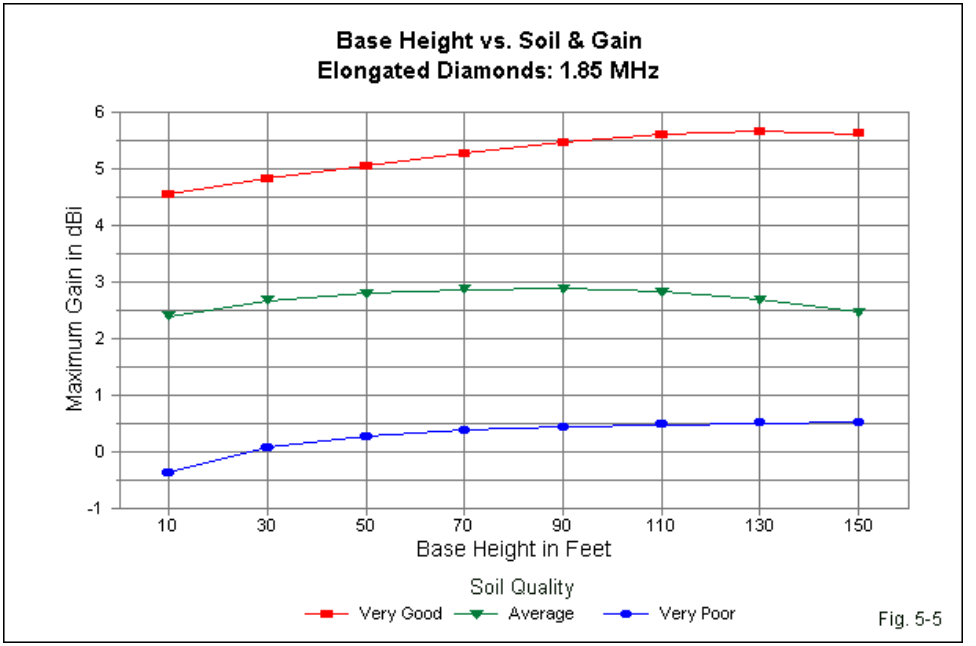

Fig. 5-5

The gain graphs for the various soil types are sufficiently similar that we might overlay one on the other and watch half of the lines disappear. The gain curves for very good and very poor soil show a flattening only at the upper end of the base-height scale. However, the gain curve for average soil peaks at about 90' above ground and then shows a definite decline in the maximum broadside gain.

We may continue the comparison at 3.55 MHz in order to assure ourselves that 160 meters is not an aberrant band. The 80-meter data appears in **Table 5-3**, while the corresponding gain graph is in **Fig. 5-6**. See **Table 4-6** and **Fig. 4-14** for the comparative right-angle delta information.

Once more, the most striking fact within the data comparison is how close together the right-angle delta and the diamond values fall. Only at the lowest base heights do the diamond data show any signs of an advantage.

Elongated Diamonds for 80 Meters					Table 5-3
Base Height and Soil Quality vs. Performance					
3.55 MHz					
Soil	Ht ft	Gain dBi	TO deg	Feed R	Feed X
VG	10	4.15	17	83.0	36.0
	20	4.37	16	72.7	14.6
	30	4.56	15	64.7	5.5
	40	4.71	13	58.0	1.4
	50	4.83	13	52.7	0.3
	60	4.88	12	48.6	0.9
	70	4.84	11	45.8	2.6
Ave	10	1.78	22	84.1	29.2
	20	1.99	20	71.3	10.8
	30	2.10	19	62.5	3.5
	40	2.14	17	55.9	0.9
	50	2.14	16	51.0	0.7
	60	2.07	15	47.6	1.8
	70	1.94	14	45.4	3.6
VP	10	-0.24	25	80.3	19.1
	20	0.21	24	66.6	6.3
	30	0.52	22	58.2	2.2
	40	0.78	21	52.7	1.4
	50	1.01	20	48.9	2.1
	60	1.21	19	46.6	3.6
	70	1.40	18	45.3	5.2

The gain curves, of course, reflect the data and show the same trends that we encountered with the right-angle delta. We find a somewhat wider gap between the gain over very good vs. average soil, and a smaller gap between average and very poor soil than we encountered on 160 meters. As well, the gain curve over very poor soil is steeper on 80 than on 160. As a result, the gain level for diamonds mounted at quite high base levels above very poor soil begins to approach the descending gain for the same antenna over average soil. Indeed, there is a numerically noticeable (although operationally insignificant) improvement in diamond performance over very poor soil relative to right-angle

delta performance over the same soil.

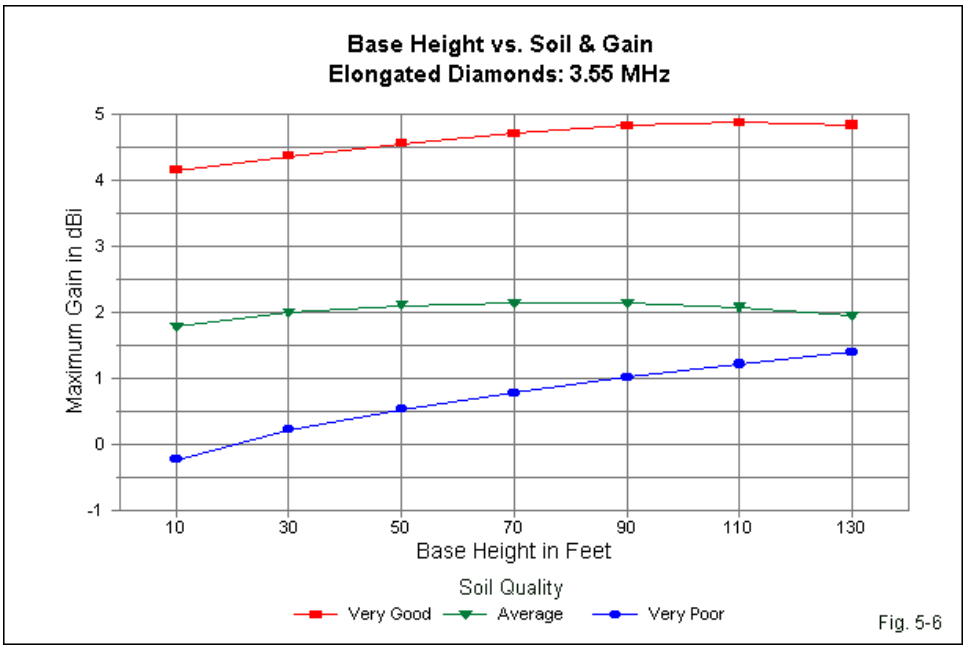

Fig. 5-6

If our examination of 160 and 80 meters has in fact produced a trend, especially with respect to the performance over very poor soil, then we ought to be able to make a fuzzy but true prediction of the 40-meter gain curves. The diamond gain curve for very poor soil should cross the gain curve for average soil at a lower height than the point we saw in the right-angle delta data and curves in **Table 4-7** and **Fig. 4-15**. The data for the elongated 7.15-MHz diamond in **Table 5-4** and the graphs in **Fig. 5-7** should tell us whether we have a true trend in hand.

Neither the data nor the graph will disappoint us. Whereas the gain data approached equality at the 35' base-height level with the right angle delta over very poor soil, the diamond shows crossing values at the 30' base height level.

Elongated Diamonds for 40 Meters					Table 5-4
Base Height and Soil Quality vs. Performance					
7.15 MHz					
Soil	Ht ft	Gain dBi	TO deg	Feed R	Feed X
VG	5	3.36	19	91.7	27.2
	10	3.56	17	79.1	6.7
	15	3.71	16	69.8	-1.8
	20	3.81	15	62.5	-5.1
	25	3.86	14	56.8	-5.6
	30	3.83	13	52.7	-4.4
	35	3.71	12	50.0	-2.4
Ave	5	1.33	23	89.8	19.7
	10	1.62	21	75.9	3.0
	15	1.80	19	66.6	-3.2
	20	1.93	18	59.8	-4.9
	25	2.01	17	55.0	-4.5
	30	2.03	16	51.8	-3.0
	35	2.00	15	49.9	-1.0
VP	5	0.23	26	82.3	12.4
	10	0.75	24	69.8	1.1
	15	1.14	22	62.1	-2.5
	20	1.48	21	57.0	-3.1
	25	1.78	20	53.7	-2.4
	30	2.05	19	51.6	-1.0
	35	2.28	19	50.5	0.6

Like the 40-meter right-angle delta curve for very poor soil, the corresponding diamond curve shows an increasing rate of gain increase per unit of base height relative to the two lower frequencies in the survey. We may also note a feature that is consistent for all diamonds, regardless of frequency: the improved performance at very low base heights. Nevertheless, for the vast majority of situations sampled by these models, the difference in performance between the right-angle delta and the elongated diamond is not sufficient to serve as a decisive factor in choosing between the two types of SCVs. Site and construction factors will likely be the keys to decision-making.

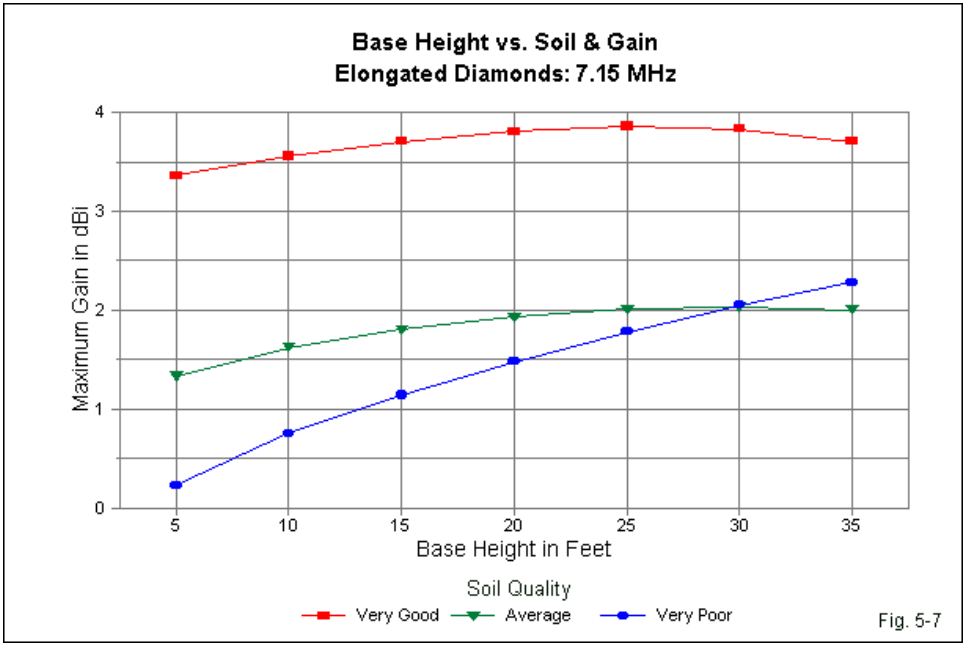

Fig. 5-7

For any given band, a right triangle will have a shorter base line and height than a corresponding elongated diamond. Even here, the difference is not as much as one might initially suspect. At 40 meters, the diamond is about 4' longer (base) and about 3.5' taller (height) than the corresponding 50-Ω right-angle delta.

The Double Diamond SCV

Just as we were able to create a double right-angle delta to increase bi-directional gain, we can multiply the single diamond to make a double diamond. In fact, we shall use the same technique of joining two diamonds at the center, with a cross wire between the upper and lower halves of the wire run. **Fig. 5-8** provides a general outline of the array, with an exploded view of the feedpoint connection. The figure also provides a set of current distribution curves to show

that the double diamond is indeed the counterpart of the double right-angle delta. The feedpoint current will be about twice the level as the current on the outer points of the array, indicating that the antenna is a form of a 3-dipole, in-phase-fed array, but with a single feedpoint and shrunken spacing between the center and outer dipoles.

Fig. 5-8

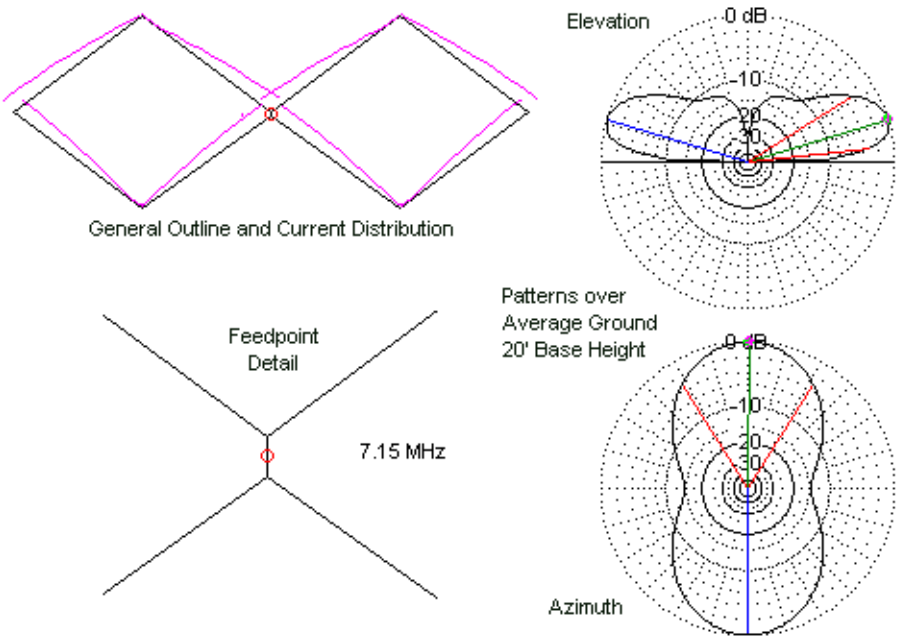

Basic Outline and Patterns of the Double (Elongated) Diamond

The figure also shows the elevation and azimuth patterns of the double diamond at a base height of 20' above average ground. The distinct nulls or insets along the plane of the wires suggest that we should see a gain improvement from the double formation.

Double Elongated Diamonds for 40 Meters					Table 5-5
Base Height and Soil Quality vs. Performance					
7.15 MHz					
Soil	Ht ft	Gain dBi	TO deg	Feed R	Feed X
VG	5	5.88	17	73.3	1.0
	10	6.09	16	63.9	5.8
	15	6.20	15	57.4	-7.5
	20	6.23	14	52.6	-6.8
	25	6.18	13	49.3	-4.9
	30	6.03	12	47.4	-2.4
	35	5.77	11	46.7	0.3
Ave	5	3.96	21	70.4	0.2
	10	4.16	19	61.5	-5.5
	15	4.28	18	55.6	-6.3
	20	4.33	17	51.6	-5.2
	25	4.32	16	49.1	-3.2
	30	4.26	15	47.8	-0.9
	35	4.14	14	47.6	1.3
VP	5	3.03	24	65.6	0.0
	10	3.42	22	58.3	-3.7
	15	3.73	21	53.9	-3.9
	20	4.01	20	51.2	-2.8
	25	4.24	19	49.6	-1.2
	30	4.44	19	49.0	0.5
	35	4.61	18	49.0	2.0

Table 5-5 provides the data to confirm our suspicion for the 40-meter model of the double diamond. Regardless of soil type, the maximum gain for the larger array is about 2.3-dB higher than for a single diamond. This gain improvement is about half-dB more than the improvement of a double-delta over a single right-angle delta, largely due to the fact that the double diamond feedpoint is optimally positioned.

In addition, the required base height for maximum gain over very good and average soil decreases relative to the required height for a single elongated

diamond. At 40 meters, the height is only about 20'. See **Fig. 5-9** for the gain curves. Note that the gain curve for very good soil parallels more closely the curve for average soil. In addition, the double diamond shows a greater rate of gain increase over very poor soil than we found with a single diamond. Hence, the gain levels cross the curve for average soil about 4' lower.

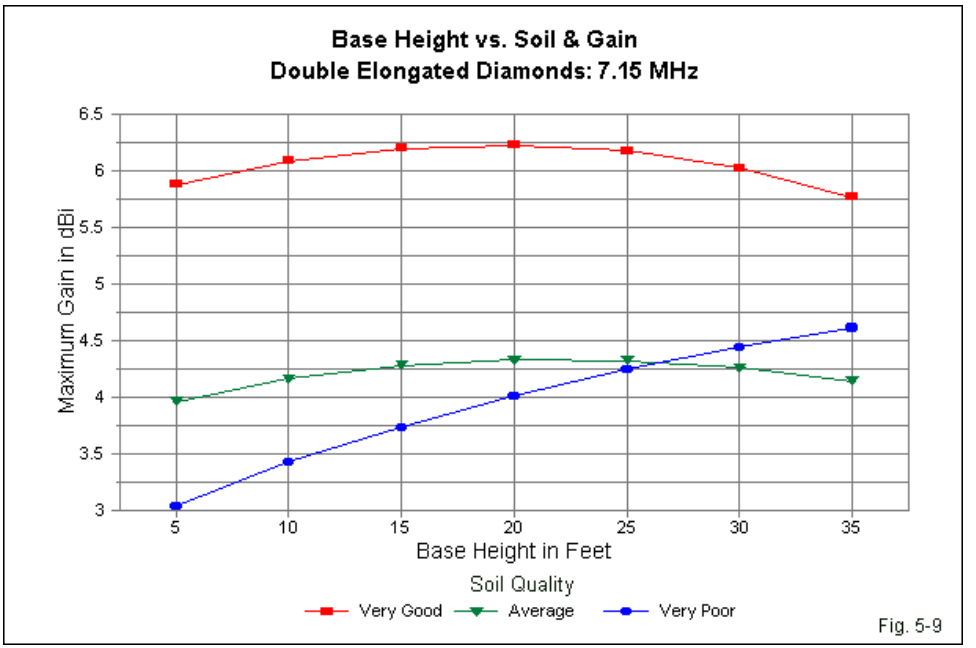

Fig. 5-9

To obtain a 50-Ω feedpoint impedance, we have to resize the diamonds somewhat relative to the dimensions for a single diamond. The single diamond had a 64.4' base and a 34' height. The 50-Ω double diamond uses a 115.6' (2 X 57.8') base with a 43' height. The requirement that we shorten the base and stretch the height indicates that a simple doubling of the single diamond would have resulted in a feedpoint impedance well below 50 Ω. If we select a base height of 20' for the array, then the top height will be about 63'. However, in all double SCVs, the feedpoint impedance will vary somewhat with the length of the

feedpoint wire. Models have a minimum length for the cross wire so that all model segments are close to the same length. As a result, the final dimensions that approach resonance may vary somewhat from the modeled dimensions.

Elevation Patterns of the Double Elongated Diamond at a Base Height of 20' above Various Soils Qualities

7.15 MHz

Soil Quality
Black: Vary Good
Blue: Average
Red: Very Poor

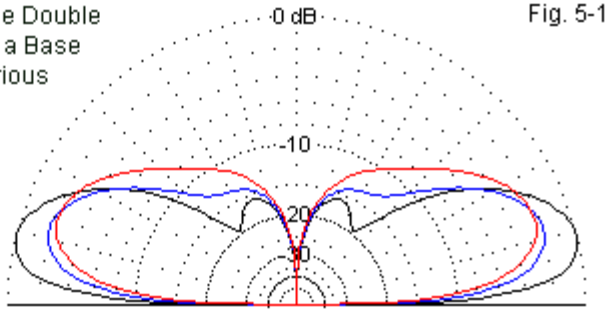

Fig. 5-10

With the base height set at 20', **Fig. 5-10** shows the resulting bi-directional elevation patterns. 20' feet is optimal for maximum gain over both very good and average soil. As well, the height is considerably less than the height for maximum gain of a single diamond over most of the soils. Consequently, the patterns in the figure all show less development of secondary elevation lobes at higher angles. For many, if not most, installations, the doublewide array will have less sensitivity to higher angle noise and signals than a single diamond at its optimal height for maximum gain.

The feedpoint impedance of the double diamond wire array is more stable with changes in base height than the impedance of a single diamond. For example, over average soil, a single diamond will show a resistance change of almost 40 Ohms as we raise the height from 5' to 35'. Over the same base height range, the reactance varies by about 25 Ω. The double diamond reduces the variation to about 23 Ω for resistance and 8 Ω for reactance. At the operating frequency, the double diamond will show no more than about than 1.4:1 50-Ω SWR over the height range of the samples. Moreover, the impedance changes slowly across the 40-meter band. **Fig. 5-11** provides a typical SWR curve for the 40-meter double diamond. It allows full coverage with a 2:1 SWR or better.

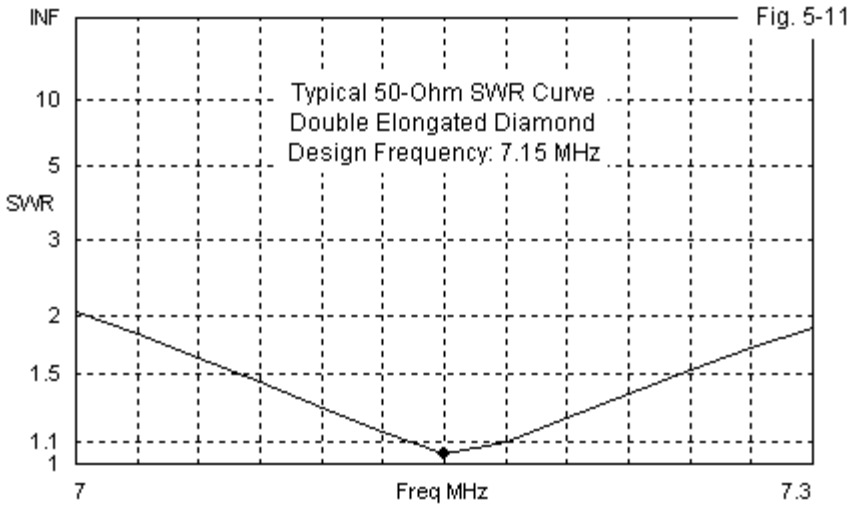

Although the single diamond seemed to be only a clone of the right-angle delta, the double diamond shows considerable promise as a bi-directional vertically polarized SCV. Of course, we may wish to withhold final decisions until we have looked at the entire SCV family. However, if the diamond has a niche among the SCVs, it is likely that it will earn its keep in double fashion.

We may also apply to the diamond all of the treatments that we tried out on the right-angle delta, especially the construction of a reversible directional parasitic beam. The similarity of performance between the delta and the diamond suggest that many of the same dimensions and techniques will be transferable between them. Rather than reviewing those elements from the preceding chapter, we shall explore some territory that we bypassed with the deltas: VHF and UHF applications. In this region, the diamond—including double and even quadruple versions—has acquired very high popularity.

VHF/UHF Diamond Drivers

In the VHF and UHF region, the diamond rarely occurs without some form of

reflector. Nevertheless, we need to examine the properties of various diamond configurations as bi-directional arrays in order to evaluate how effective the more complex antennas might be. Therefore, the place to start is with the simple side-fed diamond loop, as shown in **Fig. 5-12**.

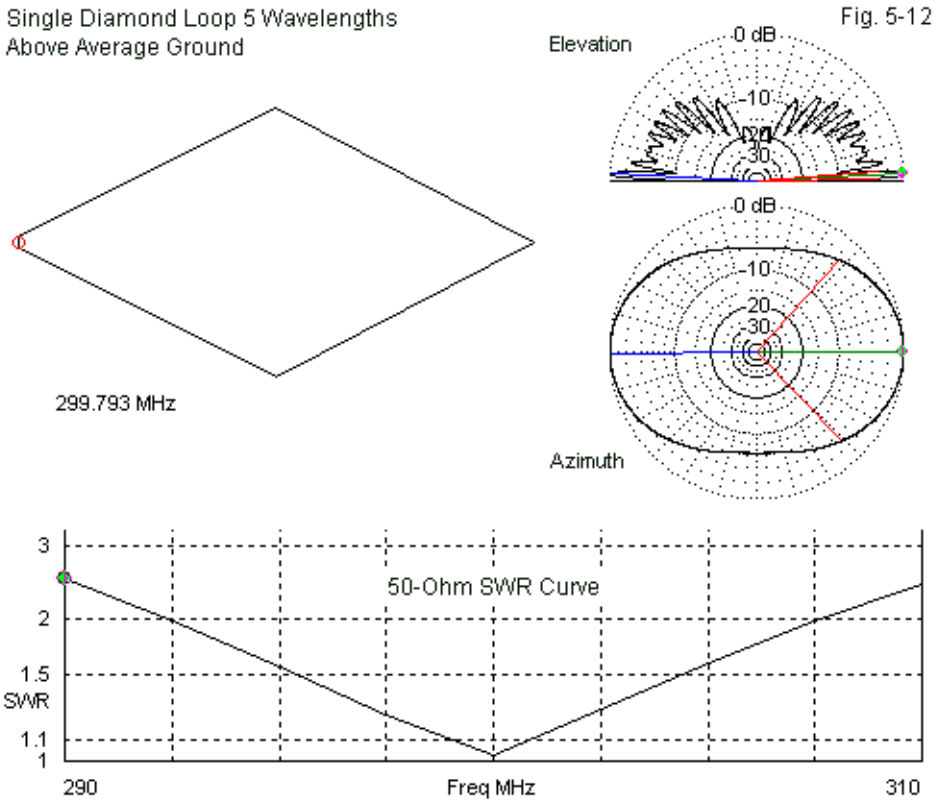

The diamond model shown in the outline portion of the figure uses 4-mm lossless material. All of the diamonds that we shall explore will use either 4-mm or 5-mm element diameters, a range that brackets the common U.S. 0.1875”

aluminum rod. For each antenna, we shall provide a summary lising of both physical and performance values derived from models. The antenna height will be 5-λ above ground, the same height that we used in Chapter 3 to explore the basic properties of dipole and certain arrays based on dipoles. At that height, a single vertical dipole showed a gain of 6.74 dBi, while a pair of dipoles, spaced ½-λ apart and fed in phase, had a maximum gain of 10.55 dBi. The gain of our initial diamond loop, a virtual pair of dipole in phase, but less than ½-λ apart, yields a gain value of 8.84 dBi. Of course, this value applies to a diamond that we have stretched and flatten only enough to yield a 50-Ω feedpoint impedance. The test frequency is 299.7925 MHz, where 1 meter equals 1 wavelength.

Single diamond 5-λ up at 299.7925 MHz

El Dia.	Base	Height	Leg	Circum.	B/H Ratio	Gain	Impedance
λ	λ	λ	λ	λ		dBi	R+/-jX Ω
0.004	0.496	0.26	0.28	1.12	1.907:1	8.84	49.1 + j0.1

The base-to-height (B/H) ratio results from a combination of ingredients, the most important of which are the desired feedpoint impedance and the element diameter. In this frequency region, we shall encounter many ratios, but a good starting point for most design work is a ratio of about 1.9:1.

Although the single side-fed elongated diamond would result in a usable bi-directional antenna, the double diamond is perhaps the most popular version in use in the VHF and UHF region of the spectrum. It provides a central feedpoint with symmetrical structures on either side. At these higher frequencies, we require very little 4-mm material to bend the antenna into shape. For our efforts, we obtain the following structure and performance.

Double diamond 5-λ up at 299.7925 MHz

El Dia.	Base	Height	Leg	Circum.	B/H Ratio	Gain	Impedance
λ	λ	λ	λ	λ		dBi	R+/-jX Ω
0.004	0.904	0.326	0.279	2.229	1.387:1	10.74	49.6 - j0.1

Note that to obtain a 50-Ω feedpoint impedance, the required base-to-height ratio decreases somewhat dramatically relative to the ratio required in a single

diamond. Although the antenna is equivalent to 3 dipoles fed in phase, they are not far enough apart for the array to yield any more gain than 2 vertical dipoles at an ideal separation. **Fig. 5-13** provides some of the graphic details. Maximum gain occurs broadside to the plane of the diamond array.

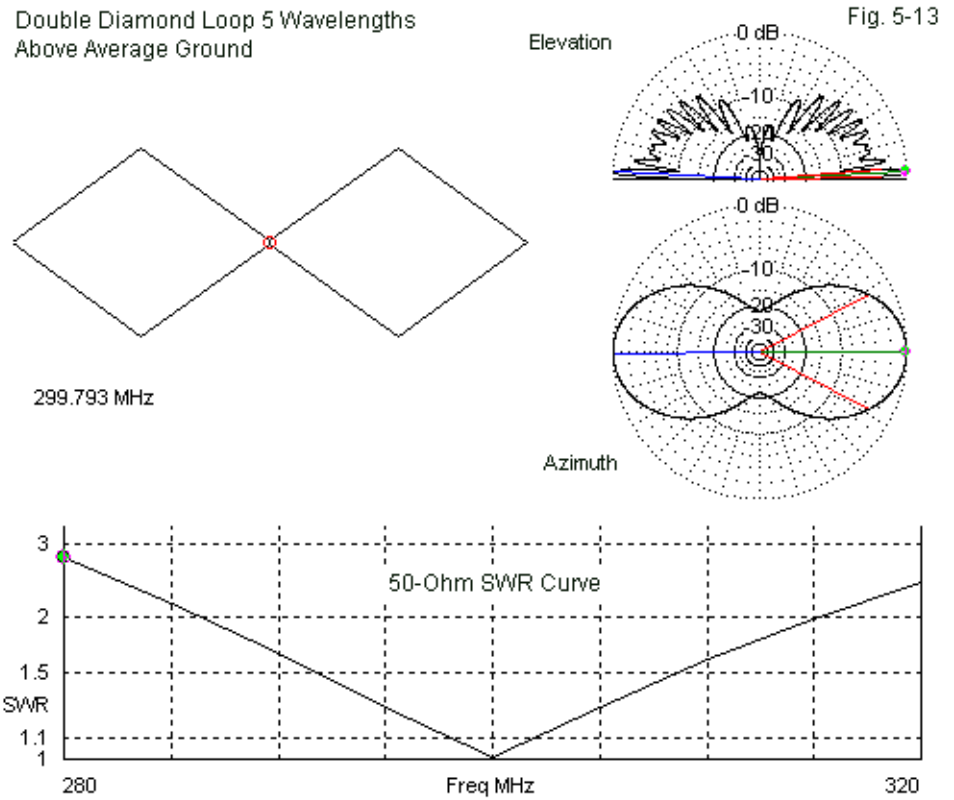

In the lower HF range, we found that the double diamond exhibited fairly broadband qualities relative to the 50-Ω SWR curve. At the boundary between the VHF and UHF ranges, we find a similar situation. Compare the SWR graphs

in **Fig. 5-12** and **Fig. 5-13**. Although the curves have a similar appearance, note the X-axis for each. The 2:1 50-Ω SWR bandwidth for the single diamond is about 15 MHz or about a 5% bandwidth. The double diamond shows about 28 MHz between 2:1 SWR points or a 9.3% bandwidth. The broadband operation of the double diamond is one of the reasons for the shape's popularity.

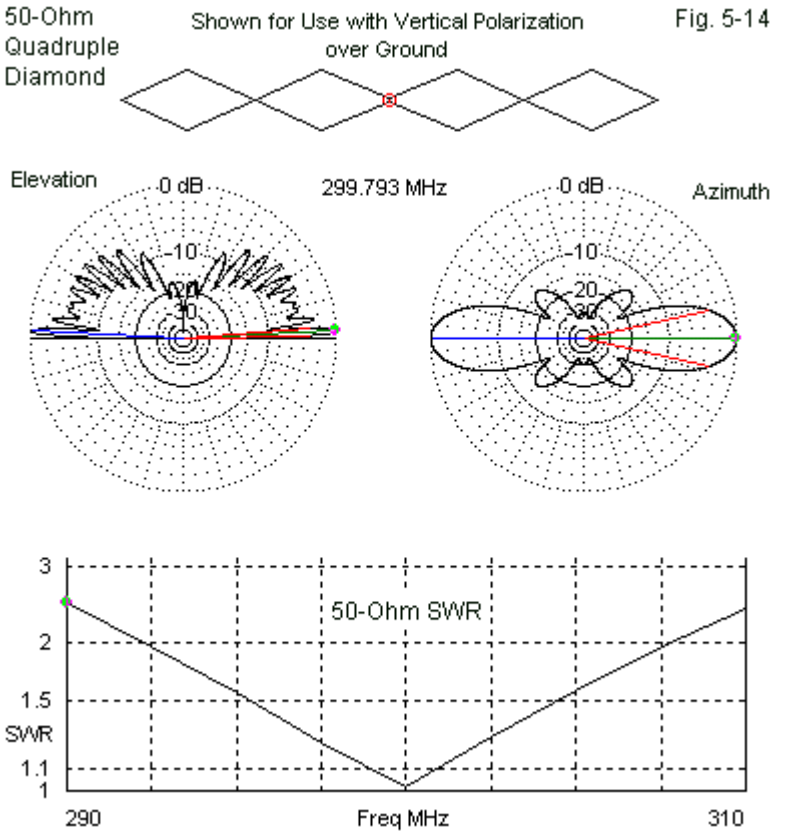

Although wholly impractical in the HF range, the quadruple diamond, outlined

in **Fig. 5-14** is useful at higher frequencies. Its SWR curve is similar to that of the single diamond, partly due to the high base-to-height ratio that we must use to obtain a 50-Ω impedance. The quad diamond yields about 3-dB of additional gain over the double diamond.

Quadruple diamond 5-λ up at 299.7925 MHz

El Dia.	Base	Height	Leg	Circum.	B/H Ratio	Gain	Impedance
λ	λ	λ	λ	λ		dBi	R+/-jX Ω
0.004	2.016	0.234	0.278	4.445	2.154:1	13.72	49.6 + j0.7

The quadruple diamond requires special care in construction. The outer diamonds do not come to a point and a junction with the inner diamonds. Instead, the wires bypass each other, as suggested in **Fig. 5-15**. As a consequence, modeling a quadruple diamond is subject to two types of variations between a physical antenna and its model. First, as we noted earlier, the length of the feedpoint segment can vary the reported feedpoint impedance. Second, the size of the gap that we leave between the crossing wires can also change the reported feedpoint impedance. As a result, NEC models are less certain guides to construction for quad diamonds than they are for single and double diamonds.

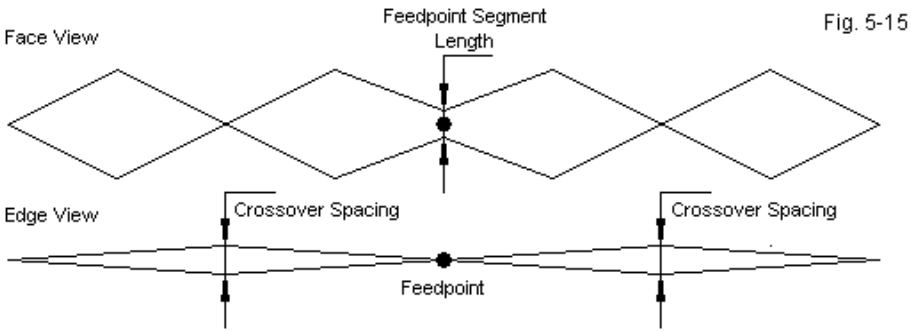

Fig. 5-15

Variables That Affect Both Model and Physical Antenna Performance

The quad diamond produces an azimuth pattern that shows sidelobes. Effectively, it represents 5 vertical dipoles fed in phase, but at less than ideal

spacing for maximum bi-directional gain from in-phase feeding. The result is the production of small sidelobes about 14-dB weaker than the main lobes.

Although the azimuth patterns for all three types of diamond arrays show considerable variation, the elevation patterns are essentially identical for all of the diamond combinations. The elevation pattern of a vertically polarized array depends upon its height above ground, as illustrated in **Fig. 5-16**. Notice that the general outline formed by the pattern lobes does not become very clear until we elevate the antenna many wavelengths above ground.

Diamond Elevation Patterns at Various Heights above Average Ground

Fig. 5-16

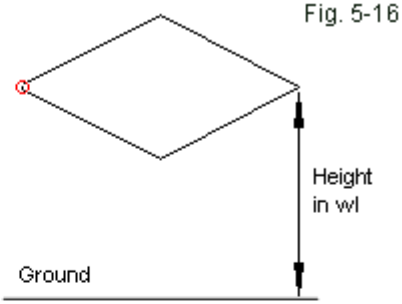

Patterns shown only for vertically polarized antenna

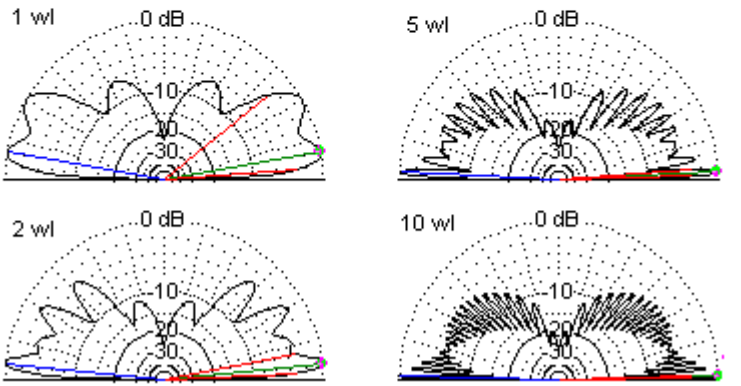

The overall outline shows a depression in both the maximum lobe gain and in the depth of the nulls between lobes. Over average soil, the angle is about 15°. Over very good soil, the angle drops to 12°, while over very poor soil, it climbs to 25°. These values are consistent for vertically polarized antennas at any height, regardless of the complexity of the array in which they occur.

In the VHF and UHF regions, we may find uses for diamonds that we orient for either vertically (long dimension horizontal) or horizontally (long dimension vertical). However, the elevation lobe structure for vertically polarized antennas differs from the elevation lobes of horizontal antennas at the same center height above ground. **Table 5-6** provides a rough sample of a single diamond oriented each way and raised above ground in regular steps.

Single Diamond Gain and TO Angle above Average Ground						Table 5-6
Subject antenna is a single diamond with a 0.005-wl diameter element.						
Test frequency: 299.7925 MHz						
Vertical Polarization				Horizontal Polarization		
Ht wl	Gain dBi	TO angle		Ht wl	Gain dBi	TO angle
Free Sp.	4.22			Free Sp.	4.22	
1	5.19	10.0		1	9.33	13.5
2	7.07	6.0		2	9.85	6.9
3	7.96	4.2		3	9.99	4.6
4	8.46	3.3		4	10.06	3.5
5	8.78	2.7		5	10.10	2.8
6	9.00	2.3		6	10.12	2.4
7	9.16	1.9		7	10.14	2.0
8	9.29	1.7		8	10.15	1.8
9	9.38	1.5		9	10.16	1.6
10	9.47	1.4		10	10.17	1.4
20	9.84	0.7		20	10.20	0.7

The table shows several significant differences between the behaviors of vertically and horizontally polarized antennas of the same type. At lower heights, the vertically polarized version shows less gain but a lower TO angle. As we elevate the antennas in tandem, the TO angles gradually come together (at a

height of about 10-λ above average ground). The vertically polarized antenna shows a more rapid rise in the gain of its lowest and main lobe. However, the gain in vertical polarization has not caught up with the gain of the horizontally polarized version even at a height of 20-λ above ground. Although we shall continue to focus upon vertically polarized diamond arrays, it is useful to be aware of the differences in the behavior of vertically and horizontally polarized versions of the same antenna.

Diamond-Driven Planar Arrays

We shall pass over the potential for using diamonds in parasitic beams. As we saw in connection with the parasitic right-angle delta for 40 meters in the preceding chapter, these beams tend to be narrow-band arrays. Most amateur applications for vertically polarized antennas require relatively broadband service, for example, to cover the entirety of an amateur sub-band designated for FM repeater serve.

For broadband service, most amateurs have turned to planar reflectors. In Chapter 3, we reviewed the basic properties of planar reflectors and applied two types of simple driver antennas, the single dipole and the pair of dipoles optimally spaced and fed in phase. As benchmarks against which we may compare the results of using diamond arrays as drivers, we may note that—at 5-λ above average ground—the single driver reported a gain of 13.84 dBi and a front-to-back ratio of 18.41 dB. When we used two dipoles fed in phase and optimally spaced, the gain climbed to 15.39 dBi, with a front-to-back ratio of 19.27 dB.

In the realm of relatively simple planar reflector arrays, we may simply replace the dipole with a side-fed single diamond driver. Once we enter this design realm, we discover that there are two interactive factors that affect the impedance of the driver: the shape of the diamond and the distance of the driver from the reflector surface. Consequently, there may be no single diamond shape that will yield a 50-Ω feedpoint impedance. In general, the greater the spacing from the reflector, the higher will be the feedpoint impedance for a driver of fixed size. At the same time, the greater the spacing value—up to about 0.3-λ or so—the broader the operating bandwidth of the array. However, with a diamond, we

also have learned that the base-to-height ratio also affects the operating bandwidth. Therefore, any set of dimensions represents a compromise between many design specifications and details. The dimensions shown for the driver, in **Fig. 5-17**, are simply one of those compromise value sets suited to the 4-mm diameter element of the driver diamond.

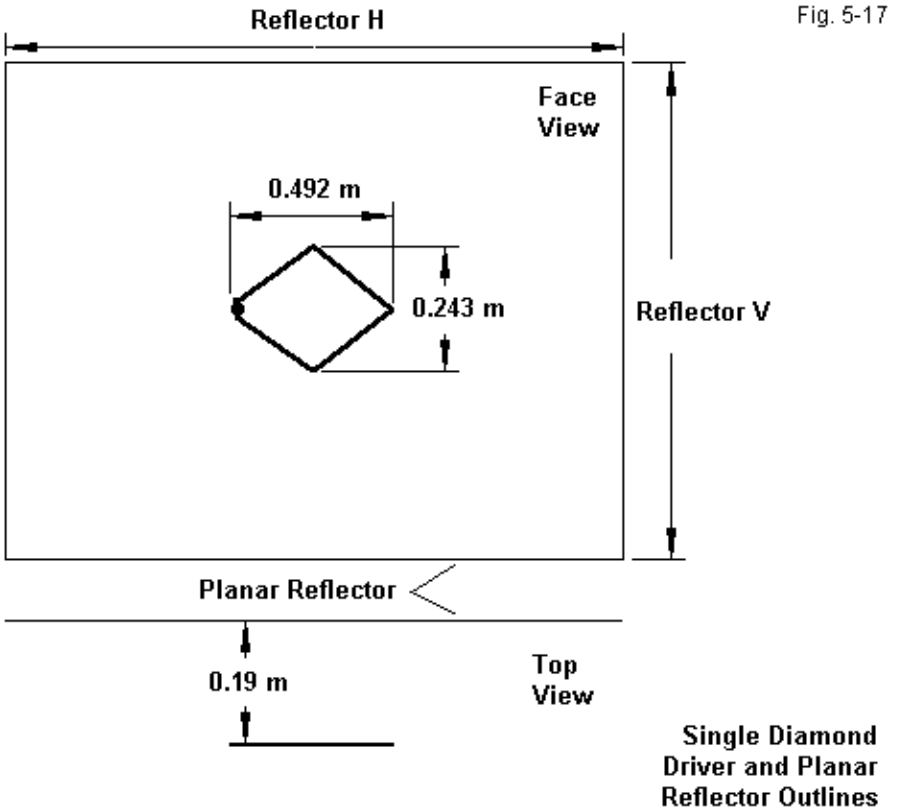

Fig. 5-17

The figure does not specify the size of the reflector. Let's examine two reflector sizes. One will be optimized at about 0.5-λ beyond the vertical and

horizontal limits of the diamond. The other will give in to the amateur tendency to minimize all dimensions. **Fig. 5-18** shows the relative reflector sizes and the resulting elevation and azimuth patterns.

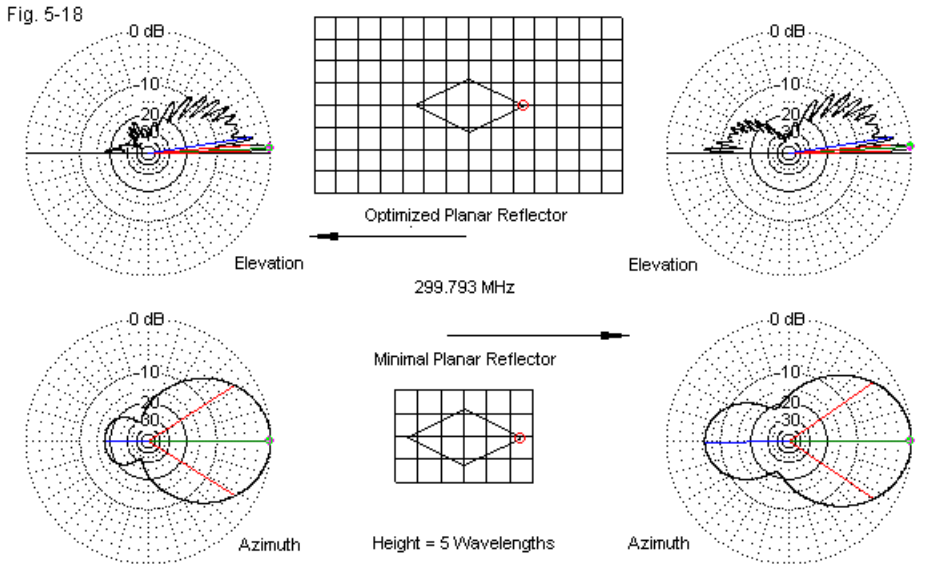

Free-Space E-Plane and H-Plane Patterns: Single-Diamond with Planar Reflectors
Minimal and Optimized Reflectors Shown

Single diamond driver and planar reflector 5-λ up at 299.7925 MHz

Dim:	El Dia. λ	El.	Length λ	Width λ	Reflector	H λ	V λ	Spacing λ
	0.004	Driver	0.492	0.243	Small	0.6	0.4	0.19
					Optimal	1.4	0.8	0.19

Performance:	Gain dBi	F-B Ratio dB	TO degrees	HplBW degrees	Impedance R+/-jX Ω
Small Ref.	13.06	6.41	2.7	69.10	35.6 + j3.2
Optimal Ref.	14.09	17.78	2.6	65.2	49.2 – j0.1

If we combine the listing of values with the graphics, we can gain a fairly clear sense of the penalties of trying to use a reflector whose size barely exceeds the dimensions of the driver assembly. A reflector based upon optical principles requires considerably more area than the driver for maximum gain. Note that even when we optimize the reflector size for forward gain, the front-to-back ratio remains below 18 dB. By increasing the reflector area further, we can improve the front-to-back ratio, but the gain will decrease slowly.

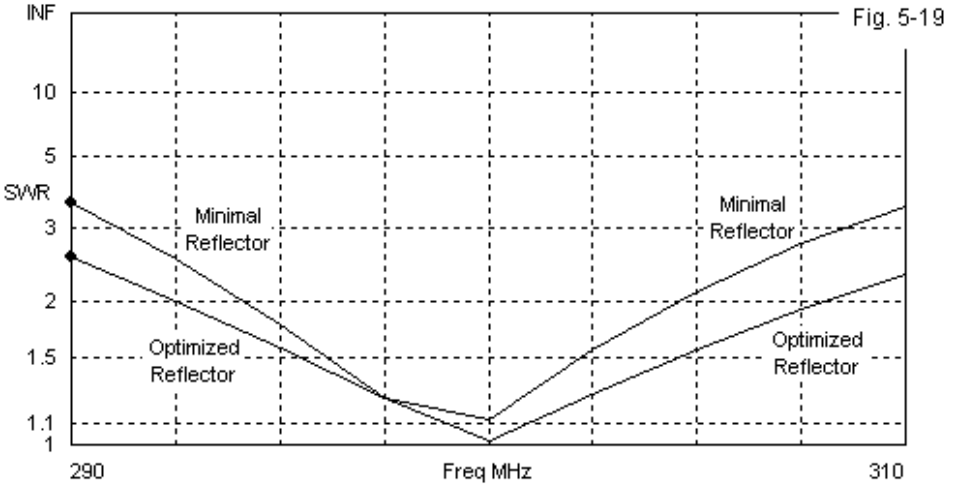

Minimizing the area of the reflector also has negative consequences for the SWR bandwidth of the array. As shown in **Fig. 5-19**, the minimal reflector achieves only about 2/3 of the operating bandwidth of the array with a more optimal reflector size.

With some justice, the double diamond antenna is perhaps the most popular driver for a planar array in the UHF region. As suggested by the outline and dimensions in **Fig. 5-20**, we may use 4-mm diameter material and fashion a sturdy driver assembly. Support relative to the planar reflector is a matter of adding insulated stand-offs at the far tips with the feedline assembly supporting

the center. Once more, we encounter the multiple variables that control the achievement of a 50-Ω total array. Hence, the driver dimensions shown are but one of several possible sets.

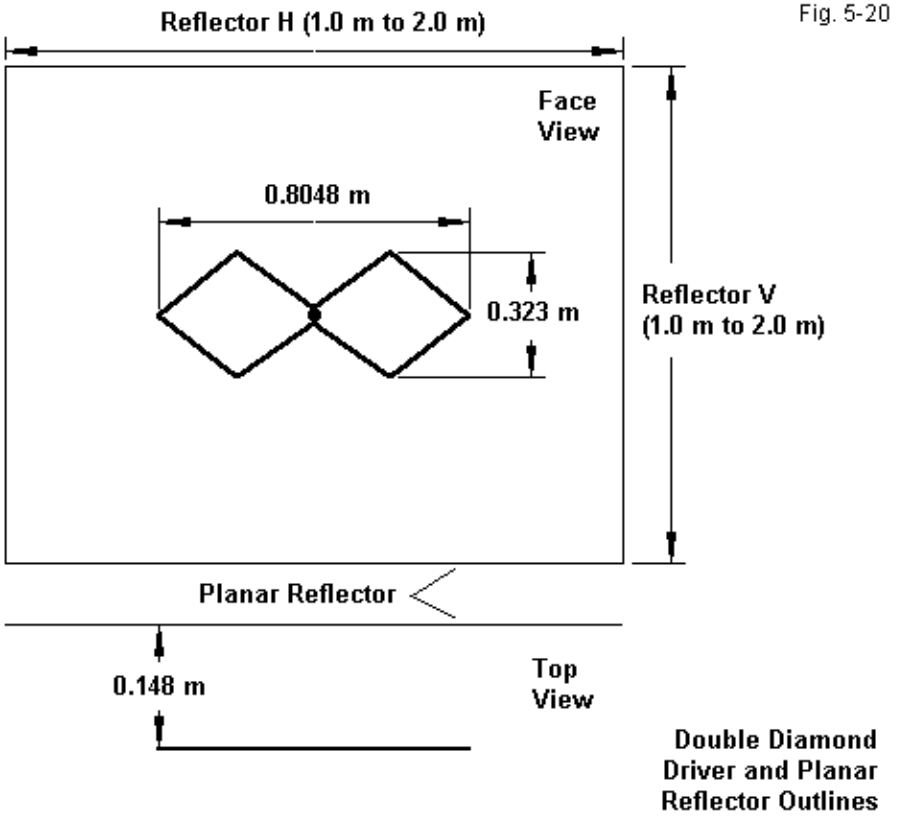

Fig. 5-21 provides a look at both minimal and optimal reflectors for the double diamond driver, while the following listing shows the performance differences. Not only does the optimal reflector provide an extra dB of forward gain, but it also controls the rear lobes to provide over 20 db of front-to-back ratio.

Moving from a single driver to a double diamond improves forward gain by about 1.5-dB and increases the front-to-back ratio by about 5-dB. Of course, the double diamond driver requires a larger planar reflector than the single diamond.

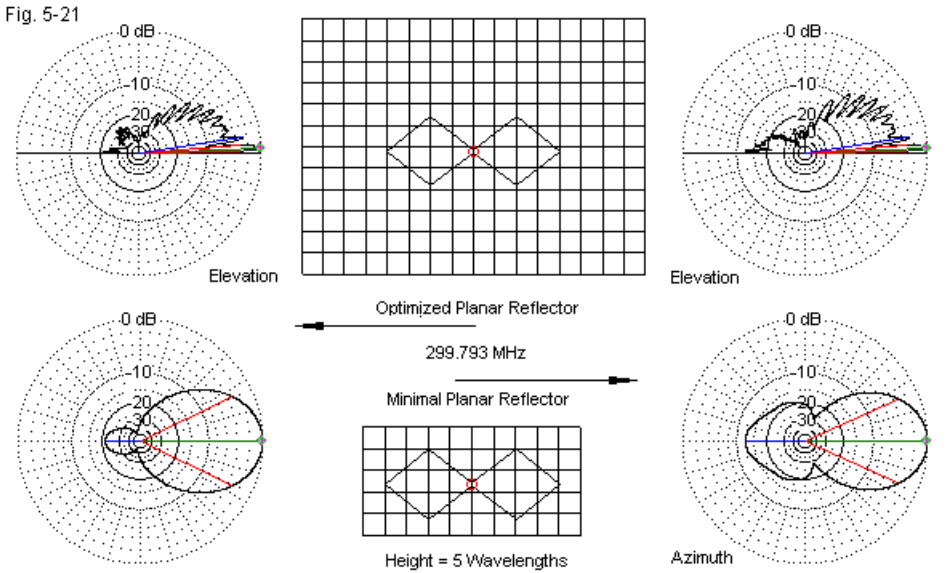

Free-Space E-Plane and H-Plane Patterns: Double-Diamond with Planar Reflectors
Minimal and Optimized Reflectors Shown

Double diamond driver and planar reflector 5-λ up at 299.7925 MHz

Dim:	El Dia. λ	El.	Length λ	Width λ	Reflector	H λ	V λ	Spacing λ
	0.004	Driver	0.805	0.323	Small	1.0	0.5	0.148
					Optimal	1.6	1.2	0.148

Performance:	Gain dBi	F-B Ratio dB	TO degrees	HplBW degrees	Impedance R+/-jX Ω
Small Ref.	14.72	12.29	2.6	48.64	43.4 + j3.4
Optimal Ref.	15.67	21.34	2.6	51.2	49.6 – j0.6

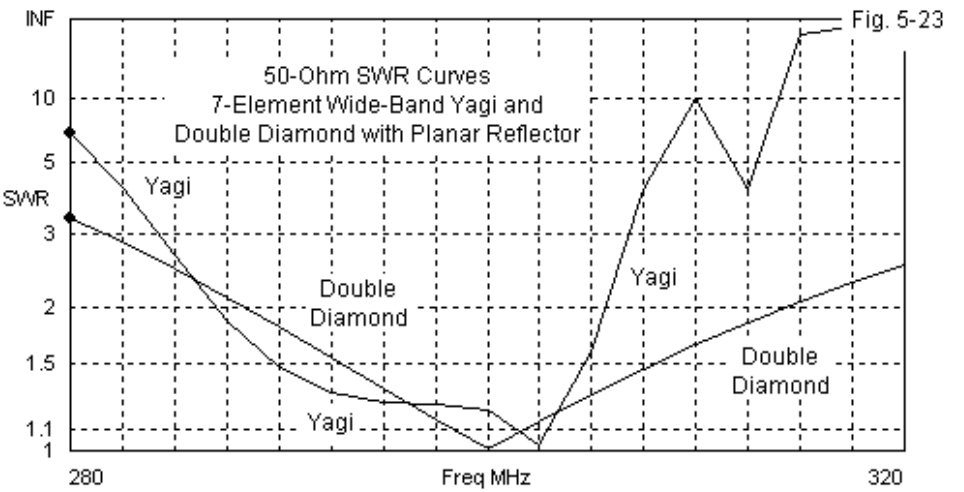

Fig. 5-22 provides a general illustration of the broad banded nature of planar

reflector arrays. With a 13% change of frequency, the forward gain changes by only 0.5-dB. The change in the front-to-back ratio is less than 1.2-dB. Although not quite linear, both curves are very straight with no anomalies.

Indeed, the limiting factor in the use of a double diamond planar array is not the pattern behavior, but the 2:1 SWR ratio. **Fig. 5-23** shows a 2:1 SWR bandwidth of about 22 MHz for the double-diamond. On the same graph, I have added the 50-Ω SWR curve for an OWA 7-element Yagi. The OWA (optimized wideband antenna) design has about the same design-frequency gain as the double-diamond-planar array and uses principles that yield some of the broadest banded shorter-boom Yagis known. However, its operating bandwidth is only about 70% as great as that of the planar array. As well, when the Yagi passes out of its primary operating bandwidth, the beam properties may also deteriorate considerably. In contrast, if we may use of the double diamond array with an SWR value as high as 3:1 (common in numerous receiving applications), we can make use of the planar antenna's relatively constant gain and front-to-back values over an even wider passband.

One technique used to achieve increased array performance is to use more than one driver assembly with an enlarged planar reflector. However, each driver requires a feedpoint connection, and multiple feedpoints require the construction of phasing lines to ensure that each driver receives the correct current magnitude and phase angle. Drivers with a single feedpoint simplify both correct driver feeding and the potential losses that accompany complex phase-line systems. For this reason, the quadruple diamond has recently grown more popular as a driver for planar reflectors. **Fig. 5-24** provides a graphic supplement to the following dimensions and modeled performance values.

Quadruple diamond driver and planar reflector 5-λ up at 299.7925 MHz

Dim:	El Dia.	El.	Length	Width	Reflector	H	V	Spacing
	λ		λ	λ		λ	λ	λ
	0.005	Driver	1.968	0.220	Optimal	3.0	1.2	0.147

Performance:	Gain	F-B Ratio	TO	HplBW	Impedance
	dBi	dB	degrees	degrees	R+/-jX Ω
	17.95	21.80	2.7	25.0	50.1 + j1.8

Quadruple-Diamond Driver with
Planar 1.2x3.0-WL Reflector

Fig. 5-24

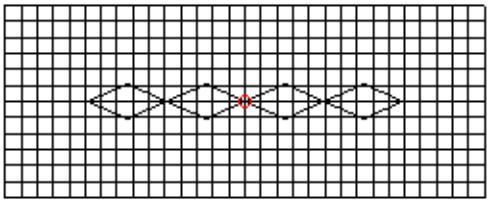

General Outline

299.793 MHz

Height = 5 Wavelengths

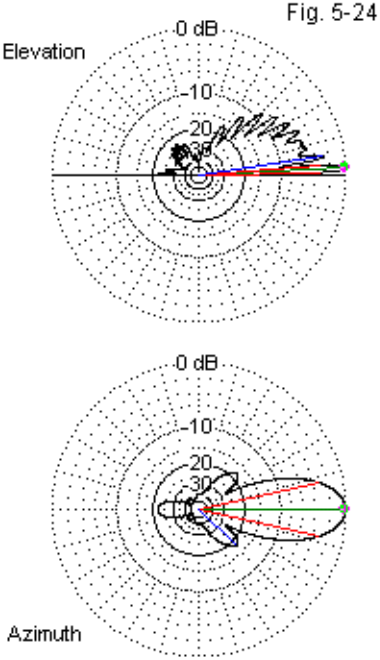

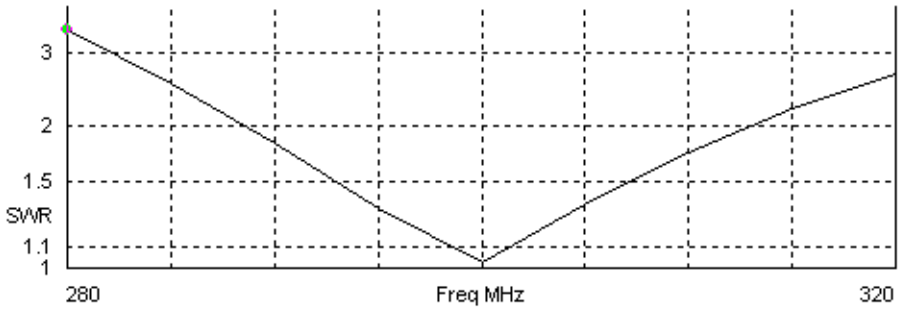

The quadruple diamond driver does not have the same dimensions as the

independent bi-directional quad array. The overall base length and the height are both less in the planar antenna. As well, the SWR bandwidth is only about the same as the bandwidth of the single diamond driver and does not match the figure achieved by the double diamond array. However, the quad diamond beam has a 2-dB gain advantage over the version with half the number of diamonds. Like the independent quadruple diamond antenna, the azimuth pattern retains its side lobes. The effectiveness of an optimized reflector shows up in the fact that the rear lobe structure is a miniature of the forward lobe structure.

Theoretically, it is possible to continue the expansion of diamond drivers without limit. Even with optimally sized reflectors, every doubling of the driver can produce a maximum of 3-dB gain increase. In practice, it is difficult to obtain the full theoretic increase. As we add more diamonds to the driver, the diamond dimensions become more critical. Additionally, the array becomes ungainly as it becomes very long and narrow. The more usual practice is to increase the array size by adding bays of quadruple diamonds to form a squarer shape.

Conclusion

The elongated diamond derives from the square diamond element by a process of stretching and flattening the side-fed element until it either reaches maximum gain or a desired feedpoint impedance. In these notes, we have selected the feedpoint impedance as the limiting factor. The basic elongated diamond performs very much like a right-angle delta in the lower HF range. However, the center-fed double diamond proved to have performance advantages over the double right-angle delta, enough of them that it becomes preferable.

The elongated diamond has not seen wide use as a lower HF SCV. However, it has become popular in the VHF and UHF region both as a bi-directional antenna and as a driver for wide-band planar arrays. The design variables for planar reflectors with complex driver elements allow for variations of base length, height, and the spacing between the driver and the reflector, even for a fixed feedpoint impedance. Nevertheless, it is possible to design a succession of diamond drivers using 1, 2, and 4 diamonds to produce beams that

show a steady rise in gain. With adequate reflector size, the arrays also show a very respectable front-to-back ratio. Typical VHF and UHF reflector materials might include solid or perforated surfaces as well as screening material with openings smaller than 0.05-λ. Screen-based reflectors normally require edge bracing.

The diamond driver owes part of its VHF/UHF popularity to the ease of construction. One may form even the most complex diamond driver from a single length of material that eventually folds back upon itself. The loop closure and the feedpoint terminals or connector are the only points requiring the use of fasteners, solder, or welding. Support of the driver from the reflector plane is equally straightforward.

The diamond derives from the square-shape diamond, with either form fed at a side corner to obtain vertical polarization. The squared diamond has a counterpart in the true square with a feedpoint at the midpoint of one vertical side. In practice, we find no essential difference in the quad loop whether we create a diamond shape or whether we place two wires parallel to the ground and two in the vertical plane. In fact, both types will exhibit the same feedpoint impedance. If this situation leads us to questions about what might happen if we stretch and flatten the true side-fed square, then we are ready for our next SCV form.

6. Rectangular SCVs

The rectangular SCV is the most effective of the closed-loop SCV forms. It derives from the common square loop with two sides horizontal and two sides vertical. Of course, for SCV use, we place the feedpoint at the center of one side to ensure vertical polarization.

The square and rectangular SCV forms are also very convenient in helping us to understand better the basic properties of these types of antennas. Therefore, let's begin our venture into the new shape with a few free-space exercises. However, as in all of the SCVs for the lower HF region, we shall continue to construct the loops from AWG #12 copper wire. **Fig. 6-1** outlines the square loop for 7.15 MHz in free space.

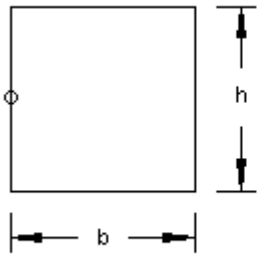

7.15-MHz Free-Space
Square Quad Loop

Dimensions

Freq.	7.15 MHz
B (base)	36.1'
H (height)	36.1'
Circumference	144.4'

Fig. 6-1

Conveniently, a square or a rectangle has only two relevant dimensions, the base (b) and the height (h). The dimensions shown yield a square that is resonant in free space, with an impedance of 124 Ω with less than 1 Ω of remnant reactance at the feedpoint. The free-space gain is 3.28 dBi. We shall use this gain value as a marker against which to compare some of our later gain values.

Amateurs widely use the square loop wherever they can appropriately use an X-shaped support frame for the element. Hence, we find the square loop used extensively in cubical quad beams, where the Xs for the elements join to a central boom. The key property of a closed square loop that is about 1-λ in circumference is that the main radiation lobes are broadside to the loop. If we reduce the circumference toward 0.5-λ or increase it past 1.5-λ, the main radiation lobes occur in the plane of the loop, that is, off its edges.

As a single element, the square shape is convenient, but it does not produce the strongest bi-directional gain that we can achieve from the rectangular shape. When we examined triangles and diamonds, we found that we could increase gain from the loops by stretching and flattening them. We should take a closer look at this process.

Appreciating SCV Variables

In the course of our studies, we have uncovered and explored several variables that affect SCV performance. In the HF and MF regions of the spectrum, soil quality plays a key role in setting the maximum gain and the TO angle for loops with base heights well under 1-λ. As in past chapters, the base height indicates the distance above ground of the lowest extent of the SCV assembly. This distance went from ground to the base wire of triangles and from the ground to the lowest peak of a diamond. The rectangular shapes that we shall meet in this chapter will show equivalent ground effects,

The second variable for relatively low SCV antennas is the frequency of operation. In most instances, the gain decreased as the operating frequency increased. The exception to this general trend occurs with very poor soil. When we have very low values of soil conductivity and relative permittivity, the gain actually rises with the operating frequency. Rectangular SCVs will not be immune to these effects.

The third variable is simply the height above ground. In the lower HF region, where we use low base heights, losses to the ground increase as we lower the base heights, regardless of the operating frequency. In fact, our basic exercises

with each SCV form include an attempt to locate in rough terms the height at which the SCV gain reaches its maximum value before the declining with the growing domination of secondary elevation lobes in the antenna's pattern. The height of maximum gain varied with both the operating frequency and the soil quality. As a result, we discover in the end that all of the main variables form an interlocking trio of mutual affects on SCV performance. Indeed, at heights well below the height of maximum gain, the feedpoint resistance and inductive reactance both increased significantly.

We have treated the fourth variable only in general terms so far. For any given frequency, we may stretch and flatten an SCV form to achieve two goals. One aim is to increase the antenna's bi-directional gain. The second is to reduce the feedpoint impedance to a convenient value. Because coaxial cable transmission lines are so commonly used, we have generally stopped the stretching-and-flattening process when we reached a feedpoint impedance of 50 Ω. Later in this chapter on rectangles, we shall use the same convention. In fact, **Fig. 6-2** outlines the basic dimensions of the single rectangles that we shall feature. Each rectangle shows a feedpoint impedance of 50 Ω in a near-resonant condition at the height above average ground at which we find maximum gain on each of the amateur bands listed. (The Appendix contains dimensions for equivalent rectangles for 160 through 30 meters.)

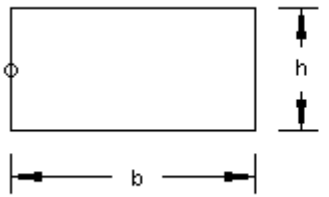

Rectangular Loop for SCV Use

Dimensions

Freq.	1.85 MHz	3.55 MHz	7.15 MHz
B (base)	196.0'	100.2'	48.8'
H (height)	79.5'	44.0'	23.2'
Circumference	551.0'	288.4'	144.0

Fig. 6-2

However, before we commit the rectangle to near-ground use, let's put the shape into free space. There are two overlooked variables in the creation of SCVs that we have not yet explored in depth. One is the limit of the extent to

which we may stretch and flatten and SCV. The other variable is the affect of using wire with a finite conductivity as our antenna element. **Table 6-1** provides the data for a stretch-and-flatten exercise in free space that uses both lossless wire (obtainable only in models) and copper wire. The test frequency is 7.15 MHz, and the wire size in both data sets is AWG #12.

7.15-MHz Rectangles in Free Space							Table 6-1
Lossless Wire: AWG #12 (0.0808" diameter)							
Nom Z	Base Len	Height	Circum	Gain dBi	BW deg	Feed R	Feed X
100	39.42	32.82	144.48	3.52	121.20	100.80	0.00
87.5	41.40	30.82	144.44	3.67	112.20	87.69	-0.15
75	43.40	28.76	144.32	3.83	104.60	75.08	-0.45
62.5	45.54	26.52	144.12	4.01	97.90	62.50	-0.55
50	47.84	24.08	143.84	4.21	91.90	50.19	-0.17
37.5	50.50	21.20	143.40	4.46	85.60	37.57	0.11
25	53.66	17.70	142.72	4.75	79.60	25.00	0.14
12.5	57.82	12.98	141.60	5.15	72.80	12.56	-0.12
Copper Wire: AWG #12 (0.0808" diameter)							
Nom Z	Base Len	Height	Circum	Gain dBi	BW deg	Feed R	Feed X
100	39.86	32.34	144.40	3.45	118.90	100.10	0.61
87.5	41.78	30.40	144.36	3.58	110.60	87.53	0.77
75	43.78	28.32	144.20	3.72	103.30	75.00	-0.05
62.5	45.96	26.04	144.00	3.88	96.60	62.44	0.29
50	48.34	23.50	143.68	4.04	90.60	49.95	0.45
37.5	51.06	20.54	143.20	4.22	84.60	37.43	0.64
25	54.30	16.92	142.44	4.37	78.40	25.03	0.03
12.5	58.86	11.74	141.20	4.32	71.30	12.49	0.51
Notes:	Nom Z = target rectangle feedpoint impedance						
	Base Len = length of rectangle base in feet						
	Height = height of rectangle (side feedpoint leg dimension) in feet						
	Circum = rectangle circumfernce in feet						
	Gain dBi = maximum free-space gain in dBi						
	BW deg = H-plane beamwidth in degrees						
	Feed R and Feed X = feedpoint impedance reported by final model						

Since we know that stretching and flattening will lower the feedpoint impedance, I used an increment of 12.5 Ω for nominal impedance values ranging

from 100 Ω down to 12.5 Ω. Then I constructed models that approach this nominal feedpoint impedance value as closely as possible. The table shows the reported impedance values obtained from the models. The dimensions for the two types of wire are not the same for any given feedpoint impedance, largely as a result of the fact that wire losses contribute to the resistive portion of the impedance. However, with both wire types, we find that the loop circumference decreases as we lengthen and flatten the structure.

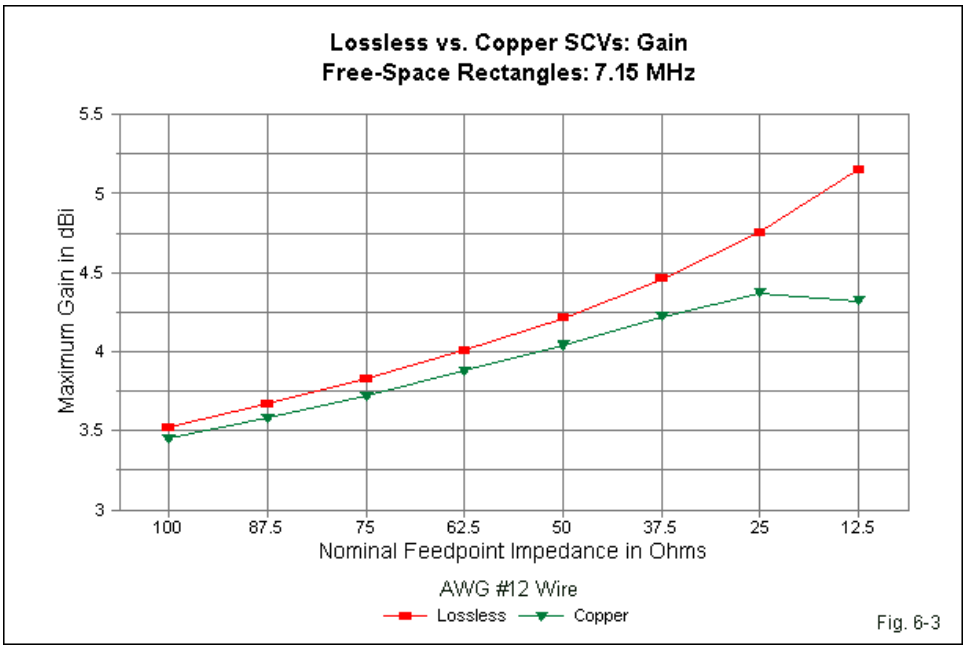

Fig. 6-3 graphs the gain for both type of wire against each increment of impedance, where the impedance decreases with the length of the loop. The lossless wire gain appears to increase without limit. However, this curve is a bit illusory. The spacing between the long wires is still about 6.5' with an impedance of 12.5 Ω. As we continue to bring the wires closer together, they will eventually become close enough to show the properties of a parallel transmission line. A

separation of under about 2' is sufficient to show these properties. As the spacing between long wires grows less, the length of those wire approaches (and passes) ½-λ. A half-wavelength transmission line shows at its feed end the same impedance that we find at the far end. Since the far end has a shorting wire, the impedance approaches zero. However, the shorting wire is too short to radiate effectively, and so our ideal flattened rectangle becomes effectively a simple transmission line. At this point, we also encounter current magnitude and phase conditions that are very different from those that we encounter when we separate the long wires enough to avoid transmission-line effects. When the log wires are too close to each other, the rectangle loses its ability to function as an antenna.

The graph also shows the gain curve for AWG #12 copper wire. Copper has a finite conductivity, often listed as 5.8E7 S/m. This value undergoes adjustment in NEC for the wire surface area and the operating frequency to recognize skin effect. The net result of using AWG #12 copper wire is to yield a gain peak in the vicinity of a 25-Ω feedpoint impedance. For rectangular shapes that produce lower impedance values, the gain will decline, even in the absence of any ground effects. Although we have generally overlooked the effect of wire losses on SCV performance by stopping the stretch-and-flatten process at a 50-Ω level, we shall have occasion in this chapter to alter that process. In fact, we shall be able to use variations of the rectangular SCV that allow us to stretch the rectangle toward its longest and flattest—and therefore, its highest-gain—shape.

As we decrease the feedpoint impedance by lengthening the rectangle, we obtain increased bi-directional gain for either wire type, even though the lossier copper wire shows a slower rate of gain rise. Accompanying the gain increase is a decrease in the beamwidth of the H-plane radiation pattern. (Over ground, we would call this pattern the horizontal or azimuth pattern. However, free-space lacks a horizon.) **Fig. 6-3** overlays three free-space E-plane patterns for lossless-wire impedance values of 87.5 Ω, 50 Ω, and 12.5 Ω. Although the impedance increments are the same for each step, we find that the step between 50 Ω and 12.5 Ω produces the greater rise in gain and the greater reduction in beamwidth. The beamwidth reduction shows up most clearly by reference to the developing side nulls in the H-plane pattern. The pattern for 87.5 Ω is an egg-shaped oval, while at 50 Ω we find a straight-sided or racetrack oval.

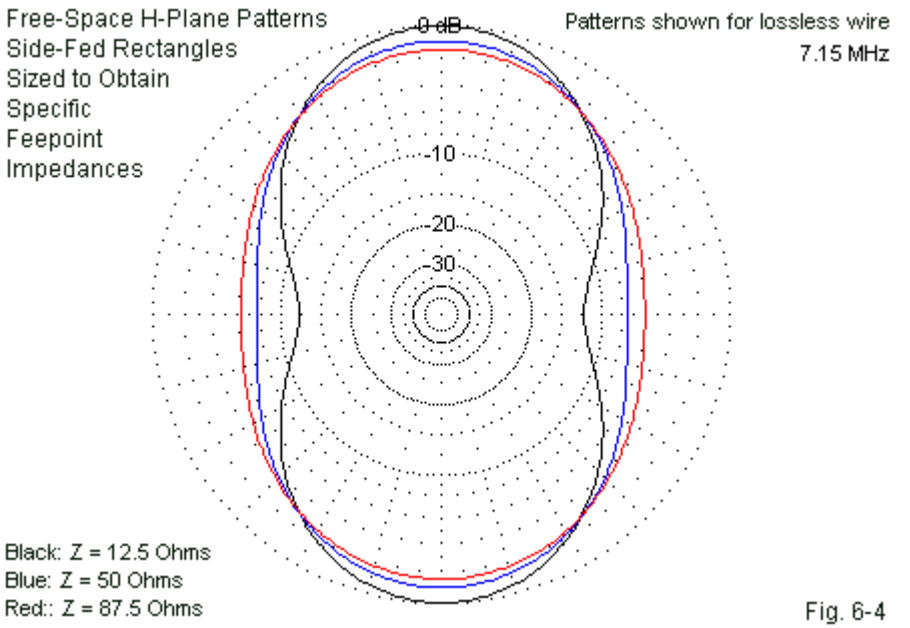

Fig. 6-4

We may legitimately ask why the rectangle continues to show increased gain as we lengthen and flatten it. **Fig. 6-5** shows that the current magnitude curves for the 100-Ω and the 12.5-Ω versions of the rectangle are virtually identical. (The graphic does not show the phase reversal that occurs at the center of each long wire.) On the surface, it would appear that the very long vertical sections of the 100-Ω version should yield a higher gain with vertical polarization, with less current involved in the virtual self-cancellation that occurs with the radiation from the horizontal portions of the antenna. We may note in passing that the peak current occurs at the feedpoint and at the point on the vertical wire opposite the feedpoint at the other end of the rectangle.

The answer largely emerges from our work in Chapter 2 of these notes. The gain of two vertical elements fed in phase increases as we increase the separation between the elements up to (and slightly past) ½-λ. As we stretch and

flatten the rectangle, the spacing between the two end-wires more closely approaches ½-λ. The rate of gain increase that results from the increased spacing is higher than the rate of gain decrease that results from shortening the vertical length of the end wires. Of course, the process has limits, partly as a function of converting a rectangle into a transmission line and partly as a consequence of losses that we encounter with real (copper) wires.

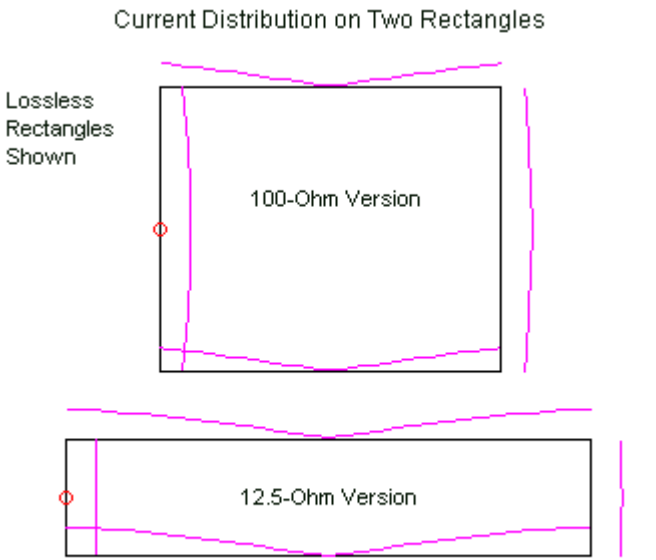

Fig. 6-5

In principle, these very same factors that define SCV performance also apply to triangles and diamonds. I have held these notes until this chapter on rectangles for three reasons. First, there has been so much to note about the earlier forms that we explored. Second, the rectangular form provides perhaps the clearest illustration of these factors at work. Finally, the use of the earlier forms has focused on the stretching and flattening process only down to the 50-Ω level. Only in common practices applied to rectangles do we find efforts to use

longer and flatter SCV shapes that usually yield very low feedpoint impedance values.

Single Rectangular SCVs

Of all the SCV forms that we have observed, the rectangle requires the least height, since it lacks any pointed vertical projections. However, in common versions, it is not sufficient to have a single very tall support supplemented by two shorter supports for the end points. The rectangle requires two moderately tall supports for the wires. In addition, since the vertical end wires are critical to antenna performance and parallel the supports, the overall installation requires further length to keep the supports far enough from the vertical wires to avoid unwanted interactions. The distance is not excessive, because the main radiation lobes are broadside to the rectangular assembly, but neither is the distance insignificant in the near field of the end wires.

Accompanying the fact that the rectangle yields the shortest SCV form is the fact that among closed SCV forms, it yields the highest gain. Indeed, the gain of a single side-fed rectangle for any of the lower HF or upper MF bands is 0.5 to 0.7 dB higher than the gain of an equivalently placed right-angle delta or a single diamond. This fact alone may give us pause to consider whether we might use a rectangular SCV in place of a contemplated delta or diamond configuration. The dimensions shown in **Fig. 6-2** reveal that the required circumference is not very different for any of the three types of SCV loops. As well, we shall soon see that the required base height for maximum gain does not significantly differ among the three configurations.

All of the single rectangles listed for the three sample bands are nearly resonant for 50 Ω at the design frequency over average ground. For any given height, the impedance does not change much as we change the ground quality. However, like all low-band SCVs, the impedance climbs fairly rapidly at low base heights above ground.

Table 6-2 lists the 160-meter data for 20’ increments of base height from 10’ to 150’. For average soil, peak gain occurs with a base height of 90’. However,

over both very good and very poor soil, peak gain occurs at or above a base height of 150'.

Rectangles for 160 Meters					Table 6-2
Base Height and Soil Quality vs. Performance					
1.85 MHz					
Soil	Ht ft	Gain dBi	TO deg	Feed R	Feed X
VG	10	4.90	17	82.4	87.7
	30	5.37	16	69.8	33.1
	50	5.61	14	62.4	14.8
	70	5.83	14	56.1	6.0
	90	6.03	13	50.6	1.8
	110	6.21	12	45.8	0.2
	130	6.33	11	42.0	0.3
	150	6.37	10	39.2	1.5
Ave	10	2.70	23	91.7	90.1
	30	3.27	21	72.5	30.0
	50	3.47	19	62.6	12.0
	70	3.58	18	55.2	4.1
	90	3.62	16	49.2	0.8
	110	3.62	15	44.6	0.0
	130	3.54	14	41.1	0.6
	150	3.39	13	38.7	2.0
VP	10	-0.16	27	101.5	78.3
	30	0.63	26	73.9	22.2
	50	0.92	23	60.8	7.1
	70	1.07	22	52.3	1.7
	90	1.14	20	46.5	0.1
	110	1.19	19	42.4	0.5
	130	1.21	18	39.7	1.7
	150	1.22	17	38.1	2.2

The gain curves based on the tabular data in **Fig. 6-6** look very similar to those for deltas and diamonds in terms of the curve shapes. Only the curve for average soil shows a distinct downturn above the peak gain base height.

However, the gain levels are about a half dB higher for any given height than those for the other SCV forms. Whether that much additional gain is a decisive factor in the selection of an SCV antenna is an operator judgment.

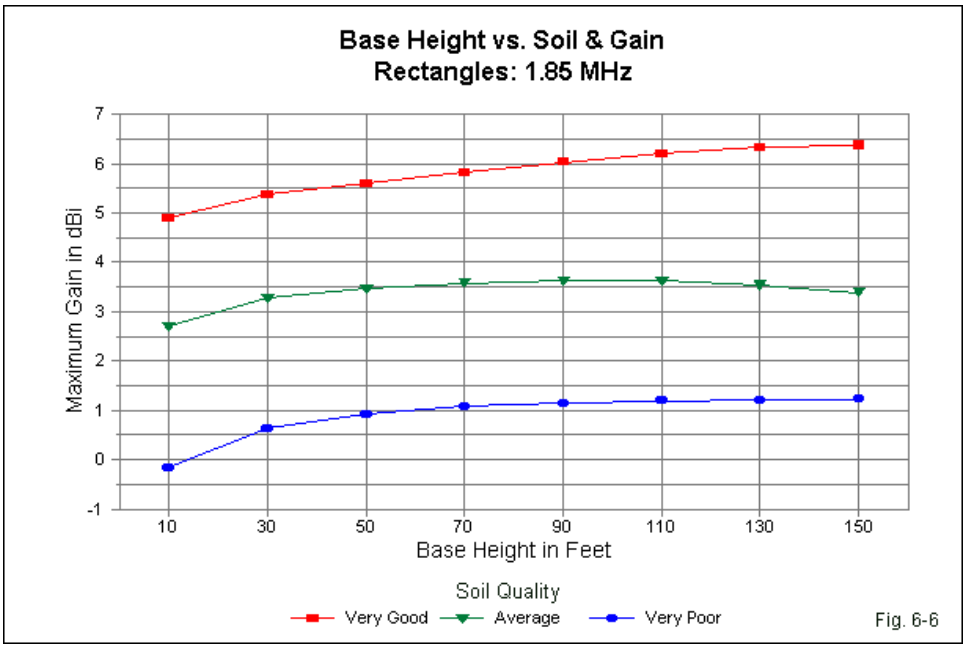

Fig. 6-6

At 3.55 MHz, the data table (**Table 6-3**) employs 10' base height increments from 10' to 80'. Over average ground, peak gain appears at a base height of about 50'. Over very good ground, the required height is 70', but over very poor ground, the base height for peak gain occurs at or above the sampling limit. The gain advantage of the rectangle over the other shapes so far examined is about a half dB. When deciding if the difference is usable, be sure to add the total array height to the base height for each SCV form under consideration. On 160 meter and 80 meters, the installation height is likely to be well below the base height for maximum gain. Therefore, a proper comparison would include gain values for the base height that would attach to each type of SCV, given whatever limits there

may be for the total antenna height. These values may differ for each SCV form under consideration.

Rectangles for 80 Meters					Table 6-3
Base Height and Soil Quality vs. Performance					
3.55 MHz					
Soil	Ht ft	Gain dBi	TO deg	Feed R	Feed X
VG	10	4.59	18	84.3	55.1
	20	4.89	17	73.5	22.3
	30	5.09	16	65.6	9.7
	40	5.26	14	58.8	2.9
	50	5.41	14	53.0	-0.1
	60	5.51	12	48.2	-0.8
	70	5.56	12	44.5	-0.1
	80	5.51	11	42.0	1.5
Ave	10	2.20	23	89.5	50.0
	20	2.57	22	73.9	18.6
	30	2.74	20	64.0	6.5
	40	2.83	19	56.6	1.3
	50	2.86	17	50.9	-0.5
	60	2.84	16	46.6	-0.4
	70	2.76	15	43.5	0.8
	80	2.62	14	41.6	2.5
VP	10	-0.02	27	88.4	36.3
	20	0.62	26	70.1	11.5
	30	0.98	24	59.6	3.2
	40	1.26	22	52.7	0.5
	50	1.49	21	47.9	0.2
	60	1.70	20	44.6	1.1
	70	1.89	19	42.6	2.5
	80	2.06	18	41.5	4.2

Fig. 6-7 provides the gain curves for the three soil types at all of the sampled base heights at 3.55 MHz. It once again shares the general characteristics of the 80-meter curves for the other SCV forms. Most strikingly, the curve for very poor

soil shows a steeper gain rise than it did on 160 meters as we increase the base height. With a base height of 80' (perhaps an unrealistic values for most amateur installations), the gain over very poor soil approaches but does not reach the gain over average soil.

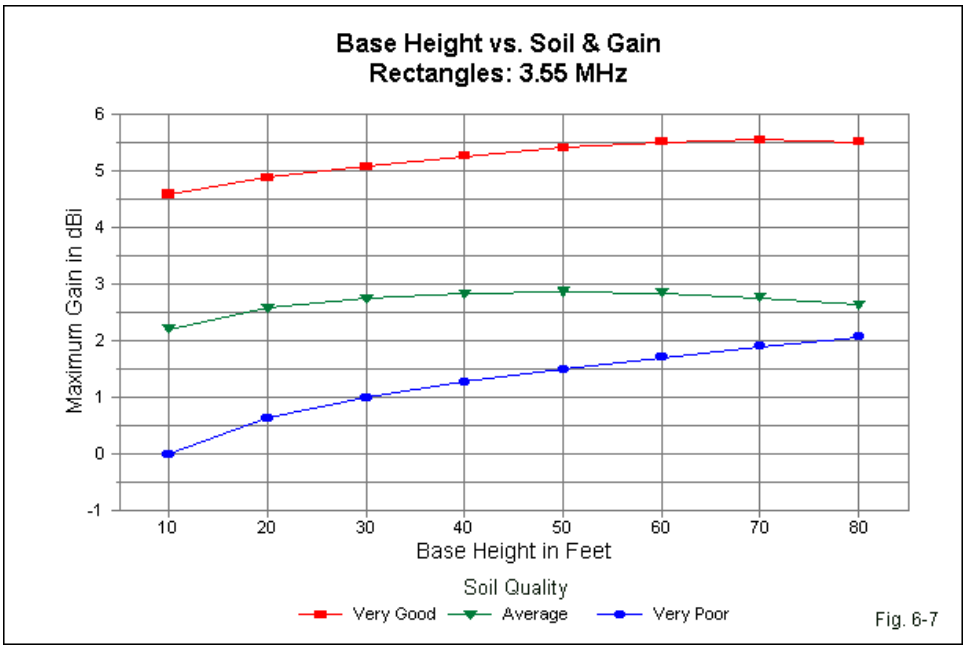

Fig. 6-7

Only on 40 meters is it very likely for a rectangular 50-Ω SCV to use a base height that displays peak gain from the antenna. As shown in the data in **Table 6-4**, the required base height for very good through average soil is between 30' and 35'. The 50-Ω SCV rectangle is only 23.2' tall, yielding a top height that is below 60'. Over very poor soil, peak gain occurs at a base height at or above 40', which allows a pair of 70' end poles (or trees) to support the 49'-long rectangle. Indeed, SCV forms are perhaps most common on both 40 and 30 meters due to the modest requirements for installation compared to the supports required to hold up 80- and 160-meter SCVs, regardless of type.

Rectangles for 40 Meters					Table 6-4
Base Height and Soil Quality vs. Performance					
7.15 MHz					
Soil	Ht ft	Gain dBi	TO deg	Feed R	Feed X
VG	5	3.77	20	95.1	55.6
	10	4.08	19	81.3	21.9
	15	4.25	17	71.6	8.0
	20	4.39	16	63.7	1.5
	25	4.48	15	57.2	-1.1
	30	4.52	14	52.1	-1.3
	35	4.48	13	48.3	-0.1
	40	4.36	12	45.9	1.9
Ave	5	1.65	25	97.0	47.1
	10	2.09	23	79.6	16.3
	15	2.33	21	68.5	5.0
	20	2.50	20	60.6	0.4
	25	2.61	18	54.6	-0.8
	30	2.67	17	50.3	-0.2
	35	2.69	16	47.4	1.3
	40	2.65	15	45.7	3.2
VP	5	0.36	28	89.6	34.4
	10	1.00	26	72.8	11.4
	15	1.45	24	63.0	3.9
	20	1.82	23	56.6	1.4
	25	2.13	21	52.1	1.1
	30	2.42	20	49.1	2.0
	35	2.67	19	47.3	3.3
	40	2.89	19	46.3	4.8

The 40-meter gain curves show their family resemblance to those of their delta and diamond kin. The curves for both very good soil and average soil display distinct downturns at the upper limits of the sampling range. The curve for very poor soil increases its rate of gain increase as we increase the operating frequency. Its curves crosses the curve for average soil at a height of about 35', the peak gain base height for average soil. However, the TO angle for very poor

soil remains about 4° higher than the corresponding TO angle for average soil. TO angles for very good soil are about 3° lower still. These general trends apply to all SCV forms.

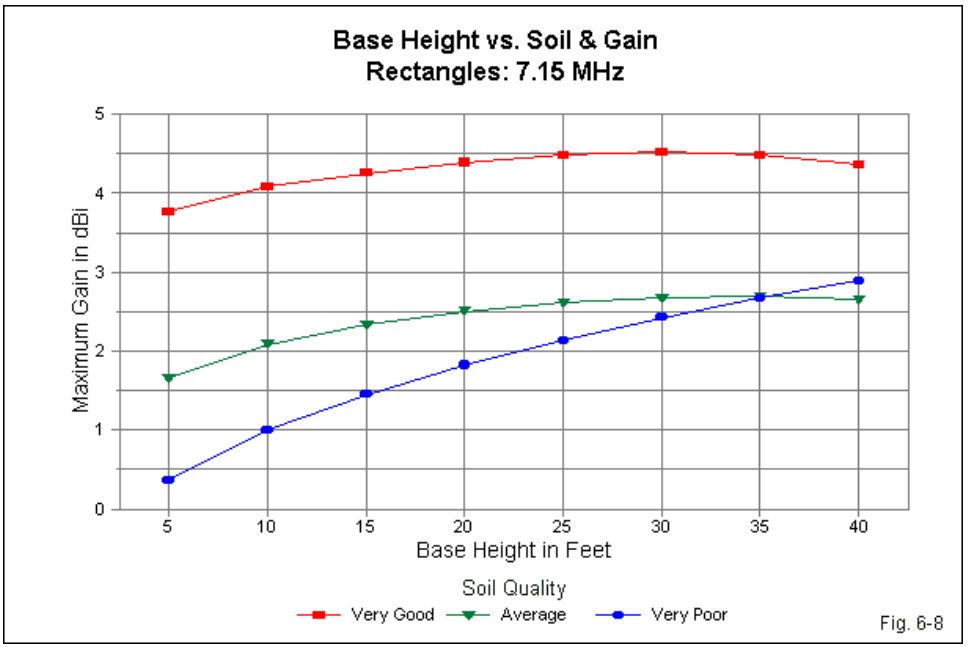

Fig. 6-8

The single 50-Ω rectangle is the shortest of the closed-loop SCV forms. Because the end wires are vertical rather than slanted, the base wire length is also shorter than the base wire of any other closed-loop SCV except the equilateral triangle. At the same time, the rectangle also exhibits a somewhat higher maximum gain than the other closed-loop SCVs. Unless there are support constraints that dictate a form other than the rectangle, our latest SCV qualifies as the best in show—so far. These comparisons are reasonably fair within the limits of modeling software, since all of the SCV models use AWG #12 copper wire over the same set of soil qualities, and none of the forms presses any of the software limits.

The Double Rectangular SCV

One technique used to increase the gain from a rectangular SCV is to double the wire, cross one set of end wires (without shorting them), and feeding only one of the vertical wires at the other end, as shown in outline form in **Fig. 6-9**. This version of the rectangle has sometimes been mis-called the "magnetic slot," as in Russell E. Prack, K5RP, "Magnetic Radiators--Low Profile Paired Verticals for HF," *The ARRL Antenna Compendium*, Vol. 2 (Newington: ARRL, 1989), pp. 39-41. However, the elongated loop or "oblong" (and its relationship to the square quad) has been well-known for a long time. See, for example, the reference to this subject in Karl Rothammel, Y21BK, *Antennenbuch* (Berlin: Militarverlag der DDM, 1984), pp. 230.

General Plan and Key Dimensions of a Double Rectangle SCV

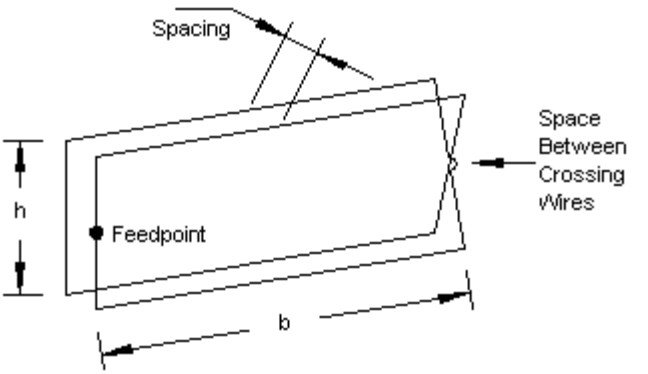

Dimensions and Base Height for Maximum Gain
Above Average Ground

Freq.	1.85 MHz	3.55 MHz	7.15 MHz
B (base)	233.0'	120.0'	58.6'
H (height)	39.4'	22.5'	12.95'
Circumference	544.8'	285.0'	143.1
Spacing	2'	2'	2'
Base Height	95'	58'	37'

Fig. 6-9

In fact, the double rectangle operates according to transmission line principles of impedance transformation that we commonly find in the folded dipole. Two reasonably closely spaced wires in this configuration will effect a 4:1 impedance transformation over a single-wire version of the same basic antenna. The crossing wire at the far end (relative to the feedpoint) of the array is necessary to set the current phase angles correctly for operation, as shown in **Fig. 6-10**. The graphic shows the relative current magnitude and phase angle relationships on the parts of a single rectangle and a double rectangle.

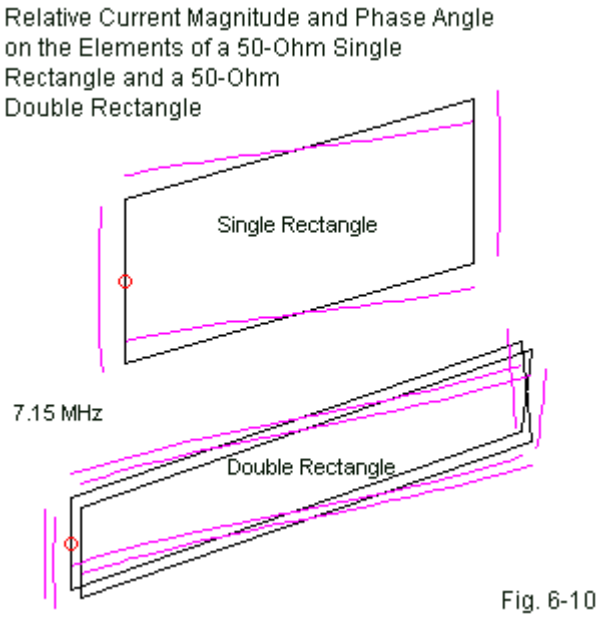

Fig. 6-10

The figure also tells us what gives the double rectangle its additional gain. The design feedpoint impedance of both antennas is 50 Ω. To arrive at 50 Ω for the double rectangle, we need a single loop impedance of about ¼ that value. (With the 2' wire spacing, the single loop of the same outline shows an impedance between 13 and 14 Ω.) However, we have already seen in this

chapter that as we stretch and flatten the rectangle to achieve a lower feedpoint impedance, the gain rises. The double rectangle simply allows us to use the naturally higher-gain version of the rectangle and still maintain our target feedpoint impedance. **Table 6-5** lists the peak gain of the double rectangle over average soil on 160, 80, and 40 meters. For comparison, the table also lists the peak gain values for a single rectangle (Gain 1R) at the same heights and the same soil quality. The column labeled "Delta Gn" shows the gain improvement that we acquire by using a longer and flatter rectangle. In fact, had we used the dimensions of a single 50-Ω rectangle as the basis for a 200-Ω double rectangle, we would find very little performance difference for our doubling of the total wire required in the antenna. (Nevertheless, the impedance might be convenient to those who prefer to feed SCVs with parallel feedline.)

50-Ohm Double Rectangles above Average Ground								Table 6-5
See Fig. 6-9 for dimensions								
Freq MHz	Base Ht	Gain dBi	TO deg	BW deg	Feed R	Feed X	Gain 1R	Delta Gn
1.85	95	4.06	18	72	49.9	0.6	3.62	0.44
3.55	58	3.52	18	74	50	0.2	2.86	0.66
7.15	37	3.48	17	75	50.3	-0.5	2.69	0.79
Notes:	Base Ht = base height in feet for maximum double rectangle gain							
	Gain dBi = maximum gain at the TO angle in dBi							
	TO deg = take-off or elevation angle of maximum gain in degrees							
	BW deg = horizontal beamwidth in degrees							
	Feed R and Feed X = feedpoint impedance reported by final model							
	Gain 1R = maximum gain of a single 50-Ohm rectangle at the same height							
	Delta Gn = gain advantage of a 50-Ohm double rectangle over a single 50-Ohm							
		rectangle (due to shape change)						

The table shows gain values for only a single sample on each band because in all other ways, the performance of the double rectangle parallels the performance of the single rectangle. Perhaps the only small difference occurs in the lesser development of secondary elevation lobes in far-field radiation patterns for the double rectangle. **Fig. 6-11** overlays patterns for all three bands. Only the pattern for 40 meters shows any trace of a secondary elevation lobe. The reason for the absence of secondary elevation lobes lies in the fact that the flatter rectangles of the double form result in a slightly lower feedpoint height, relative to single rectangles that are almost twice as tall.

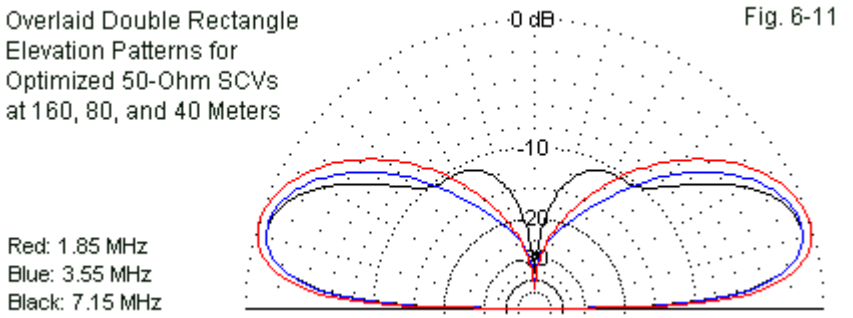

Fig. 6-11

Assuming that the cost of wire and the construction of spacers are lesser difficulties than finding space for an array much larger than a rectangle, the double rectangle may be a very usable option for someone contemplating an SCV. The double rectangle height is less than 60% of the height of a single rectangle and proportionally less than the heights of deltas and diamonds. However, the required base-wire length is only about 120% of the length of a single rectangle, which we have already noted has close to the smallest base-wire length in the SCV family.

The Open Double Rectangle

When we examined double versions of the delta and diamond configurations, we referred to two single antennas set end-to end in a simple plane with a centered feedpoint. The labeling changed when we dealt with the double rectangle, which generally refers to a pair of rectangles closely spaced to achieve a rough 4:1 impedance transformation. We may also create a double rectangle in the general fashion of the double deltas and diamonds. To distinguish it from the double that we have just explored, we may call the new version the open double rectangle. In fact, the idea has been around for quite a while. The first appearance of the array in amateur literature appears to be Lew Gordon, K4VX, "The Double Magnetic Slot Antenna for 80 Meters," *The ARRL Antenna Compendium*, Vol. 4 (Newington: ARRL, 1995), pp. 18-21. **Fig. 6-12** shows the general layout for the open double rectangle.

General Layout of an Open Double Rectangle SCV

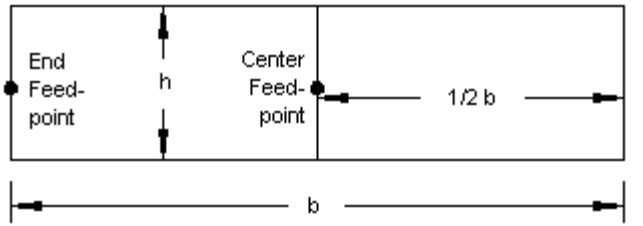

Dimensions: See Table 6-6

Fig. 6-12

The fundamental principles of the open double rectangle are identical to those of the double deltas and diamonds. The vertical portions of the array represent three vertical dipoles fed in phase. Because the halves form closed loops, we cannot attain an ideal ½-λ spacing between the vertical elements, so the array will not show the gain of a set of three full-length dipoles fed in phase using ideal spacing. The next question, then, is how much gain we may derive from the configuration, given our controlling specification of a 50-Ω feedpoint impedance.

The answer to this question depends upon where we choose to feed the array. The feedpoint that corresponds to the feedpoint position of the other double SCVs is at the center of the center vertical wire. Because double arrays exhibit a binomial current distribution, this selection results in a rectangle that—in relative terms—has a shorter base length and a greater height. The current level on the center vertical is twice the value of the current on the end wires. If we select an end wire for the feedpoint, we do not change the current distribution. However, the lower current magnitude relative to the center wire results is a higher feedpoint impedance. To obtain a 50-Ω impedance, we must stretch the rectangles and flatten them. (In fact, we may apply the same analysis to the delta and diamond doubles, although I have no record of an implementation of those configurations.) **Fig. 6-13** shows that the feedpoint position has no effect on the overall current magnitude distribution other than the amount that results from shorter or taller rectangles.

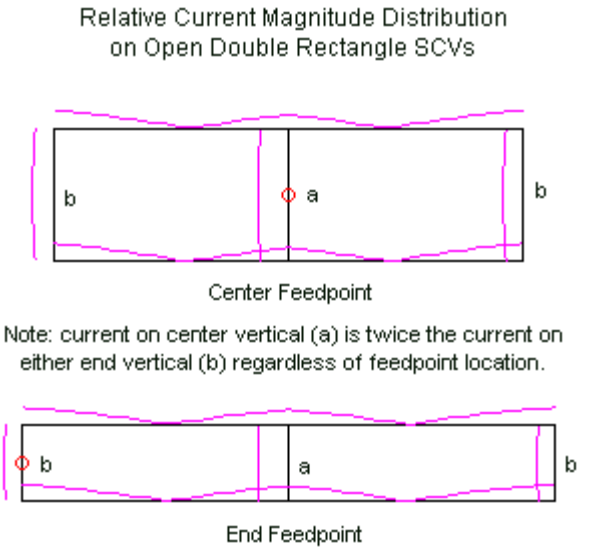

Fig. 6-13

The current distribution also shows the relative proportions of 50-Ω open double rectangles using each of the two options for the feedpoint position. Since both arrays present the same feedpoint impedance, any performance differences results from the change of base to height proportions. As we saw early in the chapter, the longer and flatter the rectangle, the more gain that we may obtain from each part of the array (within the limits shown earlier, which we do not approach in these designs). Consequently, the end-fed open double rectangle produces a higher gain value than the center-fed version. The exact gain advantage depends upon the operating frequency, but ranges from 0.3 to 0.6 dB. **Table 6-6** provides a set of dimensions and the modeled performance of open double rectangles for 160, 80, and 40 meters at optimal base heights for maximum gain over average soil. Note that the center-fed versions are about 60% to 70% taller than the end-fed versions, while the end-fed arrays are about 20% longer than their center-fed counterparts.

Dimensions and Performance: 50-Ohm Open Double Rectangles for 160, 80, and 40 Meters									Table 6-6
Freq MHz	Feedpnt	Base	Height	Base Ht	Gain dBi	TO deg	BW deg	Feed R	Feed X
1.85	Center	337.0	82.9	95	4.86	16	67	49.8	0.1
	End	413.8	47.8	95	5.15	17	57	50.8	0.1
3.55	Center	169.6	44.9	58	4.02	16	69	49.8	-0.1
	End	208.2	26.9	58	4.55	17	58	49.9	0.4
7.15	Center	83.7	23.7	37	3.81	15	70	50.2	-0.1
	End	102.4	14.8	37	4.45	16	59	49.4	0.0
Notes:	Feedpnt = location of feedpoint on either the center vertical or the end vertical								
	Base = total horizontal length of the double rectangle								
	Height = total height of the double rectangle								
	Base Ht = height above ground of the lower rectnagle horizontal wire								
	Gain dBi = maximum gain at the TO angle in dBi								
	TO deg = take-off or elevation angle of maximum gain in degrees								
	BW deg = horizontal beamwidth in degrees								
	Feed R and Feed X = feedpoint impedance reported by final model								

The double diamond that we examined in Chapter 5 obtained a maximum gain of 4.33 dBi on 40 meters. The end-fed open double rectangle shows a gain value that is not significantly higher. However, the rectangular array may prove to be the simpler to implement, considering the number of required supports in each case.

We have looked at single, double, and open-double rectangular SCVs for the lower HF range, but we have not directly compared them. All three designs provide bi-directional gain. The data tables supply a set of numbers for each type of SCV. **Fig. 6-14** overlays azimuth patterns for 40-meter models of an optimized single rectangle, an equally optimized double rectangle, and an end-fed open double rectangle. Each pattern is taken at the TO angle of the array at its base height for maximum gain. In accord with our limiting specification, each array provides an approximate 50-Ω feedpoint impedance.

The patterns show that each increment of re-design produces about the same additional gain for the array. Hence, there is nearly a 2-dB gain difference between the smallest and the largest of the rectangular arrays. The natural consequence of the gain increase is a narrowing of the azimuth pattern. By the time we reach the end-fed open double rectangle, the pattern has acquired a well-defined peanut shape.

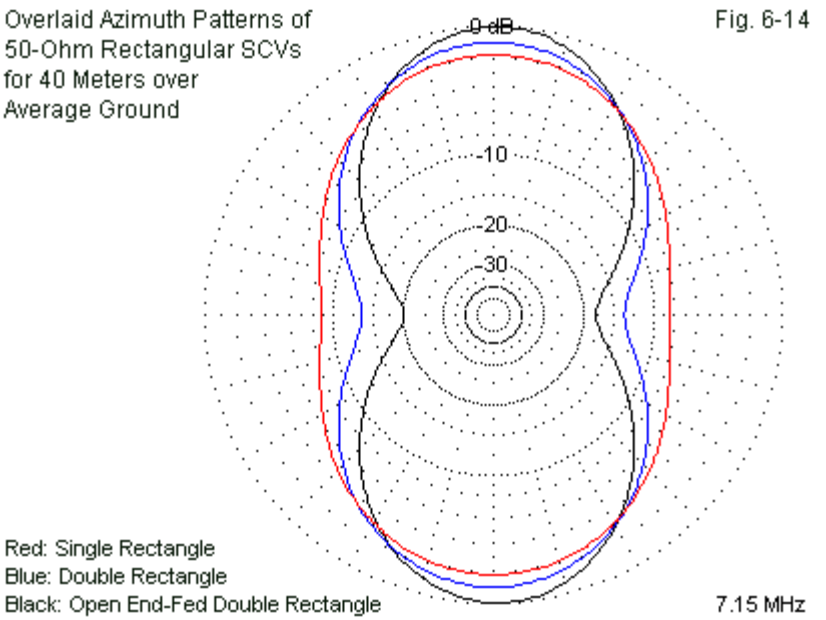

Before we close the book on lower-frequency wire rectangles, we should take a quick look at the SWR bandwidth of each major type of array. **Fig. 6-15** overlays 50-Ω SWR curves for 4 of our models, using the 40-meter band as a frame of reference. Note that none of the rectangular arrays covers the entire band with less than a 2:1 SWR ratio.

The single rectangle covers about 50% of the band within the normal SWR limits. In contrast, the impedance-transforming double rectangle covers barely 20% of the band. We may classify the array as fairly frequency specific. The end-fed open double array fares only slightly better, covering nearly 25% of the band. The center-fed open double version provides perhaps the best coverage—about 2/3 of the band within the 2:1 SWR limit. Since coaxial cable losses tend to be low and power handing ability tends to be high as we reduce the operating frequency, we may stretch the operating capabilities for the single rectangle and

the center-fed double rectangle with an antenna tuner at the equipment end of the line. However, the steeper curves for the other two types of rectangular SCVs strongly suggest that we reduce our expectations of coverage.

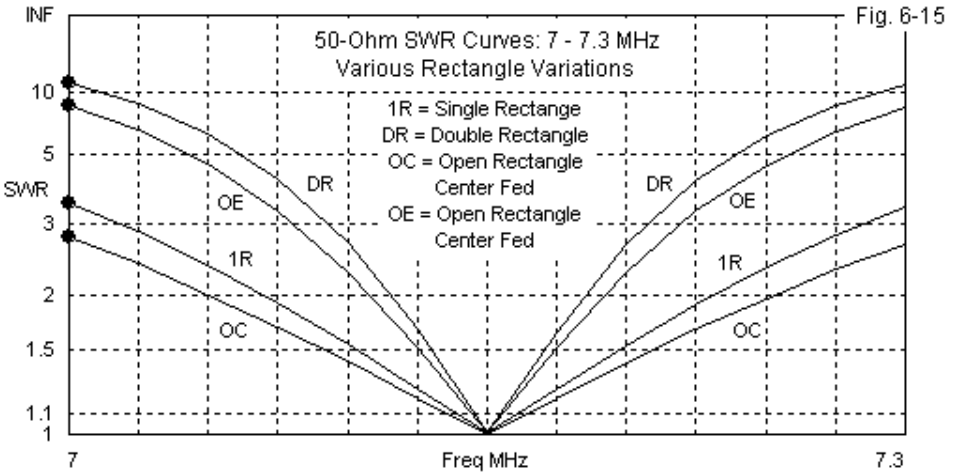

The alternative to accepting narrow frequency limits for any rectangular SCV is to add a variable matching network at the antenna feedpoint. Still, the SWR performance may influence decisions relative to which SCV to implement. For example, one might decide that the simpler physical installation requirements of an end-fed open double rectangle are more than offset by the chapter-5 SWR curve (**Fig. 5-11**) for the slightly more complex double diamond configuration that has nearly the same gain.

The Asymmetrical Double Rectangle (or Hentenna)

About 2 decades ago, Japanese amateurs developed the hentenna (where—so I am told—"hen" means "what is it?"). Although developed for horizontal polarization as a bi-directional 10-meter antenna, we may rotate the array 90° and use it as one more variation of the rectangular SCV. **Fig 6-16** shows the general outline of the hentenna.

The Asymmetrical Double Rectangle (ADR) or Hentenna as an SCV

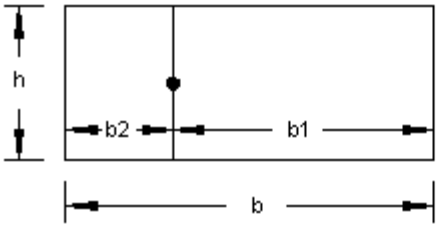

7.15-MHz Dimensions

Base (B)	68.0
B1	50.0
B2	28.0
Height	21.9
Base Height	35.0

Relative Current Magnitude and Phase Distribution

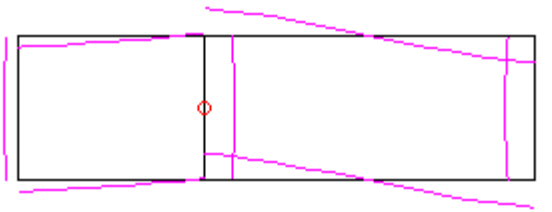

Fig. 6-16

The hentenna is an asymmetrical double rectangle that uses the off-center wire as a feedpoint. Common understandings of the arrangement generally assign the smaller rectangle the role of impedance matching, while the larger rectangle serves the role of producing the radiation. However, Dan Handelsman, N2DT, studied the antenna configuration in detail in a series of articles within the archives of *antenneX*. All three vertical wires show high current levels, but constitute a complex set of phase-angle relationships. The lower portion of the figure shows the relative current magnitude and phase angle distribution for a sample 40-meter hentenna.

N2DT coined the term asymmetrical double rectangle or ADR for the general arrangement of wires and uncovered a number of trends relative to designing them. In general, an optimized ADR yields a gain that falls somewhere between equally optimized center-fed and end-fed symmetrical double rectangles, but in a package that is shorter than the open double rectangles. The 7.15-MHz AWG

#12 copper wire example, whose dimensions appear in the figure, has a peak gain of 3.63 dBi over average soil. Under comparable conditions, a single rectangle showed a gain of 2.69 dBi, while an end-fed open double rectangle had a gain of 4.45 dBi. The ADR gain is very close to the value recorded for the double rectangle model with close-spaced elements.

The ADR remains an experimenter's antenna rather than an operator's antenna. For that reason, we shall bypass further detailed design work with it. However, the antenna experimenter may wish to consult N2DT's articles and develop a series of low-band ADRs for 160 through 40 meters.

The Single Rectangle with a Planar Reflector for VHF/UHF Service

We shall leap to the VHF/UHF range and briefly examine the use of rectangles in planar arrays. We may bypass a study of rectangles as bi-directional higher-range antennas, since we rarely find them used without a reflector. As well, even though we may apply parasitic techniques from Chapter 4 to lower-range rectangles to form beams, in the VHF and UHF ranges, we tend to find planar reflectors used almost exclusively. The chief merit of the planar reflector with a rectangular driver is a widening of the operating bandwidth. We shall begin with a single rectangle as the driver, using 4-mm lossless wire for our samples, just as we did with diamond drivers. Like the planar reflectors, we shall set the antennas at a height of 5-λ above average ground to provide comparative performance figures.

Fig. 6-17 provides the outline of a single rectangle with a planar reflector. As with earlier models, the planar reflector consists of a wire grid composed of standard size cells and a wire size that simulates a solid surface. The required spacing between the reflector and the driver is very similar to the value required by the single diamond driver (0.186-λ vs. 0.19-λ). The rectangle is shorter in both dimensions than the single diamond. However, the optimal reflector size turns out to be about 1.2-λ vertically and 1.4-λ horizontally for the vertically polarized array. The driver itself has a size that depends upon both the desired feedpoint impedance (50 Ω) and the influence of the planar reflector at the spacing needed to yield the desired impedance.

Fig. 6-17

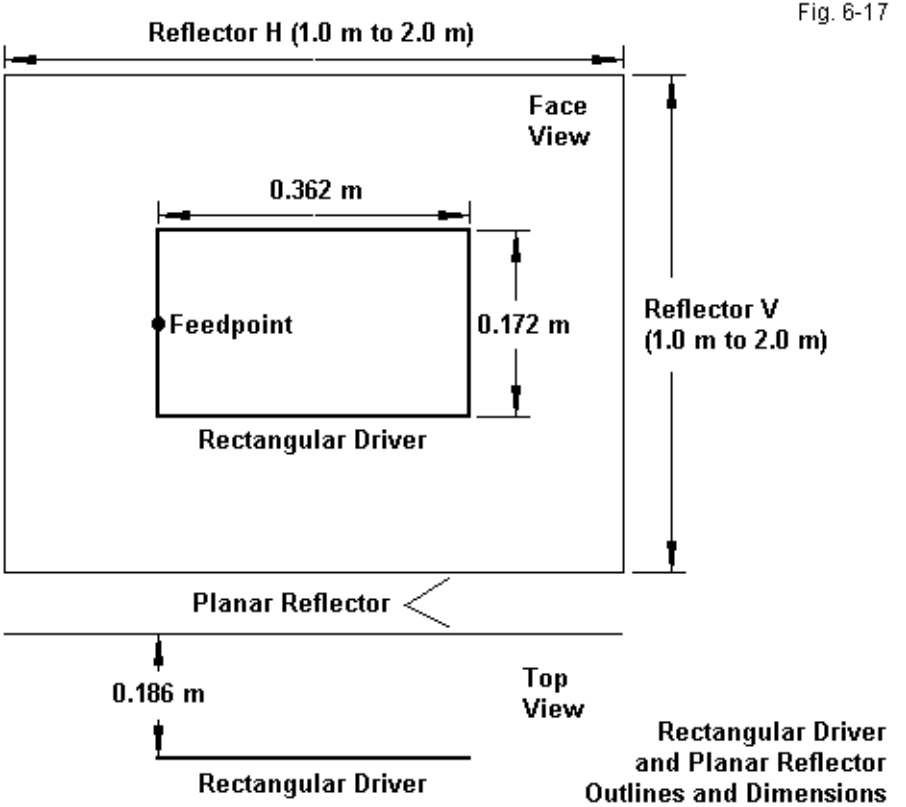

Single rectangle driver and planar reflector 5-λ up at 299.7925 MHz

Dim:	El Dia. λ	El.	Length λ	Width λ	Reflector	H λ	V λ	Spacing λ
	0.004	Driver	0.362	0.172	Optimal	1.4	1.2	0.186

Performance:	Gain dBi	F-B Ratio dB	TO degrees	HplBW degrees	Impedance R+/-jX Ω
Optimal Ref.	14.91	19.54	2.6	61.8	49.8 + j0.4

The listing shows a gain value of 14.91 dBi at 5-λ above ground. This value exceeds the gain achieved by the diamond array by about 0.8 dB. The front-to-back ratio of the single rectangle planar array is also about 1.5 dB higher than the single-diamond array value.

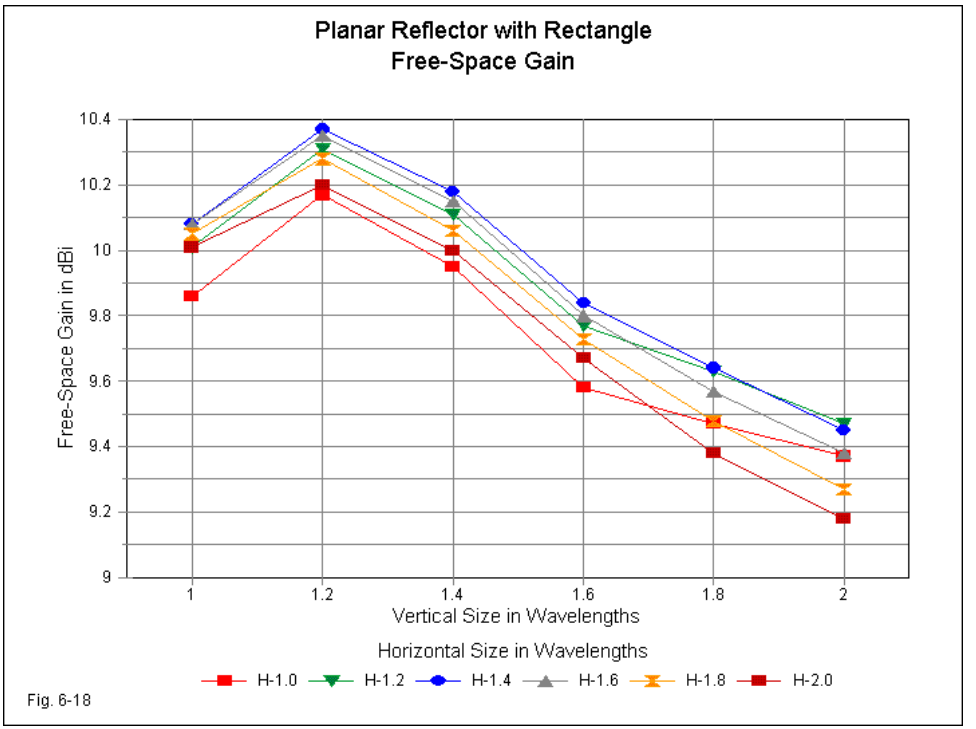

Fig. 6-18

To illustrate the effect of a planar reflector's size on the gain of a single-rectangle array, **Fig. 6-18** shows the free-space gain curves for reflectors having a wide range of vertical and horizontal dimensions. Regardless of the horizontal length, the gain peaks with a vertical length of 1.2-λ. At the vertical size, peak gain occurs with a horizontal length of 1.4-λ, although the gain difference between lengths of 1.2-λ through 1.6-λ is very small.

Fig. 6-19 provides curves for the front-to-back ratio over the same range of reflector sizes. Within the most relevant span of horizontal dimensions, the front-to-back ratio continues to increase as we increase the vertical dimension. Note that both graphs are specific to the driver involved, especially to the driver dimensions. Relative to forward gain, there is an optimal amount of reflector size excess over a driver both vertically and horizontally.

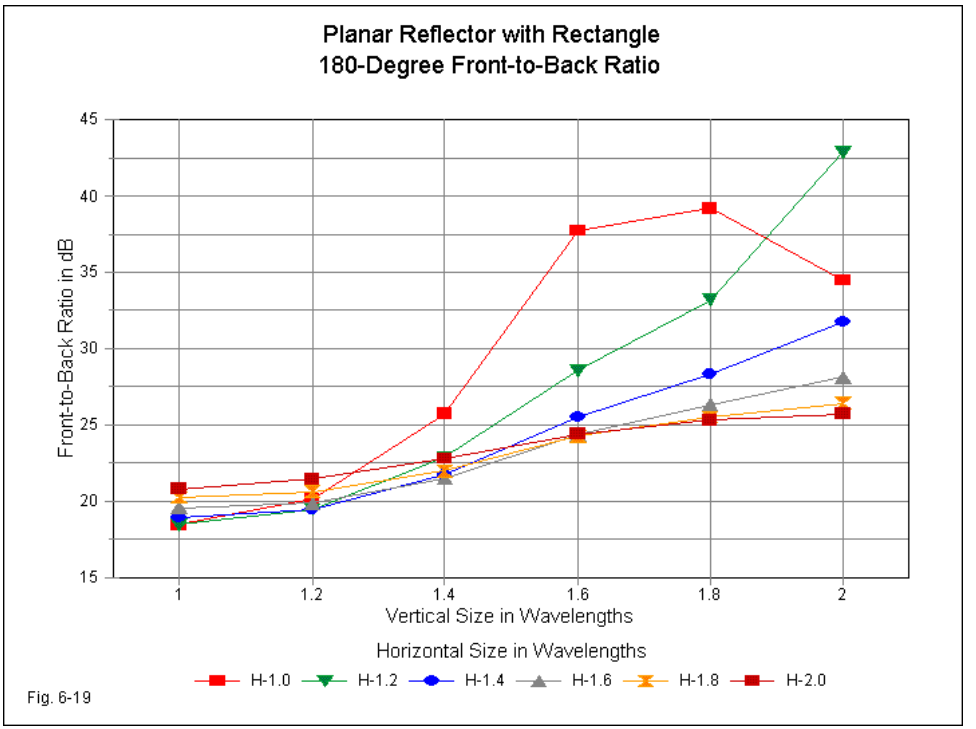

Fig. 6-19

In **Fig. 6-20**, we can see the 2:1 50-Ω SWR curve for the single-rectangle planar array. The 2:1 ratio range is about 14 MHz with a 300-MHz design frequency, about a 4.7% bandwidth. This range falls midway between the bandwidth of the 2-meter band (2.7%) and the 70-cm band (6.8%). The SWR bandwidth is slightly less than obtained by the single-diamond planar array.

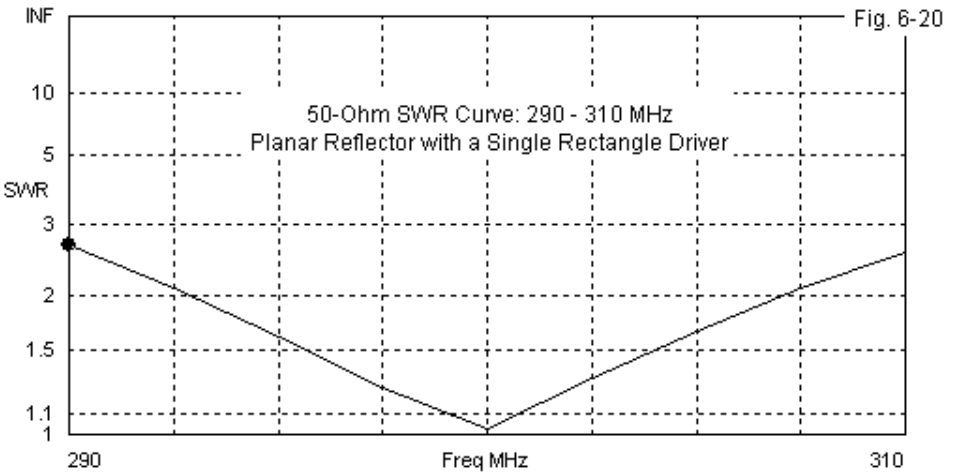

We have examined the single-rectangle planar array in some detail for two major reasons. First, the data may help us understand better how planar arrays obtain their performance. Second, the data will stand in contrast to similar data for a planar array using a center-fed open double rectangle as the driving element.

The Double Rectangle with a Planar Reflector for VHF/UHF Service

We may replace the single rectangle with a center-fed open double rectangle with suitable adjustments to the optimal reflector size. **Fig. 6-21** provides an outline of the resulting antenna. The driver turns out to be more than twice as long as the single rectangle, but somewhat shorter. The dimensions are a bit smaller in both directions than the double diamond driver shown in the preceding chapter. As a consequence of the driver dimensions, the reflector size is 1.2-λ vertically by 1.6-λ horizontally for best performance. This reflector size also proved to be optimal for the double-diamond array. Perhaps the most interesting difference between the double-rectangle array and its single-rectangle counterpart is the spacing value: 0.235-λ. This value is about 25% further away from the reflector than in the double-diamond array.

Fig. 6-21

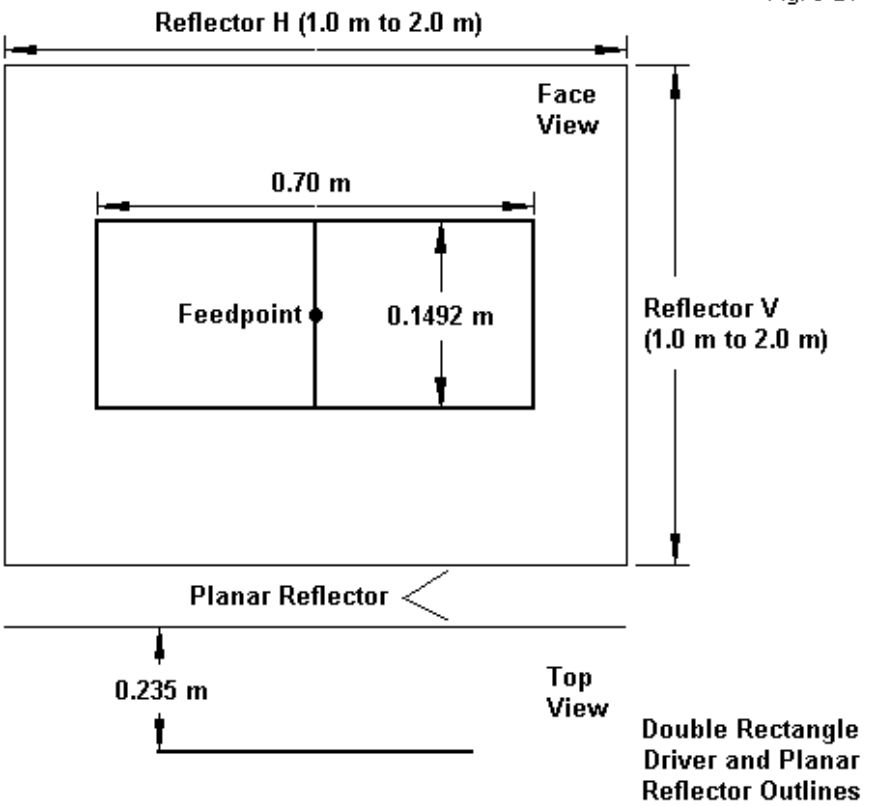

Fig. 6-22 shows the free-space gain curves that yield the optimal size for the planar reflector. As was the case for the single rectangle, the gain peaks with a vertical height of 1.2-λ, whatever the horizontal dimension may be. The optimal horizontal dimension lies between 1.6-λ and 1.8-λ and may extend to 2.0-λ without an operationally detectable drop in performance. With an array height of 5-λ above real ground, the free-space dimension values require no revision. However, you may wish to compare the gain values for both single and double

rectangle drivers.

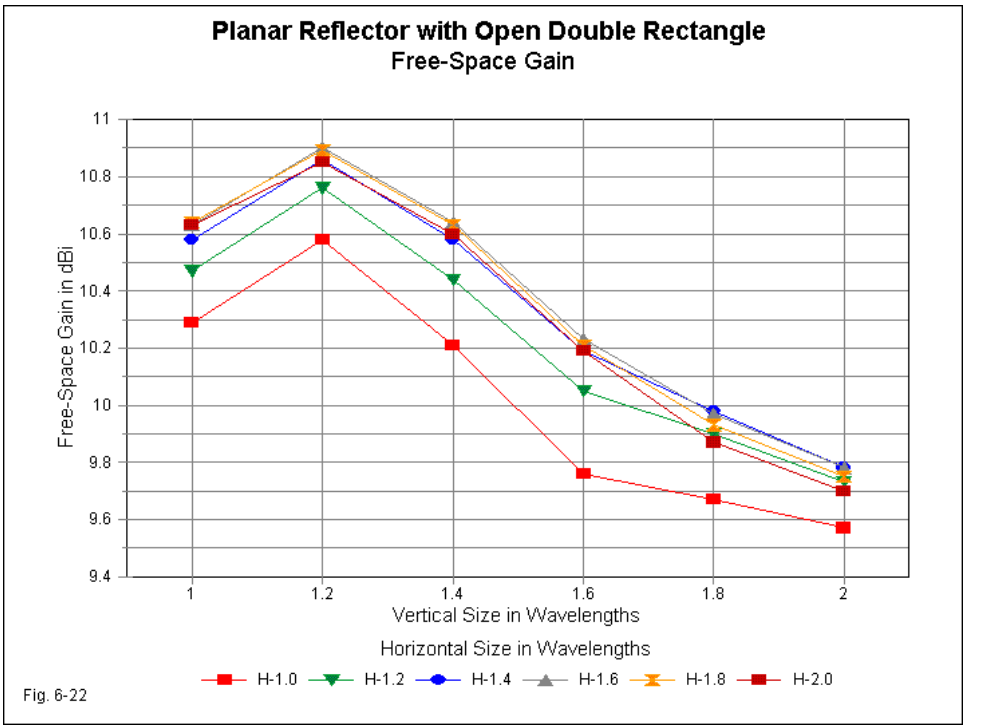

Fig. 6-22

The front-to-back data appear in **Fig. 6-23**. Like the single-rectangle curves, horizontal dimensions well below optimal for maximum gain tend to show peak front-to-back ratios within the range of sampling. For all but the horizontally shortest reflector sizes, increasing the vertical dimension increases the front-to-back ratio. These tendencies in the behavior of planar reflectors are not unique to the types of drivers that we have examined in this chapter, in Chapter 5, or in chapter 3. Rather, they are generic to planar reflector arrays in general, regardless of the type of driver involved.

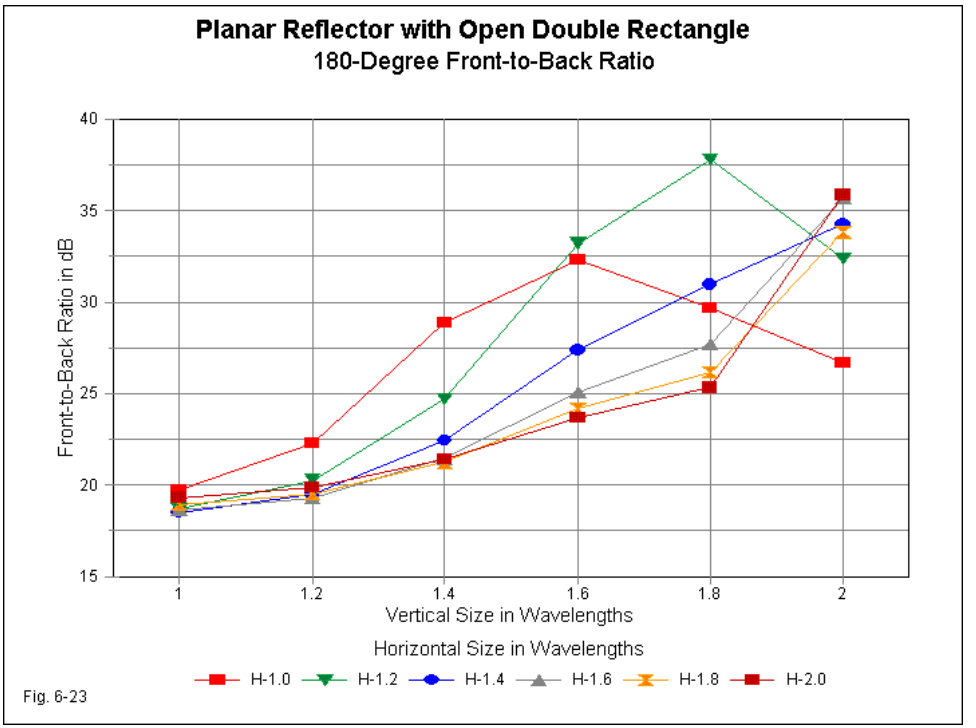

Fig. 6-23

Double diamond driver and planar reflector 5-λ up at 299.7925 MHz

Dim:	El Dia. λ	El.	Length λ	Width λ	Reflector	H λ	V λ	Spacing λ
	0.004	Driver	0.700	0.149	Optimal	1.6	1.2	0.235

Performance:	Gain dBi	F-B Ratio dB	TO degrees	HplBW degrees	Impedance R+/-jX Ω
Optimal Ref.	15.45	19.45	2.7	52.6	49.6 – j0.4

Despite the gain advantage of an isolated open double rectangle over a single rectangle, we only obtain about 0.5-dB additional gain by replacing the single rectangle driver with the double rectangle in a planar array. As well, we find almost no difference in the front-to-back ratio. Operationally, one may well

question whether there is any advantage in using a double rectangle rather than a single rectangle. For our purposes, the key question is why we obtain such a small increment of improvement after doubling the driver size.

The answer lies in the earliest parts of this chapter. To obtain higher gain from the double rectangle, we stretched and flattened the rectangles. When we created the center-fed open double rectangle, we automatically incurred a low feedpoint impedance relative to the driver's independent performance. To raise that feedpoint impedance to the 50-Ω level in the planar array, we did not resort to an end-wire feedpoint. Instead, we used the spacing from the reflector to determine in large part the driver impedance. The greater the amount of required impedance increase, the greater must be the reflector-to-driver spacing. However, as we increase the spacing, the array gain goes down. The final array performance is a consequence of those maneuvers.

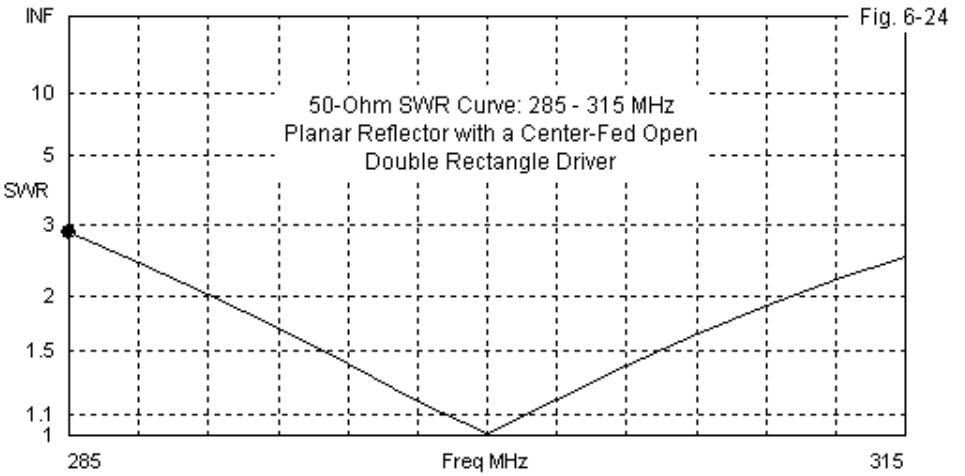

Perhaps the one major advantage offered by the double rectangle array lies in the SWR bandwidth, shown in **Fig. 6-24**. The wider spacing between the driver and the reflector that reduced the available forward gain also had the effect of broadening the SWR bandwidth for the array. The center-fed open double

rectangle driver provides about 21-MHz coverage between the 2:1-SWR points on the 50-Ω curve. The corresponding bandwidth is about 7%, enough to cover the entire 70-cm band, assuming a directly scaled array. For many VHF/UHF arrays using SCV drivers, raw gain may not be the sole decisive factor in settling upon a design.

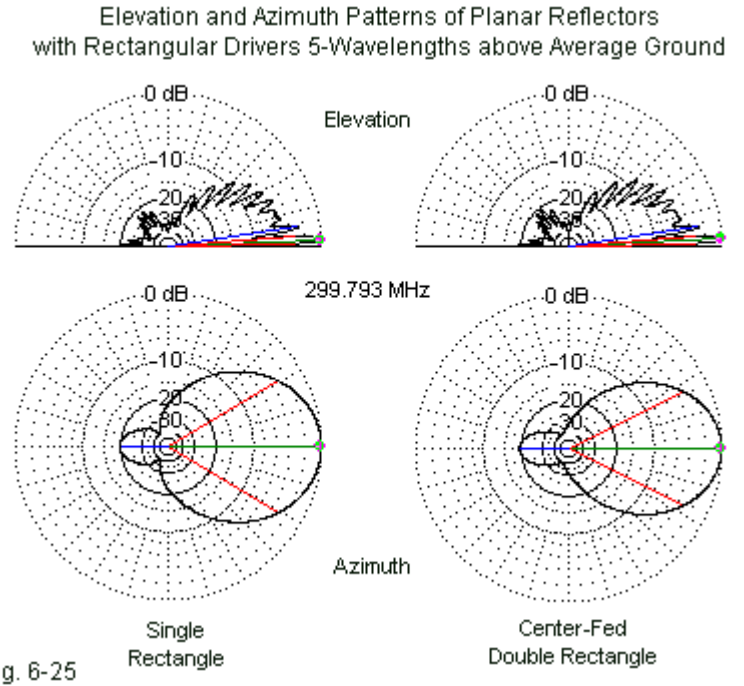

Fig. 6-25

For reference, **Fig. 6-25** provides elevation and azimuth patterns for both the single rectangle and double rectangle planar reflector arrays. The double rectangle has a slightly narrower beamwidth than its single rectangle counterpart. The elevation patterns reveal that the double rectangle array also has stronger higher-angle lobes. Since both arrays show very similar gain values, the reduction in H-plane (horizontal) beamwidth effected by the double rectangle

driver results in a wider E-plane (vertical) beamwidth. The difference would be clearer in free-space patterns, but is detectable from the elevation lobe strengths in the respective elevation patterns.

Conclusion

The journey through the rectangular SCV and the many variations upon it has led us down many paths. Beyond the single rectangle, we examined the double rectangle with close-spaced wires and two versions of the open double rectangle. Indeed, the rectangle has perhaps more practical variations than almost any other SCV form. We also examined in some detail VHF/UHF implementations of side-fed rectangles.

The core of our explorations resides in the initial portions of this chapter that looked intently at what happens when we lengthen and flatten SCVs of any shape. The rectangular shape simply proved to be the most convenient and easily understood shape to use in performing the investigation. By using a free-space environment, we could isolate the effects of SCV shape (and also wire conductivity) from the effects that involved the ground, the antenna height, and the operating frequency. In that foray into lengthening-and-flattening, we provided a basis for understanding the behavior and performance numbers of the many variations on the rectangle. As well, it allowed us to understand the performance of rectangular drivers used with planar arrays. Indeed, the general considerations relating to SCV shape apply to all forms of closed loop vertically polarized antennas.

However, not all SCV forms use closed loops.

7. Open-Ended SCVs

In this chapter, we shall depart from the closed loops that have been the trademark of all of the SCV forms that we have so far explored. Our focus will change to the open-ended SCVs, specifically, the half-square and the bobtail curtain. In amateur antenna literature, we find an interesting twist of fate, since the bobtail curtain appeared earlier than the more fundamental half-square. In fact, for many decades, antenna enthusiasts thought of the half-square as 2/3 of a bobtail curtain.

For historical information on the half-square, see Ben Vester, K3BC, "The Half Square Antenna," *QST* (March, 1974), 11-14. Additional notice appeared in *Radio Communications* for January, 1977 (p. 36). See also Robert Schiers, N0AN, "The Half-Square Antenna," *Ham Radio* (December, 1981), 48-50. All three of these early sources show the antenna as voltage-fed from one of the free ends. For the bobtail curtain, see Woodrow Smith, W6BCX, "Bet My Money on the Bobtail Beam," *CQ* (March, 1948), 21-23 and 92-95. See also Smith's follow-up articles, "The Bobtail Curtain and Inverted Ground Plane," Parts 1 and 2 in *Ham Radio* (February, 1983), 82-86, and (March, 1983), 28-30.

We shall restore electronic priorities by examining the half-square first, and the first task is to see how and why this antenna fits into the overall scheme of SCV forms. Indeed, only one fact stands between us and a clear view of the relationship. Consider a right-angle delta SCV. The apex of the triangle represents the tips of two vertical elements, a high voltage point. The junction of these two points is a structural convenience, but not an electrical necessity. We may create a small gap between the two sloping vertical elements without disturbing the performance. As we widen the gap, we may have to re-size the elements slightly, but by successive steps, we can trace the evolution of the right-angle delta (or virtually any other closed SCV loop) into the open-ended half-square. **Fig. 7-1** traces the evolution. In **Table 7-1**, we find a few of the steps a modeler might take to trace the continuous development of the open-end SCV from its closed relatives.

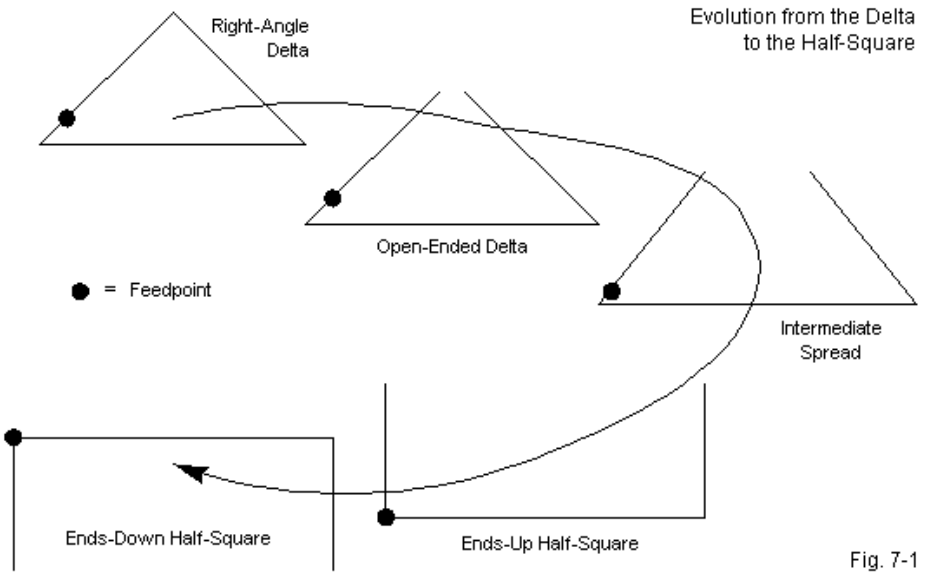

Fig. 7-1

Partial Evolution of a Right-Angle Delta to a Half-Square SCV				Table 7-1
Step	Antenna Description	Gain dBi	Feed R +/- jX Ohms	
1	Right-angle delta:			
	60.8' base; 30.4' height	3.31		51 + j 6
2	Right-angle delta: apex			
	wires separated 0.2'	3.31		51 + j 6
3	Height increase to 30.41';			
	apex spread 0.4'	3.32		51 + j 7
4	Height increase to 30.70';			
	apex spread 2.0'	3.36		51 - j 1
5	Height increase to 31.1';			
	apex spread 4.0'	3.41		53 + j 5
Note:	Frequency: 7.15 MHz			
	Wire: #12 AWG copper			
	Models are in free space			

The table does not show the complete pathway, but with the final 4' spread between vertical tips, it establishes a viable open-ended SCV. In addition, it hints at one of the benefits of using an open-ended SCV: additional gain. As we approach a pair of truly vertical elements, the array gain increases. The figure also shows a second benefit of opening the loop: we may move the feedpoint to the corner of the array and increase the spacing between vertical section to a more nearly ideal 0.5-λ. The gain will not reach the level of 2 vertical dipoles spaced 0.5-λ apart and fed in phase, since we do not have both halves of the dipole available for simple radiation duty. Half of each dipole forms the base phase-line of the array. Nevertheless, we shall obtain a higher gain than we can obtain from any of the closed loops.

The figure also shows one more feature of the half-square that is especially useful in the lower HF and upper MF ranges. We may place the base wire at the array top and let the vertical wires hang down from it. The move has two benefits. First, it simplifies construction, since we may hang a half-square between two tall supports. Second, the revised orientation overcomes the fact that each vertical leg is ¼-λ tall by lowering the optimal base height needed for maximum gain. With the base wire at the top (and an upper corner feedpoint), the high-current regions of the vertical legs are already elevated.

The Half-Square SCV for 160, 80, and 40 Meters

As we have done in all preceding chapters, we shall employ AWG #12 copper wire to construct half-squares for the lower frequency amateur bands. See **Fig. 7-2** for the outline and the dimensions that we shall eventually use.

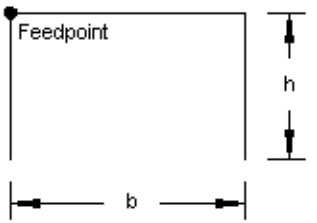

Half-Square SCV

Dimensions

Freq.	1.85 MHz	3.55 MHz	7.15 MHz
B (base)	241.0'	126.3'	62.45'
H (height)	150.0'	78.0'	39.0'
Total Wire	541.0'	282.3'	140.45'

Fig. 7-2

The half-square presents a conundrum relative to our previous practice of constructing SCVs that result in a 50-Ω feedpoint impedance. As we systematically vary the base length and the height of the vertical sections, we certainly can arrive at a version of the antenna that provides the target feedpoint impedance relative to an upper corner current feedpoint. However, that feedpoint impedance does not result in the highest gain that we may obtain from the half-square. **Table 7-2** provides the data from a free-space exercise in which I changed the length of the vertical elements for 1.85 MHz in 4' increments. Then I altered the base-wire length until the array arrived at resonance.

Shape Factor for 1.85-MHz Half-Squares				Table 7-2
Height	Base	Gain	Feed R	Feed X
154	253.6	4.48	70.9	-0.2
150	241.0	4.50	64.6	-0.3
146	248.5	4.48	59.3	0.3
142	256.0	4.42	54.9	0.6
138	263.5	4.31	51.5	0.7
134	271.0	4.14	48.8	0.5

As the table suggests—confirmed by the graph in **Fig. 7-3**—the gain is on a steep downward slope as the feedpoint impedance passes through the 50-Ω level. Peak gain occurs at a higher feedpoint impedance, in the vicinity of 65 Ω. The difference of 0.3 dB may not be earth shaking in operation, but it raises the question of which set of dimensions we should use in our exploration.

I decided upon using the dimensions that provide maximum gain for an interesting reason. Although we can feed the half-square at an upper corner and obtain good service from a coaxial cable transmission line, we have an alternative feedpoint that we shall later explore in more detail. By using a parallel tank circuit or any equivalent network that can transform a low line impedance to a high antenna impedance, we can feed the half-square at the tip of one of the two vertical legs. In fact, this system has been the mainstay for feeding both half-squares and bobtail curtains for most of their existence. The larger of the two types of arrays has been around for well over a half century.

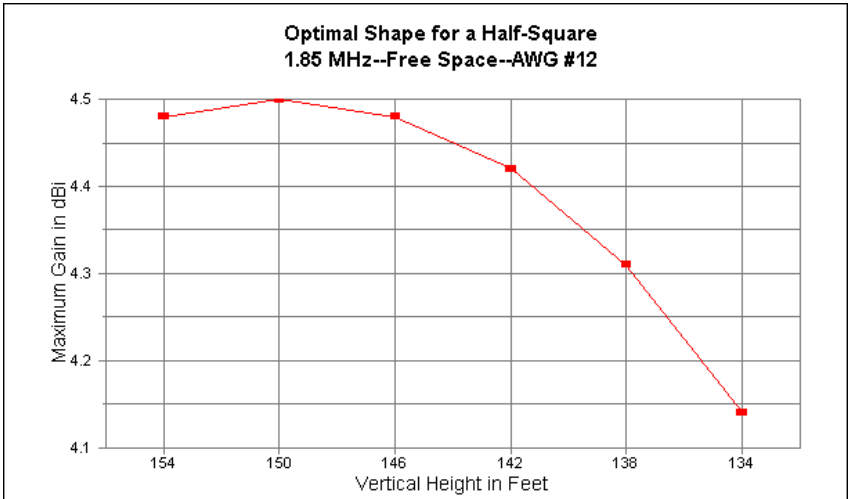
Optimal Shape for a Half-Square
1.85 MHz--Free Space--AWG #12
Maximum Gain in dBi
4.5
4.4
4.3
4.2
4.1
154
150
146
142
138
134
Vertical Height in Feet
See Table 7-2 for Corresponding Base Lengths

Fig. 7-3

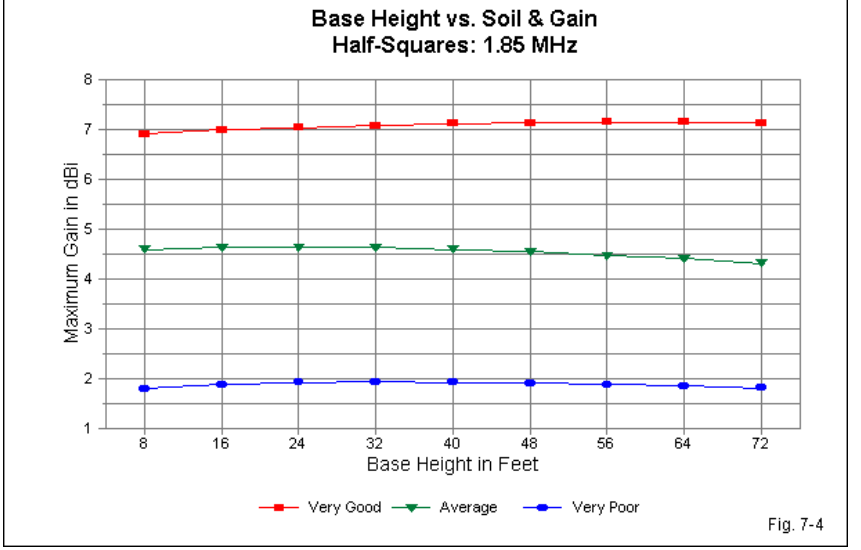
Base Height vs. Soil & Gain
Half-Squares: 1.85 MHz
Maximum Gain in dBi
8
7
6
5
4
3
2
1
8
16
24
32
40
48
56
64
72
Base Height in Feet
Very Good
Average
Very Poor

Fig. 7-4

Half-Squares for 160 Meters					Table 7-3
Base Height and Soil Quality vs. Performance					
1.85 MHz					
Soil	Ht ft	Gain dBi	TO deg	Feed R	Feed X
VG	8	6.92	14	82.6	22.0
	16	6.99	14	78.6	10.8
	24	7.04	13	75.5	4.5
	32	7.09	13	72.8	0.6
	40	7.12	12	70.5	-1.8
	48	7.14	12	68.5	-3.3
	56	7.15	12	66.7	-4.0
	64	7.15	11	65.2	-4.3
	72	7.14	11	64.0	-4.2
Ave	8	4.59	18	83.6	21.0
	16	4.63	18	78.9	10.1
	24	4.63	17	75.3	4.0
	32	4.62	17	72.4	0.4
	40	4.59	16	69.9	-1.8
	48	4.54	16	67.9	-3.1
	56	4.47	15	66.2	-3.6
	64	4.40	15	64.8	-3.8
	72	4.31	14	63.7	-3.6
VP	8	1.79	22	84.6	16.8
	16	1.88	21	78.6	7.4
	24	1.92	21	74.4	2.4
	32	1.93	20	71.2	-0.4
	40	1.92	19	68.8	-2.0
	48	1.90	19	66.9	-2.7
	56	1.87	18	65.4	-2.9
	64	1.84	18	64.3	-2.8
	72	1.80	18	63.4	-2.5

Fig. 7-4 and **Table 7-3** trace our normal exercise in examining the performance of a 160-meter antenna over a wide range of soil types (very good, average, and very poor) as we raise the base height of the antenna. In one

sense, the half-square is quite normal, and in another, it is quite abnormal. Like the single rectangle SCV, the half-square results in peak gain at a lower height over average soil than over the more extreme varieties. Both very good soil and very poor soil show distinct base heights for peak gain on this upper MF band, although the base height for peak gain is highest over the best soil of the group.

Compared to the single rectangle and all of the closed-loop SCVs, the base height required for a half square to reach peak gain is considerably lower. Indeed, one may operate an SCV with a very low base height without losing much gain potential at all. This fact gives considerable confidence to the practice of voltage feeding one of the wire tips of the half-square array. However, given the dimensions that we have selected for our exercises, a 160-meter vertical leg still requires supports that are at least 150' tall. In many 1.85-MHz installations, builders sacrifice a little gain to enable the use of more moderately tall supports. The most convenient method of shortening the half-square without increasing the base-wire length is to fold the tips of the vertical legs inward toward each other. Because these folds occur in relatively low current regions of the elements, the array does not lose too much gain, although the lower overall height will also exact a price. As well, those who shorten the height must also contend with changes in the corner feedpoint impedance.

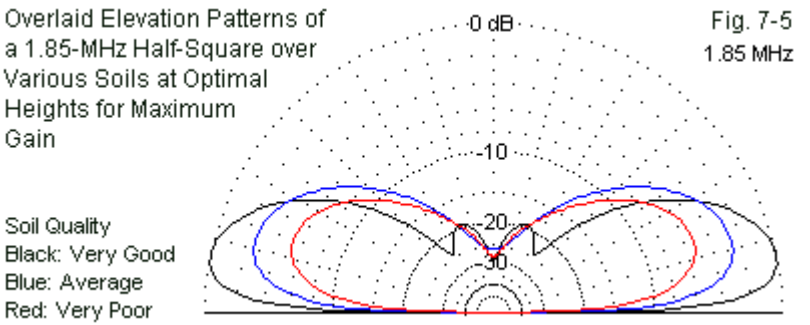

The low base height required to optimize gain over any soil type has another advantage. **Fig. 7-5** overlays the elevation patterns for 160-meter half-squares,

with each antenna at the base height needed for maximum gain. The patterns for very poor and average soils show no signs of an emergent secondary, higher-angle, elevation lobe to increase the antenna's sensitivity to high-angle noise and signal sources. Even over very good soil, the secondary elevation lobes are 20 dB lower than the maximum gain from the bi-directional array.

When we turn to 80-meter versions of the half-square, we encounter similar trends. At this stage of our examination, let's simply replicate the 160-meter free-space exercise, but change the dimensions to those appropriate to 3.55 MHz. In this case, I used a range of vertical legs from 72' to 80' in the free-space test to find the shape that produces maximum gain and the shape that produces a 50-Ω feedpoint impedance. In each case, I selected a base length that yielded resonance at the upper corner feedpoint. (Since there is no earth in free space to define the vertical and the horizontal, terms like "upper" are relative only to the conventions used in the modeling software.) **Table 7-4** shows the results of these efforts.

Shape Factor for 3.55-MHz Half-Squares				Table 7-4
Height	Base	Gain	Feed R	Feed X
80	122.6	4.58	68.6	-0.5
78	126.3	4.60	62.7	-0.4
76	130.0	4.58	57.7	-0.4
74	133.8	4.53	53.6	0.8
72	137.5	4.43	50.4	0.4

As shown in both the table and in the graph in **Fig. 7-6**, we lose about 0.2 dB by insisting upon a 50-Ω feedpoint impedance. The gain decrease is not as large as on 160 meters. However, the peak free-space gain shown by the 3.55-MHz half-square is slightly higher than the peak gain achieved by the 1.85-MHz counterpart. Like all such differences, we cannot tell from just two samples whether we have a trend or merely a difference.

Using the dimensions for peak gain, we may explore the effects of base height on gain over various soils. For this data set, examine **Fig. 7-7** and **Table 7-5**.

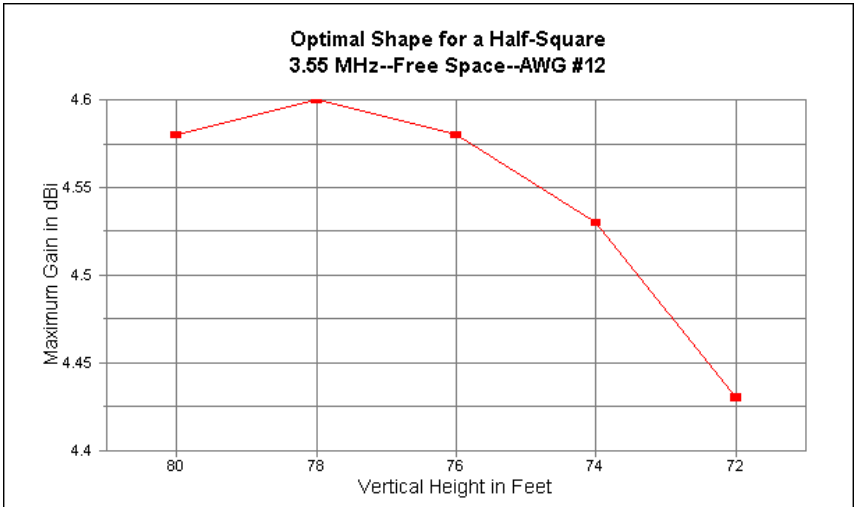

See Table 7-4 for Corresponding Base Lengths

Fig. 7-6

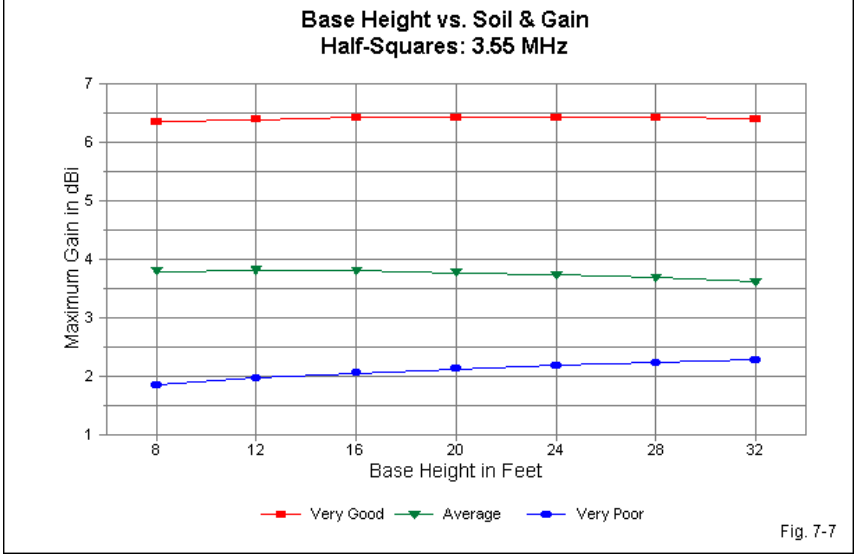

Fig. 7-7

Half-Squares for 80 Meters					Table 7-5
Base Height and Soil Quality vs. Performance					
3.55 MHz					
Soil	Ht ft	Gain dBi	TO deg	Feed R	Feed X
VG	8	6.35	15	77.1	11.6
	12	6.39	14	73.8	5.2
	16	6.42	14	71.2	1.2
	20	6.43	14	68.9	1.3
	24	6.43	13	66.9	-2.8
	28	6.43	13	65.2	-3.6
	32	6.40	13	63.7	-4.0
AV	8	3.79	19	77.4	10.5
	12	3.81	19	73.7	4.6
	16	3.80	18	70.7	1.0
	20	3.77	17	68.3	-1.2
	24	3.73	17	66.3	-2.5
	28	3.68	17	64.2	-3.1
	32	3.61	16	63.3	-3.3
VP	8	1.84	23	76.2	6.9
	12	1.96	22	72.2	2.5
	16	2.05	22	69.3	0.0
	20	2.12	21	67.0	-1.5
	24	2.18	21	65.3	-2.2
	28	2.23	20	63.9	-2.5
	32	2.27	20	62.9	-2.4

As we discovered while looking at the closed-loop SCVs, the 80-meter half-square over very poor soil does not show a peak gain within the limits of the sampled base heights. Peak gain over very good soil is actually a very broad range of heights from about 16' to 28' above ground. As usual, peak gain over average soil occurs at the lowest base heights. Nevertheless, the half-squares show a significant gain advantage over any of the closed-loop SCV forms, especially over average to very good soil. As in the case of 160-meter half-squares, builders without tall enough supports sometimes resort to bending the lower vertical ends to fit the antenna within their installation limits.

Fig. 7-8 provides 80-meter azimuth patterns for a half-square over each of the soil qualities. Each pattern uses the TO angle applicable to the base height that yields maximum gain. The obvious reading from these patterns is that the depth of the side nulls in the plane of the wires is directly proportional to the bi-directional gain. For these patterns, the base wire connecting the vertical runs horizontally across the page.

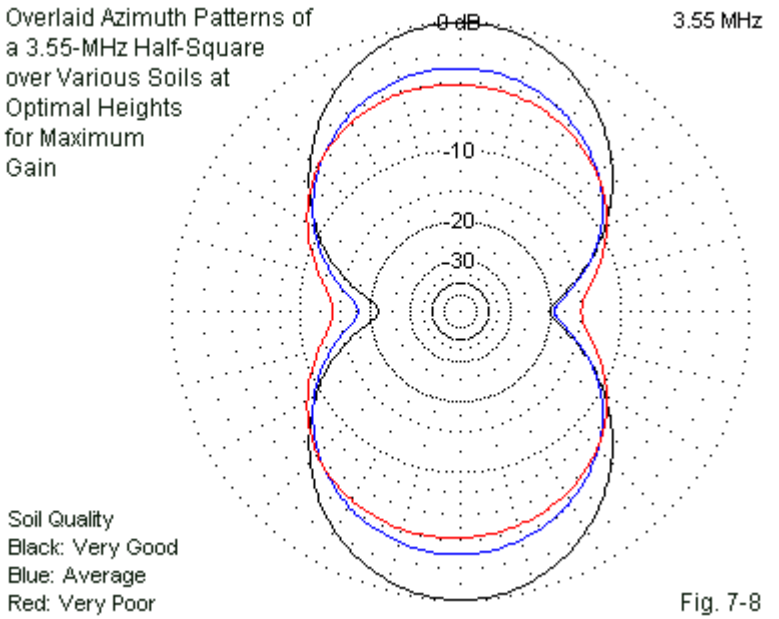

Fig. 7-8

The less evident fact about half-square azimuth patterns is that they are not perfectly symmetrical. Corner feeding plus copper-wire losses in the base wire produce very small but noticeable differences in the depth of the side nulls regardless of the soil quality. In operation, we would not be able to detect these differences, although they will tend to grow, especially as we increase the element diameter as a fraction of a wavelength. As a result, what we can scarcely notice in these thin-wire half-squares will become quite evident in fat-

element VHF and UHF versions of the antenna.

Our final sample for in-depth examination is for 7.15 MHz. (The Appendix, of course, contains some recommended maximum-gain half-square dimensions for 160 through 30 meters, including 75 meters.) In general, the dimensions of a 40-meter half-square are highly manageable for most amateur installation sites. A pair of 50' supports separated by perhaps 70' or so will anchor a full-size and optimized half-square SCV.

The shape-factor data in **Table 7**-6 (and the graph in **Fig. 7-9**) tend to confirm a trend that we suspected after reviewing the 80-meter data. As the frequency rises, the free-space half-squares shaped for maximum gain show a slow but regular increase in the maximum gain value. As well, we find a significant physical difference between the overall shape of the half-square that produces maximum gain and the version that shows a 50-Ω feedpoint impedance. Even at 7.15 MHz, the two base-wire lengths differ by over 5', while the vertical portions differ by 3'.

Shape Factor for 7.15-MHz Half-Squares				Table 7-6
Height	Base	Gain	Feed R	Feed X
40	60.60	4.65	69.3	-0.5
39	62.45	4.68	63.1	-0.1
38	64.30	4.67	57.9	0.2
37	66.10	4.63	53.7	-0.9
36	68.00	4.54	50.2	0.2

When we explore the behavior of the maximum-gain version of the half-square over various ground qualities, we find some properties in common with other SCV forms. For example, at 40 meters, peak gain over very good ground occurs at a lower height than over average ground, a reversal of the 80-meter situation. The gain over very poor soil does not reach a peak value within the sampling range. The data for these models appear in **Table 7-7**, with the gain curves graphed in **Fig. 7-10**. Note that, unlike the closed-loop SCVs, the gain for very poor soil does not climb high enough to cross the gain curve for average soil within the sampling range of the exercise.

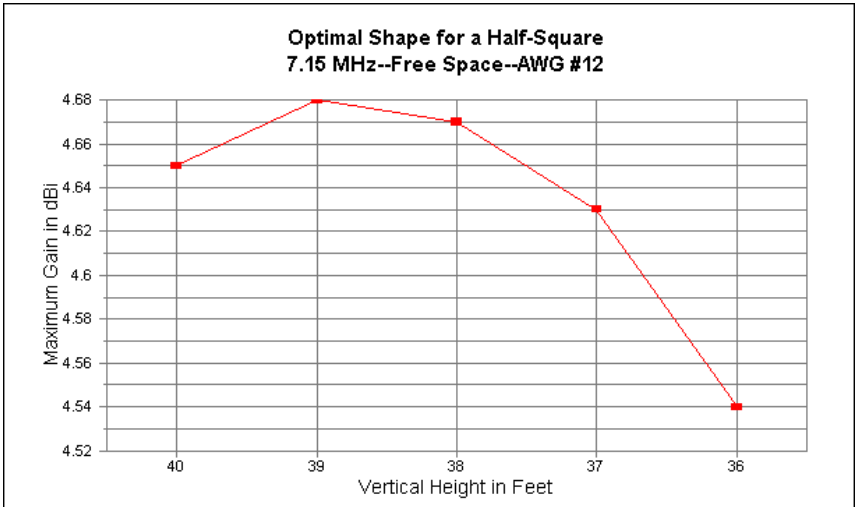

See Table 7-6 for Corresponding Base Lengths

Fig. 7-9

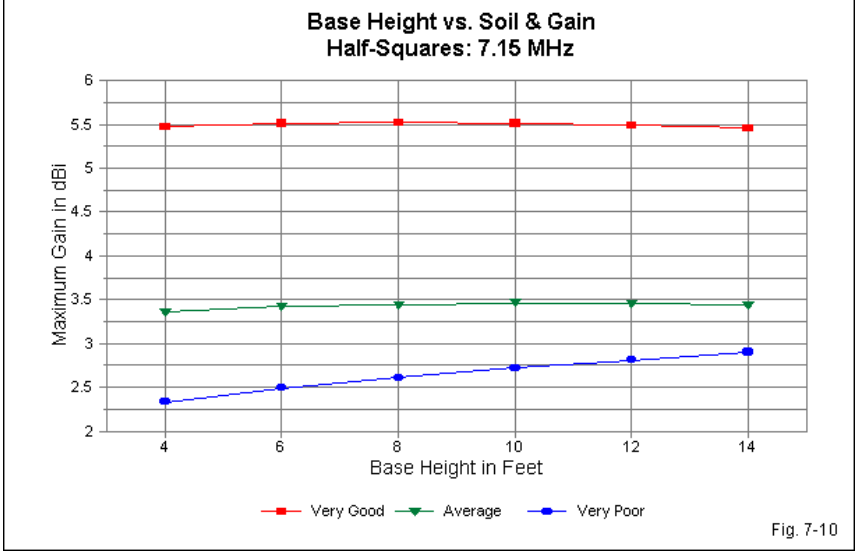

Fig. 7-10

Half-Squares for 40 Meters					Table 7-7
Base Height and Soil Quality vs. Performance					
7.15 MHz					
Soil	Ht ft	Gain dBi	TO deg	Feed R	Feed X
VG	4	5.48	17	78.0	11.0
	6	5.51	16	74.4	4.7
	8	5.52	16	71.5	0.8
	10	5.51	15	69.1	-1.5
	12	5.49	15	67.0	-2.9
	14	5.46	14	65.3	-3.6
Ave	4	3.36	20	77.7	9.2
	6	3.42	20	73.8	3.7
	8	3.44	19	70.8	0.5
	10	3.46	19	68.4	-1.4
	12	3.45	18	66.4	-2.5
	14	3.44	18	64.8	-2.9
VP	4	2.33	23	75.0	6.7
	6	2.49	23	71.6	2.6
	8	2.61	22	69.0	0.3
	10	2.72	22	67.1	-1.0
	12	2.81	21	65.5	-1.7
	14	2.90	21	64.3	-2.0

An interesting facet of this collection of half-square designs (including those in the Appendix through 30 meters) is the nearly constant base-wire length and vertical leg length across the entire frequency span—when we measure these values in wavelengths. Using AWG #12 copper wire, all of the half square base-wires are just about 0.454-λ long, while all of the vertical sections are 0.282-λ long. We may note in passing that a half-square yields maximum gain with a spacing between the vertical sections that is less than 0.5-λ, the ideal spacing for vertical dipoles fed in phase.

One danger of uncovering relationships of this sort is that they all too often find their way into cutting formulas that quickly lose the required qualifications that yield accurate outcomes. The constant lengths apply to AWG #12 copper wire,

which grows a bit thicker as a fraction of a wavelength with rising frequency. Significantly different wire sizes would yield different base-wire and leg lengths. Since skin effect is not a linear function, the values might well not be as constant. As well, we find a very small but telling amount of drift when we reach 30 meters, suggesting that further increases in frequency would reveal values that do not fit the listed constants. Nevertheless, use of the constants within the qualifications of frequency, wire size, and wire material will yield very close to optimal half-squares for the lower HF and the upper MF amateur bands.

The Bobtail Curtain for 160, 80, and 40 Meters

Among open-ended SCVs, the analog to the double delta, the double diamond, and the open double rectangle is the bobtail curtain. The name is a coinage by the antenna's developer, Woodrow Smith, and arose in an era in which cute names overrode descriptive accuracy in the assignment of antenna labels. When Smith named the array, amateurs still dreamed of large wire arrays, including the now passé Sterba curtain. The "bobtail" portion of the name derives from the appearance of having cut off the bottom half of the curtain. Unfortunately, the misnomer can mislead: the Sterba array was horizontally polarized, while the bobtail is vertically polarized, as Smith well knew. The proper electrical analog to the bobtail curtain is a set of three vertical dipoles (or monopoles), all fed in phase with the correct current distribution for maximum gain. The set of three dipoles requires a complex network to assure that the feedpoint currents are in phase and that the end dipoles receive exactly half the current magnitude as the center dipole. In contrast, the bobtail curtain requires only a single feedpoint, with the base wires providing the correct phasing among elements. This simplification opens the antenna to extensive amateur use.

Fig. 7-11 shows the outlines of a bobtail curtain along with the dimensions that we shall use in these exercises. The relative current magnitude and phase-angle distribution along the antenna wires appears in **Fig. 7-12**. Whereas the half-square has a single base wire for setting the opposing vertical to a correct phase-angle condition, the bobtail curtain has two such base wires referenced to the center vertical leg. The relative current at the top of the center vertical—the nominal feedpoint—is twice the magnitude of the current at the top of each outer

vertical leg.

Bobtail Curtain SCV

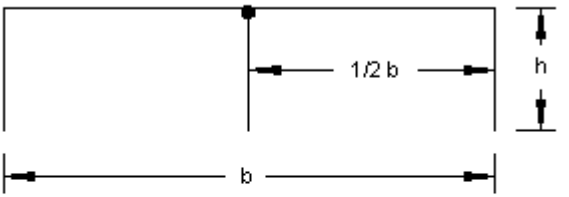

Dimensions

Freq.	1.85 MHz	3.55 MHz	7.15 MHz
B (base)	570.0'	296.5'	152.2'
½ B	285.0'	148.25'	76.1'
H (height)	130.0'	68.0'	33.0'

Fig. 7-11

Relative Current Magnitude and Phase-Angle
Distribution on a Bobtail Curtain
Optimized for Maximum Gain

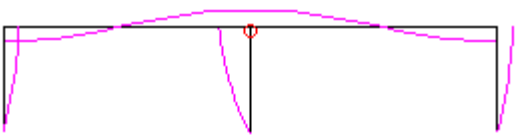

Fig. 7-12

Like the half-square, the bobtail curtain has different dimensions for a 50-Ω feedpoint impedance and for maximum gain. **Fig. 7-11** shows the dimensions for maximum gain, the ones that we shall subsequently use when exploring the behavior of bobtails at various heights above various soil qualities. The dimensions for maximum gain do not reveal any constants when measured in

terms of wavelengths. Instead, as we raise the operating frequency, the base wires grow slowly longer, while the vertical legs become slightly shorter.

Bobtail Curtain Dimensions and Free-Space Performance							Table 7-8
Freq MHz	Version	H (vert)	B (horiz)	Gain dBi	BW deg	Feed R	Feed X
1.85	Opt Gn	130.0	570.0	6.20	46	27.3	-0.1
	50-Ohm	152.0	447.0	5.87	54	50.0	0.2
3.55	Opt Gn	68.0	296.5	6.34	45	26.7	-0.2
	50-Ohm	79.5	232.8	5.95	53	49.7	0.9
7.15	Opt Gn	33.0	152.2	6.47	45	24.5	0.2
	50-Ohm	39.5	116.0	6.01	53	49.0	0.0
Notes:	Opt Gn = dimensions optimized for maximum gain						
	50-Ohm = dimensions optimized for a 50-Ohm feedpoint impedance						
	H (vert) = array height in feet						
	B (horiz) = total array length in feet; spacing between verticals is 1/2 B						
	All bobtail curtains use AWG #12 copper wire						

In 1988, Kent Svensson, SM4CAN, produced a small booklet called *Practical Bobtail Layouts*. He recommends a base-wire length of 0.480-λ between verticals and 0.227-λ for the vertical legs. Note that these values fall about half-way between the 50-Ω values and the maximum gain values. Kent derived his values strictly from empirical experimentation using base-feeding methods.

The maximum-gain versions of the bobtail curtain require spacing values between vertical legs that are just over 0.5-λ. The sample free-space models use values between 0.535-λ and 0.553-λ. In contrast, the 50-Ω versions of the array call for spacing values just under 0.5-λ, about 0.42-λ for all three bands. (The vertical legs of these three versions fall between 0.286-λ and 0.287-λ, yielding more constant dimensional values than the maximum-gain versions.) The dimensional differences appear in the overlaid free-space azimuth patterns for the 40-meter versions of the bobtail curtain. Of course, the maximum gain version has slightly more gain. However, the interesting aspect of the pattern lies in the side-null regions. The 50-Ω version with narrower spacing between vertical legs has distinct side nulls. However, when we increase the bobtail spacing to a value higher than 0.5-λ between verticals, we find the beginnings of sidelobes. These lobes are operationally insignificant, but hold considerable interest. They

are the same sidelobes that we noted would appear when we slightly stretch the ideal spacing of in-phase-fed vertical dipoles in order to maximize array gain. In both cases, if we increase the spacing further, we actually end up with less broadside gain, because the side lobes grow rapidly.

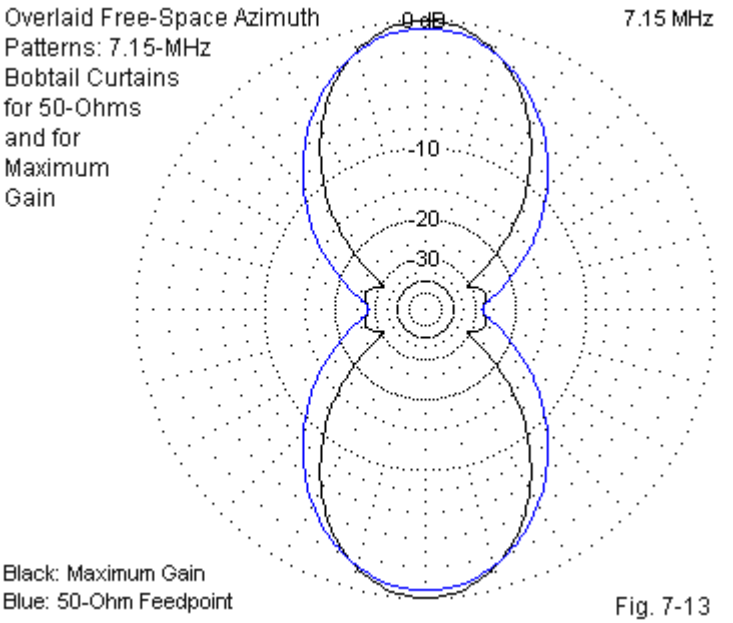

Fig. 7-13

With respect to the base height and the soil quality of a bobtail curtain, we find a general replication of the patterns that we uncovered for the half-square array. The required height above ground is largely a function of the "inverted" arrangement of the open-ended SCV that places the low-current, high-voltage tips closer to ground. On 160 meters, average soil calls for the lowest base height that yields maximum gain. Both very good soil and very poor soil show distinct heights at which maximum gain occurs. The peak over very poor soil is unique to 160 meters and does not occur at the higher frequencies used in this collection of samples.

Table 7-9 and **Fig. 7-14** provide the relevant data in both tabular and graphical formats. Compare the gain values with the half-square information in **Table 7-3** and **Fig. 7-4**. The bobtail curtain provides about 1.5 to 1.6 dB higher gain potential over the half-square, regardless of the soil type. This gain value rests in both cases on the use of the maximum gain dimensions and the maximum gain base height applicable to each antenna and soil type.

Bobtail Curtains for 160 Meters					Table 7-9
Base Height and Soil Quality vs. Performance					
1.85 MHz					
Soil	Ht ft	Gain dBi	TO deg	Feed R	Feed X
VG	8	8.52	14	37.3	23.5
	16	8.57	14	35.6	14.7
	24	8.60	14	34.2	9.4
	32	8.63	13	33.0	6.0
	40	8.65	13	32.0	3.6
	48	8.66	12	31.2	2.0
	56	8.66	12	30.4	0.9
	64	8.66	12	29.8	0.1
Ave	8	6.16	19	39.2	23.0
	16	6.21	19	36.7	14.1
	24	6.22	18	34.8	8.9
	32	6.21	17	33.3	5.6
	40	6.19	17	32.1	3.3
	48	6.09	16	31.1	1.8
	56	6.02	16	30.2	0.7
	64	4.40	15	29.5	0.0
VP	8	3.19	23	41.7	19.6
	16	3.35	23	37.8	11.7
	24	3.44	22	35.1	7.2
	32	3.48	21	33.2	4.3
	40	3.49	21	31.7	2.4
	48	3.48	20	30.6	1.2
	56	3.45	19	29.7	0.4
	64	3.43	19	29.0	-0.1

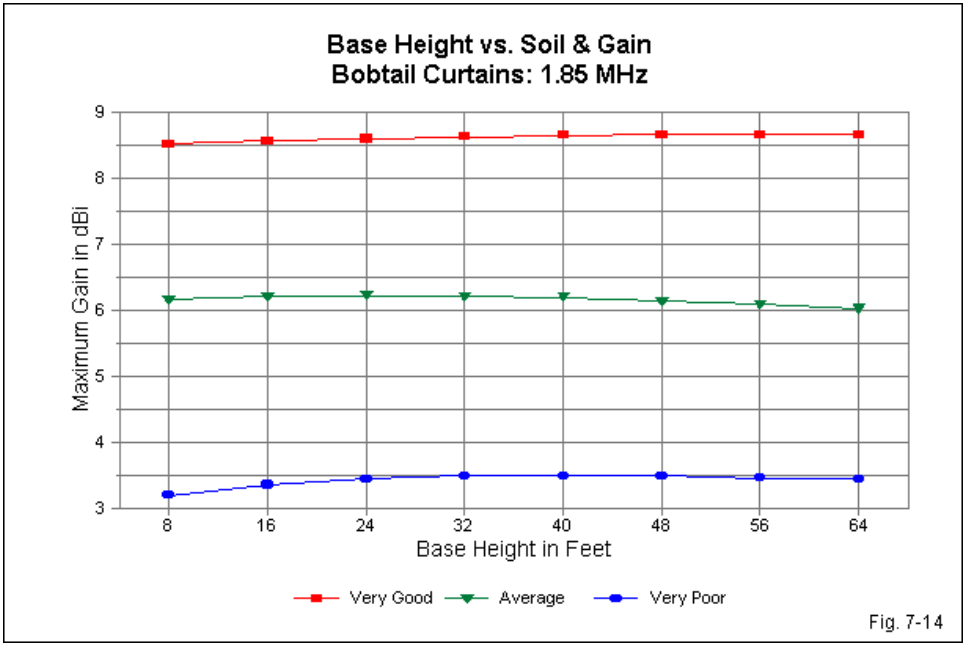

Fig. 7-14

At 3.55, the general patterns relating to base height and soil type also replicate those we uncovered for the half-square. The data for base height between 8' and 32' appear in **Table 7-10**, with a graphic portrayal of the gain curves in **Fig. 7-15**. The base heights over average soil for both the half square and the bobtail curtain occur between 12' and 16' above ground. Over very good soil, the proper height range is 16' to 28', a comparatively wide range. For the 80-meter arrays over very poor soil, the sampling range does not show a peak gain maximum height. Finally, for both arrays, the rate of gain increase with an increase in base height over very poor soil is steeper at 3.55 MHz than at 1.85 MHz. Hence, the gain cure for that soil quality begins to approach the curve for average soil at the top sampled base height.

We may also note that the lowest base height in the sampling range—at least over very good through average soil—does not show a radical drop in the array

gain (for either the half-square or the bobtail curtain). Therefore, many bobtail users prefer to place the antenna tips relatively close to ground level. The practice is convenient for base feeding methods, but is subject to several limitations. As we saw in an early chapter, the poorer the soil quality, the more an antenna with less than very good soil may benefit from local ground improvement, such as the addition of a very large-area ground screen. In addition, the lower tips of half-square and bobtail curtain elements show very high voltages during transmission. Safety concerns dictate that no one (human or pet animal) should be able to touch the element ends.

Bobtail Curtains for 80 Meters					Table 7-10
Base Height and Soil Quality vs. Performance					
3.55 MHz					
Soil	Ht ft	Gain dBi	TO deg	Feed R	Feed X
VG	8	7.96	16	35.6	14.9
	12	7.98	15	34.0	9.6
	16	8.00	15	32.8	6.2
	20	8.01	14	31.7	3.8
	24	8.01	14	30.8	2.1
	28	8.00	14	30.0	0.9
	32	7.98	13	29.3	0.1
AV	8	5.35	20	36.9	13.9
	12	5.39	20	34.8	8.8
	16	5.40	19	33.1	5.5
	20	5.38	18	31.8	3.3
	24	5.36	18	30.7	1.8
	28	5.31	17	29.8	0.8
	32	5.26	17	29.0	0.0
VP	8	3.22	24	37.0	10.3
	12	3.39	23	34.4	6.3
	16	3.52	22	32.5	2.8
	20	3.62	22	31.1	2.2
	24	3.69	21	30.0	1.1
	28	3.76	21	29.1	0.4
	32	3.81	20	28.5	-0.1

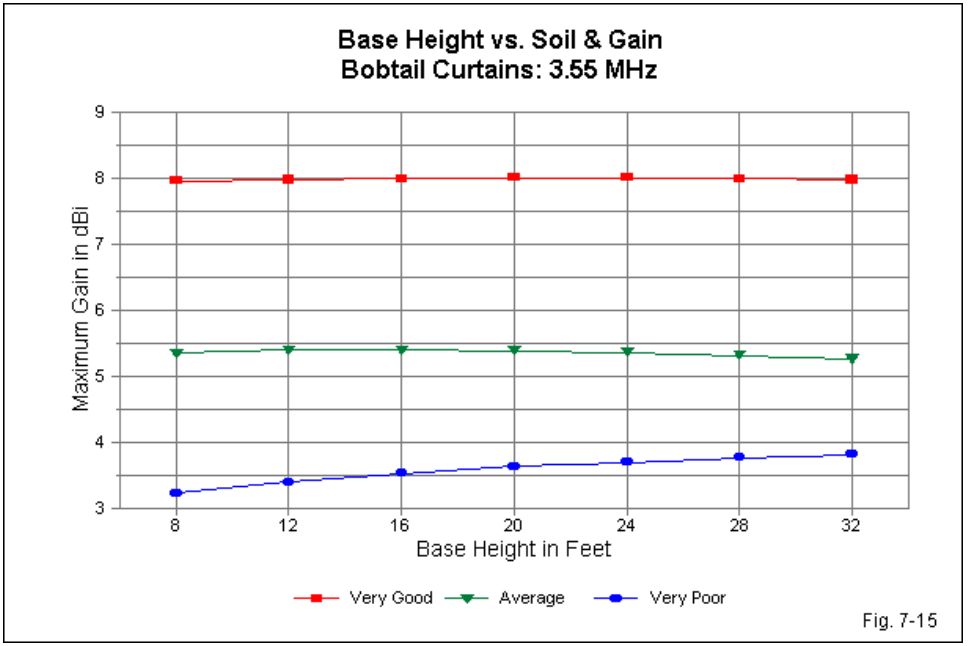

Fig. 7-15

On 40 meters, we find small but distinct variations in the behavior of bobtail curtains relative to the half-squares that we explored earlier. The bobtail's gain advantage remains between 1.5 and 1.6 dB over the half-square. However, the base heights that yield maximum gain differ. The half-square shows maximum gain over very good through average soil at a somewhat lower height than the bobtail curtain. However, the gain curves are very broad, so that for base height differences of up to 6' or so, the gain difference would not be operationally noticeable. The base height for maximum gain over very poor soil occurs above the sampling limit of 18'. Like the 40-meter gain curve for the half-square over very poor soil in **Fig. 7-10**, the corresponding curve for the bobtail in **Fig. 7-16** does not reach the average soil curve. As you may recall, the closed-loop SCVs showed an intersection between those curves on 40 meters.

The data for 40 meters appears in **Table 7-11**. Like all of the SCV data for

double forms, the models presume a flat plane formed by the vertical elements. Potential SCV users with limited installation space face the temptation to bend the double SCV to form a V in the base wires. Do not give in to this temptation. Even shallow angles reduce the spacing between the end verticals, and the result is a severe reduction in gain. SCV gain over a single vertical dipole largely rests upon using the maximum spacing up to about 0.5-λ between verticals.

Bobtail Curtains for 40 Meters					Table 7-11
Base Height and Soil Quality vs. Performance					
7.15 MHz					
Soil	Ht ft	Gain dBi	TO deg	Feed R	Feed X
VG	4	7.07	18	36.1	26.3
	6	7.12	18	33.8	16.9
	8	7.15	17	32.1	11.4
	10	7.16	17	30.8	7.7
	12	7.15	16	29.6	5.1
	14	7.13	16	28.7	3.3
	16	7.10	15	27.9	2.1
	18	7.06	15	27.2	1.1
Ave	4	4.69	23	38.4	23.5
	6	4.83	22	35.2	14.9
	8	4.92	21	32.9	9.9
	10	4.98	20	31.2	6.6
	12	5.01	20	29.8	4.4
	14	5.03	19	28.7	2.8
	16	5.03	19	27.8	1.7
	18	5.02	18	27.0	1.0
VP	4	3.31	25	37.7	18.0
	6	3.60	25	34.3	11.3
	8	3.81	24	31.9	7.4
	10	3.99	24	30.2	4.9
	12	4.13	23	28.9	3.3
	14	4.25	22	27.9	2.1
	16	4.26	22	27.1	1.4
	18	4.46	21	26.5	0.9

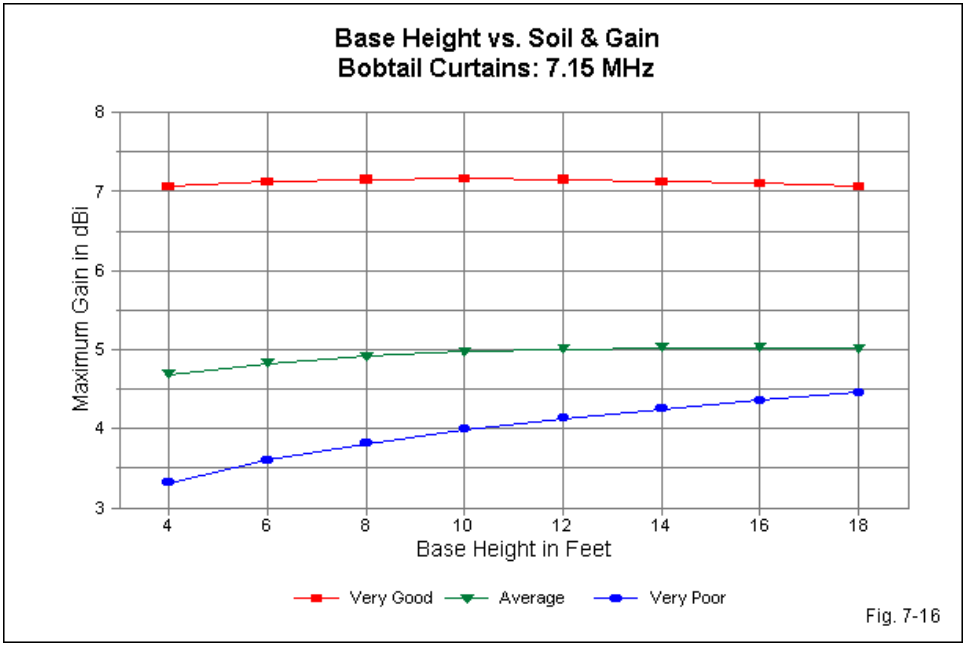

Fig. 7-16

We have found that the open-ended SCVs achieve the highest gain among the SCV forms relative to the number of vertical sections within an array. We noted in Chapter 6 that the open double rectangle shows the highest gain among double closed-loop SCV forms. Therefore, we may find it useful to perform a simple comparison between the bobtail curtain and the open double rectangle on each of the sampled bands when we place each antenna at the base height for maximum gain over average soil. **Table 7-12** provides the relevant information. The double rectangles use an end-fed version to arrive at a maximum-gain value.

Note that the gain improvement is more incremental than radical. As well, the gain improvement of the bobtail varies with the operating frequency, as it generally decreases as the frequency rises. Since these values are for optimized shapes and base heights, we cannot extrapolate the differences to shape variations occasioned by limitations of the installation site or to differences in the

base height chosen. For example, for equivalent and low base heights, the double rectangle's gain value would suffer more than the bobtail curtain's value.

A Comparison of Bobtail Curtains and					Table 7-12
Open Double Rectangles for 160, 80, and 40 Meters					
Freq MHz	Type	Gain dBi	Base Ht	Ant Ht	Total Ht
1.85	Dbl Rect	5.15	95	47.8	142.8
	Bob Cur	6.22	24	130.0	154.0
Difference		1.07			11.2
3.55	Dbl Rect	4.55	58	26.9	84.9
	Bob Cur	5.40	16	78.0	94.0
Difference		0.85			9.1
7.15	Dbl Rect	4.45	37	14.8	51.8
	Bob Cur	5.03	14	39.0	53.0
Difference		0.58			1.2
Notes:	Dbl Rect = open double rectangle				
	Bob Cur = bobtail curtain				
	Base Ht = distance from ground to lowest point on				
		antenna in feet			
	Ant Ht = antenna vertical dimension in feet				
	Total Ht = Base Ht + Ant Ht in feet				
	All antennas use the base height for maximum gain				
		over average soil			

The table also lists the base height, the antenna height, and the total array height. As we increase the operating frequency, the difference in the total height between an optimized double rectangle and an optimized bobtail curtain becomes nearly non-existent from the perspective of practical construction. Since the gain values are very similar, with only a half-dB advantage for the half square, either antenna may serve equally well. At lower operating frequencies, both the height and the gain show larger differences that any prospective user must weight carefully. Considerations of overall size of the installation plot, safety for people and pets, available supports, interfering objects, the height vs. gain equation, and a number of other matters fold into the SCV planning exercise.

Base-Feeding the Half-Square and the Bobtail Curtain

All of the open-ended SCV models that we have sampled use a current-maximum point as the array feedpoint. The half-square used an upper corner, while the bobtail curtain placed the feedpoint at the upper end of the center vertical. Both feedpoint placements assure as close as possible to the proper current distribution along the array. However, we need not use those feedpoints. Through about 1990 or so, almost all half-squares and bobtail curtains used base feeding, that is, voltage feeding, as some call the technique. The technique is equally applicable to the vertical dipole that we explored in Chapter 1 and to the current pair of open-ended SCVs. **Fig. 7-17** reviews the general principle involved.

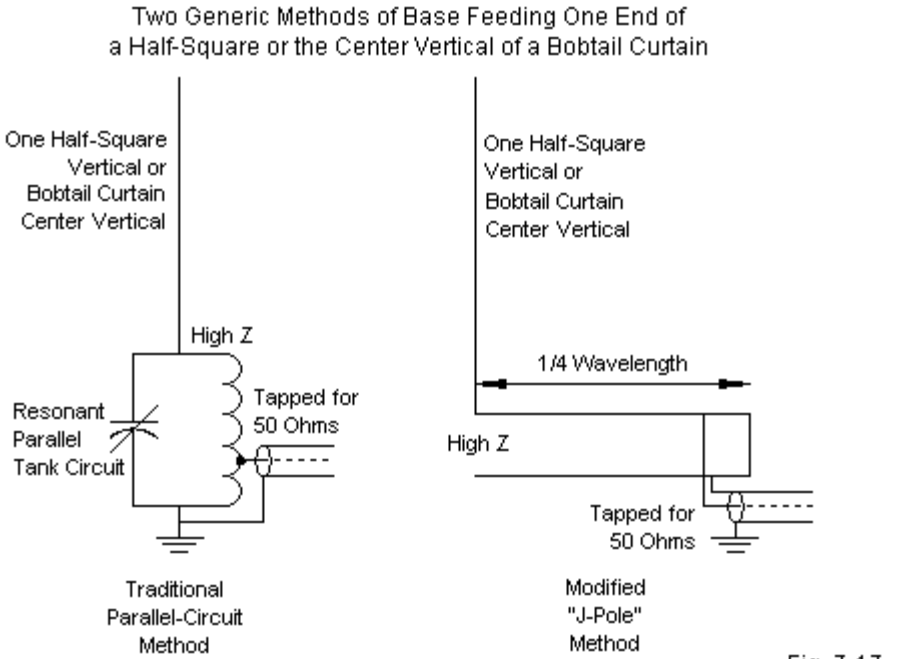

Fig. 7-17

The sketch shows two general methods of feeding an element tip at a high-voltage, low-current point, such as the end of a vertical dipole or the end of an SCV element. The version called the “modified J-pole method” has an old name, the quarter-wave Zepp match. (If anything distinguishes the two names, it may be that the Zepp version generally leaves the far end of the line open, while the J-pole version generally shorts the end of the ¼-λ line.) Whatever the name, the method relies on the fact that a ¼-λ of parallel transmission line forms an impedance transformer. For any given practical line impedance (usually 450 Ω to perhaps 800 Ω), the antenna element end shows a much higher impedance. Hence, the other end of the line will show a much lower impedance than the line impedance. The usual practice is simply to find experimentally tapping points near the far end of the line that yield a desired impedance value. For most amateur installations, the required value is 50 Ω to match the characteristic impedance of common coaxial cables.

The left side of the sketch shows a parallel tank circuit that is resonant at the operating frequency. The circuit presents a very high impedance relative to the earth ground. A very good earth ground and virtually zero voltage difference between this point and the equipment end of the main feedline is a requisite for high efficiency in any voltage-fed system. The sketch shows a tap for the 50-Ω feedline. However, one may equally use a small link coil to effect physical isolation between the main feedline and the antenna-to-ground circuit. The sketch also simplifies reality by showing the connection between the tank circuit and the antenna element at the very top of the coil. Alternatively, one may refine the match by selecting a tap on any turn of the coil. The result is a variable network capable of transforming relatively low line impedances up to very high impedances required by the antenna element. Therefore, one may replace the very traditional tank circuit with any network capable of the same matching range with good efficiency. For example, one of the waterproof remotely controlled antenna tuners might perform the matching task.

The benefits of having a variable network, whatever its construction, become more evident when we consider where to place the circuit. Half-squares and bobtail curtains perform best when elevated above ground, but the matching circuit generally finds its best home close to ground, with the shortest possible

lead to the good earth ground system. In fact, if we elevate the matching network, the ground lead becomes part of the center element of the bobtail of the end element of the half-square. Hence, unless we lower antenna efficiency by placing it very near to the ground, we shall automatically lengthen the wire that we chose to end feed.

Fig. 7-18

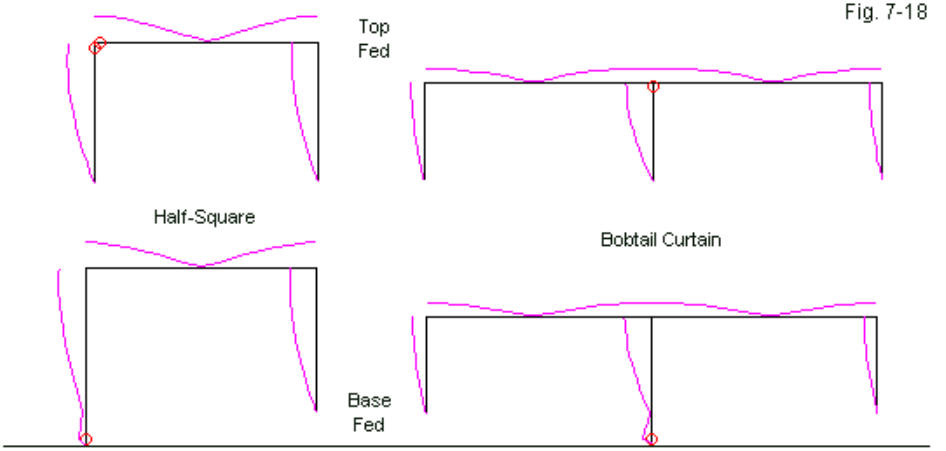

Relative Current Magnitude Distribution on a Half-Square and on a Bobtail Curtain
With Both Antennas 10' above Average Ground Using Top and Base Feeding

Using an elevated antenna position for greater performance and extending the fed vertical leg creates no problems with respect to current distribution along either a half-square or a bobtail curtain. **Fig. 7-18** shows the current magnitude distribution of corner fed and base fed versions of each antenna. In principle, the antenna performance remains unchanged. Both models use a 10' base height for a 40-meter array. TO angle values do not vary between each pair of models. The gain variation is under 0.05 dB.

The impedance at ground level in each case is no longer as high as it would be at the tip of an element where the current goes toward zero. Therefore, variability in the matching system become more important, since the network

must match the impedance that appears at ground level, that is, at the terminals of the matching network. Variability, weatherproofing, and a good earth ground are the hallmarks of an effective base-feeding system for either the half-square or the bobtail curtain.

Base feeding overcomes some of the inconveniences associated with feeding the arrays at higher-level positions. Cable routing that avoids common-mode current inducement becomes a perennial practical problem for these arrays. In addition, coaxial cables add weight to a wire antenna structure, sometime leading to seemingly insurmountable problems of sagging and strain. Hence, the base feeding methods retain considerable popularity among half-square and bobtail users.

One final feeding note relative to the bobtail. We saw that there is a performance difference between the 50-Ω and the maximum-gain versions of the antenna. The maximum gain versions showed feedpoint impedances at the upper junction that were considerably less than 50 Ω. The use of a 1:2 balun—a somewhat rare item—would overcome the difficulty. An alternative solution is to feed the antenna part way down the center vertical at a 50-Ω impedance point. In most cases, a position about 1/3 of the way down from the element top will yield close to 50 Ω for a roughly 25-Ω top position impedance. Good common-mode current attenuation will be important to the use of this “off-center” feedpoint.

Open-Ended SCV Beams

Like all SCVs, the half-square and the bobtail curtain produce bi-directional patterns. Although the gain yielded by these arrays is clearly a significant advantage, the levels are modest in the total scheme of amateur HF antennas. Therefore, wire antenna fans have sought to add a second array to the first—with suitable spacing—in order to create a directional beam.

Adhering to traditional vertical antenna practice, many attempts to form a beam from the half-square or the bobtail have used phasing techniques. These methods require carefully tuned networks to arrive at the proper current magnitude and phase-angle at the feedpoints of each array to yield an acceptable

pattern. Parasitic methods produce very competent performers with far simpler construction and no tuning after an initial field adjustment period. Let's use 40-meters as perhaps the most reasonable band on which to develop a couple of very usable designs. On 40, the total installation site territory required by the 2-element driver-reflector parasitic beam is quite reasonable (but not necessarily small). **Fig. 7-19** outlines the two beams that we shall consider.

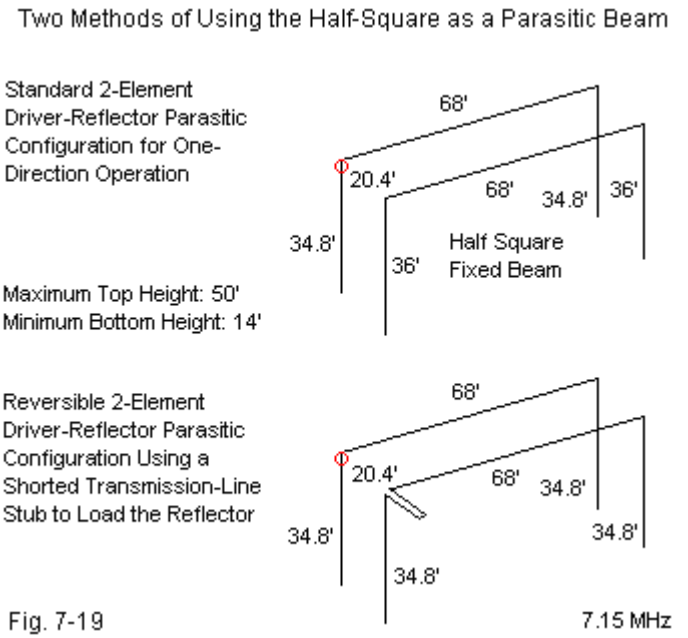

The beams use some common limitations. First, all elements are AWG #12 copper wire. Second, the beams have a top height of 50' above ground. (The samples use average soil quality as the ground beneath them.) As a result, the base height of each element above ground is 50' minus the vertical leg length shown in the sketch. The elements use a constant base-wire length of 68'. The spacing is fixed at 20.4'. Thus, we tune the elements to a desired condition by adjusting only the length of the vertical legs, a task that we can perform from the

ground or with no more than a stable stepladder. Both beams shown use top-corner feedpoints, so that the feedline is a 50-Ω coaxial cable.

The top sketch shows a directional beam that uses driver and reflector elements tailored to the task. It has a fixed orientation and requires that the user orient the beam toward a favored target region. Fixed parasitic beams, however, normally benefit from the application of techniques that allow the user to reverse the beam's direction. The lower sketch shows such a scheme. We cut both elements to the specifications for a driver element. On the reflector, at the position corresponding to the feedpoint, we attach a loading inductive reactance that will electrically lengthen the element so that it functions as a reflector. The required inductive reactance is just about 50 Ω.

We have several choices among methods to arrive at the required loading inductive reactance. We might install a coil with an inductance that shows j50-Ω reactance at 7.15 MHz, the design frequency. 1.11 μH would do the job. We may also use a shorted length of transmission line. Since the main feedline is 50-Ω, let's use the same cable for the line. The electrical length that we need is just about 17'. However, the physical length will be the electrical length times the line's velocity factor (VF). If we use a solid-dielectric cable with a VF of 0.66, the physical length will be about 11.2'. For a foam-dielectric cable with a VF of 0.78, the physical length is about 13.25'.

Let's install the selected line not only on the reflector, but also at the feedpoint of the driver. The two cables are long enough to meet half way between the elements. At this point, we may install a remotely operated switching system, using the schematic (or a variant of it) shown earlier in **Fig. 2-10**. In one position, a selected line receives a short across the two conductors. In that same position, the other line connects to the main cable and becomes simply a short extension of the main feedline. Reversing the switch position also reverses the connections and therefore the functions of the two elements. The beam is now reversible.

The beam works quite effectively because moderately loading a reflector has very few consequences for the driver and for overall beam performance. The following listing shows the modeled performance of the two versions of the 40-

meter half-square beam. The patterns in **Fig. 7-20** confirm the generally good performance of the reversible version relative to the fixed version.

Modeled performance of 2 parasitic 40-meter half-square beams

Version	Gain dBi	TO Angle degrees	Front-Back Ratio dB	Beamwidth degrees	Feedpoint Z R +/- jX Ω
Fixed Beam	6.52	17	25.09	76	59.6 + j0.0
Reversible	6.50	17	19.65	76	53.5 + j1.7

Fig. 7-20

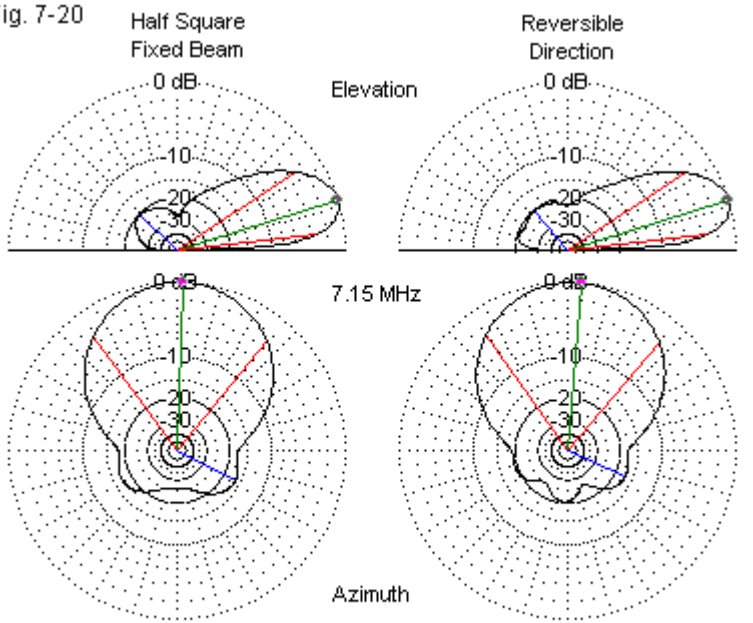

Elevation and Azimuth Patterns of Fixed and Reversible
40-Meter Half-Square Beams

The forward gain, TO angles, and beamwidth values of both beams are equivalent. There are two small differences in the patterns and data worth noting.

First, the fixed beam has a higher front-to-back ratio due to better overall regulation of the current distribution along the wires. The larger of the two quartering rear lobes on the reversible pattern is away from the feedpoint-loading side of the array. Second, the slight angle in the forward lobe that is offset from directly broadside to the antenna is about 3° farther off center in the reversible version of the antenna. However, with a forward lobe beamwidth of 76°, the slight angle would be operationally unnoticeable. The angles between points at which the forward gain is 1 dB less than maximum—the minimum that might be noticeable under highly controlled conditions—is about 30°.

A directional beam using the half-square as a foundation is both straightforward and beneficial. Either version of the 40-meter beam has a forward gain that is about 1.5 dB higher than the bi-directional gain of a bobtail curtain. As well, the beamwidth is larger. The final advantage is the very respectable front-to-back ratio that reduces both signals and noise from the rear of the beam.

For any installation site and frequency, the design process should consider using antenna-modeling software that takes into account the operating frequency, the proposed installation height, and the soil quality beneath the antenna. Expect to spend some time making final adjustments in the field. However, by varying the model dimensions systematically, you will be prepared to understand what your initial results mean and in what directions your adjustments must go. Parasitic half-square beams are not wide-band devices. The operating bandwidth is similar for both the fixed and reversible versions. The 50-Ohm SWR will rise much more quickly below the design frequency than above it. Hence, a version of the array design for the CW end of 40 meters will require a design tailored to that end of the band.

VHF/UHF Open-Ended SCV Applications

As we suddenly jump from the lower HF region to the VHF/UHF region, we must once more change our methods of construction for SCV arrays. The test frequency will be 299.7925 MHz, where 1 meter = 1 wavelength. We shall use 4-mm diameter lossless wire for all elements. We shall also place all sample

antennas 5-λ above average ground to facilitate comparisons of present samples with those appearing in other chapters.

In the VHF/UHF region, we place antennas sufficiently high that we may use either possible orientation of an open-ended SCV, that is, with tips up or tips down. **Fig. 7-21** shows the outlines of a half-square with the open side up and with it down. However, only one set of patterns appears in the figure. The reason is simple. Both half squares show a maximum gain of 9.2 dBi at a TO angle of 2.6° above the horizon when we place them at a height of 5-λ above ground. The beamwidth in each major direction is 79°, and each version of the array has a feedpoint impedance within 0.4 Ω of the desired 50 Ω.

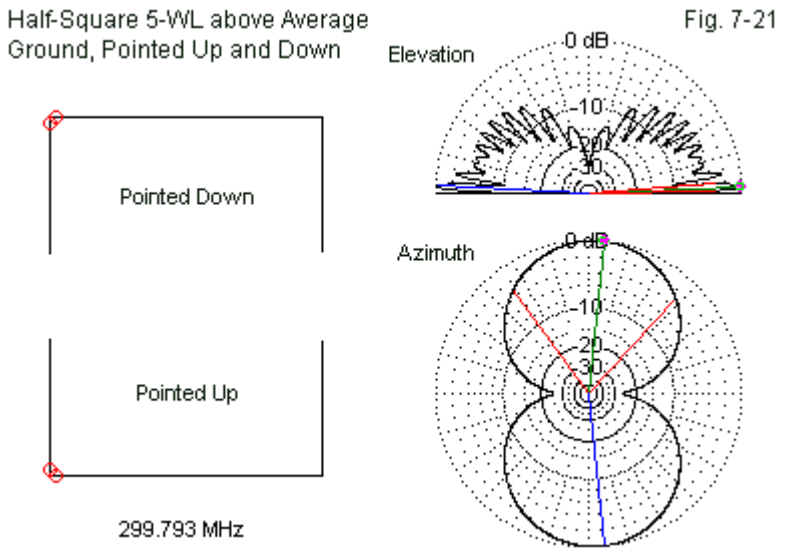

The azimuth pattern shows a seemingly greater departure from a true broadside pattern. The pattern has two sources. In the lower HF region, our arrays were close to the ground, which has some affect on straightening the pattern. However, the more significant contributing factor is the much greater

wire diameter, as measured in terms of a wavelength. At 300 MHz, the 4-mm (0.1575") wire diameter is 0.004-λ. At 40 meters, the AWG #12 wire (0.0808") is 0.000049-λ.

The half-square's bi-directional nature yields broadside gain and side nulls that are quite deep. This feature can be very useful in situations where we require vertical polarization, but without the usual wide beamwidth that accompanies it. A vertical dipole might have a gain of about 7 dBi at the 5-λ height, but the pattern would be omni-directional. Even a 2-element Yagi will have a beamwidth of about 135° when we orient it for vertical polarization. In some situations, we want a vertically polarized beam with a narrower beamwidth.

The 40-meter fixed parasitic half-square beam is highly adaptable to use at VHF frequencies, where the size of a full planar reflector might be prohibitive. However, we shall have to make some adjustments. For example, we shall place the tips of the array upward so that the feedpoint becomes a lower corner. This position eases the problem of routing the feedline. Next, we shall have to adjust the dimensions to suit the use of 4-mm elements. Since we shall be using the common 50-Ω coaxial cables as a feedline, we shall design the array for that feedpoint impedance. However, we shall retain the use of a constant base-wire length for both elements and let the vertical sections show the differences between the driver and the reflector elements. Of course, the antenna will be light enough to rotate, so we may bypass any thought of creating a reversible beam. The following listing shows the results of our redesign efforts. **Fig. 7-22** provides the outline of the antenna, elevation and azimuth patterns at the 5-λ height, and the 50-Ω SWR curve for the antenna.

2-element half-square parasitic beam 5-λ up at 299.7925 MHz

Dim:	El Dia.	El.	Length	Width	El.	Length	Width	Spacing
	λ		λ	λ		λ	λ	λ
	0.004	Driver	0.516	0.2395	Refl.	0.516	0.259	0.135
Performance:		Gain	F-B Ratio	TO	HplBW	Impedance		
		dBi	dB	degrees	degrees	R+/-jX Ω		
		12.76	18.97	2.6	72.4	50.1 + j0.4		

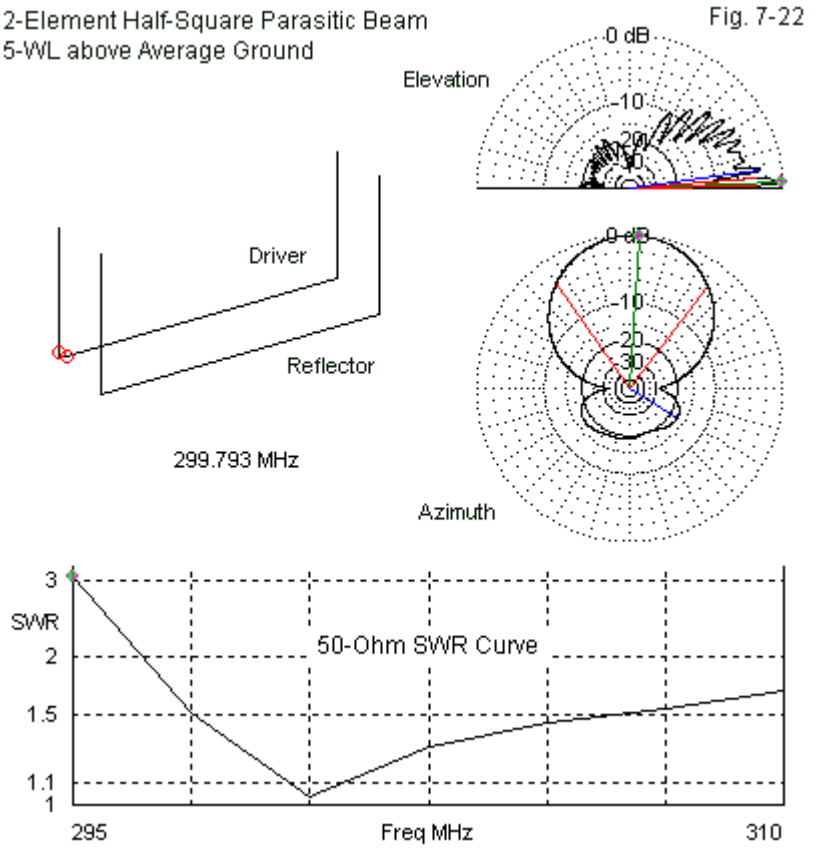

The dimensions shown in the listing are scalable, but only with a scaling of the element diameter. For 6- and 2-meter versions of the antenna, re-design using the proposed element diameter will be necessary in most cases. If the base-wire is fatter as a support for thinner elements at these frequencies, you may wish to turn to a version of MININEC to overcome NEC's difficulty with angular junctions of wires having different diameters. However, be certain to use a version of MININEC that has been corrected for the frequency drift inherent in

the raw version of MININEC 3.13.

The performance promise of the half-square beam is very respectable. The forward gain is about he same as from a 3-element Yagi oriented vertically. So too is the front-to-back ratio, although the rear lobes of the half-square array shows a slight asymmetry. However, the half-square beamwidth is narrower. Depending upon design, a vertical 3-element Yagi has a beamwidth between 100° and 120°. The half-square beam lowers that figure to about 72°. Like the 40-meter half-square beam, the SWR curve for the parasitic VHF/UHF beam shows a high degree of difference in the rates of rise above and below the design frequency. Note that the graphic begins at 295 MHz but extends up to 310 MHz, with the lowest SWR at 300 MHz. The 5% SWR bandwidth would just about cover 2 meters, but might not be sufficient to cover the entire FM portion of 6 meters. To add to our concerns, the operating bandwidth in terms of the forward gain and front-to-back ratio may be—depending upon the operating needs—narrower than the SWR bandwidth.

If we wish to obtain a beamwidth that is narrower than the value (72°) offered by the 2-element half-square beam, we can create a 2-element beam using the bobtail curtain as the basic element. We shall use a feedpoint at the junction of the center vertical and the base wire and set the impedance for 50 Ω. As in the case of the half-square beam, we shall use the same base-wire length for both elements and adjust the beam properties by adjusting the length of the vertical legs. 4-mm lossless wire is still the element material of choice for consistency within the entire set of VHF/UHF models. **Fig. 7-23** shows the beam outline, the azimuth and elevation patterns, and the 50-Ω SWR curve that goes with the data in the following listing.

```
2-element bobtail curtain parasitic beam 5-λ up at 299.7925 MHz
Dim:      El Dia.   El.      Length    Width     El.      Length    Width     Spacing
          λ                  λ         λ                  λ         λ         λ
          0.004     Driver   1.000     0.2505    Refl.    1.000     0.2675    0.168
Performance:  Gain      F-B Ratio   TO          HplBW       Impedance
              dBi       dB          degrees     degrees     R+/-jX Ω
              14.11     19.74       2.6         47.2        49.7 - j0.0
```

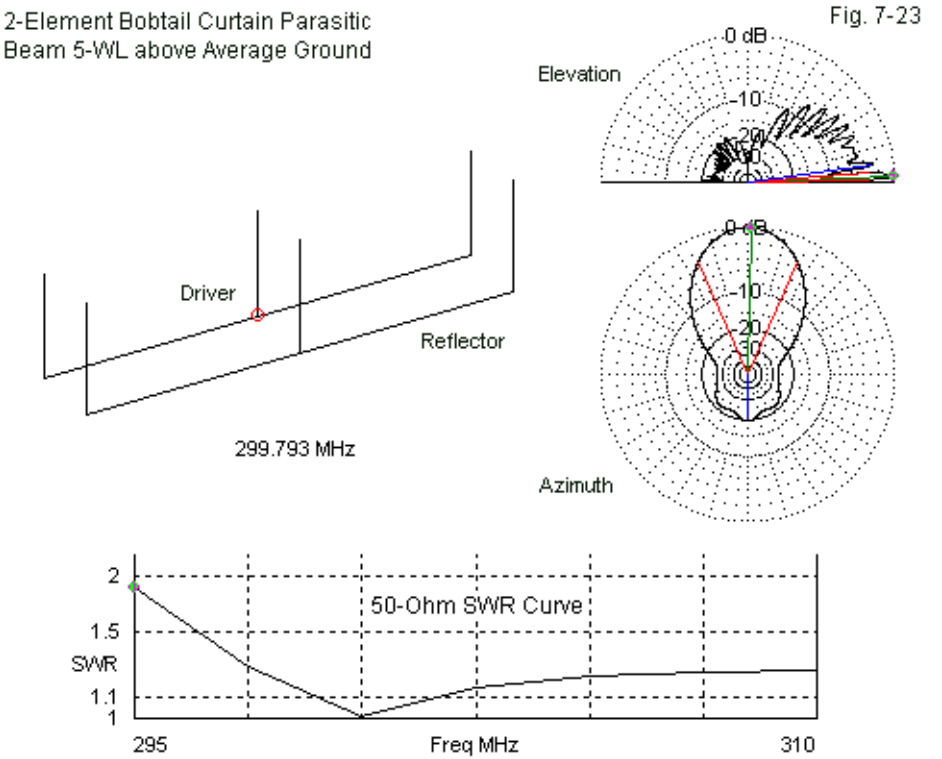

The parasitic bobtail is exactly 1-λ long, with vertical legs set for driver and reflector operation. At about 47°, the horizontal beamwidth is down by near half relative to the half-square. However, the bobtail gain is about 1.4 dB higher, with a very comparable front-to-back ratio. The 50-Ω SWR curve indicates a narrow operating bandwidth, especially below the design frequency. Above the design frequency, the relatively flat SWR line through 310 MHz may be deceptive, because the gain and front-to-back properties may not hold up as well as the feedpoint impedance values. Nevertheless, for use on a specific frequency or a narrow band of frequencies, the bobtail parasitic beam may prove highly effective.

Although I have for convenience referred to the half-square and bobtail beams as 2 element arrays, they are actually parasitic arrangements of complex arrays. Hence, the half-square's true element count is 4, and the bobtail count is 6. Alternatively, we may think of the beams as sets of 2 or 3 2-element parasitic beams fed in phase.

The off-center feedpoint of the half-square does not lend itself to as effective use with a planar reflector as the centered feedpoint of the bobtail curtain. The 3-element vertical array works well with a planar reflector. The relatively short vertical dimension of a bobtail curtain results in a reflector that is 1.2-λ vertically by 2-λ horizontally. For the present sample, I have sacrificed about 0.4 dB of forward gain by using a square reflector that is 2.0-λ by 2.0-λ. The increased vertical dimension of the reflector increases the front-to-back ratio by about 10 dB. **Fig. 7-24** shows the outline of the bobtail curtain driver with a planar reflector. As the sketch and the following listing show, the required dimensions of the 4-mm driver element do not match those of the elements in the parasitic beam. Since the element spacing from the reflector plays a role in setting the feedpoint impedance, it also affects the required driver dimensions.

Bobtail curtain driver and planar reflector 5-λ up at 299.7925 MHz

Dim:	El Dia.	El.	Length	Width	Reflector	H	V	Spacing
	λ		λ	λ		λ	λ	λ
	0.004	Driver	0.900	0.271	Max FB	2.0	2.0	0.185
Performance:		Gain	F-B Ratio	TO	HplBW	Impedance		
		dBi	dB	degrees	degrees	R+/-jX Ω		
Max FB Ref.		14.99	30.86	2.6	49.0	49.8 + j4.0		

The forward gain exceeds the value obtained from the parasitic beam. Had we used a reflector optimized for maximum forward gain, the gain value would exceed 15.4 dBi and match the value obtain from the open-double rectangle driver. The beamwidth of the array is about 49°, close to the value obtained from the bobtail parasitic beam. **Fig. 7-25** shows the model outline, including the wire-grid reflector, along with the elevation and azimuth patterns and the 50-Ω SWR curve.

Fig. 7-24

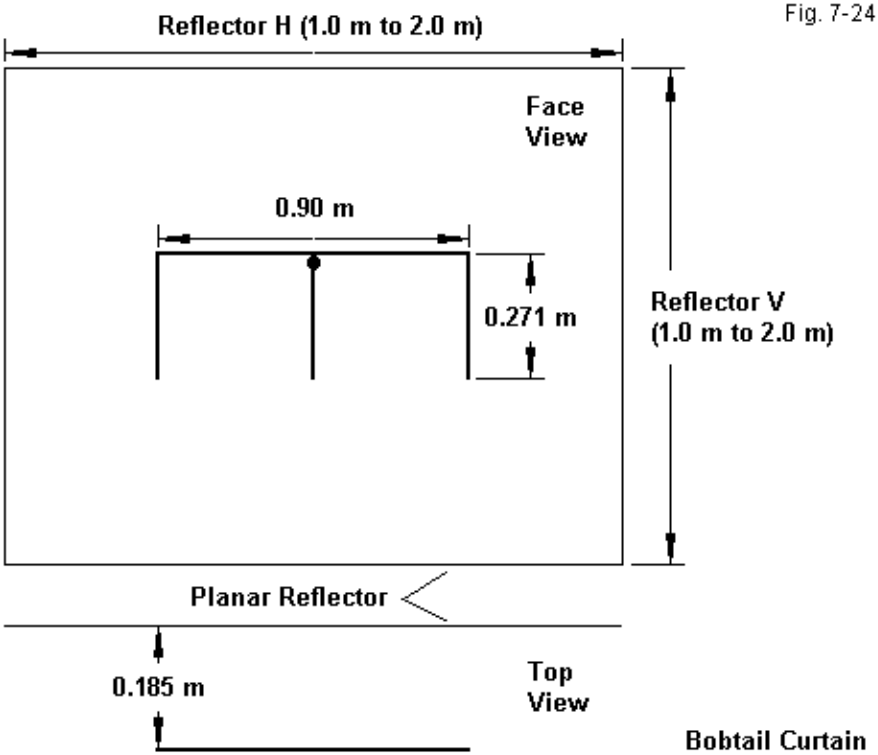

Bobtail Curtain Driver and Planar Reflector Outlines

The patterns produced by the bobtail-planar array are very clean, with a single forward lobe and a single rearward lobe. Compare the rearward lobes in **Fig. 7-25** with those in **Fig. 7-22** and **Fig. 7-23**. The freedom from either forward or rearward sidelobes is an advantage of a planar reflector over most parasitic reflectors, so long as the planar element is sufficiently large. As a result, the planar reflector finds favor above 300 MHz, as the required physical size of the reflector diminishes to manageable proportions. On the 70-cm band, a 2-λ

reflector will be about 55” on a side—large but within reason.

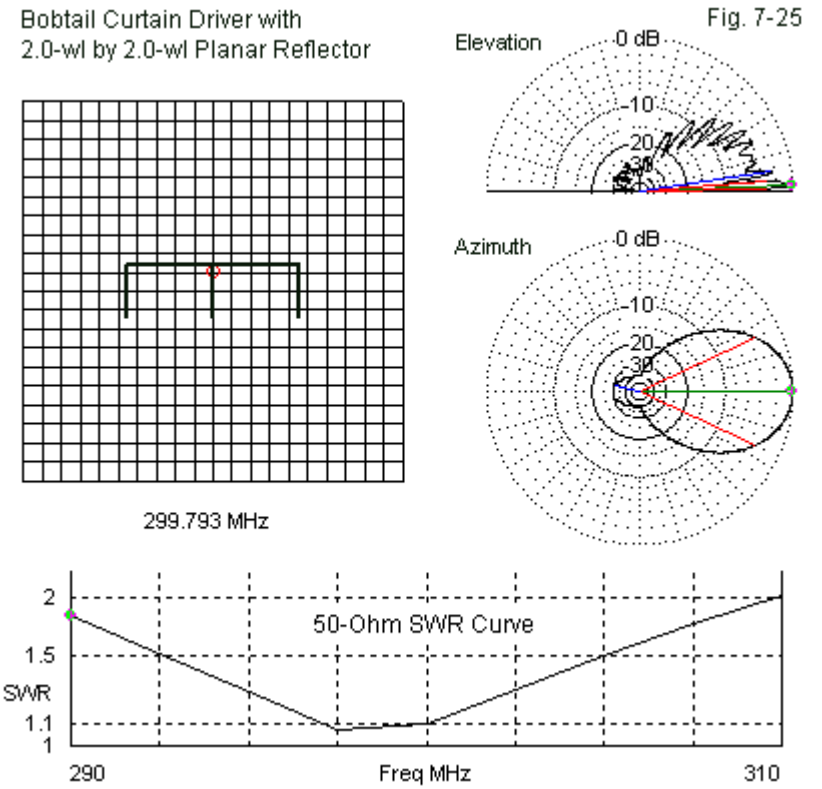

The planar array’s SWR curve is well-behaved, with roughly equal rates of increase on each side of the slightly off-centered curve that results from leaving j4 Ω of reactance on the feedpoint at the design frequency. As a result, the array is usable across the span from 290 to 310 MHz, a 6.7% bandwidth. More specifically, the array is usable with respect to the 50-Ω SWR. We have not yet established that such operating parameters as gain and front-to-back ratio hold up across the entire 20 MHz span.

A Comparison of Half-Square and Bobtail Curtain 2-Element Parasitic Beams and a Bobtail Curtain with a Planar Reflector						Table 7-13
Antenna	Freq MHz	Gain dBi	FB dB	Feed R	Feed X	SWR 50
HS Par	295	13.12	7.97	23.2	-30.7	3.10
	300	12.76	18.97	50.1	0.4	1.01
	305	11.99	11.57	69.4	10.2	1.45
	310	11.45	8.05	72.2	22.5	1.68
BC Par	295	14.27	9.25	29.8	-14.5	1.88
	300	14.11	19.74	49.7	0.0	1.01
	305	13.61	14.25	61.1	1.5	1.22
	310	13.21	9.47	60.5	6.4	1.25
BC Pl Ref	290	14.84	30.85	46.0	-28.8	1.82
	295	14.92	30.90	47.8	-22.9	1.28
	300	14.99	30.86	49.8	4.0	1.08
	305	15.06	30.70	52.3	21.0	1.51
	310	15.12	30.50	55.0	37.2	2.02
Notes:	HS Par = 2-element parasitic half-square beam					
	BC Par = 2-element parasitic bobtail curtain beam					
	BC Pl Ref = bobtail curtain with a planar reflector					

Table 7-13 provides us with one kind of answer to the unfinished question. It provides modeled operating data for all three VHF/UHF arrays that we have sampled. The data for the parasitic arrays cover 295 to 310 MHz, while the planar array data cover 290 to 310 MHz.

The planar array information shows that the most variable parameter is the feedpoint reactance, which is a function of the bobtail curtain dimensions. The feedpoint resistance changes by only 9 Ω. We find similarly small changes in the other operating specifications. The forward gain changes by less than 0.3 dB, while the front-to-back ratio shows only a 0.4-dB range. In effect, like the other planar arrays that we examined in preceding chapters, the limiting factor in planar array performance is the feedpoint SWR. Many commercial planar arrays, especially the ones once designed for UHF television use, employed higher feedpoint impedances with wider spacing between the driver and the reflector. The result was less gain but a broader operating bandwidth, especially if we

extended the usable SWR to 3:1 in a receiving-only application. (Many such antennas also employed bowtie-shaped drivers for added operating bandwidth.)

The table also provides data for the parasitic arrays. Both arrays share a common feature: the rapid decrease in the rearward performance, as revealed by the high rate of decrease in the front-to-back ratio as we move away from the design frequency. Even with a narrower SWR bandwidth to define the scanned range, the front-to-back values at the passband edges may be less than satisfactory for most applications. Additionally, the forward gain varies more across 15 MHz than we found with the planar reflector across 20 MHz. The half-square beam shows a gain range of almost 1.7 dB, while the bobtail beam shows over 1 dB. Compare these gain variations to the 0.3-dB range shown by the bobtail-planar array.

Adequately sized planar reflectors are exceptionally useful to create beams using relatively simple drivers that form a single plane that is parallel to the reflector plane. A planar reflector should exceed the driver dimensions by between 0.4-λ and 0.5-λ in each dimension for maximum gain. They find only scattered use in amateur installations below the UHF range. However, there are a few lazy-H arrays that use planar reflector in the upper HF range. In the lower HF range, we find such reflectors below arrays used for NVIS service. Perhaps the greatest numbers of HF planar reflectors are in service with short-wave broadcast stations.

Conclusion

The open-ended SCVs—namely, the half-square and the bobtail curtain—provide the highest gain of any of the SCV forms that we have explored, at least in the lower HF and the upper MF amateur bands. Although the unchangeable labels given to these arrays are uninformative of their operation, they have proven not only to be SCV forms, but also to be derivable from the closed SCV forms that we explored in earlier chapters. Although the true vertical legs of the open-ended SCVs produce antenna heights that are greater than those we met with the elongated rectangles, the overall array heights are comparable, since the open-ended forms achieve peak gain with much lower base heights. In addition, they

tend to lose less gain as we reduce the base height below the optimal value, since the high current region of the elements remains well elevated.

Unlike most of the closed SCV forms, the open-ended arrays are well suited to parasitic beams, especially in the lower HF and in the VHF regions of the spectrum. The chief limitation of these 2-element beams is the narrow operating range as defined by a rapidly deteriorating front-to-back ratio away from the design frequency. Planar reflectors can overcome most of the operating bandwidth limitations. Nevertheless, the double diamond and the double rectangle remain perhaps the most favored driver shapes as a function of their physical structure that permits simple attachment methods.

In one sense, we have completed our survey of SCV forms, at least the ones we normally think of when considering a self-contained vertically polarized antenna form. However, we should consider one more array that has both historical interest and current interest: the Bruce array. In fact, if we think about the Bruce array long enough, we can derive it from a side-fed square quad loop.

8. The Bruce Array

The Bruce Array owes its name to Edmond Bruce, one of the truly innovative antenna developers of the 1920s and 1930s. His curtain array appeared in the late 1920s, but he is perhaps more famous for his diamond antenna design, an array renamed the rhombic only a few years after its first appearance. If we may believe a story attribute to John Kraus, W8JK, Bruce would have preferred that the rhombic should bear his name rather than the array that we in fact call the Bruce. The Bruce array languished in relative obscurity until *The ARRL Antenna Book* revived interest in recent editions (pp. 8-42 to 8-47 in the 19th Edition) in a section written by Rudy Severns, N6LF.

Fig. 6-1 outlines the general idea of the array. We may fold vertical dipoles into S-shaped structures 1/8-λ on each side of the feedpoint. Next, we may join the vertical dipole tips to form a chain of deformed dipoles that is as long as we may desire. We then bend the 1/8-λ end tips either inward or outward. The sketch shows may possible feedpoints, although normally, we select only one (or possibly 2) for the actual transmission-line connection.

Fig. 8-1

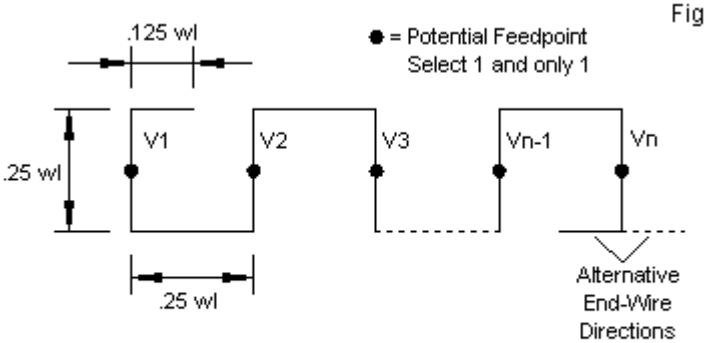

The Bruce Array (or Curtain): General Specifications

The result of our exercise in antenna origami is a collection of vertically polarized dipoles at ¼-λ intervals, all in phase with each other. The sketch shows the generalized dimensions that we might find in an old textbook, but in practice, we may tweak them just a bit to optimize array performance for any overall length that we select. As a preview of things to come, we might note in passing that for any given array length among all of the SCV forms, the Bruce array manages the highest bi-directional gain.

From Loop to Bruce

Like the half-square and the bobtail curtain, the Bruce array derives from the common close loop that we call the quad element. **Fig. 8-2** shows the evolution. We begin with a closed loop. If we model the loop as a continuous ribbon, with one wire for each of the four sides, we shall find an interesting set of reports. The dotted line marks the loop center that cuts through the high-voltage, low-current points along the elements. At these points, the current table will show a reversal of current phase so that the alternative or virtual feedpoint on the side opposite the side actually fed will be 180° out of phase with the current that we assign to the source point. Since the modeled voltage at the virtual source point will also be out of phase with the voltage at the actual source, we end up with two dipoles in phase with each other.

Fig. 8-2

Evolving the Basic Bruce Array from a Quad Loop

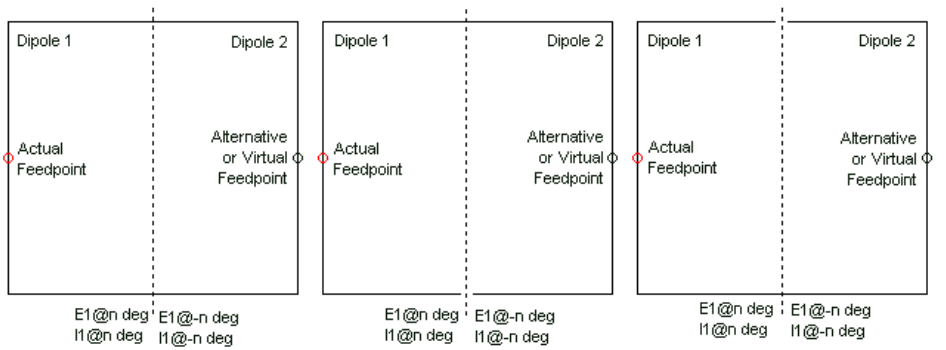

The reversal of current and voltage phase is an artifact of our modeling practices. If we had modeled each dipole half of the loop from the dotted line outward, then up (or down) the vertical side to end at the other intersection with the dotted line, we would find that the voltage and current at the actual and virtual feedpoints would be in phase with each other. The Appendix contains a small exercise set that demonstrates the manner in which the way we set up the wires in a model affects the output reports of current phase.

For our purposes, the continuous ribbon method of modeling loop wires will work fine in developing the Bruce array. The next step is to open a small gap either at the bottom or the top of the side-fed vertically polarized loop. The gap makes no significant difference to the antenna's performance, as illustrated by the 40-meter data in **Table 8-1**. We find almost no change in the dimensions, the bi-directional gain, or the feedpoint impedance. In fact, we may bend the end wires created by cutting the gap in an outward direction without much change in performance. However, we must adjust the length of these end wires to restore resonance.

Evolving the Bruce Array from the Quad Loop								Table 8-1
Antenna		Base Len	Height	Gap	Gain dBi	TO deg	Feed R	Feed X
Closed Loop		0.278	0.25		1.85	16	113.8	4.8
Gap at Top		0.280	0.25	0.01	1.86	16	112.4	-3.5
Gap at Bottom		0.280	0.25	0.01	1.89	16	112.1	-3.1
Bot. Ends Outward		0.534	0.25		1.76	16	119.3	0.1
Notes:	All dimensins in wavelengths			Test frequency 7.15 MHz			Base height: 0.21 wl	
	All antennas composed of AWG #12 copper wire						Soil Quality: Average	
	Base Len = horizontal dimension of the antenna							
	Height = vertical height of the antenna (add base height to obtain antenna top height)							
	Gap = distance between wire ends for open loops with wires inward							
	Bot. Ends Outward = open loop with bottom end wires pointed outward							
		Base length is the total horizontal length. Base length of loop is 0.28 wl.						
		End wires are each 0.138-wl long, adjust in length for resonance.						

From the single loop, we may use outward bends to create longer strings of vertical dipoles or half-loops. **Fig. 8-3** shows the general process. Conventionally, we bend the unconnected end wire inward, although many older texts show an outward bend. Of course, we must bend the end that meets a new

dipole outward in order to create the junction. In theory, we may extend the Bruce array endlessly, although practical considerations of support normally limit the size of the array that we build.

Fig. 8-3

Growing Larger Bruce Arrays

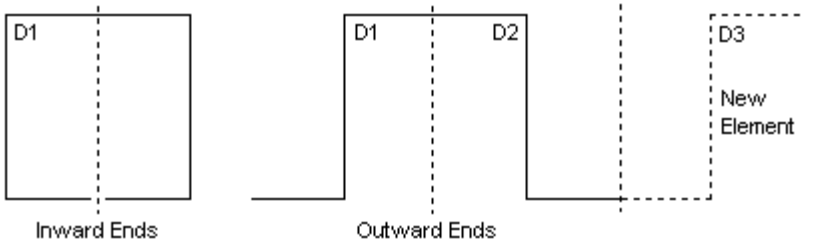

While we are looking at these basic forms, we may note that our discussion of the Bruce array will alter a few of the conventions used in earlier chapters of these notes. We shall retain 40 meters (7.15 MHz) as the frequency for general ideas applicable to all Bruce arrays. Instead of listing dimensions and antenna heights in feet, as we have previously done, we shall list them in wavelengths. Because we shall alter the theoretical Bruce dimensions a bit, expressing the new dimensions in wavelengths is convenient. At our current test frequency, a wavelength is 137.56', so you may easily translate any dimensions to English units of measure. For example, the models shown in **Table 8-1** had a base height of 0.21-λ or 28.9' above average soil.

Size Makes a Difference

A Bruce array places the high-current portions of vertical dipoles at intervals of about ¼-λ. This spacing does not yield the highest gain that we may obtain from a pair of vertical dipoles, but it does permit us to connect the dipoles in a single continuous string with a single feedpoint. In the space of a half-wavelength, we may fit 3 dipoles, each in phase with the adjacent one for a bi-directional pattern that is broadside to the plane of the array. The gain will exceed the gain of a half-square, our previous gain leader for arrays that are ½-λ

long. Five elements will require just about a full wavelength in total array length, the same overall lengths as a bobtail curtain. However, the Bruce will again yield higher gain. We shall find that the Bruce requires a bit more top height, since the ¼-λ vertical dimension and a higher optimal base height combine to reach greater heights, but the difference is not great. Finally, a Bruce needs more total wire than a corresponding half-square or bobtail, although wire may not be the most significant factor in large wire array design for the lower HF and upper MF amateur bands.

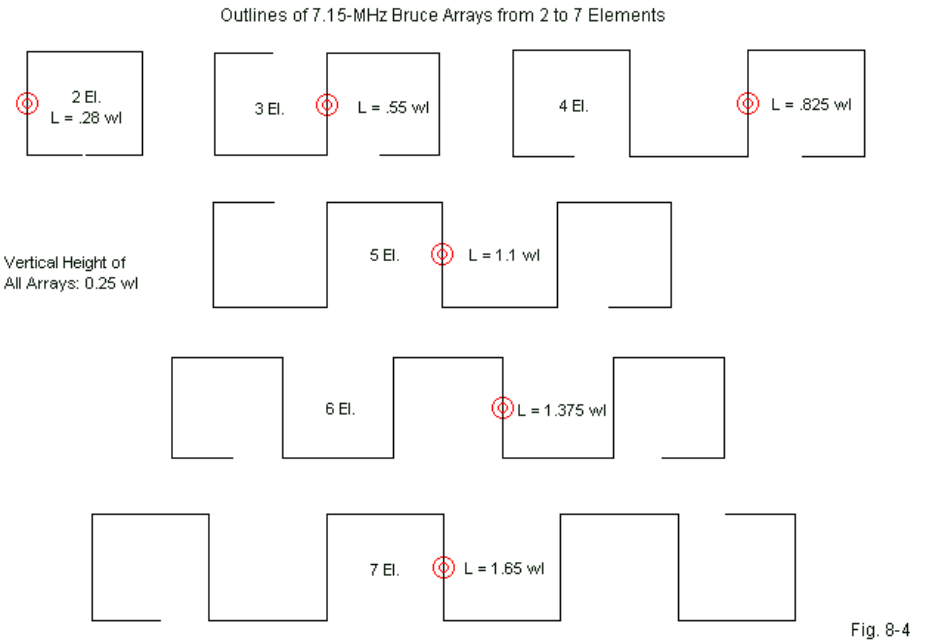

Fig. 8-3 outlines the relative sizes of Bruce arrays ranging from 2 to 7 elements. Each sketch lists the overall length for versions of the arrays with inward end wires. Models of each Bruce size for 7.15 MHz used a common base height of 0.21-λ, and all use AWG #12 copper wire. At 40 meters, the ideal

height of each loop in the array is 0.25-λ, for a total antenna height of 0.46-λ (58.2'). Except for the 2-element version, all horizontal increments are 0.275-λ (37.8'). Between 3 and 7 elements, the only variable dimension is the length of the end wires, which I adjusted to yield a resonant feedpoint impedance. As we increase the overall size of a Bruce array, the length of the end wires increases slowly. **Table 8-2** provides dimensional information for the entire set of arrays.

40-Meter Bruce Arrays from 2 to 7 Elements										Table 8-2
All antennas use AWG #12 copper wire with a base height of 0.21-wavelength over average soil at 7.15 MHz.										
No. El.	Base Len	Height	End Len	Tot. Len	Gain dBi	Gain Add	TO deg	BW deg	Feed R	Feed X
2	0.280	0.25	0.1357	0.280	1.89		16	130	112.3	-0.1
3	0.275	0.25	0.1430	0.550	3.78	1.89	16	72	176.1	-0.1
4	0.275	0.25	0.1475	0.825	5.15	1.37	16	52	206.5	0.0
5	0.275	0.25	0.1490	1.100	6.19	1.04	16	40	256.0	0.7
6	0.275	0.25	0.1570	1.375	6.75	0.56	16	34	313.4	0.0
7	0.275	0.25	0.1625	1.650	7.56	0.81	16	28	363.5	-0.6
Notes:	See Fig. 8-4 for outlines of the subject arrays. All end wires are inward.									
	Base Len = horizontal length of each array loop in wavelengths									
	Height = loop height; add base height for antenna top height (wavelengths)									
	End Len = length of each end wire in wavelengths.									
	Tot. Len = total array length in wavelengths.									
	Gain Add = increment of gain increase in dB over preceding array size.									

The table also lists the modeled performance of the arrays over average soil. The constant 16° TO angle indicates that each array is the same height above ground. As we increase the size of the Bruce array, we find a rising value for the resonant feedpoint resistance. By convention, we have assign the feedpoint position to the center vertical wire for arrays with odd numbers of vertical elements and to the vertical nearest the center for arrays with even numbers of elements. We shall explore alternative feedpoints later in these notes. Nevertheless, at the outset, we can see that most sizable Bruce arrays are best suited for use with parallel transmission lines. However, the 4-element array, with a feedpoint impedance close to 200 Ω, might well use a 4:1 balun and a coaxial cable feedline. Indeed, the 4-element array might use a length of home-made 200-Ω transmission line for some distance from the array and place the weightier balun and coaxial cable closer to ground level.

As we increase the size of the array, the bi-directional gain increases and the beamwidth decreases. In the 1920s and 30s, both Bell Labs and RCA developed antennas for trans-oceanic city-to-city service in the communication of

commercial and governmental messages. Hence, they leaned toward very large arrays to narrow the antenna beamwidth and to achieve the highest possible gain. Amateur service with fixed wire antennas has different requirements. In most cases, we are interested in relatively broad coverage, for example, all of Europe from a U.S. site. To achieve this goal, one may sometimes have to sacrifice gain for the sake of coverage, since I am unaware of anyone being able to develop a rotatable Bruce array for 40 meters or lower.

As we increase the array size, we find the usual shrinking gain increment. As well, we also see some variability in the increment from one step to the next. The reason for this variability lies in the development of side lobes. **Fig. 8-5** can help us sort out the phenomena.

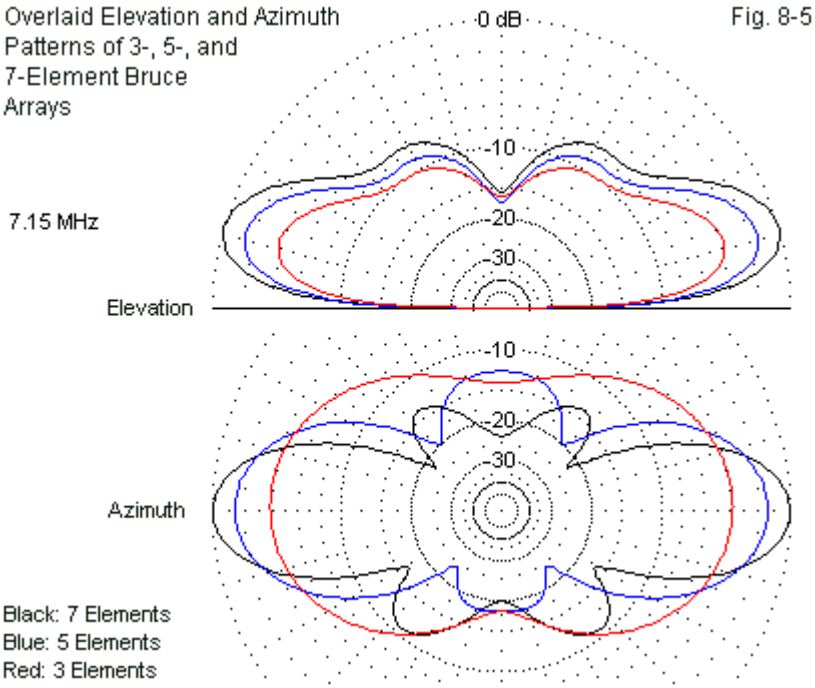

The elevation patterns for all sizes of Bruce arrays are very well behaved. As the upper portion of the figure shows, the only difference that we see in the elevation patterns for 3-, 5-, and 7-element arrays is a proportional growth in strength with each size increase.

The azimuth patterns tell a different sort of story. Bruce arrays up to 4 elements show very "neat" patterns, with a deepening side null as gain increases. However, from 5 elements upward, we find the development of sidelobes in the azimuth pattern. The strength and shape of the sidelobes vary with each added element. The only general rule of sidelobe develop is that as we increase the number of elements, the number of sidelobes increases and the angle of some lobes extends farther toward the main axis of bi-directional gain.

We can also see an interesting, even if minor, phenomenon in the patterns, all of which are for arrays with odd numbers of elements. The patterns are not perfectly symmetrical despite the use of a centered feedpoint position. Reference to **Fig. 8-4** provides a clue to the asymmetry. Odd element numbers produce end wires such that one is at the array bottom while the other is at the array top. The null region is deeper in the direction of the bottom end wire and shallower in the direction of the top end wire. The outlines reflect the models from which I took the azimuth patterns, and the figure contains examples with the top end wire at different ends of the array. The azimuth patterns reflect those differences.

In **Table 8-2**, we may note that the gain of the 5-element Bruce array is 6.19 dBi. The array's overall length is 1.1-λ. An optimized 40-meter bobtail curtain has exactly the same overall array length. The modeled gain for this array over the same average soil is 5.03 dBi. (An open double rectangle under the same conditions is 0.744-λ long with a bi-directional gain of 4.45 dBi.) Although the Bruce array requires more wire for its length than the bobtail, the array gain is significantly higher.

While we are considering an array as large as 5 elements, we might review the matter of bending the end wires inward vs. bending them outward. **Fig. 8-6** shows the alternative forms in which I have only modified the end wires, leaving the interior loops identical. Below the figure, **Table 8-3** shows the modeled data

for the two forms. Just as we found with the basic loop, outward bending of the end wires calls for a different end-wire length than the inward bent version.

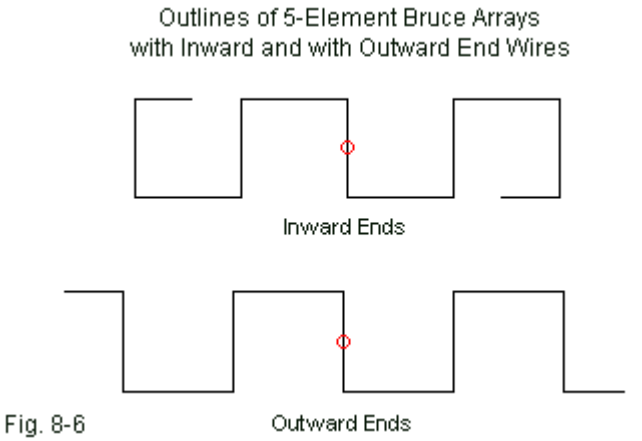

Fig. 8-6

5-Element Bruce Array with Inward and with Outward End Wires									Table 8-3
Type	Base Len	Height	End Len	Tot. Len	Gain dBi	TO deg	BW deg	Feed R	Feed X
Inward	0.275	0.25	0.149	1.100	6.19	16	40	256.0	0.7
Outward	0.275	0.25	0.146	1.392	6.07	16	40	265.1	0.2
Notes:	See Fig. 8-6 for outlines of the antenna variations.								
	See Table 8-2 for explanations of dimension entries.								

The difference in the feedpoint impedance values is slight, relative to the general level of the feedpoint resistance. The outward bend yields a gain that is 0.12-dB lower than the array with inward bends. This difference is virtually identical to the gain difference that we found with our initial bending exercise with only 2 elements. Even though two data points are insufficient to yield a trend, the result is highly suggestive. Since normal construction would support the top and bottom of a Bruce array with a pair of horizontal RF-inert ropes, the inward bend is both convenient and economical with space. Hence, it is the more common Bruce form. Nevertheless, we likely could not detect a performance difference between using either termination system.

5-Element Bruce Arrays for 160, 80, and 40 Meters

As we have done in the case of all of the basic SCV forms, we shall explore both dimensional and performance differences among Bruce arrays at 1.85, 3.55, and 7.15 MHz. We shall use AWG #12 copper wire construction for all arrays, but optimize the shape for each band to account for the fact that the wire diameter changes from band to band when measured as a fraction of a wavelength. The use of a 5-element Bruce array yields an antenna that is comparable to the bobtail curtain in the preceding chapter. Hence, you may wish to compare the data for both antennas. For each array and frequency, we shall sample the performance at various heights above very good, average, and very poor soils.

However, as earlier noted, we shall set dimensions and heights in terms of wavelengths. Base heights (that is, the height from the ground to the array's bottom wire or wires) will appear in 0.03-λ increments for all antennas surveyed.

A 5-Element Bruce Array for 160 Meters

A wavelength at 1.85 MHz is 531.66', so the increments of 0.03-λ used in the base-height table are each about 15.95'. The dimensions for an AWG #12 copper Bruce array on 160 meters are not identical to those for 40 meters. Each horizontal wire is 0.27-λ (143.55'), except for the end wires, which are each 0.14-λ (74.43'). The vertical distance between the top and bottom wires is 0.255-λ (135.57'). You may vary these dimensions slightly to conform to installation needs. As well, you may bring the array to resonance by adjusting the length of the end wires.

Table 8-4 provides the performance data for the 160-meter 5-element Bruce array at base heights between 0.03-λ and 0.27-λ. As we have seen in the case of other SCV forms, on 160 meters, the antenna will show an optimal base height over all three soil types. The optimal base height over average soil is the lowest at 0.15-λ (79.75'), with higher levels indicated for very good soil (0.21-λ or 111.65') and very poor soil (0.24-λ or 127.6'). The graph in **Fig. 8-7** confirms the peak values in the shapes of its curves.

5-Element Bruce Arrays for 160 Meters					Table 8-4
Base Height and Soil Quality vs. Performance					
1.85 MHz		1 wl = 531.66'		Increments: 15.95'	
Soil	Ht wl	Gain dBi	TO deg	Feed R	Feed X
VG	0.03	8.82	15	471.3	188.4
	0.06	9.09	14	414.8	83.6
	0.09	9.32	13	373.5	38.5
	0.12	9.52	12	340.2	17.9
	0.15	9.70	12	313.2	10.9
	0.18	9.83	11	291.9	12.3
	0.21	9.90	11	276.3	19.2
	0.24	9.89	10	266.1	29.2
	0.27	9.80	10	261.2	40.4
Average	0.03	6.62	19	481.4	167.4
	0.06	6.86	18	413.6	68.7
	0.09	7.00	17	368.2	29.3
	0.12	7.08	16	333.8	13.6
	0.15	7.12	15	307.4	10.3
	0.18	7.09	14	287.8	14.2
	0.21	7.01	14	274.3	22.3
	0.24	6.85	13	266.2	32.4
	0.27	6.62	12	262.8	42.8
VP	0.03	3.97	24	476.8	121.8
	0.06	4.32	22	397.1	44.6
	0.09	4.51	21	349.4	18.1
	0.12	4.64	20	317.0	11.0
	0.15	4.71	19	294.7	13.3
	0.18	4.75	18	279.6	20.6
	0.21	4.77	17	270.3	29.9
	0.24	4.78	17	265.7	39.7
	0.27	4.76	16	265.1	48.7

Except for showing higher gain values throughout and having optimal base heights that are unique to the antenna, the 160-meter data parallel those of the other SCV forms. On this band, the average-soil gain curve is about mid-scale

between the other curves and shows the greatest drop in gain with increased height above ground.

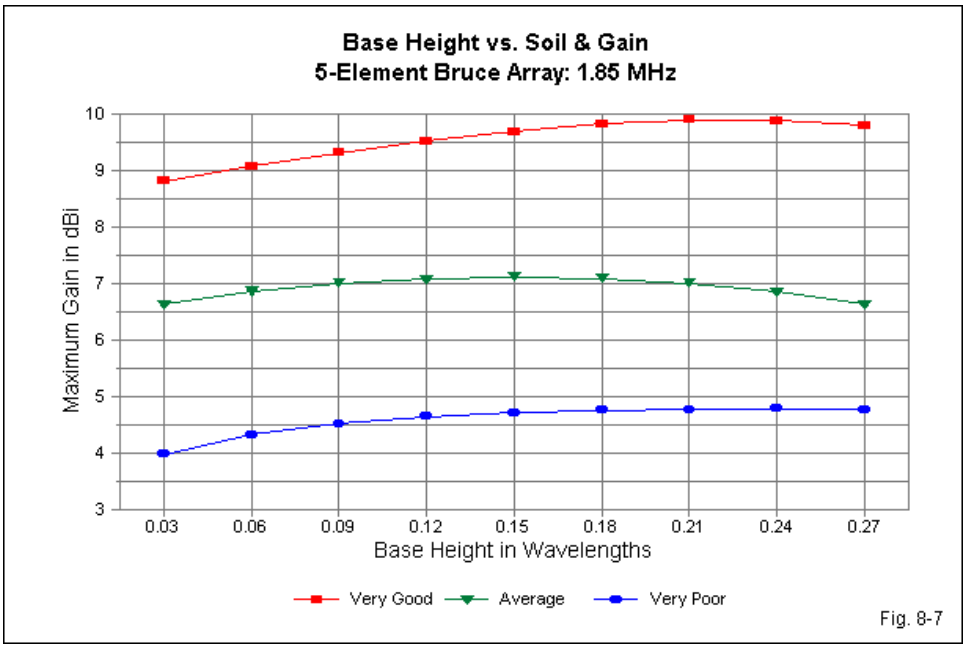

Fig. 8-8 provides overlaid elevation patterns for the array over each soil type, with each pattern recorded for the optimal base height applicable to the soil type. At its lower height, the pattern for average soil shows the least development of secondary elevation lobes. The patterns for very good and very poor soil show more distinct secondary lobe development. Only over very poor soil do the secondary gain peaks reach a level that is only about 4-dB down from the strength of the main lobe. Over very poor soil at the height of maximum gain, the array (and virtually any other SCV form similarly situated) would show a greater sensitivity to noise and signals from high angles. (At the risk of repetition, one of the reasons for using an SCV array in the first place is to maximize low-angle signal strength while minimizing sensitivity to higher-angle radiation.)

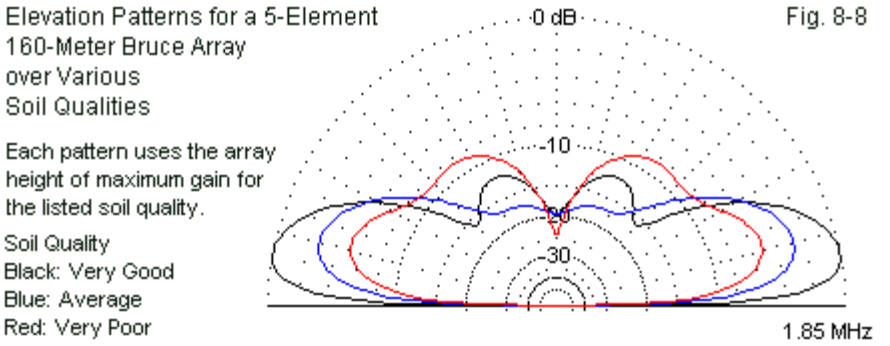

A 5-Element Bruce Array for 80 Meters

At 3.55-MHz, a wavelength is 277.06', so the 0.03-λ increments in the base-height entries are each 8.31'. Like the 160-meter array, an 80-meter Bruce array composed of AWG #12 copper wires calls for horizontal sections that are 0.27-λ (74.81'). The distance between the bottom and top wires is 0.255-λ (70.65'). The inward end wires are each 0.145-λ (40.17'). Only the end-wire dimension differs from the 160-meter version, although I tested dimensions only in 0.005-λ increments to settle in on the values shown. These values emerge from setting the array over average soil at its eventual optimal base height for maximum gain. You might find very slightly different values over very good or very poor soil. However, the performance differences that emerge would not be operationally significant.

Table 8-5 provides the data gleaned from the survey of base heights over the three soils. Like the 160-meter version of the array, the 80-meter Bruce shows the lowest base height for maximum gain over average soil, and the value is the same as for 160-meter: 0.15-λ (41.55'). Over very good soil, the optimal base height rises to 0.21-λ (58.18'). When we change the soil type to very poor, the gain curve shows no peak through the end of the scanning range (0.24-λ or 66.48'). These results are consistent with the results for a bobtail curtain, which we surveyed in the preceding chapter. Indeed, the effects of soil quality on each band are consistent for all SCV forms, although specific numbers vary.

5-Element Bruce Arrays for 80 Meters					Table 8-5
Base Height and Soil Quality vs. Performance					
3.55 MHz		1 wl = 277.06'		Increments: 8.31'	
Soil	Ht wl	Gain dBi	TO deg	Feed R	Feed X
VG	0.03	8.16	16	472.1	176.3
	0.06	8.43	15	411.7	74.4
	0.09	8.63	15	369.1	31.4
	0.12	8.79	14	335.9	12.5
	0.15	8.92	13	309.0	6.7
	0.18	9.00	12	288.4	8.8
	0.21	9.01	12	273.5	15.9
	0.24	8.95	11	264.0	25.7
Average	0.03	5.75	21	477.5	146.8
	0.06	6.03	20	405.7	56.4
	0.09	6.18	19	359.8	21.6
	0.12	6.27	18	326.2	8.8
	0.15	6.30	17	301.2	7.4
	0.18	6.28	16	283.1	12.3
	0.21	6.21	15	271.0	20.6
	0.24	6.08	14	269.2	30.3
VP	0.03	3.76	25	453.3	98.5
	0.06	4.26	24	379.5	35.4
	0.09	4.58	22	336.5	15.0
	0.12	4.84	21	308.2	10.7
	0.15	5.05	20	289.2	13.9
	0.18	5.23	19	276.6	20.8
	0.21	5.39	19	269.1	29.2
	0.24	5.53	19	265.6	37.6

Fig. 8-9 converts the gain figures into graphic form to facilitate several types of comparisons. First, we may interrogate each curve to note the rate of gain change per increment of base-height change in order to reach decisions on installation issues. Over average soil, for example, the rate of gain decrease is slowest as we reduce the base height. The curves for both very good soil and very poor soil are considerably steeper at lower base heights.

Second, as we have done for the other SCV forms, we may note how the 80-meter curves differ from those for 160 meters. Perhaps the most vivid feature is the rise in the general level of the curve over very poor soil. As we increase the operating frequency, average gain levels drop over both very good and average soil. However, the increase in operating frequency results in higher average gain values over very poor soil.

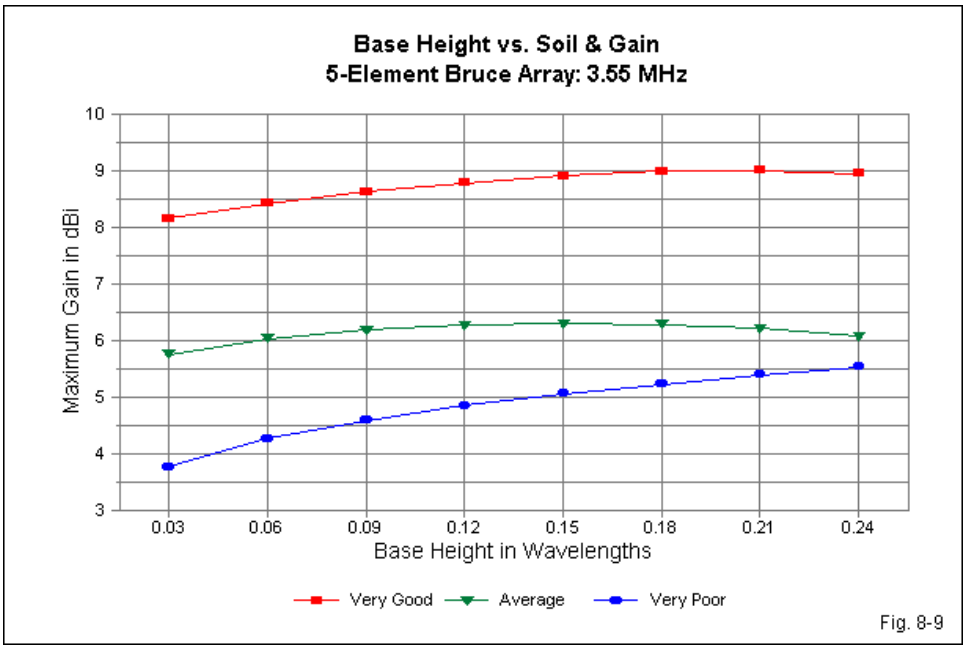

Fig. 8-10 allows us to compare the azimuth patterns of the 5-element Bruce array over each soil type, with each pattern taken at the TO angle for the base-height that yields maximum gain. Two features stand out. First, the general shape of the patterns does not change with the soil type (as it did for the 160-m elevation patterns). Each of the three overlaid patterns has the same general shape, so that even the sidelobes appear to be roughly proportional to the differences in the gain in the main lobes.

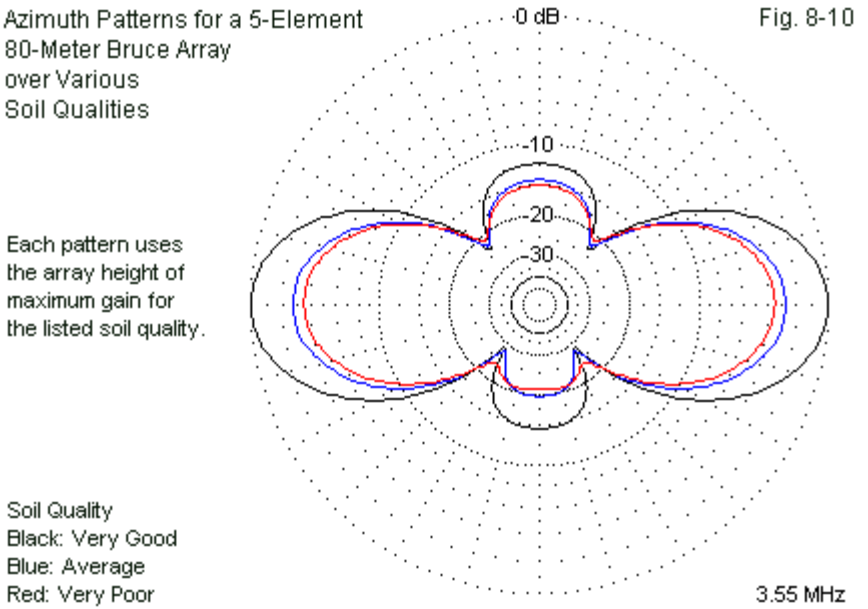

Second, patterns for average and for very poor soil are much closer together than they were in the 160-meter elevation patterns. Taking each versions of the antenna at its optimal base height, we find less than 1-dB difference in the bi-directional gain for the two soil types. However, had we used the average-soil base height of 0.15-λ for each pattern, we would have found an additional half-dB of gain difference.

A 5-Element Bruce Array for 80 Meters

At 7.15-MHz, a wavelength is 137.56'. Therefore, each 0.03-λ increment in base height is 4.13'. As we have noted in our general discussions of Bruce array properties, the horizontal wires in the antenna are each 0.275-λ (37.83'), while the distance from the bottom to the top wires is 0.25-λ (34.39'). For the 5-element array, the end wires are each 0.15-λ (20.63'). **Table 8-6** provides the

performance data for an AWG #12 copper 5-element Bruce array for base heights from 0.03-λ through 0.24-λ.

5-Element Bruce Arrays for 40 Meters					Table 8-6
Base Height and Soil Quality vs. Performance					
7.15 MHz		1 wl = 137.56'		Increments: 4.13'	
Soil	Ht wl	Gain dBi	TO deg	Feed R	Feed X
VG	0.03	7.35	19	455.5	149.6
	0.06	7.61	17	392.5	52.4
	0.09	7.78	16	350.2	12.5
	0.12	7.90	15	317.9	-4.6
	0.15	7.98	14	292.7	-9.6
	0.18	8.01	14	273.6	-7.3
	0.21	7.98	13	259.8	-0.8
	0.24	7.87	12	251.1	8.1
Average	0.03	5.28	23	448.4	114.7
	0.06	5.64	21	379.4	34.1
	0.09	5.86	20	336.7	3.9
	0.12	6.01	19	306.2	-6.8
	0.15	6.12	18	283.8	-7.4
	0.18	6.18	17	267.8	-2.7
	0.21	6.19	16	257.2	4.8
	0.24	6.16	15	251.2	13.4
VP	0.03	4.14	26	412.9	79.8
	0.06	4.70	25	351.1	23.3
	0.09	5.09	23	315.0	4.6
	0.12	5.41	22	291.3	-0.2
	0.15	5.68	21	275.2	1.4
	0.18	5.93	21	264.5	6.4
	0.21	6.14	20	257.8	12.7
	0.24	6.32	19	254.3	19.3

On 40 meters, we find further gain decreases over very good and average soils, but additional gain increases over very poor soil. In fact, the gain values for the Bruce array at the optimal base height (0.21-λ or 28.88') over average soil are

almost identical to the gain for the array over very poor soil at the same height. **Fig. 8-11** shows the crossing gain lines and also shows the more rapidly rising very-poor soil gain curve that we have come to expect on 40 meters. In addition, on 40 meters, the curve for very good soil reaches a peak gain value at a lower base height than the curve for average soil, a reversal of the situation that we found on both 80 and 160 meters.

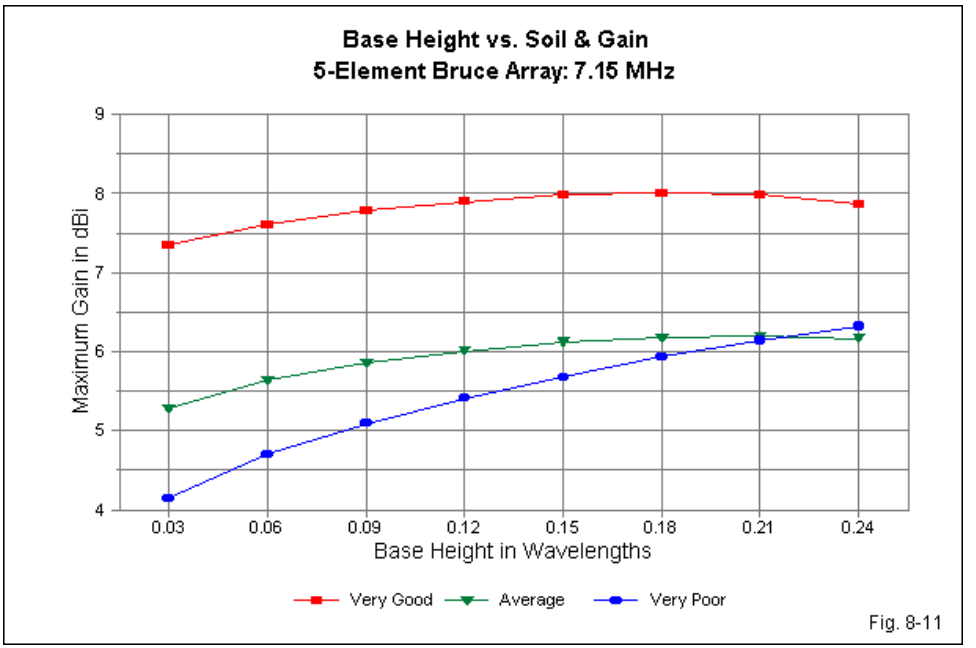

Fig. 8-11

Regardless of the type of SCV array that you may select, the gain data and curves for the three bands and the three soil types are very useful planning tools. You may reliably interpolate virtual curves for values of conductivity and permittivity that apply to your region but which fall between the extreme cases that we have used in the surveys. Almost every amateur installation involves compromises among the many elements that go into a major wire antenna assembly, including the support system, the available skills for erecting the array,

methods of feeding the antenna, and all of the safety concerns that surround antennas near a home. Hopefully, the survey data will provide useful planning information to arrive at the best possible installation of an SCV, whatever the circumstances.

Feeding the Bruce Array

For all basic and survey data, we have used a feedpoint that represents a current feed position at the center of the vertical wire either at or closest to the middle of the antenna. For reasons that will shortly become apparent, the selected feedpoint position has been a good one. But, it is not the only possible feedpoint position, and current feeding of the antenna is not the only way to handle this task. In fact, feeding the center of the middle element may be the least convenient way to deal with the weight and the routing of transmission line used in conjunction with the Bruce array. We have several options at our disposal.

To see a few of our options, let's study **Table 8-7** and **Fig. 8-12** together. The figure shows an outline of our 5-element array with a potential feedpoint at the center of each vertical section. As the data in the table reveal, we may select any one of the five feedpoint positions without creating any major changes in either the array performance numbers or the feedpoint impedance. The feedpoint resistance changes by about 5% from minimum to maximum values, an amount that is at the error limits of most impedance meters.

Feedpoint Position Consequences				Table 8-7
5-Element 7.15-MHz Bruce Array				
0.21 WL above Average Ground				
Position	Gain dBi	TO deg	Feed R	Feed X
1	6.16	16	261.9	0.1
2	6.25	16	262.0	-8.8
3	6.19	16	257.2	4.8
4	6.16	16	262.5	-8.6
5	6.20	16	271.3	0.4
Notes: See Fig. 8-12 to locate feedpoint positions.				

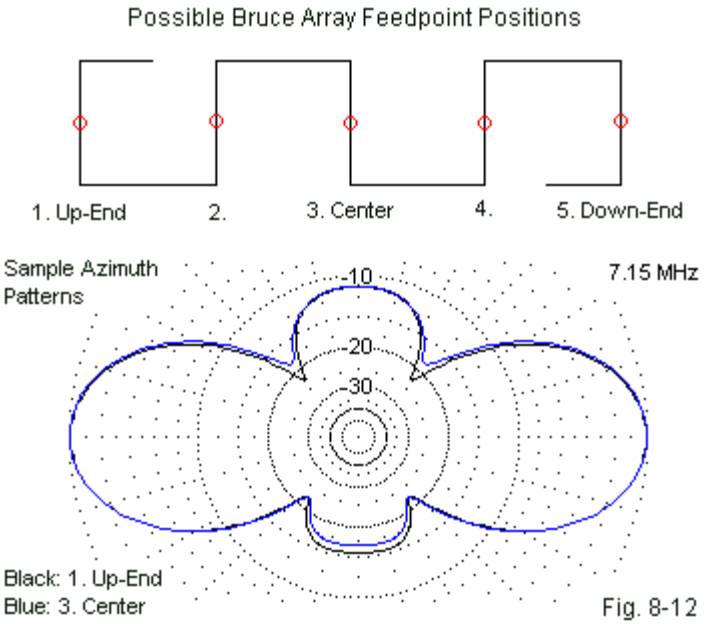

Fig. 8-12

The overlaid azimuth pattern in the figure shows the most radically different patterns produced by moving from one feedpoint position to another. (Had I overlaid all 5 patterns, the graphic would show a single fat line.) Since the pattern does not change if we move the feedpoint position from one vertical to the next, we might wish to consider feeding the array on an end wire. We would route the transmission line along a support that is outside the end wire and then across to the element. Not only is the run short, producing the least stress on the wire, but as well it lies in the plane of the antenna, where far-field radiation is weakest. End-feeding the array may prove to be the most convenient method of current feeding, although the impedance levels strongly suggest the use of parallel transmission line.

Before we invest in a Bruce array, we should examine the operating bandwidth. Some SCV forms displayed wider operating bandwidths than others.

The idea of the operating bandwidth includes not only the feedpoint impedance, but other key operating parameters as well. In this case, the bi-directional gain is one of those parameters. **Fig. 8-13** shows the gain across the entire 40-meter amateur band of Bruce arrays ranging from 2 to 7 elements.

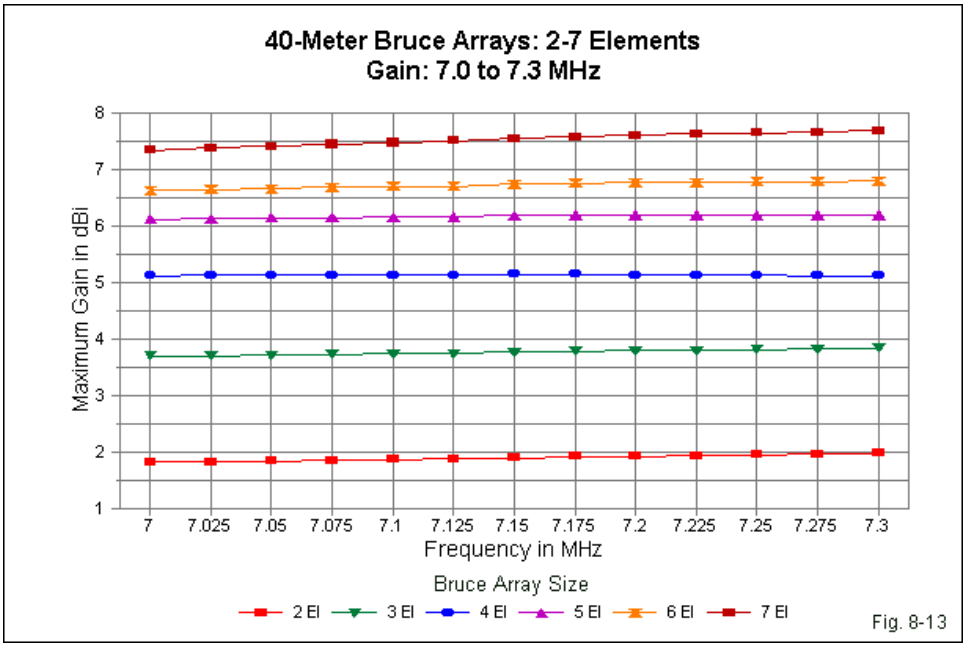

Fig. 8-13

Whatever the size of the array, it shows very stable gain over the 40-meter band. In most cases, the curve shows a very slight rise with frequency, although some bands are essentially flat within 0.05 dB for the entire 300 kHz spread. The maximum range of gain is under 0.35 dB. The importance of checking this parameter lies in the fact that a very wide SWR bandwidth would be meaningless if the gain changed radically across the passband.

Returning to our feedpoint concerns, **Fig. 8-14** shows the feedpoint resistance of the same collection of Bruce arrays. These data reflect the use of a

centered feedpoint, although the data would not change significantly for other feedpoints.

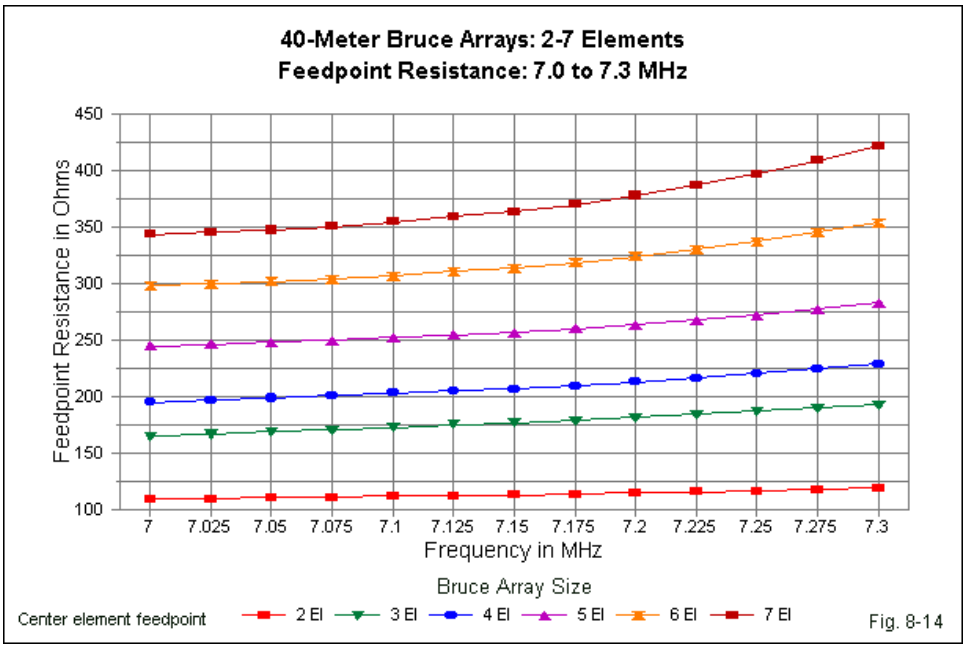

Fig. 8-14

The feedpoint resistance across the band rises modestly, regardless of the array size. The small 2-element Bruce shows a feedpoint resistance range that is under 10 Ω. As the number of elements increases, the feedpoint resistance at the center of the band also rises, and the range of that resistance is roughly proportional to the value at the band's center. Above the 2-element size, the resistance range is between 15% and 20% of the feedpoint resistance at 7.15 MHz. The small resistance range suggests that one might control the overall impedance range (or the SWR range relative to the feedpoint resistance) by controlling the feedpoint reactance.

Fig. 8-15 provides a graph of the feedpoint reactance for the same collection

of Bruce arrays over the same set of frequencies. Like the feedpoint resistance, the reactance range increases as we increase both the number of elements and the feedpoint resistance at the center of the band. Since each array in the collection is very close to being resonant at 7.15 MHz, all line cross at that frequency. Note that each line is virtually linear.

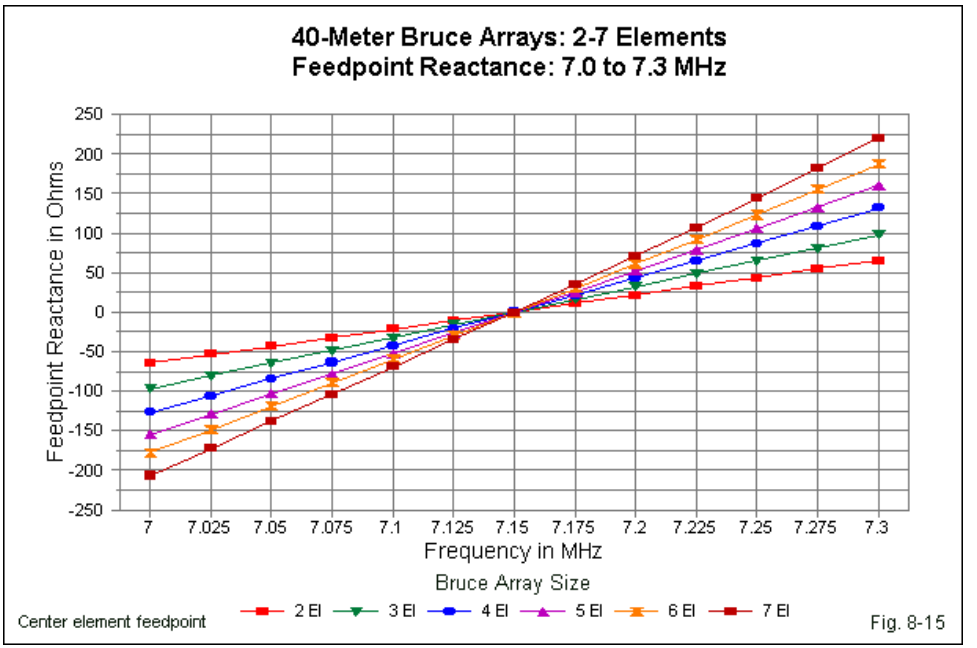

Fig. 8-15

One might easily set the reactance of an array to show a low inductive reactance at 7.0 MHz, allowing the reactance to rise across the band. Under those conditions, a series capacitor—either manually or remotely controlled—could compensate for the reactance, leaving essentially a purely resistive impedance. A transmission line with the same impedance as the remaining feedpoint resistance would provide matched conditions from the series capacitor(s) to the equipment end of the line.

However, the level of mismatch created by the range of the reactance swing across 40 meters is not high. **Table 8-8** summarizes the data ranges that we have discussed in connection with the graphs, but it also has a further column. The data labeled "delX/R" provides the ratio of the reactance swing to the 7.15-MHz feedpoint resistance. The low ratios shown indicate a relative small SWR swing for a parallel transmission line. In turn, the low swing indicates that the voltage and current excursions on the line will have limited values, in virtually all cases falling well below the level at which a parallel transmission line shows significant losses. Therefore, the use of a parallel transmission line using a common characteristic impedance (300 Ω to 600 Ω) with a balanced antenna tuner at the equipment end of the line is equally appropriate in feeding the Bruce array.

Bruce Array Size vs. 7-MHz to 7.3-MHz Performance						Table 8-8
All arrays 0.21-WL above average ground.						
No. El.	Gain dBi	Delta Gn	Feed R	Delta R	Delta X	delX/R
2	1.89	0.16	112.3	9.6	129.9	1.16
3	3.77	0.15	176.1	28.1	194.7	1.11
4	5.15	0.03	206.5	33.7	258.7	1.25
5	6.19	0.08	256.4	37.9	314.9	1.23
6	6.75	0.16	313.4	56.0	365.9	1.17
7	7.56	0.34	363.5	78.5	427.3	1.18
Notes:	Delta Gn = gain range across band in dB					
	Gain dBi and Feed R are values at 7.15 MHz					
	Delta R = feedpoint resistance range across band in Ohms					
	Delta X = feedpoint reactance range across band in Ohms					
	delX/R = ratio of reactance range to mid-band resistance					

Bruce arrays that use an even number of elements—usually 4 or 6—present a different opportunity when it comes to feeding them. Of course, we may use one of the standard feedpoints. If we do so, we obtain the current distribution shown in the outline sketch in **Fig. 8-16**. I have overlaid the outline of the far-field pattern for reference, with the understanding that the two pictorial elements have little other than positional relationships. A proportional representation of the antenna itself relative to the far-field pattern outline would be an invisible dot,

which would obscure our view of the current distribution curves on the four vertical elements. However, the presence of the azimuth pattern outline (along with the data in **Table 8-8** does reveal why the 4-element version of the Bruce is an amateur favorite. At the cost of a little gain, the antenna is shorter than the 5-element array and yields an azimuth pattern with no sidelobes.

Fig. 8-16

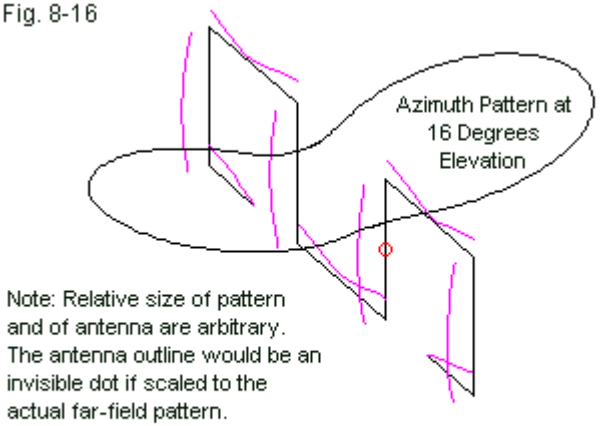

4-Element Bruce Array with Relative Current Distribution
and Azimuth Pattern Oriented to Antenna

Those who wish to use a feedline system based on coaxial cable can use a version of the standing-H feed system that we examined in Chapter 2. Instead of feeding only one vertical, we shall feed both central vertical. To do so, we shall employ two equal lengths of line to a center point. A T-fitting allows us to use 50-Ω coaxial cable from the junction to the equipment.

In this particular case, the minimum physical length for the two phase lines is 0.135-λ (18.57), since the distance between the verticals is 0.27 (37.14'). If we allow a bit of extra, say lines that are 0.1375-λ (18.91') long, then we will be assured of a fit and the electrical length will be even longer. RG-62 has a characteristic impedance of 93 Ω with a velocity factor of 0.84. The electrical

length of each phase line for our sample case is 0.164-λ. Using a pair of these lines, the junction shows a feedpoint impedance of 42.8 –j3.6 Ω. As well, the performance of the antenna does not change, with a bi-directional gain of 5.18 dBi at a TO angle of 16°. **Fig. 8-17** shows the outline of the system, along with the current distribution.

4-Element Bruce Array with Center Verticals Fed In Phase with 93-Ohm Transmission Line

Fig. 8-17

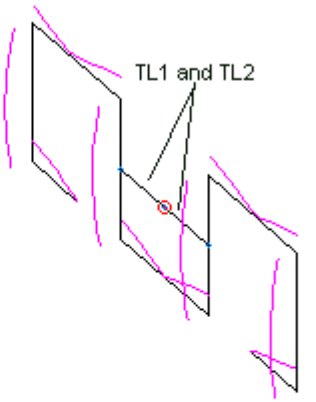

Note: Compare relative current distribution to Fig. 8-16.

50-Ohm SWR Curve

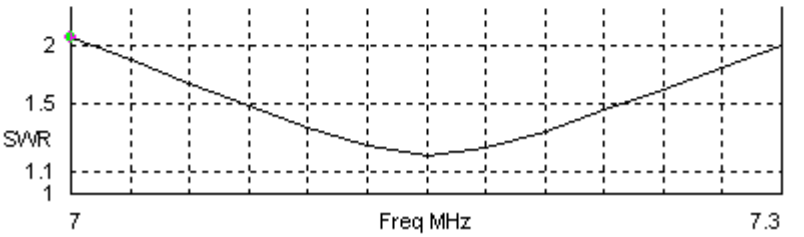

The SWR curve shows that the phased feed system provides 2:1 SWR coverage for the entire band relative to a 50-Ω standard, despite the fact that the design frequency impedance is not exactly 50 Ω. Moreover, the phase-line lengths are not critical within reasonable levels of variation. A non-conductive support post at the center of the array could easily support the coaxial cable and prevent its weight from placing undue stress on the array wires.

Like any of the other SCV forms, it is possible to substitute a high-voltage, low-current feed system for the Bruce array. We may usefully review the right way and the wrong way to achieve a voltage feed. If we use any one of the current feed systems that we have noted, we obtain the elevation pattern shown on the left in **Fig. 8-18**. The pattern is for a 4-element Bruce array at a base height of 0.21-λ over average ground. A voltage feed system should also produce this pattern within close tolerances.

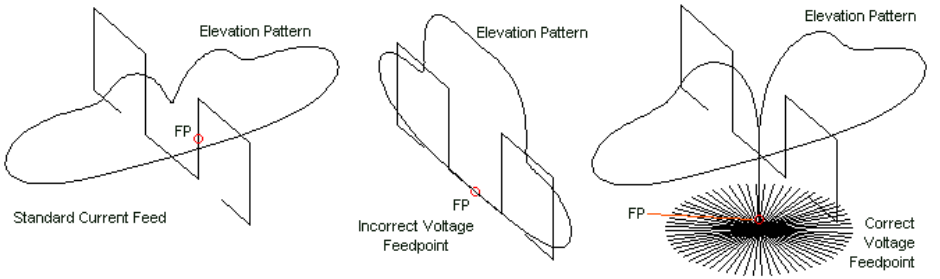

Fig. 8-18 Voltage Feeding the Bruce Array (4-Element Version Shown)

The center portion of the figure shows a temptation for many amateur, that is, to effect a voltage feed by placing the transmission line at the center of a horizontal wire. However, if we simply break the line and insert the transmission line, we obtain a very weak pattern that is in the plane of the array rather than broadside to it. Obviously, the technique is incorrect.

The correct manner to implement a voltage feed system is to connect a single wire between the center of the horizontal wire and the ground, with the feedpoint transferred to a point very near to the ground. We shall need a very good RF ground, simulated in the model by 64 buried ¼-λ radials from the point of contact with the vertical wire. Now the broadside elevation pattern has returned.

Fig. 8-19 provides the elevation and azimuth patterns produced by the 4-element Bruce array set up for voltage feed. Because the area immediately below the antenna represents improved ground of significant but not

overwhelming proportion, the elevation pattern shows larger secondary lobes than the corresponding pattern for one of the standard methods of providing a current feed. As well, the azimuth pattern shows a small increase in gain to 5.31 dBi, with a 3° shrinkage in the beamwidth. Note the small sidelobe bulges in the azimuth pattern.

Fig. 8-19

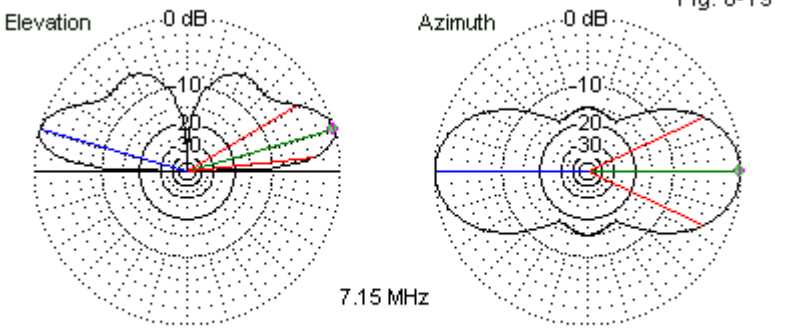

Elevation and Azimuth Patterns of a Voltage-Fed
4-Element Bruce Array 0.21-WL above Average Soil

Nonetheless, the operating performance of the antenna will be indistinguishable from a current-fed version. In addition, the voltage-feed system places the main feedline close to the ground. We should note that the impedance at ground level is not the very high impedance that occurs at the junction of the vertical wire with the horizontal array wire. The wire is about 0.21-λ, allowing a large transition from the high impedance at the junction to a lower impedance at the feedpoint. With a perfectly straight wire and the excellent ground system, the near-ground feedpoint shows an impedance of 202 – j83 Ω. The value obtained at any installation will depend upon the base height of the antenna and the length of the vertical wire to ground, as well as the quality of the RF ground itself. With careful experimentation, it is usually possible to set the system for a 50-Ω coaxial cable feedline running at ground level. You may need to install a 4:1 impedance transformer or balun at the near-ground feedpoint. Alternatively, one might use a network of fixed components to effect the

necessary impedance transformation.

All in all, the Bruce array provides a considerable number of feeding possibilities. At least one of them should meet the needs of the user and the limitations of the installation site.

Conclusion

Although we have stricted ourselves to Bruce arrays using 2 through 7 elements, we might extend the size of the array indefinitely. For most amateur installations, even at 40 meters, an array of 5 elements presses the boundaries of the installation site, and the 4-element array is a more modest favorite. Although not as horizontally long as a bobtail curtain, the 4-element Bruce array matches the bobtail in gain. Smaller Bruce arrays are possible, as these notes have shown, but the more complex wire arrangement usually gives a more favored place to other SCV forms.

The Bruce array yields the highest level of gain for any horizontal length of any of the SCV forms. It replaces ideal ½-λ spacing between vertical elements with an ingenious arrangement of wires to produce a collection of vertical wires at ¼-λ spacing and interconnected for in-phase feeding of each vertical section. In addition, we may feed any one of the vertical wires from end to center with no significant change in either the performance or the feedpoint impedance. As well, the antenna is amenable to voltage feeding, if correctly implemented.

Nevertheless, the Bruce array has some limitations. Installations for 160 and 80 meters usually require pre-existing supports of very great height. Hence, we normally find amateur Bruce arrays for these bands in forests of redwood or Douglas fir trees. In addition, the Bruce array is not open to modifications that allow for lower heights. For example, we might fold the lower ends of a half-square inward to lower its top height. The Bruce array does not allow for such variations, although one might experiment with loops that have a lower vertical dimension and a wider horizontal length. Although we might also apply the Bruce array as a driver with a planar reflector, I am aware of no VHF or UHF applications of the array.

The Bruce array brings us to the end of our exploration of SCV forms. As the most complex and highest-performing antenna of the group, the Bruce is a good place to close our journey. The self-contained vertically polarized antenna has proven to be highly useful on the lower HF and upper MF amateur bands, with additional applications for many forms in the VHF and UHF regions of the spectrum. Only in recent years have we recognized the electronic family to which all of the members belong. These notes have tried to create a family reunion, along with enough detailed data to allow a prospective user to select and design the version that is best for a given installation situation. Along the way, we may have also improved the expectations that we have for such antennas as we change their height above ground, the operating frequency, and the soil quality beneath them.

As with any family reunion, there are undoubtedly missing cousins that I have not included in this book of portraits. I hope that you will be able to recognize such arrays by their family resemblances to the members that we have featured.

Appendix

Dimensions, Performance and Models

Dimensions of "Ideal" SCVs for 160 to 30 Meters

This appendix contains three types of information. The first is a series of dimensions for basic SCVs of various types composed of AWG #12 copper wire for the amateur bands between 160 and 30 meters. Each table lists the dimensions for single SCVs that are near resonance within a few Ohms at the optimal height for maximum gain over average soil. All SCVs are set for an impedance of 50 Ω except the half-squares. Each entry lists the base height, the base or horizontal dimension, and the height or vertical dimension. You may need to make adjustments for other soil qualities or for heights much closer to ground level. All dimensions are in feet. Multiply by 0.3048 for dimensions in meters.

For each listing, the attached nn.ez-format files contain a model using these dimensions at the listed height. Each type of SCV shows a 2-letter code, such as EQ for equilateral delta. File names will then add the amateur band. For example, file eq-160.ez is the file for the 160-meter (1.85-MHz) equilateral delta SCV model.

Equilateral Deltas (EQ)

Freq. MHz	Base Height	Base Length	Height	Circumference
1.85	90	186.6	161.6	559.8
3.55	40	97.6	84.52	292.8
3.95	40	87.8	76.0	253.4
5.368	35	64.7	56.0	194.1
7.15	30	48.8	42.3	146.4
10.125	25	34.4	29.8	103.2

Right-Angle Deltas (RA)

Freq.	Base Height	Base Length	Height	Circumference
1.85	90	232.6	116.3	561.5
3.55	40	121.7	60.85	293.8
3.95	40	109.5	54.75	264.3
5.368	35	80.8	40.4	195.1
7.15	30	60.8	30.4	146.8
10.125	25	43.0	21.5	103.8

Diamonds (DI)

Freq.	Base Height	Base Length	Height	Circumference
1.85	90	254.0	117.0	559.3
3.55	50	131.4	64.4	292.7
3.95	45	118.0	57.9	262.9
5.368	35	86.9	43.1	194.0
7.15	30	64.4	34.0	145.6
10.125	25	45.4	24.4	103.1

Rectangles (RE)

Freq.	Base Height	Base Length	Height	Circumference
1.85	90	196.0	79.5	551.0
3.55	50	100.2	44.0	288.4
3.95	45	90.1	39.6	259.4
5.368	35	65.8	29.8	191.3
7.15	30	48.8	23.2	143.9
10.125	25	34.0	16.9	101.9

Half-Square (HS)

Freq.	Base Height	Base Length	Height	Wire Length
1.85	16	241.0	150.0	541.0
3.55	12	126.3	78.0	282.3
3.95	12	113.5	70.0	253.5
5.368	10	82.9	52.0	186.9
7.15	10	62.45	39.0	140.45
10.125	8	43.45	28.0	99.45

Comparative Performance

The second data element is a comparison of the performance of single 40-meter (7.15-MHz) SCVs at their optimum height for maximum gain over each soil type (very good, average, and very poor). The data is extracted from tables in the preceding chapters and forms a general guide to performance expectations. Installations at other heights or at other operating frequencies will generally show a proportional increase or decrease in the performance numbers. Nevertheless, the general trends will remain valid.

Where performance values are close, allow the antenna dimensions and the parameters of the installation site to drive the final selection of an SCV. Indeed, in many cases, the performance values will be moot due to installation site limitations.

Very Good Soil (conductivity 0.0303 S/m, permittivity 20)

Antenna Type	Base Ht feet	Gain dBi	TO deg	BW deg	Feedpoint Z R +/- jX Ω
EQ	25	3.33	14	---	125.7 – j0.2
RA	30	3.88	14	112	53.0 – j1.7
DI	25	3.86	14	106	56.8 – j5.6
RE	30	4.52	14	91	52.1 – j1.3
HS	8	5.52	16	70	71.5 + j0.8

Average Soil (conductivity 0.005 S/m, permittivity 13)

Antenna Type	Base Ht feet	Gain dBi	TO deg	BW deg	Feedpoint Z R +/- jX Ω
EQ	30	1.47	17	---	122.3 + j2.3
RA	30	2.01	17	117	51.6 – j0.4
DI	30	2.03	16	107	51.8 – j3.0
RE	35	2.69	16	92	47.4 + j1.3
HS	10	3.46	19	80	68.4 – j1.4

Very Poor Soil (conductivity 0.001 S/m, permittivity 5)

Antenna Type	Base Ht feet	Gain dBi	TO deg	BW deg	Feedpoint Z R +/- jX Ω
EQ	35	1.65	19	---	113.7 + j13.7
RA	40	2.13	19	130	48.5 + j4.7
DI	35	2.28	19	107	50.5 + j0.6
RE	40	2.89	19	93	46.3 + j4.8
HS	14	2.90	21	95	64.3 – j2.0

To supplement the performance tables for single SCV forms, we may add performance values for double forms, including the double right-angle delta (RAD), the double diamond (DID), the open double rectangle (ODR), and the bobtail curtain (BC). The values are for the array at an optimal base height above average soil. The open double rectangle uses end feeding. The bobtail curtain is dimensioned for maximum gain rather than for a 50-Ω feedpoint impedance.

Antenna Type	Base Ht feet	Gain dBi	TO deg	BW deg	Feedpoint Z R +/- jX Ω
RAD	20	3.78	20	73	38.7 + j2.2
DID	20	4.33	17	64	49.1 – j3.2
ODR (end)	37	4.45	16	59	49.4 – j0.0
BC	14	5.03	19	50	28.8 + j1.8

Modeling Conventions and Results

I have written these notes on SCVs from a modeler's perspective, although the data reflects real-antenna performance. The modeler's perspective appears in certain references to what happens to the current and the voltage on an SCV form as we pass a high-voltage, low-current position along the antenna wire. In virtually all of the attached models, I have followed what appear to be "normal" modeling conventions, creating loops and similar structures from a continuous wire "ribbon." Wire 1, End 2 of the first part of the SCV connects to Wire 2, End 1 of the next part. Under these conditions, modeling reports will show a reversal of

the phase of the current as it passes a high-voltage position. Since the elements are in phase, we therefore assume a comparable voltage phase angle reversal. However, NEC does not provide a voltage report, so we may find it difficult to verify the latter assumption.

Let's go through some simple exercises to establish the phase-reversal condition within the continuous-ribbon model of an SCV. We shall start with 2 vertical dipoles (set up for 7.15 MHz and composed of AWG #12 copper wire, of course). We shall space the dipoles ½-λ apart. Each dipole wire will run from near the ground (4') to a higher point (71'). Under these basic modeling conditions, we shall place a source or feedpoint on each wire's center segment, assigning a current of 1.0 A at 0° phase angle. We customarily think of this set-up as proper for in-phase feeding of the dipoles. **Fig. App-1** shows the set-up at the left, with the resulting relative current magnitude and phase angle distribution.

Fig. App-1

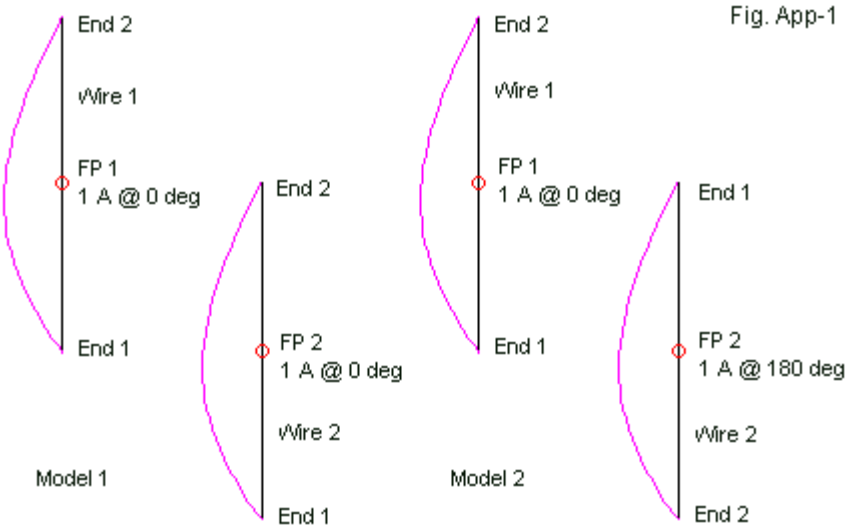

In-Phase Feeding vs. Model Wire Set-Up

The right portion of the figure shows an alternative set-up for the two dipole wires. The first dipole remains unchanged, but we reverse the set-up direction of the second dipole. We model this wire from the top (End 1) downward to the bottom (End 2). To obtain in-phase feeding of the two dipoles, the second wire source is set at 1 A at 180°. For both the left and the right figures, the voltage on the Wire-1 source will show 72.9 v at –22.40°. The voltage for Wire 2 of the left figure is 72.0 v at –22.4°, just as we would expect. With the second wire reversed in its set-up direction on the right and the source current set at 180°, the source voltage report shows 72.0 v at 157.6°. Like the phase angle of the source current, the phase angle of the source voltage has changed by exactly 180°.

Wire direction does make a difference to all models of antennas using either 2 or more sources or having virtual feedpoint positions that we could have provided with a second (or subsequent) source. The dipoles have a physical separation between them and therefore require individual sources for in-phase feeding. Even so, if we reverse the direction of a wire set-up relative to a first and fixed wire set-up, we must adjust the source on the second wire accordingly. (There are models of both dipoles attached to this chapter. As an exercise, you may wish to change the source phase angle of the second model to a 0° phase angle and watch the broadside pattern turn into an edgewise pattern relative to the plane formed by the dipoles.)

SCV forms typically use a single feedpoint. Therefore, we do not often find reports of the virtual source voltage, although we can check the current tables for key values. To illustrate the situation, let's perform a series of small modeling experiments on a half-square, the simplest SCV to model. Again, we shall set the half-square at 7.15 MHz and use AWG #12 copper wire for all four of the models in the set. **Fig. App-2** shows the modeling set-up and the distribution of relative current magnitude and phase angle on each of the models.

The first model is the simplest and perhaps the most normal or common. We start with Wire 1, working from the ground upward to the first corner. We next set a horizontal wire (Wire 2) from the first corner to the second corner. Finally, we set the last wire, working from the upper corner to the loose end close to ground (Wire 3). The single (split) source at the upper end of Wire 1 has a current of 1 A

at 0° phase angle. Vertical wires have 11 segments, while the horizontal wire has 21 segments.

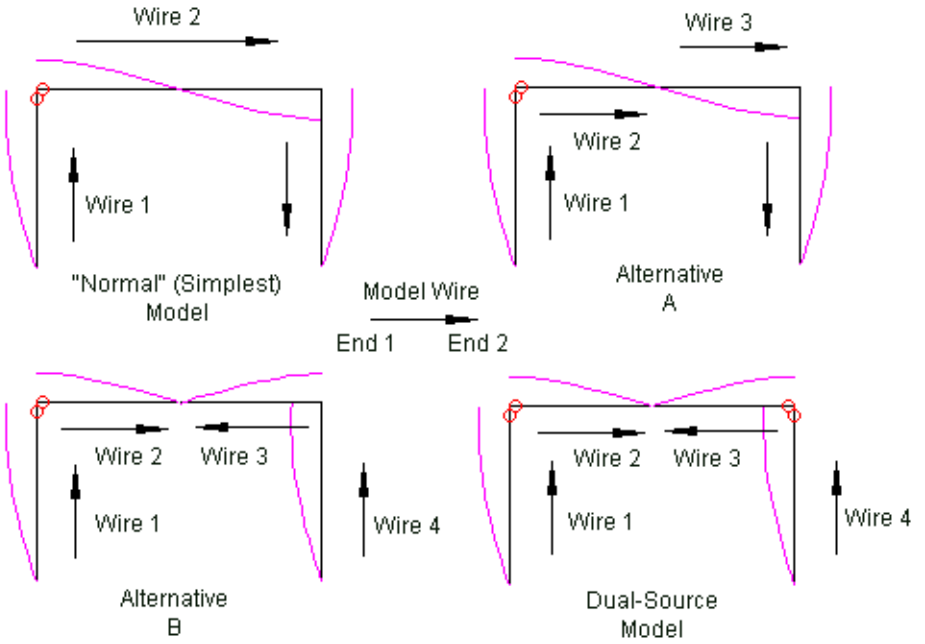

SCV Modeling: Half-Square Example
Set-Up Conventions and Results

Fig. App-2

The current distribution curves show a phase reversal at the approximate center (allowing for copper losses) of the horizontal wire. The current curve on the second vertical element (Wire 3) shows the opposite phase angle relative to the current on Wire 1. Next let's check the current reports. The top of Wire 1 shows 1 A at 0°, since that is the source location with its assigned value. The top of Wire 3 shows a current of 1.01 A at –179.2°, about as close as we can come to a full 180° phase reversal using lossy wire. At the center of the horizontal wire

(Wire 2) we find a report of 0.06 A at –83.4°. The current is passing through a zero magnitude, and the phase angle has shifted almost 90° along the route to the upper corner of Wire 3.

As an intermediate exercise, let's break the horizontal wire into two wires, both set up in the continuous-ribbon orientation. Both Wire 2 and Wire 3, which combine to form the horizontal wire, use 11 segments. The current curves in the upper right section of the figure show no change. We can read the currents on the segments on each side of the horizontal wire center point and find phase angle readings of –40.7° and –132.6°. The phase-angle change across the center of the horizontal wire is exceptionally rapid. You may refine the rate of current phase-angle change simply by populating all wires in the model with many more segments, keeping segment lengths about equal throughout.

Next, without changing the half-square's dimensions, we shall make two small changes, as shown on the lower left in the sketch. The second vertical (Wire 4) will now run from the ground upward, and Wire 3 will run from the corner to the center. In this maneuver, we replicate in the half-square model the set-up that we normally use for the vertical dipole models on the left in **Fig. App-1**. The change makes no difference to the half-square's performance: the gain is 3.46 dBi with a TO angle of 19 for all three models so far.

The changes do make a difference to the current distribution curves and to the current reports. The top segment of the unfed vertical wire (Wire 4) still reads a current magnitude of 1.01 A. However, the reported phase angle is 0.8°, exactly 180° different from the previous report. The difference also shows up in the current distribution curves, which now show an in-phase condition. The segments on each side of the junction between Wire 2 and Wire 3 now show phase angles of –40.7° and 47.4°. The change across the junction is still close to 90°. The size of the graphics does not permit showing the vector of the current in the second axis at the very low current magnitude levels.

Now let's confirm that the model form in our preceding exercise is correct for in-phase feeding relative to a physical antenna. We may do this simply by adding a source at the upper corner of the previously un-fed vertical element. The lower

right corner shows this option. Under these conditions, both vertical top segments show a current—as assigned—of 1.0 A at 0°. The voltage at both corners is 33.6 v at –3.5°. Note that the current distribution curves do not change from the identical model minus the extra source.

You may expand this set of models to gather further insight into the ways in which how we set up model wires may affect performance. However, for the purposes of these notes, our work is done. We have shown that the idea of a phase reversal applies to SCV forms that we set up in the normal continuous-ribbon method of modeling. Under those conditions, in-phase feeding from a single feedpoint effects a phase reversal of both current and voltage at the actual and the virtual feedpoint(s) of the SCV form. We may overcome the need for viewing the models in this way by reconstructing them so that all elements proceed in common directions, just as we normally do when working with vertical dipoles.

Other Publications

We hope you've enjoyed this Volume of the **SCV Notes.** You'll find many other very fine books and publications by the author L.B. Cebik, W4RNL (SK) in the ***antenneX Online Magazine BookShelf*** at the web site shown below.

Published by
antenneX Online Magazine
http://www.antennex.com/
POB 271229
Corpus Christi, Texas 78427-1229
USA

ISBN: 1-877992-46-1
